A Study of Viral and Cellular Factors in the Regulation of the Influenza Virus RNA-dependent RNA Polymerase

Ashley D York



Sir William Dunn School of Pathology
and
Brasenose College

A thesis submitted for the degree of Doctor of Philosophy
at the University of Oxford, Trinity Term 2014

ASHLEY YORK
BRASENOSE COLLEGE

DOCTOR OF PHILOSOPHY
TRINITY TERM, 2014

ABSTRACT

The segmented negative-sense vRNA genome of influenza A virus is replicated via a complementary RNA (cRNA) intermediate by the viral RNA-dependent RNA polymerase (RdRP). The replicative intermediate has been thought to exist as a complementary ribonucleoprotein (cRNP) complex. Development of an RNA-based affinity-purification strategy for the isolation of viral ribonucleoprotein complexes enabled the structural and functional characterisation of the previously uncharacterised cRNP complex. The cRNP exhibits a filamentous double-helical organisation with defined termini, containing the viral RdRP at one end and a loop structure at the other end. *In vitro* characterisation of cRNP activity led to a proposal of a model of vRNA synthesis that relies on a *trans*-activating RdRP.

The viral RdRP is an important host range determinant indicating that its function is affected by interactions with cellular factors. However, the identities and the roles of most of these factors remain unknown. Affinity-purification followed by mass spectrometry was performed to identify cellular proteins that interact with the viral RdRP. 171 cellular proteins were found to co-purify with the viral RdRP, the most abundant of which were chaperones, cytoskeletal proteins, importins, proteins involved in ubiquitination, kinases and phosphatases, mitochondrial and ribosomal proteins. Among the phosphatases, three subunits of the cellular serine/threonine-protein phosphatase 6 (PP6) were identified. PP6 was found to interact directly with the PB1 and PB2 subunits of the viral RdRP, and siRNA-mediated knockdown of the catalytic subunit of PP6 in infected cells resulted in the reduction of viral RNA accumulation and the attenuation of virus growth. Taken together, these results suggest that PP6 interacts with and positively regulates the activity of the influenza virus RdRP.

DECLARATION

I declare that this thesis is entirely my own work, and except where otherwise stated, describes my own research.

Ashley York

Oxford, July 2014

ACKNOWLEDGEMENTS

I would like to thank my supervisor Professor Ervin Fodor for all of his help, encouragement and generosity during my D.Phil. studies. His knowledge and never-ending enthusiasm have been an inspiration, and it has been the greatest pleasure to work under his guidance. I am also grateful to Dr. Nicole Robb and Jane Sharps for their help and advice during my time in the lab. I would also like to thank Dr. Ed Hutchinson for all of his assistance and expert help in mass spectrometry analyses. I am also grateful to all of the present and past members of the Fodor lab for making my time here enjoyable and entertaining. I was lucky enough to collaborate with Dr. Juha Huiskonen, who was always helpful and friendly. His stellar electron microscopy skills and knowledge base were pivotal for driving some of the work in this thesis. I would like to thank the Medical Research Council for studentship funding.

I am also indebted to previous teachers and mentors without whom it would have been impossible for me to study for a D.Phil. at the University of Oxford. In particular, I would like to acknowledge Professor Peter Rich and Dr. Bambos Charalambous for strong support and encouragement during my undergraduate studies at University College London. I would like to thank Dr. Tonia Schofield and Judy Potter (Hills Road Sixth Form College, Cambridge) for inspirational teaching of biology and chemistry that led me to pursue a career in science.

I would like to thank my friends Matthew, Sophie, Damien, Amanda, Aisling, Emma, Jack, Seann, Daniel J, Mark and Daniel C for many fond memories I will take with me from my time in Oxford. Lastly, I would like to thank my Mum, Dad and Nan for all of their love and support.

TABLE OF CONTENTS

Abstract I
Declaration II
Acknowledgements III
Table of Contents IV
Abbreviations IX

Chapter 1: Introduction

1.1 General introduction 1
1.2 Influenza virus taxonomy and nomenclature 4
1.3 The influenza A virion 5
1.4 The influenza A virus life-cycle 9
1.4.1 Attachment and entry 11
1.4.2 Fusion, uncoating and nuclear import 12
1.4.3 Viral gene expression 13
1.4.4 Nuclear export and traffic of vRNP complexes 15
1.4.5 Genome packaging 16
1.4.6 Virion assembly and egress 18
1.5 Influenza virus RNA synthesis 19
1.5.1 Overview 19
1.5.2 Viral ribonucleoprotein (RNP) complexes 21
1.5.3 The viral RNA-dependent RNA polymerase and nucleoprotein 25
1.5.4 Viral RNA promoters 33
1.5.5 Viral mRNA synthesis, processing and transport 34
1.5.6 vRNA replication 39
1.5.7 Regulation of the viral RdRP 41
1.6 The influenza virus transcription/replication machinery and host-pathogen interactions 47
1.6.1 Overview 47
1.6.2 Host-adaptation of the viral transcription/replication machinery 48
1.6.3 Approaches to study interactions between the viral transcription/replication machinery and the host cell 50

1.7 Thesis objectives and outline 54

Chapter 2: Materials and Methods

2.1 Materials 57
2.1.1 General reagents 57
2.1.2 Enzymes 58
2.1.3 Radiochemicals 58
2.1.4 Synthetic oligodeoxyribonucleotides and oligoribonucleotides 58
2.1.5 Antibodies 59
2.1.6 Bacteria and bacterial culture medium 59
2.1.7 Cell culture media 60
2.1.8 Cell lines 60
2.1.9 Viruses 61
2.1.10 Plasmids 61
2.2 Cloning 62
2.2.1 Plasmid construction 62
2.2.2 Transformation into competent *E. coli* 66
2.2.3 Plasmid preparation and sequencing 67
2.3 Eukaryotic cell culture 68
2.4 Virus culture and handling 68
2.4.1 Reverse genetics 68
2.4.2 Plaque assay 69
2.4.3 Infection of eukaryotic cells with influenza A virus 70
2.4.4 Growth curve analysis 70
2.5 RNA analyses 71
2.5.1 RNP reconstitution assay 71
2.5.2 TRIzol extraction of RNA 71
2.5.3 Primer extension analyses 72
2.6 SDS-PAGE 74
2.6.1 Gel electrophoresis of proteins 74
2.6.2 Western blotting 75
2.6.3 Silver and Coomassie staining of proteins 75

2.7 Isolation of viral ribonucleoprotein (RNP) complexes by RNA-based affinity purification 76
2.8 Recombinant influenza virus RdRP purification 78
2.9 *In vitro* activity assays 80
2.10 Strep-tag affinity-purifications 81
2.11 GST-pulldown assay 83
2.12 RNA interference of PPP6C 84
2.13 Mass spectrometry 85
2.13.1 Sample preparation and mass spectrometry 85
2.13.2 Analyses of mass spectrometry 85
2.14 Microscopy 87
2.14.1 Electron microscopy and image processing 87
2.14.2 Indirect immunofluorescence and confocal microscopy analysis 88

Chapter 3: RNA-based affinity purification of influenza virus ribonucleoproteins
3.1 Introduction 90
3.2 Rationale and strategy for the insertion of an RNA tag into the influenza virus genome 92
3.3 Accumulation of tagged viral RNAs in RNP reconstitution assays 98
3.4 Generation of recombinant influenza A viruses containing a PP7 RNA tag in the NA or NS gene segments 102
3.5 Accumulation of viral RNAs containing a PP7 RNA tag in infected cells 105
3.6 Generation of a stable cell line that expresses the coat protein of the *Pseudomonas aeruginosa* PP7 bacteriophage 109
3.7 Purification of influenza virus cRNP and vRNP complexes separately from infected cells 111
3.8 Discussion 117
3.9 Summary 121

Chapter 4: Characterisation of the complementary ribonucleoprotein of influenza virus
4.1 Introduction 122
4.2 Influenza virus cRNP exhibits a double-helical arrangement 125
4.3 Isolated vRNPs, but not cRNPs, can synthesise RNA *in vitro* 128

4.4 A *trans*-activating RdRP is required for vRNA synthesis 130

4.5 A *trans*-activating RdRP acts cooperatively with the resident RdRP, which carries out vRNA synthesis 132

4.6 Discussion 135

4.7 Summary 141

Chapter 5: Interactome of the influenza virus transcription/replication machinery

5.1 Introduction 142

5.2 Isolation of influenza A virus cRNP and vRNP complexes and the identification of co-purifying cellular factors 145

5.3 Isolation of influenza A virus RdRP complexes and the associated interactome from infected cells 158

5.4 Identification of the interactome of the influenza A virus replication machinery by mass spectrometry 160

5.5 Discussion 169

5.6 Summary 178

Chapter 6: Protein phosphatase 6 is required for efficient replication of influenza virus

6.1 Introduction 180

6.2 PP6 co-purifies with viral RdRP complexes from infected cells 184

6.3 PB1 and PB2 subunits of the viral RdRP interact directly with a regulatory subunit of PP6 184

6.4 Down regulation of PPP6C significantly attenuates influenza A virus replication 190

6.5 Down regulation of PPP6C reduces viral RNA accumulation in influenza A virus infected cells 193

6.6 Reduced nuclear export of vRNPs is observed in PPP6C knockdown cells infected with influenza A virus 200

6.7 Discussion 208

6.8 Summary 212

Chapter 7: Summary and Discussion

7.1 Introduction 214

7.2 Isolation of influenza virus RNP complexes by RNA-based affinity purification . 215

7.3 Molecular architecture of the influenza virus cRNP complex.....217
7.4 A *trans*-activation model of vRNA synthesis.....218
7.5 Identification of cellular factors that interact with the viral replication/transcription machinery.....223
7.6 Cellular PP6 interacts with the viral RdRP and acts a positive regulatory factor in influenza virus replication 224

Chapter 8: References.....228

Appendices 265

ABBREVIATIONS

UNITS

In addition to SI units and derived units, the following additional units are used:

a.u.	arbitrary units
bp	Base pair
Ci	Curie; 1 Ci = 3.7×10^{10}
Da	Dalton
g	Standard gravity: 9.80665 m/s^2
h	Hour(s)
kb	Kilobase
kDa	Kilodalton
min	Minute(s)
MOI	Multiplicity of infection (defined as virus sufficient to initiate detectable infection)
nt	nucleotide
PFU	Plaque-forming unit (not to be confused with Pfu DNA polymerase, an enzyme used in PCR)
pH	$-\log_{10} c$, where c is $[H^+]$ in mol/l
rpm	Revolutions per minute
s	Second(s)
U	Enzyme unit (the amount of enzyme to catalyse the transformation of 1 µmol of substrate per minute under defined conditions)

OTHER ABBREVIATIONS

A	Adenine / Alanine
AP	Affinity-purification
ATP	Adenosine-5′-triphoshate
Au	Gold
BCE	Before the common era
BSA	Bovine serum albumin
C	Cysteine / Cytidine
CBC	Cap binding complex
CCD	Charge-coupled device
cDNA	Complementary DNA
CHX	Cycloheximide

CIP	Calf intestinal alkaline phosphatase
CPFP	Central proteomics facilities pipeline
cRNA	Complementary RNA
cRNP	Complementary ribonucleoprotein
CTD	C-terminal domain
CTP	Cytidine-5′-triphoshate
D	Aspartic acid
DAPI	4',6-diamidino-2-phenylindole
ddH_2O	Double distilled water
dH_2O	Distilled water
DMEM	Dulbecco's modified Eagle's medium
DNA	Deoxyribonucleic acid
dNTP	Deoxynucleotide-5′-triphosphate
DTT	Dithiothreitol
E	Glutamic acid
ECL	Enhanced chemiluminescence
EDTA	Ethylenediaminetetraacetic acid
EMDB	Electron microscopy data bank
F	Phenylalanine
FCS	Foetal calf serum
FDR	False discovery rate
FISH	Fluorescence *in situ* hybridization
G	Glycine / Guanine
GFP	Green fluorescent protein
GO	Gene ontology
GST	Glutathione *S*-transferase
GTP	Guanosine-5′-triphoshate
H	Histidine / Hygrogen
HA	Haemagglutinin
HEPES	4-(2-hydroxyethyl)-1-piperazineethanesulfonic acid
HRP	Horseradish peroxidase
IFN	Interferon
IPTG	Isopropyl β-D-1-thiogalactopyranoside
K	Lysine
M1	Matrix protein 1
M2	Matrix protein 2
MEM	Minimal Essential Medium
mRNA	Messenger ribonucleic acid
MWCO	Molecular weight cut-off
N	Asparagine / Any nucleic acid base

NA	Neuraminidase
NEP	Nuclear export protein (formally known as NS2)
NES	Nuclear export protein
Ni	Nickel
NLS	Nuclear localisation signal
NP	Nucleoprotein
NS	Non-structural
NS1	Non-structural protein 1
NT60	Influenza A/NT/60/68 virus
NTA	Nitrilotriacetic acid
ORF	Open reading frame
p.i.	post-infection
p.t.	post-transfection
PA	Polymerase acidic protein
PAGE	Polyacrylamide gel electrophoresis
PB1	Polymerase basic protein 1
PB1-F2	PB1 reading frame 2
PB2	Polymerase basic protein 2
PBS	Phosphate buffered saline
PCR	Polymerase chain reaction
PDB	Protein data bank
PMSF	Phenylmethylsulfonyl fluoride
PNK	T4 polynucleotide kinase
poly(A)	Polyadenylic acid
poly(U)	Polyuridylic acid
PP6	Serine/threonine-protein phosphatase 6
PPM	Protein phosphatase metallo-dependent
PPP	Phosphoprotein phosphatase
PPP6C	Protein phosphatase 6 catalytic subunit
PPPR1	Protein phosphatase 6 regulatory subunit 1
PPPR2	Protein phosphatase 6 regulatory subunit 2
PPPR3	Protein phosphatase 6 regulatory subunit 3
RdRP	RNA-dependent RNA polymerase
RNA	Ribonucleic acid
RNP	Ribonucleoprotein
rRNA	Ribosomal ribonucleic acid
S	Serine
S.O.C.	Super Optimal broth with Catabolite repression
SAPS	Sit4-associated protein subunit
SD	Standard deviation

SDS	Sodium dodecyl sulfate
SINQ	Normalised spectral index quantitation
siRNA	Small interfering RNA
ss	Single-stranded
T	Threonine
TAP	Tandem affinity purification
TBE	Tris-borate-EDTA
TEMED	*N*,*N*,*N'*,*N'*-Tetramethylethylenediamine
TEV	Tobacco etch virus protease
TP	Transcription product
TRIM22	Tripartite motif containing 22 protein
Tris	Tris (hydroxymethyl) aminomethane
U	Uracil
UTP	Uridine-5'-triphosphate
UTR	Untranslated region
vRNA	Viral ribonucleic acid
vRNP	Viral ribonucleoprotein
WHO	World Health Organisation
WSN	Influenza A/WSN/33 (Wilson-Smith Neurotropic)
WT	Wild type
Y	Tyrosine

Chapter 1: Introduction

1.1 General introduction

Influenza viruses cause highly contagious respiratory disease that is characterised by the sudden onset of fever, cough, throat pain, headache, nasal congestion, sneezing, muscle aching and malaise (Eccles, 2005). Hippocrates of Cos, an ancient Greek physician, described an illness that resembled influenza in 412 BCE and thus, these viruses have been with us for millennia. Influenza virus derives its name from the Italian word for "influence", reflecting a fifteenth century belief that this illness was attributed to the influence of the stars (Potter, 2001). Influenza viruses are responsible for significant mortality and morbidity in the form of seasonal epidemics and worldwide pandemics. In the Northern and Southern Hemispheres, influenza epidemics occur every winter, leading to a significant rise in hospitalisations and deaths. The

World Health Organisation (WHO) has estimated that annual epidemics result in 3 to 5 million cases of severe illness and 250,000 to 500,000 deaths worldwide (WHO, 2014a). Occasionally, influenza virus is able to spread on a global scale and cause a pandemic which is the consequence of strains of influenza virus passing to humans from another animal species. This zoonotic virus then spreads worldwide and infects a large proportion of the human population. In the twentieth century the world experienced four pandemics. The 'Spanish influenza' pandemic of 1918 is the most severe that has been recorded in human history (Taubenberger & Morens, 2006). Caused by an H1N1 influenza A virus, it is estimated to have infected 500 million people across the globe, representing a third of the total world population at the time. It is estimated that 50–100 million people lost their lives as a consequence, making this pandemic one of the severest natural disasters in human history. The second and third pandemics of the twentieth century were the 1957 'Asian influenza', caused by a H2N2 subtype, and the 1969 'Hong Kong influenza', which was caused by a H3N2 subtype influenza A virus (Morens & Taubenberger, 2011). These pandemics were not as severe as the 1918 pandemic, but still resulted in an estimated 1–4 million deaths globally. In 1977 a fourth pandemic occurred due to the reappearance of an H1N1 virus. This virus first came to attention in the Union of Soviet Socialist Republics and was thus named the 'Russian influenza'. This virus was found to be virtually identical to an H1N1 virus that had circulated prior to 1950 and consequently this pandemic was mild due to pre-existing immunity, affecting mostly young adults and children. Since the twentieth century there has been one influenza virus pandemic. First described in April 2009, this pandemic H1N1 virus resulted when a triple reassortant of bird, swine and human influenza viruses combined with a Eurasian swine influenza virus, and was thus named

'swine flu' (Neumann *et al.*, 2009). It is estimated that up to 20–40% of the total population in some regions of the world, particularly in Africa and Southeast Asia, were infected by this virus and that 284,500 people died within the first twelve months of the pandemic (Dawood *et al.*, 2012).

Since 1997, a number of highly pathogenic avian influenza viruses have emerged that can directly infect humans (Claas *et al.*, 1998). Currently, three avian strains are considered to be a serious threat to human health, H5N1, H7N9 and H10N8, of which H5N1 has caused the greatest number of human infections. To date, 650 laboratory-confirmed cases of human infections by H5N1 virus in sixteen countries have been reported by the WHO with fatality in 60% of cases (WHO, 2014b). Although these viruses are able to cause severe disease in humans, transmission between humans has not been observed. A major concern is that these viruses will serve as a precursor for a pandemic virus as a number of transmission studies have shown that avian influenza viruses require relatively few mutations in order to become transmissible in ferret and guinea pig models (Herfst *et al.*, 2012; Imai *et al.*, 2012; Zhang *et al.*, 2013). Future influenza pandemics are inevitable and therefore gaining an in-depth understanding of the molecular biology of virus replication is vital to enable the design and development of novel antiviral strategies and for pandemic preparedness.

In this chapter a general overview of the current understanding of the influenza A virus life-cycle will be described. Description of RNA synthesis, viral ribonucleoprotein complexes and host-pathogen interactions will be given in more detail as these areas are particularly relevant to this thesis.

1.2 Influenza virus taxonomy and nomenclature

Influenzaviruses A, *B* and *C* represent three genera in the *Orthomyxoviridae*, a family of single-stranded, negative-sense RNA viruses with segmented genomes. Three further genera are present in this family, *Thogotovirus*, *Isavirus* and *Quaranfilvirus* (Palese & Shaw, 2013). Due to the segmented nature of these virus genomes they are able to undergo genetic reassortment and readily exchange genetic information. Reassortment between different genera, however, has not been reported. Influenza B viruses can infect humans, seals and ferrets, and influenza C viruses have been found to infect humans, dogs and swine. Influenza A virus has a broader host-range. Aquatic birds are the major reservoir, however, they can infect a range of species including swine, horses, bats, seals, whales, poultry and humans (Wright *et al.*, 2013). Influenza A viruses are further classified according to their serologic subtype, which are grouped according to their antigenic cross-reactivity against antisera directed against the viral haemagglutinin (HA) and neuraminidase (NA) glycoproteins. Currently there are 18 recognised HA subtypes (H1-H18) and 11 NA subtypes (N1-N11) (Palese & Shaw, 2013; Tong *et al.*, 2013). Conventionally, influenza A virus isolates are named according to their genera, host species, geographical location of isolation, strain identification number, year of isolation and the HA and NA subtype. Therefore, an influenza A virus isolated in 1956 from a horse in Prague with a strain number of E5203 and a subtype of H7N7 would be named A/equine/Prague/E5203/1956 (H7N7). If the influenza virus was isolated from a human then the species name is omitted (Wright *et al.*, 2013).

1.3 The influenza A virion

Influenza A virus particles are enveloped with a lipid bilayer and are pleomorphic, assuming spherical, filamentous or bacilliform morphologies. The morphology of the virion is dependent on the virus strain and the host cell from which it derives (Bourmakina & Garcia-Sastre, 2003; Mosley & Wyckoff, 1946; Roberts & Compans, 1998; Roberts *et al.*, 1998). The sizes of these different morphological forms of influenza A virus particles can vary substantially. Spherical particles are approximately 100 nm in diameter, whereas filamentous particles can be greater than 1 μm in length and can be visualised by light microscopy (Calder *et al.*, 2010; Harris *et al.*, 2006). A schematic diagram of the virus particle and electron micrographs of influenza virus particles are presented in Figure 1.1. The influenza A virion acquires a lipid envelope from the host cell during budding. During virus assembly the trimeric HA, tetrameric NA and tetrameric M2 membrane proteins are incorporated into the virion. It has been estimated that there are approximately four HA trimers for every NA tetramer, while numbers of the M2 tetramer are much lower (Harris *et al.*, 2006; Palese & Shaw, 2013). Underneath the lipid envelope is a network of the matrix protein (M1) and a core of eight individual viral ribonucleoprotein (vRNP) complexes which represent the influenza A virus genome. Each vRNP is composed of single-stranded viral RNA (vRNA) that is encapsidated by the viral nucleoprotein and bound at the 5′ and 3′ ends by the viral RNA-dependent RNA polymerase (RdRP) which is a heterotrimer made up of polymerase basic 1 (PB1), polymerase basic 2 (PB2) and polymerase acidic (PA) subunits (Arranz *et al.*, 2012; Moeller *et al.*, 2012). A summary of the segmented genome and the encoded proteins is presented in Table 1.1. A description of the

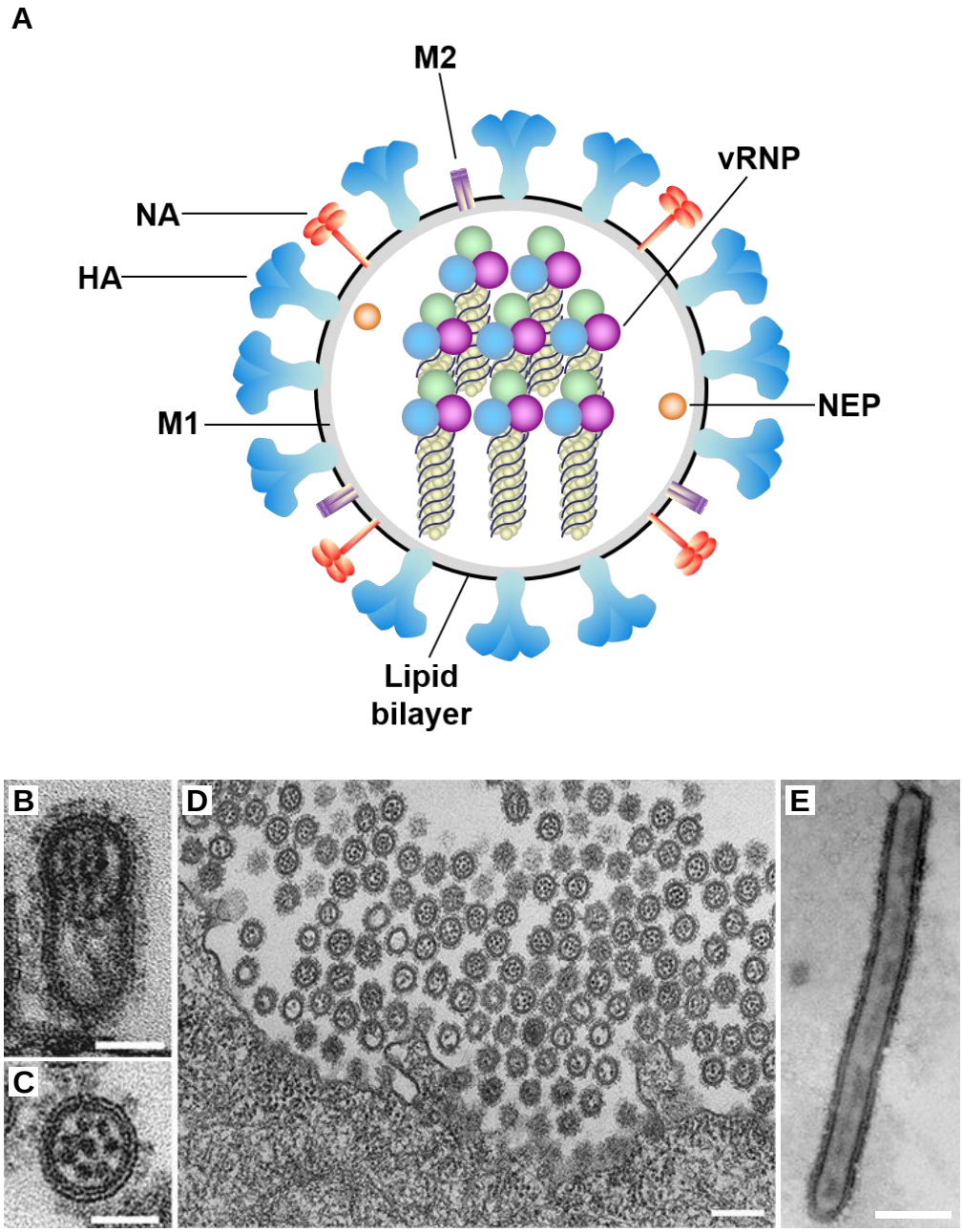


Figure 1.1 The influenza A virion. (A) Schematic of the influenza A virion showing structural proteins, including vRNP complexes. Negative stain electron microscopy of single influenza A/WSN/33 (H1N1) virions in the (B) vertical and (C) horizontal planes, and of (D) budding virions from Madin-Darby Canine (MDCK) cells. Adapted from Noda *et al*., 2006. (E) Negative stain electron microscopy of a single filamentous influenza A/Udorn/72 (H3N2) virion in the vertical plane. Adapted from Rossman *et al*., 2012. Scale bars, 50 nm (B and C), 200 nm (D) and 100 nm (E).

Table 1.1 A summary of the genome and encoded polypeptides of influenza A virus.

Segment	Length (nucleotides)	Encoded polypeptide(s)	Length (amino acids)	Reference
1	2341	PB2	759	Fields & Winter, 1982
2	2341	PB1	757	Winter & Fields,1982
		PB1-N40	718	Wise *et al.*, 2009
		PB1-F2	87	Chen *et al.*, 2001
3	2233	PA	716	Fields & Winter, 1982
		PA-X	252	Jagger *et al*., 2012
		PA-N155	562	Muramoto *et al*., 2013
		PA-N182	535	Muramoto *et al*., 2013
4	1778	HA	566	Winter *et al*., 1981a
5	1565	NP	498	Winter & Fields, 1981
6	1413	NA	454	Fields *et al*., 1981
7	1027	M1	252	Winter & Fields, 1980
		M2	97	Winter & Fields, 1980
		M42	99	Wise *et al*., 2012
8	890	NS1	230	Winter *et al*., 1981b
		NEP	121	Winter *et al*., 1981b
		NS3	188	Selman *et al*., 2012

Table 1.2 A summary of the influenza A virus encoded polypeptides and their function.

Encoded polypeptide	Function
PB2	RdRP subunit, cap binding. Innate immune antagonist.
PB1	RdRP subunit, promoter binding and harbours RNA polymerase catalytic domain.
PB1-N40	Unknown function.
PB1-F2	Apoptosis regulator and virulence factor.
PA	RdRP subunit, endonuclease activity.
PA-X	Modules host response. Contains endonuclease activity.
PA-N155	PA-related protein. Unknown function.
PA-N182	PA-related protein. Unknown function.
HA	Trimeric transmembrane surface glycoprotein. Binds to sialic acid on the surface of host cell surface glycoprotein receptors. Host range and cell tropism determinant. Virulence factor.
NP	Encapsidates vRNA and cRNA and the major constituent of viral ribonucleoprotein complexes. Necessary for transcription and replication.
NA	Tetrameric transmembrane surface glycoprotein. Cleaves sialic acid on the surface of host cells to facilitate virus release.
M1	Major structural protein of the virion. Essential for virus assembly and budding. Binds vRNP complexes and HA/NA.
M2	Tetrameric transmembrane protein. Acts as a proton ion channel that acidifies the virion and facilitates vRNP release. Important for viral morphogenesis, budding and membrane scission.
M42	M2-related protein with an antigentically distinct ectodomain. Largely retained in the Golgi compartment.
NS1	Interferon antagonist. Binds to dsRNA. Inhibits polyadenylation of pre-mRNAs. Binds to CPSF30 and PABPII.
NEP	Minor component of the virion. Binds M1 and Crm1 for nuclear-export of vRNPs. Regulates transcription and replication.
NS3	NS1-related protein. Potential role in host adaptation.

functions of each virally encoded protein is described in Table 1.2. The genome of influenza A viruses is relatively small, comprising a total of approximately 13.6 kilobases (kb). The size of the segments range from approximately 0.9 to 2.3 kb in length (Palese & Shaw, 2013). Electron microscopy of the influenza virion has shown that eight individual vRNPs are packaged in a 7+1 arrangement (Fournier *et al.*, 2012b; Noda *et al.*, 2006; Noda *et al.*, 2012). Within the virion a number of minor constituents are also present including the viral nuclear export protein (NEP) (Richardson & Akkina, 1991) and a number of host factors (Shaw *et al.*, 2008).

1.4 The influenza A virus life-cycle

Influenza A viruses primarily replicate in the cells of the respiratory and gastrointestinal tract epithelia (Wright *et al.*, 2013). Influenza A viruses can also replicate in alveolar macrophages and dendritic cells (Hofmann *et al.*, 1997; Seo *et al.*, 2004; Smed-Sorensen *et al.*, 2012). During the virus life-cycle many interactions occur between the virus and the host cell and these interactions are relevant to pathogenesis and restriction of host range (Cauldwell *et al.*, 2014; Matsuoka *et al.*, 2013). The life-cycle of influenza virus is, as one would expect of an acute infection, relatively short (8–10 hours in tissue culture) (Wright *et al.*, 2013). Nevertheless, infection of a cell results in the exponential growth of virus. A schematic diagram of the influenza A virus life-cycle is presented in Figure 1.2.

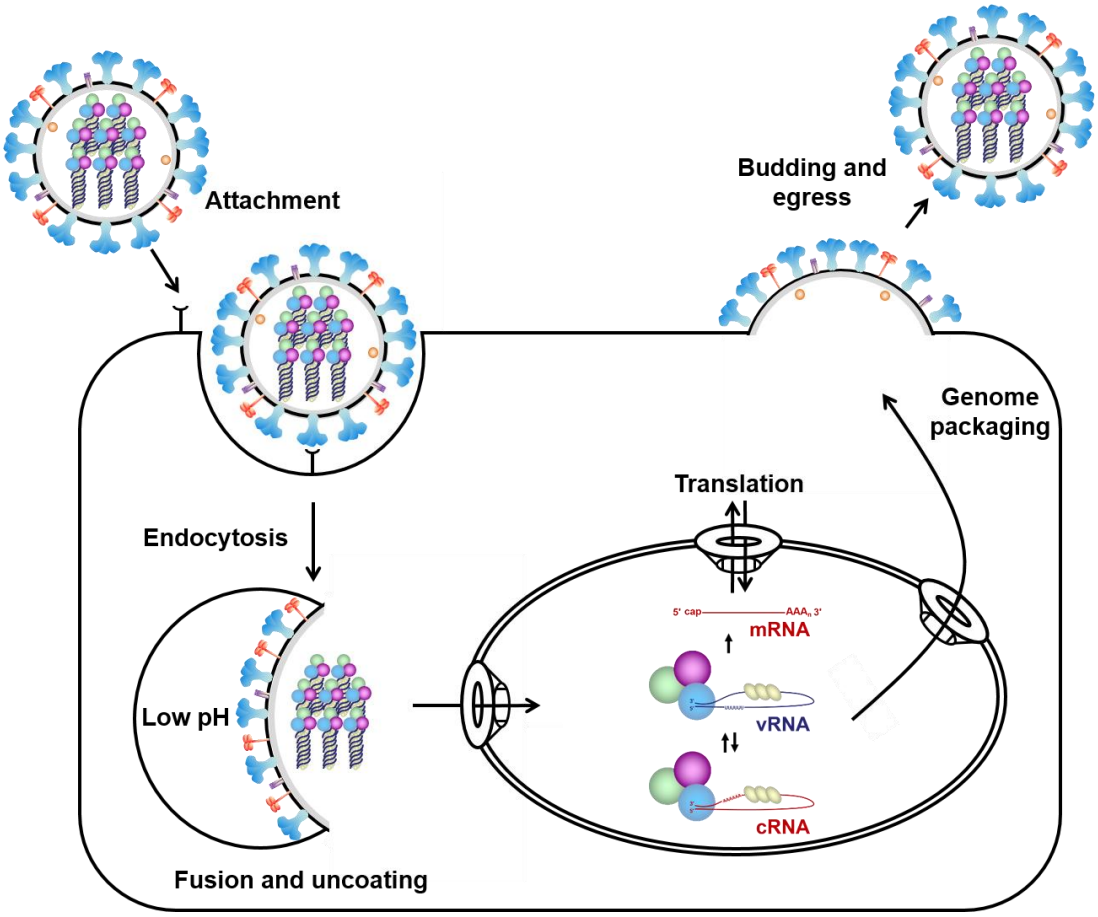


Figure 1.2 Schematic of the influenza A virus life-cycle. Influenza A virus infection begins with attachment via the viral HA glycoprotein to host cellular receptors that contain terminal α-2,3-linked or α-2,6-linked sialic acids. Viral entry occurs by receptor-mediated endocytosis. Acidification of the endosome results in a conformational change in the viral HA protein, exposing a fusion peptide that facilitates viral-endosome membrane fusion, releasing vRNP complexes into the cytoplasm. vRNP complexes are subsequently imported into the host cell nucleus, where the vRNA genome is transcribed and replicated by the viral RdRP. Genomic vRNA is replicated via a complementary positive-sense cRNA. Viral mRNAs are exported to the cytoplasm for translation of viral proteins. Progeny vRNP complexes are exported to the cytoplasm and are packaged into progeny virions at the plasma membrane along with M1, M2 and NEP. Progeny virions are released by budding.

1.4.1 Attachment and entry

Influenza A virus entry into a host cell initiates with the binding of the viral HA to sialic (*N*-acetylneuraminic) acid on cellular receptors that are present on the surface of the plasma membrane. The sialic acid linkage that is present on cell surface glycoproteins is an important determinant of host tropism. The different subtypes of viral HA that are encoded by influenza A viruses (HA1-HA18) preferentially bind to sialic acid depending on sialic acid linkage to a penultimate galactose in an N-linked glycan chain on the receptor (Connor *et al.*, 1994; Nelson *et al.*, 1993). Sialic acids that are linked from their C2 to C3 of galactose (α-2,3-linked sialic acid) are preferentially bound by avian influenza A viruses and are predominantly found in the gastrointestinal tract of birds and in the lower respiratory tract of mammals. Conversely, sialic acids that are linked from their C2 to C6 of galactose (α-2,6-linked sialic acid) are preferentially bound by mammalian influenza A viruses and are predominantly found in the upper respiratory tract of mammals. Epithelia can have a mixed population of α-2,3 and α-2,6-linked sialic acids, particularly in swine. Swine have been described as a 'mixing vessel' for genetic reassortment as their epithelia cells can be infected with avian and mammalian influenza viruses simultaneously (Ito *et al.*, 1998).

Once a virus particle has attached to a cell surface receptor, it is internalised into the host cell by receptor-mediated endocytosis. Although clathrin-mediated endocytosis has been the traditional model for influenza virus entry, caveolae-dependent, macropinocytosis-dependent, caveolae-independent and clathrin-independent pathways have been described (Edinger *et al.*, 2014; Mercer *et al.*, 2010). Whichever route is

taken for entry, likely to be dictated by the cell type and polarisation properties of the cell, the virion is enclosed in an early endosome from which the genome must escape to establish a productive infection.

1.4.2 Fusion, uncoating and nuclear import

Fusion of the virion and endosomal membranes for the release of vRNP complexes into the host cytoplasm is dependent on the viral HA glycoprotein and it is an event triggered by a decrease in pH in the acidifying endosome (Hamilton *et al.*, 2012). For fusion of virion and endosomal membranes to occur the viral HA must first be cleaved from the HA_0 precursor to HA_1 and HA_2 subunits by host-specific proteases (Boulay *et al.*, 1987; Chen *et al.*, 1998). Highly pathogenic avian influenza viruses possess multibasic cleavage sites which are cleaved by ubiquitously expressed subtilisin-like proteases, thought to enhance the virulence of these viruses (Stieneke-Grober *et al.*, 1992). During the acidification of the endosome the low pH environment triggers a conformational change in the HA protein, exposing a hydrophobic fusion peptide in HA_2 that is inserted into the endosomal membrane, bringing virion and endosomal membranes into juxtaposition for fusion (Bullough *et al.*, 1994). This fusion results in the formation of a pore that enables vRNP complexes to move from the virion interior into the cytoplasm. In addition to HA-mediated fusion, the viral M2 ion channel pumps H^+ ions from the endosome into the virion, thus decreasing the pH of the virion interior (Pinto *et al.*, 1992). This decrease in pH weakens interactions between M1 and vRNP

complexes, allowing the genomic material to transfer from the virion to the cytoplasm (Bui *et al.*, 1996).

Once vRNP complexes have been released into the cytoplasm they are actively transported into the cell nucleus by components of the α/β-importin pathway (Hutchinson & Fodor, 2012). All protein constituents of vRNP complexes contain at least one nuclear localisation signal (NLS), however, import is achieved by the presence of NLSs present on the NP protein (Cros *et al.*, 2005; Martin & Helenius, 1991b; Oneill *et al.*, 1995). Nuclear import of vRNP complexes is achieved through the binding of importin-α to NP, which in turn is bound by importin-β, allowing these complexes to dock at the nuclear pore complex (NPC) and translocate into the nucleus.

1.4.3 Viral gene expression

Once vRNP complexes have been transported into the nucleus, the viral RdRP is responsible for transcribing viral messenger RNA (mRNA) and for replicating vRNA via a complementary RNA (cRNA) intermediate (Fodor, 2013; Resa-Infante *et al.*, 2011). An in-depth introduction to viral transcription and replication will be given in section 1.5. Viral mRNAs are exported to the cytoplasm from the nucleus where viral proteins are synthesised by the host translational machinery. Viral proteins are not expressed to equivalent levels at the same time during the virus life-cycle, indicating that gene expression is regulated (Enami *et al.*, 1985; Hatada *et al.*, 1989; Shapiro *et al.*, 1987). Viral NS1 and NP mRNAs and proteins are synthesised at high levels early in

the life-cycle, whereas the bulk of HA, NA and M1 synthesis occurs at later time points post-infection (Hatada *et al.*, 1989; Hay *et al.*, 1977; Shapiro *et al.*, 1987; Smith & Hay, 1982). The mechanisms of temporal regulation of viral gene expression in infected cells are not completely understood, however, differential RNA synthesis, RNA stability and regulation of translation have been proposed (Shapiro *et al.*, 1987; Smith & Hay, 1982; Yanguez & Nieto, 2011). One control mechanism, specific to the expression of viral RdRP subunits, is a difference in the vRNA promoter sequence (Lee & Seong, 1998). The RdRP subunit genes contain a "C" at position 4 from the 3′ end of the vRNA, whereas all other segments ordinarily have a "U" residue. The promoter that contains a C4 is associated with down-regulation of viral mRNA synthesis and an up-regulation of replication products. Structural analyses of these different promoters has led to the proposal that the viral RdRP interacts differentially with C4 and U4-containing promoters (Lee *et al.*, 2003). The temporal expression of viral genes reflects the diverse roles viral proteins have during infection (Palese & Shaw, 2013). For example, high levels of NP are required for genome replication (Turrell *et al.*, 2013) and NS1 is essential for antagonism of the cellular innate immune response (Hale *et al.*, 2008), so the early expression of these viral proteins would be beneficial for virus replication. Conversely, M1 has been shown to be inhibitory to viral RNA synthesis (Perez & Donis, 1998; Watanabe *et al.*, 1996) and it is required for nuclear export of vRNP complexes (Baudin *et al.*, 2001; Bui *et al.*, 2000; Martin & Helenius, 1991a), so expression at a later time point would be favourable for virus replication. Similarly, viral HA and NA glycoproteins are required for virus assembly which takes place at the final stage of the virus life-cycle. A recent study proposed that influenza A virus can use suboptimal splicing to coordinate timing during infection (Chua *et al.*, 2013). It was

found that the use of a suboptimal splice site in NS1 mRNA leads to the gradual accumulation of NEP over time. Modulation of this transcriptional event led to improperly timed nuclear export of vRNP complexes in infected cells, indicating that the coordination of the virus life-cycle is controlled by a "molecular timer" that is set by inefficient splicing of NS1 mRNA.

1.4.4 Nuclear export and traffic of vRNP complexes

After vRNA synthesis and the assembly of progeny vRNP complexes in the nucleus they are exported to the cytoplasm for their journey to the apical plasma membrane for packaging into nascent virions. Two viral proteins, M1 and NEP have been shown to be essential for this process (Paterson & Fodor, 2012). M1 protein associates with vRNP complexes and it has been proposed that this interaction is functional and assists in their assembly (Huang *et al.*, 2001). Preventing nuclear import of M1 has been shown to block export of vRNPs, strongly indicating that M1 is necessary for this process (Bui *et al.*, 2000; Martin & Helenius, 1991a). Although M1 was shown to be necessary for vRNP export, it is not sufficient. NEP has been proposed to act as an adaptor between the vRNP-M1 complex and the importin-β protein Crm1 in a daisy chain model of nuclear vRNP export (Neumann *et al.*, 2000; O'Neill *et al.*, 1998). In this model M1 binds to the vRNP via an interaction with NP, which in turn is bound by NEP, masking an NLS which is thought to prevent re-import after nuclear export. Crm1 then recognises an N-terminal nuclear export signal (NES) in NEP which directs the export of the complex via the NPC to the cytoplasm. After nuclear export of vRNPs they

accumulate at the perinuclear microtubule organising centre (MTOC) and form an interaction with Rab11, possibly mediated by PB2. They then traffic to the plasma membrane via vesicular anterograde microtubule transport in association with Rab11 (Amorim *et al.*, 2011; Bruce *et al.*, 2010; Momose *et al.*, 2011). A recent study that employed four-colour fluorescence *in situ* hybridization (FISH) to visualise individual vRNAs in cells infected with a virus that encodes a PA-GFP RdRP subunit concluded that vRNP segments form subcomplexes in the cytoplasm and that these subcomplexes further assemble into the larger vRNP complex that is observed within virions en route to the plasma membrane (Lakdawala *et al.*, 2014).

1.4.5 Genome packaging

Packaging at least one copy of each gene segment of influenza virus is essential for replication competency and productive infectivity. This outcome is most likely to be achieved if a selective model of genome packaging has been adopted, as opposed to random incorporation of gene segments by chance. Historically, two independent models have existed for the packaging of eight vRNA molecules into a single virion; one that relies on selection of vRNA over cellular RNA, but does not discriminate between different gene segments, and a selective model that relies on the formation of an intermolecular network of RNA-RNA interactions between all genomic vRNAs (Gerber *et al.*, 2014; Hutchinson *et al.*, 2010). There is increasing experimental evidence that influenza A virus specifically packages a single copy of each vRNA during assembly. A number of observations have led to the conclusion that packaging is

mediated by specific RNA-RNA interactions. Electron microscopy and tomography revealed that the relative positions of each of the eight vRNPs within virions is not random and that a typical arrangement of vRNPs is observed with a central vRNP surrounded by seven additional vRNPs (Fournier *et al.*, 2012b; Noda *et al.*, 2006; Noda *et al.*, 2012). In these tomograms, electron densities were observed between each of the vRNPs, which were hypothesised to correspond to RNA-RNA interactions. Biochemical and FISH analyses revealed that the majority of influenza virions package one copy of each gene (Bergmann & Muster, 1995; Chou *et al.*, 2012; Smith & Hay, 1982). Deletion mutagenesis and reverse genetics in combination with sequencing defecting interfering vRNAs led to the identification of specific bipartite packaging signals, mostly located in the 5′ and 3′ untranslated regions (UTRs) of vRNAs (Hutchinson *et al.*, 2010). Strong evidence for a specific packaging mechanism that relies on intermolecular RNA-RNA interactions came from the identification of regions of RNA that interacted *in vitro* between all vRNAs of influenza A/Moscow/10/99 (H3N2) virus (Fournier *et al.*, 2012a; Fournier *et al.*, 2012b). This enabled the construction of an interaction network of vRNAs in the virus genome. Identification of RNA sequences that interact between a pair of vRNAs was later reported by the same group using a *trans*-complementary approach (Gavazzi *et al.*, 2013). In this method silent mutations were introduced into regions that were hypothesised to interact, resulting in packaging defects and failure to generate virus by reverse genetics. Insertion of compensatory mutations into the interacting vRNA restored the observed packaging defects and resulted in the generation of infectious virus. This study therefore demonstrated for the first time that a functional direct interaction existed between two vRNA molecules.

1.4.6 Virion assembly and egress

Influenza A viruses assemble and bud from the apical surface of the plasma membrane of polarised cells (Rodriguez Boulan & Sabatini, 1978), preferentially from lipid raft domains which are regions of membrane that contain sphingolipids and cholesterol into which membrane proteins become incorporated (Brown & Rose, 1992; Scheiffele *et al.*, 1999; Simons & Ikonen, 1997). The viral transmembrane proteins HA, NA and M2 traffic from sites of protein synthesis at the endoplasmic reticulum via the Golgi apparatus to the apical membrane. The targeting of HA and NA glycoproteins to lipid raft domains cause coalescence and broadening of these domains (Chen *et al.*, 2007; Leser & Lamb, 2005; Takeda *et al.*, 2003). Clustering of HA and NA is thought to cause membrane deformation and the initiation of budding (Chen *et al.*, 2007), however, the precise details of budding initiation remain unclear. M1 is recruited to sites of virion assembly through the binding to cytoplasmic tails of HA and NA where it can then polymerise and form a network on the interior leaflet of the budding virion (Ali *et al.*, 2000; Noton *et al.*, 2007; Zhang *et al.*, 2000). M1 acts as a platform for the incorporation of vRNP complexes through protein-protein interactions (Noton *et al.*, 2007). M2 recruitment to sites of virion budding is also thought to be mediated by M1 (Chen *et al.*, 2008; McCown & Pekosz, 2006), at which point M2 can alter the membrane curvature at the neck of the budding virus, resulting in scission of the membrane and release of the nascent virion into the extracellular environment (Rossman *et al.*, 2010; Rossman & Lamb, 2011). The extent to which cellular factors mediate budding is unknown, however, Rab11 has been shown to support the budding of spherical and filamentous virions (Bruce *et al.*, 2010). Once membrane scission has

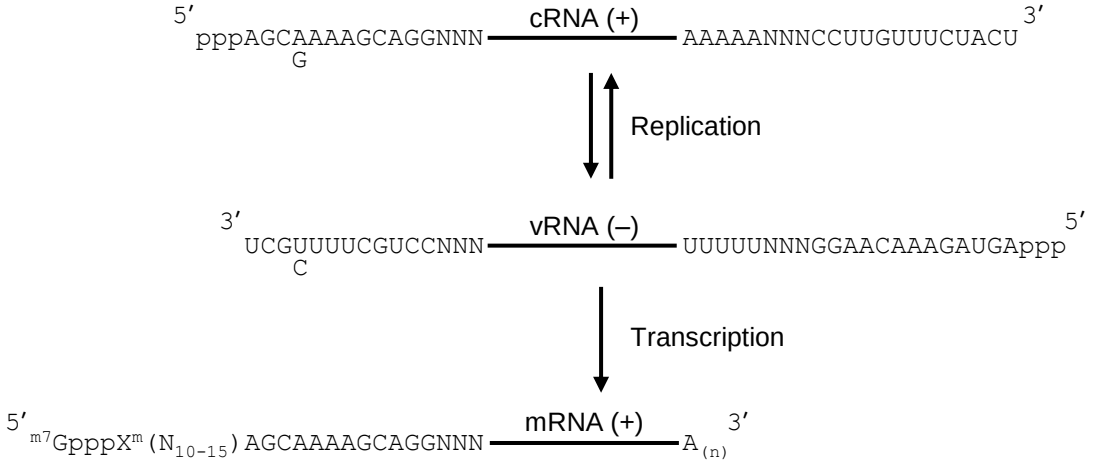
occurred, the sialidase activity of the viral NA is required to hydrolyse sialic acid from the cell surface, so as to prevent re-attachment of the virion and super-infection (Air & Laver, 1989; Huang *et al.*, 2008).

1.5 Influenza virus RNA synthesis

1.5.1 Overview

During the virus life-cycle vRNP complexes enter the host cell nucleus where the vRNA genome is transcribed and replicated by the viral RNA-dependent RNA polymerase (RdRP) (Herz *et al.*, 1981; Jackson *et al.*, 1982). A schematic of influenza A virus RNA synthesis is presented in Figure 1.3A. Transcription is performed using a primer-dependent mechanism where short 10–15 nt long RNA molecules with a 5′ 7-methylguanosine cap are cleaved from cellular pre-mRNAs and are used for primer-dependent transcription (Bouloy *et al.*, 1978; Plotch *et al.*, 1981). Polyadenylation of viral mRNAs is also performed by the viral RdRP, which results in an mRNA that contains a 5′ cap structure and a 3′ poly(A) tail. Replication of the vRNA genome is primer-independent and occurs in two stages. First, a full-length positive-sense copy of the vRNA genome is synthesised *de novo*, known as complementary RNA (cRNA). The cRNA does not possess a 5′ cap or a 3′ poly(A) tail. Second, the cRNA is used as a template to synthesise multiple copies of vRNA. Although transcription and replication are both performed by the viral RdRP using vRNA as a template, disparate mechanisms of RNA synthesis during transcription and replication have evolved. A graph showing

A



B

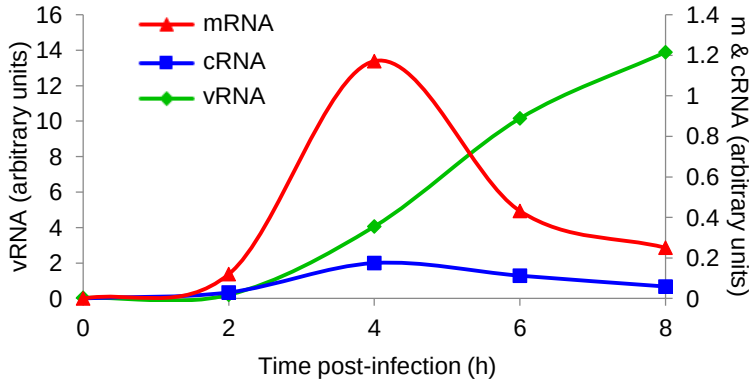


Figure 1.3 Influenza A virus RNA synthesis. (A) Schematic of the influenza virus RNA species synthesized by the viral RdRP. The parental negative-sense vRNA is shown in the center with the conserved non-coding sequences at each terminus, adjacent to segment-specific nucleotides (NNN). The polyadenylation signal consists of a poly(U) stretch at the 5′ end of the vRNA. Viral mRNA derives its cap and 10–15 5′ nucleotides from host pre-mRNAs and has a 3′ poly(A) tail. The vRNA genome is replicated via cRNA which is an exact copy of the parental vRNA. The variation at position 4 in the 3′ vRNA non-coding region is shown. Adapted from Palese & Shaw, 2013. (B) Kinetics of viral RNA species accumulation. Comparison of viral RNA species accumulation in a single replication cycle. Viral mRNA accumulation predominates early in the life-cycle, while vRNA steadily accumulates throughout the life-cycle. cRNA levels accumulate to lower levels than mRNA and vRNA and remain at a constant level throughout infection. Adapted from Vreede *et al.*, 2011.

the temporal accumulation of viral RNA species is presented in Figure 1.3B. Viral mRNA accumulation predominates early in the life-cycle, peaking at approximately 4–6 hours post-infection, while vRNA steadily accumulates throughout the life-cycle. cRNA levels accumulate to lower levels than mRNA and vRNA, peaking at approximately 4–6 hours and then remain at a constant level throughout infection (Hay *et al.*, 1977; Smith & Hay, 1982).

1.5.2 Viral ribonucleoprotein (RNP) complexes

Each influenza virus vRNA segment exists as an individual vRNP complex in which vRNA is encapsidated by multiple copies of the viral nucleoprotein (NP), assembling into a long double helical filament in which vRNA forms a hairpin with a closing loop at one terminus and the opposite terminus is bound by a single copy of the viral RdRP (PB1, PB2 and PA subunits). When vRNP complexes have been isolated from virions and studied by negative-stain electron microscopy, they appear as closed superhelical structures with a ribbon-like appearance (Figure 1.4) (Compans *et al.*, 1972; Heggeness *et al.*, 1982; Pons *et al.*, 1969). The overall structural features of the RNP are inherent in the oligomerisation properties of NP, as NP-RNA and NP in the absence of RNA can form helical structures resembling RNPs *in vitro* (Ruigrok & Baudin, 1995; Yamanaka *et al.*, 1990). The viral NP is a positively charged protein that contains multiple basic residues, reflecting its role in the encapsidation of vRNA. The interaction between vRNA and NP is sequence-independent and mediated by the negatively charged phosphate backbone of vRNA and positively charged patches on NP (Baudin *et al.*,

1994; Elton *et al.*, 1999; Ng *et al.*, 2008; Ye *et al.*, 2006). Each NP monomer within the vRNP complex binds to approximately 24 nt of RNA (Ortega *et al.*, 2000). High resolution cryogenic electron microscopy (cryo-EM) of vRNP complexes has shown that vRNP complexes have three major regions; a central filament and two termini, one containing the viral RdRP and the other a loop structure (Figure 1.4) (Arranz *et al.*, 2012; Moeller *et al.*, 2012). Reconstruction of the central filament revealed a dihedral helix with two opposite-polarity NP strands. The double helix contains both a minor groove and a major groove. The helical parameters in two independently reported vRNP structures were similar, with a rise of approximately 30 Å per monomer with a twist of approximately 60–70° per turn of the helix, corresponding to five or six NP monomers. NP in the helix interacts with neighbouring NP monomers in the same strand (intra-strand interactions) and also interacts with NP monomers in the opposing strand (inter-strand interactions). The vRNA within the vRNP complex has been modelled to follow a positively charged pathway on the surface on the NP oligomer with bases exposed. This model of RNA binding by NP is consistent with the observation that vRNA within influenza virus RNPs is particularly sensitive to ribonuclease treatment compared to vRNA of other negative-strand RNA viruses (Duesberg, 1969; Ruigrok *et al.*, 2010). The structure of the loop end of the filament revealed the presence of three NP monomers in one study (Arranz *et al.*, 2012) and five to seven monomers in a different study (Moeller *et al.*, 2012). The RdRP-containing terminus in one reported structure adopted two different conformations (Arranz *et al.*, 2012). In particular it was found that a large domain within the RdRP shifted in one conformation relative to the other conformation (Figure 1.5A). In another reported vRNP structure the RdRP-end contained two domains, a large domain and a smaller

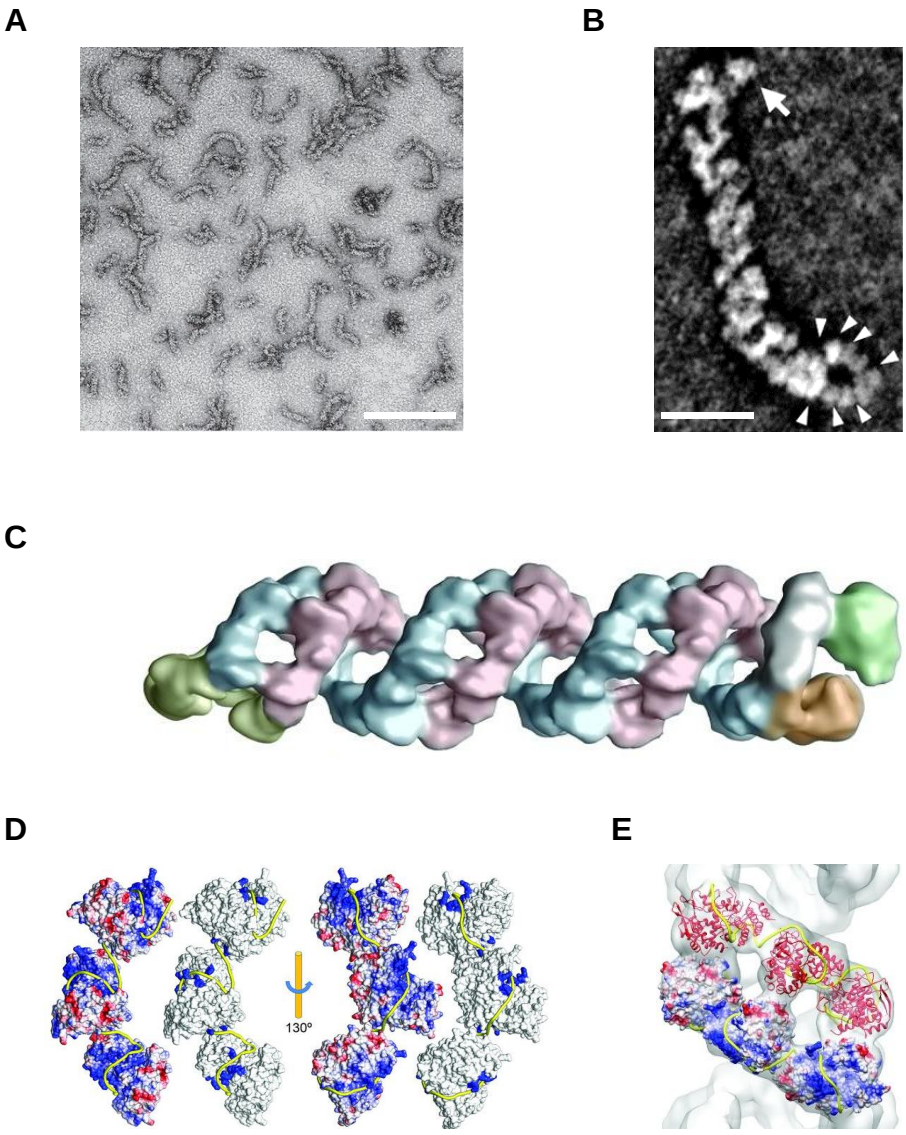


Figure 1.4 Structure of the influenza virus vRNP complex. (A) Negative stain electron microscopy of vRNP complexes isolated from influenza A/PR/8/34 (H1N1) virions. (B) Reconstruction of a view of a single vRNP by scanning transmission electron microscopy. NP molecules form a loop structure (small arrowheads) at one end, while the opposite terminus forms a morphologically distinct structure that corresponds to the viral RdRP (large arrowhead). Scale bars, 200 nm (A), 25 nm (B). Adapted from Sugita *et al*., 2013. (C) Cryo-electron microscopy model for the structure of the influenza A/WSN/33 virus vRNP. Double-helical central filament (blue and pink), terminal NP loop (yellow) and the viral RdRP (green, grey and brown) are shown. (D) Model for the localisation of vRNA (yellow thread) in the helical vRNP structure. Residues that when mutated reduce NP-RNA interactions are highlighted in blue. (E) Model for vRNA localisation (yellow thread) in the vRNP structure showing one NP strand with surface potential and the opposite strand as a ribbon representation. Adapted from Arranz *et al*., 2012.

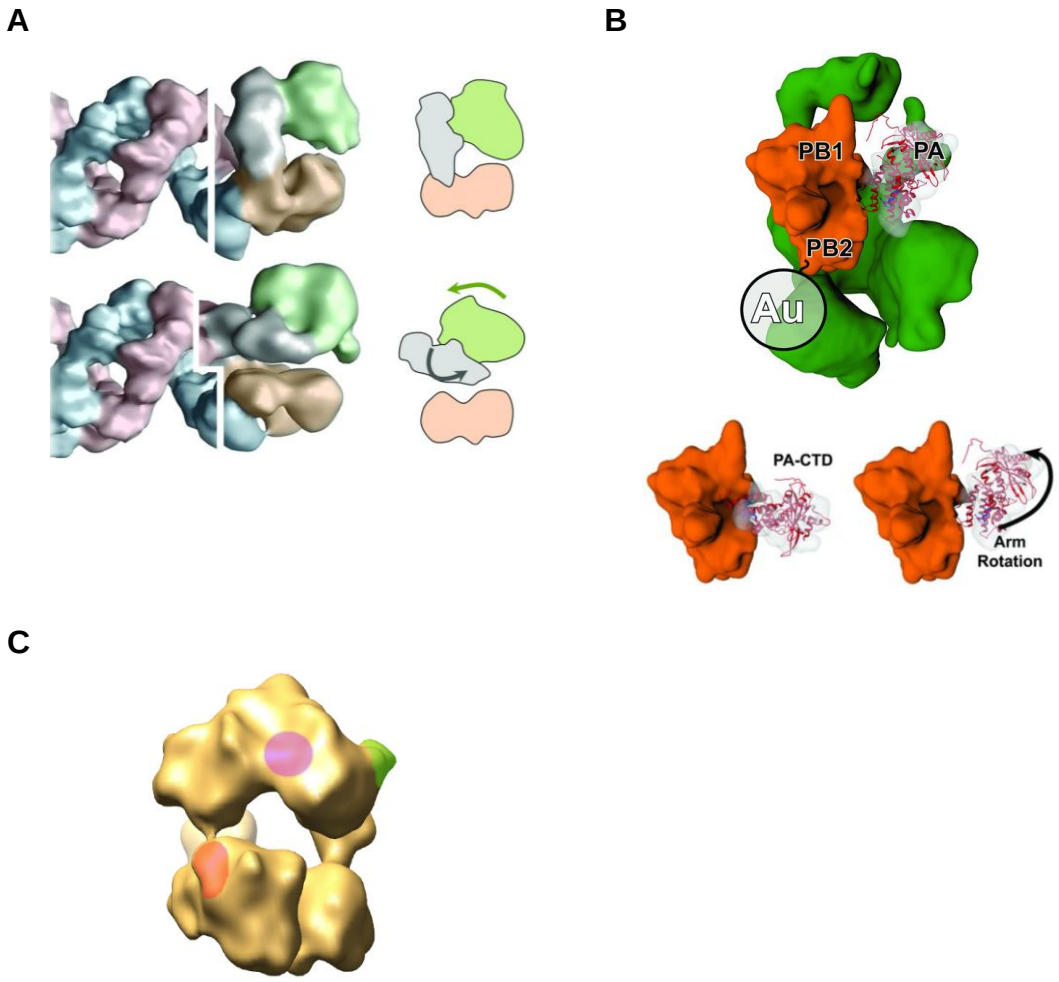


Figure 1.5 Structural models of the influenza A virus RdRP within vRNP complexes. Three-dimensional models for the influenza A virus RdRP present in vRNP complexes as reported by different studies. (A) Two different conformations of the viral RdRP were observed in vRNP complexes derived from virions. Structural changes are indicated on the right. Adapted from Arranz *et al*., 2012. (B) Cryo-electron microscopy structure of viral RdRP within recombinant vRNP complexes (left) indicating a putative PA-CTD location based on PA-CTD docking into the electron density map. Location of the PB2 C-terminus was determined by immunogold labeling, as indicated by the circle labeled Au. Cryo-electron microscopy structure of free viral RdRP (right) revealing that it contains a large domain (orange) and an arm domain putatively containing PA-CTD (red). The arm domain has been proposed to rotate when incorporated in vRNP complexes. Adapted from Moeller *et al*., 2012. (C) Structure of RdRP within a recombinant mini-vRNP containing a nonameric NP ring. The location of specific domains in the PB1 (green), PB2 (red) and PA (purple) subunits are shown. From Coloma *et al*., 2009.

flexible arm domain (Moeller *et al.*, 2012). In this structure the flexible arm domain was proposed to correspond to the C-terminal domain (CTD) of the PA protein (Figure 1.5B). This region of PA has been crystallised and the structure of the PA-CTD was docked into the flexible arm domain (He *et al.*, 2008). It was hypothesised that the PA-CTD plays a role in feeding the RNA template into the RdRP active site. The structure of the RdRP within a biologically active recombinant RNP containing nine monomers of NP arranged in a nonameric ring does not corroborate the finding of a flexible arm within the RdRP. On the contrary, in this structure the RdRP was reported to form a more compact structure (Figure 1.5C) and the mapping of specific RdRP subunits within this structure using monoclonal antibodies allowed the docking of the PA-CTD (Area *et al.*, 2004; Coloma *et al.*, 2009).

A complementary RNP (cRNP) complex containing cRNA, NP and the viral RdRP has been assumed to form an analogous structure to the vRNP complex, however, these complexes have not been isolated and therefore their structure remains uncharacterised.

1.5.3 The viral RNA-dependent RNA polymerase and nucleoprotein

1.5.3.1 The heterotrimeric RNA polymerase complex

The RdRP of influenza A virus is a 250 kDa complex consisting of three proteins: PB1, PB2 and PA (Braam *et al.*, 1983). The interaction between the three subunits has been studied using a combination of biochemistry and genetics. These approaches indicate

that the PB1 subunit is at the core of the complex (Digard *et al.*, 1989) and interacts with the C-terminus of PA via its N-terminus and with the N-terminus of PB2 via its C-terminus for a linear arrangement of PA-PB1-PB2 of the subunits (Figure 1.6) (Gonzalez *et al.*, 1996; Perez & Donis, 1995; Toyoda *et al.*, 1996; Zurcher *et al.*, 1996). Additionally an interaction between the N-terminus of PA and PB2 has been described (Hemerka *et al.*, 2009). Some of these interactions have also been confirmed using X-ray crystallography (He *et al.*, 2008; Obayashi *et al.*, 2008; Sugiyama *et al.*, 2009). A three-dimensional atomic structure for the heterotrimer is not available, however, studies of the RdRP by electron microscopy using RNPs (Area *et al.*, 2004; Arranz *et al.*, 2012; Coloma *et al.*, 2009; Moeller *et al.*, 2012), RNA-devoid RdRP (Moeller *et al.*, 2012; Torreira *et al.*, 2007) and RdRP in association with vRNA (Resa-Infante *et al.*, 2010) have been performed to give insight into the overall molecular architecture of this RNA synthesis machine (Figure 1.7). Three of these studies indicate that the RdRP has a compact structure but that it exhibits a degree of flexibility and can undergo conformational changes depending on whether template is associated (Figure 1.7A) (Coloma *et al.*, 2009; Resa-Infante *et al.*, 2010; Torreira *et al.*, 2007). The highest resolution structure available was obtained by cryo-EM of an RdRP within a recombinant RNP (Coloma *et al.*, 2009). This structure has a resolution of 18 Å with defined domains. The latest electron microscopy structure of the RdRP to be reported is a 20 Å structure of a template-devoid RdRP (Moeller *et al.*, 2012). This structure does not corroborate previous structural observations of the RdRP (Figure 1.7B). Specifically, a large flexible arm was observed in the structure which was hypothesised to correspond to the PA-CTD due to its overall shape and size. Detailed understanding

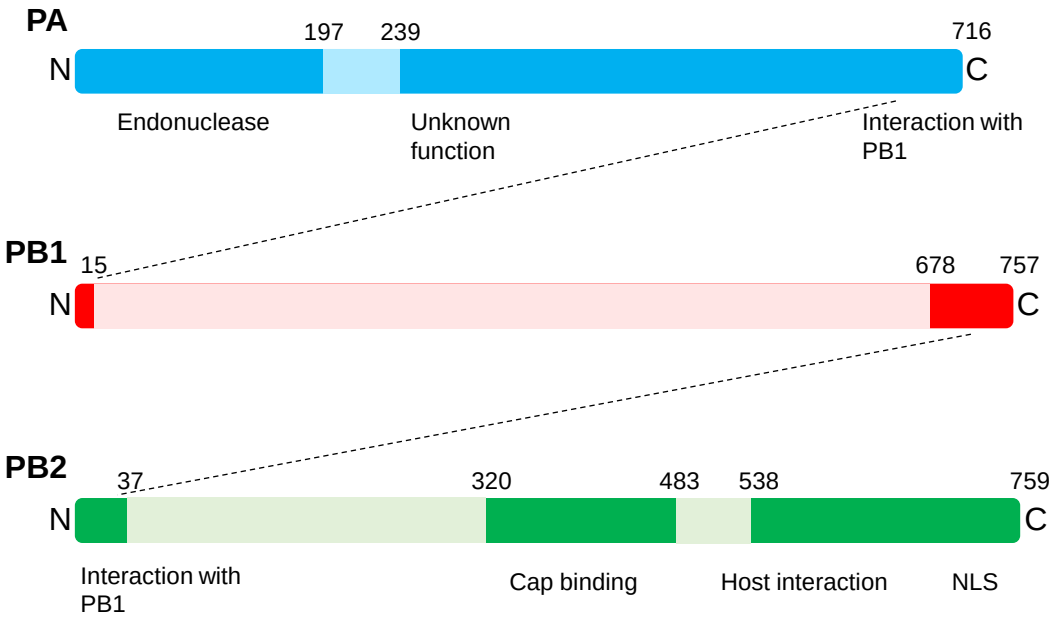


Figure 1.6 Diagram of the intersubunit interactions in the influenza A virus RdRP. Viral RdRP subunits are represented as bars with the N- and C-terminal regions that interact indicated by dashed lines. The regions of each of the viral RdRP subunits for which there is atomic structural information available are indicated by dark colours. Relevant functional domains are also indicated.

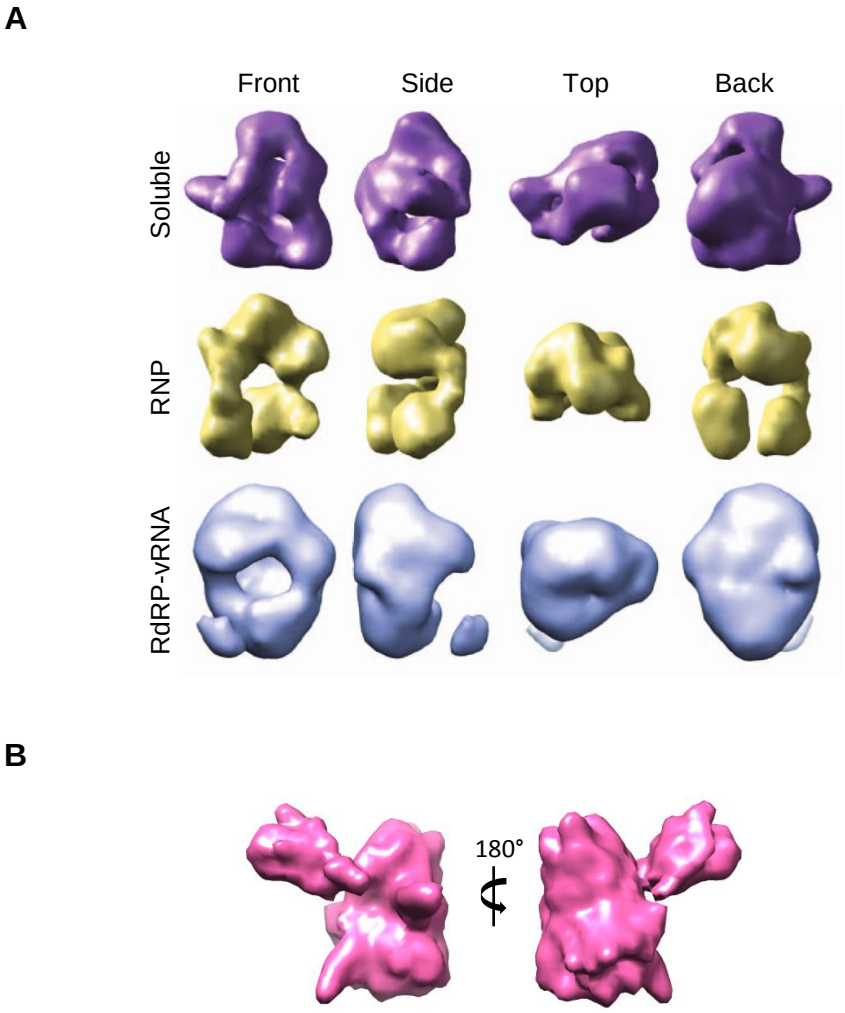


Figure 1.7 Comparison of influenza A virus RdRP cryo-electron microscopy structures. (A) Different views are shown to compare viral RdRP cryo-electron microscopy structures with a similar overall architecture, including soluble trimer that is template-free (top) (From Torreira, *et al*., 2007), trimer within a recombinant mini-vRNP (middle) (From Coloma *et al*., 2009), and RdRP in association with template vRNA (bottom) (Resa-infante, *et al*. 2010). Adapted from (Resa-infante *et al*., 2011). (B) Two different views of a cryo-electron microscopy structure of the viral RdRP with a side arm that has been proposed to correspond to PA-CTD. From Moeller *et al*., 2012. EMDB code: 2213.

of the architecture of the trimeric RdRP and how the individual subunits are arranged will come from determination of the atomic structure by X-ray crystallography.

1.5.3.2 Polymerase basic 1 protein

The PB1 protein catalyses the condensation of nucleotides during RNA synthesis (Braam *et al.*, 1983). Within the amino acid sequence are consensus motifs that are conserved between nucleic acid polymerases including the active site for polymerisation of nucleotides, the S-D-D motif at positions 444–446 (Biswas & Nayak, 1994). Mutation of the aspartic acid residues in this motif to alanine abolishes RNA synthesis by the RdRP (Biswas & Nayak, 1994; Vreede *et al.*, 2004). PB1 binds to the promoters of both vRNA and cRNA for the initiation of both transcription and replication (Gonzalez & Ortin, 1999a; b; Li *et al.*, 1998).

PB1 is believed to be the central scaffold within the trimeric RdRP, interacting with both PA and PB2 (Digard *et al.*, 1989). The majority of the atomic structure of PB1 is unknown, however, the extreme N- and C-terminal domains that interact with PA and PB2 respectively have been crystallised. Crystal structures of residues 1–15 have been reported in complex with the PA-CTD (He *et al.*, 2008; Obayashi *et al.*, 2008). The PB1 C-terminus (residues 678–757) has been crystallised in complex with residues 1–37 of PB2, revealing the presence of three helices (Sugiyama *et al.*, 2009).

1.5.3.3 Polymerase basic 2 protein

PB2 plays a major role in the initiation of transcription by binding 5′ 7-methylguanosine cap structures of cellular pre-mRNAs for subsequent cap-snatching (Blaas *et al.*, 1982; Guilligay *et al.*, 2008). Additionally, the PB2 subunit of the viral RdRP has been shown to be critical for replication of the vRNA genome with residues in the N-terminus critical for this activity (Perales & Ortin, 1997), however, mutations in this region do not affect transcription (Gastaminza *et al.*, 2003).

Crystal structures of three regions of the PB2 protein have been reported. The N-terminal 1–37 residues of PB2 adopt a three helical structure that interacts with three helices at the C-terminus of PB1 (Sugiyama *et al.*, 2009). The next region of PB2 that has been crystallised is the cap binding domain (residues 320–483) in which four residues H357, E361, K376 and F404 were shown to be essential for cap binding (Guilligay *et al.*, 2008). The third region of PB2 that is crystallised is a region that contains the so called 627 domain, named after amino acid residue 627 which is predominantly a lysine in mammalian influenza viruses and a glutamic acid in avian influenza viruses (Tarendeau *et al.*, 2008). The difference in amino acid at this position has been hypothesised to play an important role in host adaptation and pathogenesis (Subbarao *et al.*, 1993). The structure of this domain (residues 538–759) revealed that the 627 residue falls within a mostly positively charged region of PB2 and therefore the presence of either a lysine or a glutamic acid at this position can alter the overall electrostatic potential of this region of PB2. The differences in electrostatic potential depending on the presence of a lysine or a glutamic acid has been hypothesised to

influence the interaction with a host-specific cellular factor (Tarendeau *et al.*, 2008). The C-terminus of PB2 (678–759) has been crystallised in complex with importin-α5 (Tarendeau *et al.*, 2007). This region contains a classical bipartite NLS which makes extensive interactions with importin-α.

1.5.3.4 Polymerase acid protein

The PA subunit of the RdRP is essential for generating 5′ capped RNA primers for transcription initiation by cleaving cellular pre-mRNAs 10–15 nt downstream of the 7-methylguanosine cap structure. Crystallisation of the N-terminal domain (residues 1–197) of PA yielded important mechanistic insight into the workings of this subunit (Dias *et al.*, 2009; Yuan *et al.*, 2009). Previously it was thought that the endonuclease activity that is required for the generation of 5′ capped RNA primers resided in the PB1 subunit (Li *et al.*, 2001). Two independent crystal structures revealed the presence of a domain that had a fold similar to that of type II restriction endonucleases and importantly, the N-terminal domain had bivalent cation-dependent endonuclease activity against both RNA and DNA. The C-terminal domain of PA interacts with the N-terminal domain of PB1 and crystal structures of this region (residues 239–716) of PA have been reported (He *et al.*, 2008; Obayashi *et al.*, 2008), however, the precise role of this region of PA has yet to be determined.

1.5.3.5 Nucleoprotein

NP is the major component of the vRNP complex. As well as NP playing a structural role, it is essential for replication and transcription of full-length genomic vRNAs (Huang *et al.*, 1990), but has been shown to be entirely dispensable for replication and transcription of short viral RNA-like templates in cell culture (Resa-Infante *et al.*, 2010; Turrell *et al.*, 2013). This finding indicates that NP acts as an elongation factor for the viral RdRP. NP has historically been proposed to play a role in whether the RdRP performs transcription or replication on vRNA templates via a switching mechanism, although the mechanism of this action has been unclear and does not reconcile with the ability of the viral RdRP to perform both transcription and replication in the absence of NP (Turrell *et al.*, 2013). The atomic structure of NP has been solved by X-ray crystallography, revealing that NP has three major domains: a head, body and tail loop domain (Ng *et al.*, 2008; Ye *et al.*, 2006). Between the head and body domains exists a deep groove with a number of exposed basic amino acids that have been shown to be essential for RNA binding and homo-oligomerisation. NP has been shown to interact with the viral RdRP via PB1 and PB2 subunits (Biswas *et al.*, 1998; Poole *et al.*, 2004) and with numerous host factors including UAP56 and Tat-SF1 which have been proposed to act as chaperones in order to facilitate the incorporation of NP into nascent RNPs (Momose *et al.*, 2001; Naito *et al.*, 2007).

1.5.4 Viral RNA promoters

Influenza virus vRNA segments contain non-coding regions (NCRs) at the 5′ and 3′ termini which flank the coding region (Robertson, 1979; Skehel & Hay, 1978). Some of the NCR sequences are segment-specific, however, the termini are conserved in all influenza vRNA segments. At the 5′ end there are 13 nt and at the 3′ end there are 12 nt conserved residues. *In vitro* activity assays have demonstrated that both 5′ and 3′ termini are necessary for RdRP activity (Fodor *et al.*, 1994; Tiley *et al.*, 1994). A number of structural models of the vRNA promoter have been proposed. The 5′ and 3′ termini have partial and inverted complementarity (Desselberger *et al.*, 1980), which led to the proposal that the vRNA promoter adopts a panhandle structure due to Watson-Crick base-pairing (Hsu *et al.*, 1987). This model is supported by cross-linking experiments which showed that vRNA has a circular configuration and by structural analyses using nuclear magnetic resonance (NMR) spectroscopy of naked RNA (Bae *et al.*, 2001; Hsu *et al.*, 1987). An RNA-fork model has also been proposed where the extreme termini of the vRNA remain single-stranded (Fodor *et al.*, 1994; 1995; Kim *et al.*, 1997). Currently, the most favoured model is the corkscrew model in which single-stranded regions of vRNA in each of the 5′ and 3′ termini base-pair to form secondary RNA structures (Flick & Hobom, 1999; Flick *et al.*, 1996). The main features of the RNA corkscrew are two short hairpin loop structures, each with a stem of two base-pairs and a tetraloop that are formed by residues in the termini. This model is supported by the observation that 5′ and 3′ stem loops are important for endonuclease activity (Leahy *et al.*, 2001a; Leahy *et al.*, 2001b) and that a 5′ stem loop is necessary for polyadenylation of viral mRNA (Pritlove *et al.*, 1999). It is plausible that the vRNA

promoter adopts different conformations prior to or upon binding of the viral RdRP. It has been shown that secondary RNA structures in the 5′ and 3′ termini are important for binding to and stabilising the viral RdRP (Brownlee & Sharps, 2002), further strengthening evidence for a corkscrew model.

The cRNA promoter is complementary to the vRNA promoter and mutagenesis experiments of the cRNA promoter found that base pairing in the stems of both 5′ and 3′ hairpin loops is required for vRNA synthesis in cell culture, indicating that the cRNA promoter adopts a corkscrew structure analogous to the vRNA promoter (Azzeh *et al.*, 2001; Crow *et al.*, 2004).

1.5.5 Viral mRNA synthesis, processing and transport

1.5.5.1 Transcription

Influenza virus mRNA synthesis is reliant on cellular RNA polymerase II activity as viral mRNA synthesis requires a 5′ capped primer that is snatched from a cellular pre-mRNA (Engelhardt & Fodor, 2006). Viral transcription requires the concerted action of all three subunits of the viral RdRP. Transcription begins with the binding of a 5′ cap of a pre-mRNA to PB2 (Cianci *et al.*, 1995; Li *et al.*, 1998). Subsequently, endonuclease activity that resides in the PA subunit cleaves 10–15 nt downstream of the cap, usually after a purine residue (Beaton & Krug, 1981; Dias *et al.*, 2009; Plotch *et al.*, 1981; Yuan *et al.*, 2009). Transcription then proceeds with the addition of a G residue at the

catalytic site within the PB1 subunit (Biswas & Nayak, 1994), directed by the penultimate C residue in the 3′ end of the vRNA template (Beaton & Krug, 1981). It has also been reported that in some cases a C residue can be the first nucleotide to be incorporated, templated by the G residue at position 3 of the vRNA template (Fodor *et al.*, 1995). RNA synthesis continues along the vRNA template until the RdRP encounters a stretch of uridine residues approximately 16 nt from the 5′ end of the vRNA which is a signal for polyadenylation of the transcript.

1.5.5.2 Polyadenylation

Cellular mRNAs that are synthesised by RNA polymerase II contain an AAUAAA signal that is required for both cleavage and subsequent polyadenylation of the transcript through the action of a number of cleavage/polyadenylation factors and polyadenylate polymerase (Proudfoot, 2011; Proudfoot & Brownlee, 1976). Influenza virus mRNAs do not possess this signal and therefore polyadenylation of viral mRNAs is not performed by cellular enzymes. Instead, polyadenylation is performed by the viral RdRP. All vRNA segments contain a short stretch of 5–7 uridine residues approximately 16 nt from the 5′ end of the vRNA template which is required for polyadenylation of viral mRNAs (Robertson *et al.*, 1981). The current model of polyadenylation proposes that the 5′ end of the vRNA template remains associated to the viral RdRP throughout transcription and as the RdRP approaches the 5′ end of the vRNA template it cannot proceed to the end of the template due to steric hindrance (Fodor *et al.*, 1994). Consequently, the viral RdRP stutters on the stretch of uridine residues which results in the synthesis of a poly(A) tail. Replacement of the uridine

stretch of residues with a stretch of adenosines has been shown to result in polyuridylation of transcripts, which fail to be properly processed and exported from the nucleus (Poon *et al.*, 2000; Poon *et al.*, 1999).

1.5.5.3 Splicing

Splicing of mRNAs occurs co-transcriptionally and is performed by the splicesome, a complex of small nuclear RNAs (snRNAs) and proteins that coordinate the removal of introns between splice donor and acceptor sites (Matera & Wang, 2014). The two smallest of the eight influenza A virus gene segments can produce both spliced and unspliced transcripts. The M segment gives rise to M1 mRNA which encodes the M1 protein, however, this mRNA transcript can be alternatively spliced into various forms of mRNA, the most important of which is the M2 mRNA that encodes the M2 ion channel (Lamb & Choppin, 1981; Lamb *et al.*, 1981). Further spliced transcripts can be produced from M1 mRNA, including $mRNA_3$ which is of unknown function (Shih *et al.*, 1998) and for some influenza virus strains, the M4 mRNA that encodes the M42 ion channel, a variant of M2 with an antigenically distinct ectodomain and a putative 54 amino acid polypeptide that corresponds to an internally deleted M1 protein (Wise *et al.*, 2012). The NS segment gives rise to the unspliced NS1 mRNA that encodes the multifunctional NS1 protein that antagonises the cellular innate immune response (Hale *et al.*, 2008), and a spliced transcript that gives rise to the NEP protein (Lamb & Lai, 1980). A further spliced transcript that derives from NS1 mRNA has been found in some virus strains which results in the expression of a NS1 protein with an internal

deletion, which has been termed NS3 (Selman *et al.*, 2012). It has been shown that splicing of viral mRNAs is performed by the cellular splicing machinery (Lamb & Horvath, 1991), however, the precise molecular mechanisms of the splicing of viral transcripts is not fully understood. Within infected cells splicing is tightly regulated such that approximately 10% of viral transcripts are spliced, dissimilar to cellular mRNAs that are efficiently spliced (Lamb *et al.*, 1980; Lamb *et al.*, 1981). Both host and viral proteins have been shown to be involved in regulating splicing, including NS1, as well as *cis*-acting RNA signals. NS1 has been shown to be involved in the regulation of splicing of M1 mRNA, affecting the accumulation of M1 spliced transcripts in an RNA binding dependent manner (Robb & Fodor, 2012). NS1 has also been proposed to regulate splicing of the NS1 mRNA transcript (Garaigorta & Ortin, 2007; Smith & Inglis, 1985), however, these data are controversial and were not supported by a study that found that splicing of NS1 mRNA is independent of NS1, suggesting that an alternative mechanism exists for regulating the splicing of NS1 mRNA (Robb *et al.*, 2010). Recently, a study found that the host proteins NS1-BP and heterogeneous nuclear ribonucleoprotein K (hnRNP K) are involved in regulating splicing of the M1 mRNA and down regulation of these host proteins resulted in a change in M1/M2 mRNA ratios, decreasing the expression of M2 and inhibiting virus replication (Tsai *et al.*, 2013). The viral RdRP acting with cellular splicing factor SF2/ASF has also been proposed to regulate splicing of the M1 mRNA (Shih & Krug, 1996; Shih *et al.*, 1995), however, another study did not find RdRP associated to viral mRNA (Bier *et al.*, 2011). Splicing of NS1 mRNA has been proposed to coordinate the timing of infection through the use of a suboptimal splice site that allows the gradual

accumulation of NEP during the course of the life-cycle, serving as a "molecular timer" (Chua *et al.*, 2013).

1.5.5.4 Viral mRNP assembly and transport

Cellular mRNP processing is closely coupled to RNA polymerase II for capping, splicing and polyadenylation, as well as for assembly into an export-competent mRNP for delivery to the cytoplasm (Moore & Proudfoot, 2009). The assembly and nuclear export of viral messenger ribonucleoprotein (mRNP) complexes is also reliant on numerous cellular factors and ongoing host RNA polymerase II transcription (Amorim *et al.*, 2007; Read & Digard, 2010; Tokunaga *et al.*, 2006; York & Fodor, 2013). During mRNA synthesis mRNAs co-transcriptionally acquire a myriad of RNA binding proteins including the cap-binding complex (CBC), hnRNP proteins, exon junction complex (EJC) proteins, poly(A)-binding proteins and components of the transcription export (TREX) complex (Cheng *et al.*, 2006; Kelly & Corbett, 2009; Reed, 2003). A component of the TREX complex, known as REF/Aly recruits the nuclear RNA export factor 1 (NXF1) and its functional co-factor p15 to direct the nuclear export of mRNPs to the cytoplasm via the nuclear pore complex (Katahira, 2012). There is strong evidence that influenza virus mRNPs are exported from the nucleus using the NXF1-p15 pathway as NXF1 is required in the early stages of infection as determined by a small interfering (siRNA) screen (Hao *et al.*, 2008), viral mRNAs have been shown to interact with NXF1 (Wang *et al.*, 2008), and down regulation of NXF1 inhibited the nuclear export of viral mRNPs and virus growth (Read & Digard, 2010).

It is possible that viral mRNPs are exported from the nucleus by an alternative export pathway and a number of RNA nuclear export pathways exist within the cell, the best characterised of which is the Crm1 export pathway (Carmody & Wente, 2009; Kohler & Hurt, 2007). Pharmacological blockade of the Crm1 export pathway using the antibiotic leptomycin-B suggests that export of viral mRNPs does not depend on this pathway (Amorim *et al.*, 2007; Elton *et al.*, 2001; Read & Digard, 2010; Wang *et al.*, 2008).

The viral NS1 protein has been shown to inhibit the nuclear export of cellular mRNPs by binding to the cellular factors cleavage and polyadenylation specificity factor 30 (CPSF30) and poly(A)-binding protein II (PABPII) to prevent 3′ processing of pre-mRNA (Chen & Krug, 2000). NS1 has also been proposed to form an inhibitory complex with NXF1 and p15 to block export of mRNPs (Satterly *et al.*, 2007). Additionally, NS1 has been proposed to inhibit splicing of its own mRNA (Garaigorta & Ortin, 2007) and it has been found to co-purify with viral mRNA and NXF1 (Wang *et al.*, 2008), suggesting a role for NS1 in the regulation of viral mRNP export.

1.5.6 vRNA replication

Replication of the vRNA genome proceeds in two separate stages. During the first stage, a full length positive-sense cRNA copy of vRNA is synthesised (vRNA→cRNA), while in the second stage cRNA is copied back into vRNA (cRNA→vRNA). Both cRNA and vRNA do not possess a 5′ cap or a 3′ poly(A) tail and therefore their

synthesis require an initiation and termination mechanism that is distinct to that of mRNA synthesis. Both cRNA and vRNA possess a 5′ triphosphate, strongly suggesting that initiation of their synthesis occurs *de novo* in the absence of a primer (Hay *et al.*, 1982; Honda *et al.*, 1998; Lee *et al.*, 2002). For cRNA synthesis, primer-independent initiation occurs at the 3′ terminus of vRNA and it has been proposed that the first nucleotide to be incorporated by the RdRP is GTP, directed by the penultimate C residue in the vRNA, followed by the formation of a phosphodiester bond with ATP that is directed by position 1, resulting in a pppApG dinucleotide that is extended by the viral RdRP (Vreede *et al.*, 2008). In an alternative model of cRNA synthesis initiation, it has been proposed that initiation from the vRNA promoter is directed by the penultimate residue from the 3′ end only after a non-templated residue (preferentially a purine) has been added to the vRNA template by a cellular ribonucleotidyltransferase in order to make a complete copy of the vRNA (Zhang *et al.*, 2010). Once the RdRP has initiated, the template is threaded through the active site to synthesise a full-length copy of vRNA. The newly synthesised cRNA associates with NP and the viral RdRP for the synthesis of multiple copies of vRNA. Initiation of vRNA synthesis on the cRNA promoter has been proposed to occur by a distinct mechanism. It has been proposed that pppApG is synthesised internally, directed by positions 4 and 5 from the 3′ end of cRNA, which then realigns to positions 1 and 2 for subsequent elongation by the viral RdRP (Deng *et al.*, 2006). Differences in the modes of initiation of RNA synthesis between cRNA and vRNA promoters could be due to slight differences in promoter structure and their affinity and binding properties for the viral RdRP (Azzeh *et al.*, 2001; Crow *et al.*, 2004; Gonzalez & Ortin, 1999b). Newly synthesised vRNAs

associate with NP and are bound at their 5′ and 3′ termini by the viral RdRP and are subsequently exported to the cytoplasm.

1.5.7 Regulation of the viral RdRP

The genomic vRNA templates that are introduced into infected cells act as both a template for mRNA and cRNA synthesis, however, it has remained an enigma as to how the viral RdRP switches between cRNA or mRNA synthesis on the same vRNA template. Transcription is known to occur predominantly early in infection, peaking at approximately 4–6 hours post infection, while replication products are preferentially synthesised later in infection (Hay *et al.*, 1977; Smith & Hay, 1982). A substantial body of research has been devoted to understanding the molecular mechanisms that underlie what determines whether a RdRP synthesises mRNA or cRNA and a number of models have been proposed which involve viral factors (NP, *cis*- and *trans*- acting RdRPs, NS1, NEP and small viral RNAs (svRNAs)) and a number of host-specific factors (reviewed in (Resa-Infante *et al.*, 2011)). It is the aim of this section to give an overview of the proposed models of how the activity of viral RdRP is regulated.

It has been proposed that the viral RdRP that performs transcription is structurally distinct to the RdRP that performs replication. In support of this theory it has been shown that different domains of PB1 are involved in the binding of vRNA and cRNA (Gonzalez & Ortin, 1999b). The cap-binding and endonuclease functions of the viral RdRP are only required for transcription and not for replication, therefore structural

rearrangement of the RdRP could allow modulation of these activities on different templates.

The availability of viral NP has historically been proposed as the trigger that controls the switch between transcription and replication. In support of this theory products of replication appear within the cell only after the synthesis of NP and RdRP, suggesting that it is the availability of viral proteins that determines whether an RdRP synthesises mRNA or cRNA (Barrett *et al.*, 1979; Hay *et al.*, 1982). Furthermore, cRNA synthesis but not mRNA synthesis is affected in the presence of temperature-sensitive NP mutants at non-permissive temperatures (Krug *et al.*, 1975; Medcalf *et al.*, 1999; Shapiro & Krug, 1988). NP that is not associated to an RNP has also been proposed to act as an anti-termination factor that enables the RdRP to read through the polyadenylation signal at the 5′ end of the template for the synthesis of full length cRNA (Beaton & Krug, 1986; Shapiro & Krug, 1988). The molecular basis of this model is not clear, but it has been proposed that NP may bind to vRNA to melt the panhandle promoter to prevent steric hindrance at the stretch of uridines. It has also been proposed that NP binds to the RdRP to directly modulate transcriptase or replicase activity (Biswas *et al.*, 1998; Mena *et al.*, 1999; Newcomb *et al.*, 2009). However, these models have been widely and intensely disputed. It has been shown that increasing NP concentrations has no effect on the promotion of replication over transcription (Mullin *et al.*, 2004). Furthermore, a stabilisation role was proposed for the viral RdRP and NP protein which disputes the ability of NP to cause a switch between transcription and replication (Vreede *et al.*, 2004). In this model, incoming vRNP complexes are able to synthesise both mRNA and cRNA from the outset, but cRNA does not accumulate to

detectable levels until sufficient NP and RdRP have been synthesised in order to stabilise the cRNA product and prevent its degradation by cellular nucleases. However, this model does not explain what determines whether the viral RdRP initiates primer-dependent or primer-independent synthesis on the same vRNA template. Additional evidence that NP is not required for switching between transcription and replication came from the observation that short vRNA genome segments up to 76 nt in length, with large internal deletions but which preserve 5′ and 3′ terminal sequences, are able to transcribe and replicate in cell culture in the absence of NP, resulting in authentic 5′ capped and 3′ polyadenylated mRNA products and authentic replication products (Resa-Infante *et al.*, 2010; Turrell *et al.*, 2013).

A model that mRNA synthesis is performed in *cis* and that cRNA synthesis is performed in *trans* has gained support in recent years (Moeller *et al.*, 2012). In this model a viral RdRP that is distinct to the resident RdRP within the vRNP performs cRNA synthesis, while mRNA synthesis is performed by the resident RdRP. In this *trans*-acting RdRP cRNA synthesis model the 3′ end of the vRNA would need to be released by the resident RdRP to be copied by the *trans*-acting RdRP for synthesis of the nascent 5′ end, which would then bind to the *trans*-acting RdRP. In support of this model of replication, examination of purified viral RNPs from transfected cells by negative stain electron microscopy revealed RNP complexes with a branched arrangement in which a smaller nascent RNP appears to branch from a full length RNP (Moeller *et al.*, 2012). Labelling of the RdRP using immunogold revealed the presence of an RdRP at the branch point, however, simultaneous labelling of the branch point and the termini was not shown. This model is not compatible with the observation that

vRNPs isolated from virions can produce cRNA *in vitro* and vRNPs introduced into cells early in infection can synthesise cRNA in the presence of cycloheximide, an inhibitor of protein synthesis (Vreede & Brownlee, 2007; Vreede *et al.*, 2004). It also remains unclear how the 5′ end of the vRNA would be released by the resident RdRP to be allowed to be copied by the *trans*-acting RdRP.

Fundamental mechanistic and regulatory differences are also expected to exist between viral RdRP activity on cRNA and vRNA templates. A number of biochemical and genetic studies suggest that RdRP activity on cRNA and vRNA templates is different. It was reported that cRNA and vRNA promoters interact with different regions of the viral RdRP (Gonzalez & Ortin, 1999a; b) and that initiation of cRNA and vRNA synthesis are performed by distinct mechanisms as previously discussed (Deng *et al.*, 2006; Vreede *et al.*, 2008; Zhang *et al.*, 2010). It has been proposed that vRNA synthesis on a cRNA template is performed in *trans* by a newly synthesised RdRP (Jorba *et al.*, 2009). Complementation experiments in cell culture using RdRP complexes that are defective in either transcription or replication have established a model that proposes that an RdRP distinct from the replicating RdRP is incorporated into a progeny vRNP. Transfection of replication-defective vRNP complexes into cells that express transcription-defective but replication-competent mutant polymerase led to the proposal that replication is performed in *trans*.

It has been proposed that the viral protein NEP is involved in the regulation of viral RNA synthesis. Specifically, it was observed that co-expression of NEP in RNP reconstitution assays in cell culture resulted in an increased accumulation of cRNA and

vRNA and a decrease in mRNA (Robb *et al.*, 2009). Furthermore, it was found that adaptive mutations in NEP can compensate for defective replication by a non-adapted RdRP from an H5N1 influenza A virus in mammalian cells (Manz *et al.*, 2012). Another study proposed that NEP regulates viral RNA synthesis by promoting the synthesis of svRNAs that are 22–27 nt in length and correspond to the 5′ end of each vRNA segment (Perez *et al.*, 2010). svRNAs were found to be expressed at high levels in infected cells and their synthesis correlates with the accumulation of vRNA and a shift from transcription towards genome replication. It was shown that svRNAs promote RdRP activity *in vitro*, while their absence inhibited viral RNA synthesis (Perez *et al.*, 2012). It was proposed that svRNAs promote replication by binding to a putative RNA binding cleft in the PA subunit of the RdRP which results in an allosteric effect to enhance RdRP activity (Perez *et al.*, 2012).

The multifunctional viral NS1 protein has also been shown to have an effect on RNA synthesis and could play a role in the regulation of the viral RdRP. Early experiments using temperature-sensitive mutations in NS1 were shown to reduce the levels of vRNA accumulation, but cRNA and mRNA levels were unaffected (Wolstenholme *et al.*, 1980). This observation was confirmed years later using viruses with C-terminal truncations of NS1, supporting a view that NS1 plays a role in regulating viral RNA synthesis (Falcon *et al.*, 2004). The addition of purified NS1 protein to an *in vitro* viral RNA synthesis system resulted in the counteraction of a putative ‘polymerase regulating factor’ (Shimizu *et al.*, 1994). It has also been proposed that NS1 interacts directly with the viral RdRP through amino acid positions 123 and 124 to regulate the timing of vRNA synthesis (Min *et al.*, 2007). Alanine mutations at these sites resulted

in the deregulation of the accumulation of viral RNAs over the course of infection. In support of this hypothesis, NS1 has previously been shown to co-purify with vRNP complexes (Kuo & Krug, 2009; Marion *et al.*, 1997). It was later found that NS1 interacts with NP via its RNA-binding domain (Robb *et al.*, 2011). It is important to note that a recombinant influenza virus that lacks an NS1 gene has previously been shown to replicate in interferon-deficient cells (Garcia-Sastre *et al.*, 1998) and therefore the contribution of NS1 to the regulation of RdRP activity remains to be fully elucidated.

It is possible that the localisation of vRNP complexes to particular nuclear microenvironments or structures could determine whether mRNA or cRNA synthesis proceeds. It has been reported that the concentrations of nucleotide triphosphates required for *de novo* initiation are higher than those concentrations that are required for primer-dependent RNA synthesis and therefore this difference may determine the mode of initiation (Vreede & Brownlee, 2007; Vreede *et al.*, 2008). The viral RdRP has been shown to associate with serine-5 phosphorylated carboxyl terminal domain of the large subunit of RNA polymerase II in infected cells (Engelhardt *et al.*, 2005). It has been proposed that this interaction allows the viral RdRP to gain access to host pre-mRNAs for subsequent cap-snatching for viral mRNA synthesis and therefore this association may stimulate the RdRP to act as a transcriptase (Engelhardt & Fodor, 2006; Engelhardt *et al.*, 2005). Alternatively, the involvement of specific cellular factors cannot be excluded and a number of host factors have been described to stimulate viral RNA synthesis. For example the minichromosome maintenance (MCM) helicase complex has

been proposed to regulate *de novo* replication by increasing the efficiency and processivity of cRNA synthesis (Kawaguchi & Nagata, 2007).

1.6 The influenza transcription/replication machinery and host-pathogen interactions

1.6.1 Overview

Viruses are obligate intracellular parasites that have been compelled by evolutionary processes to encode a minimal number of proteins for the completion of an infectious life-cycle, in order to infect naïve hosts and to persist in nature. This is particularly exemplified by influenza viruses, the genomes of which are compact and therefore they greatly rely on the exploitation and subversion of host cellular proteins, structures and pathways to facilitate virus replication (Holmes, 2013; Mehle & Doudna, 2010; Muller *et al.*, 2012; Watanabe *et al.*, 2010). A comprehensive understanding of host-virus interactions greatly improves our understanding of the influenza virus life-cycle and could potentially lead to the identification of novel strategies to prevent or treat virus infections.

The viral transcription/replication machinery and components thereof engage with numerous cellular factors during the course of the virus life-cycle which are believed to be important to their function. Likewise, viral restriction factors that are present within the cell can also interact and act as an intracellular block to viral replication.

Furthermore, components of the viral transcription/replication machinery are major determinants of species tropism and pathogenicity, and are key players in the adaptation of avian influenza A viruses to mammalian hosts. These characteristics are also thought to be governed by numerous interactions with cellular factors (Cauldwell *et al.*, 2014; Manz *et al.*, 2013). Consequently, many studies have been carried out in order to identify interactions between viral proteins and the host cell with the aim of understanding the underlying molecular mechanisms of replication.

1.6.2 Host-adaptation of the viral transcription/replication machinery

Influenza viruses that circulate in wild waterfowl, a reservoir for influenza A viruses, can occasionally infect new species including humans, swine, horses and sea mammals (Wright *et al.*, 2013). In order for influenza virus to become established in a new host it must overcome species-specific barriers and adapt to interact successfully with host-specific cellular factors to achieve efficient virus replication. It is known that the RdRP from avian influenza viruses are unable to function well in mammalian cells and that mutations in the RdRP and NP subunits are required for host adaptation (Cauldwell *et al.*, 2014; Manz *et al.*, 2013; Naffakh *et al.*, 2008). The enormous potential for genetic variation in influenza viruses occasionally enables this transformation to take place.

The primary viral contributor to host restriction is a component of the viral transcription/replication machinery, the PB2 subunit of the RdRP. Early studies of host adaptation identified that the ability of an avian virus to form viral plaques on mammalian cells was dependent on the origin of the PB2 gene (Almond, 1977). The

ability of the PB2 gene to confer mammalian adaptation was better defined over a decade later when it was discovered that a single amino acid change at position 627 (E627K) allowed an avian PB2-possessing virus to replicate in mammalian cells (Subbarao *et al.*, 1993). The PB2 627 position is a glutamic acid in almost every avian influenza A virus isolate, whereas in mammalian influenza A virus isolates it is mostly a lysine. One notable exception to this rule was the 2009 swine origin pandemic virus (Garten *et al.*, 2009). Further studies revealed that substitution of a glutamic acid for a lysine at position 627 resulted in enhanced RdRP activity in mammalian cells. Currently, the molecular mechanism for this is unclear and numerous models have been proposed in recent years (reviewed in (Cauldwell *et al.*, 2014; Manz *et al.*, 2013), however, it is a widely-held view that host-specific interactions play an important role. RdRP activity assays in heterokaryons of human and avian cells concluded that mammalian cells express a dominant inhibitory factor that restricts a PB2-627E RdRP, while another study concluded that the activity of a PB2-627E within a human cell was enabled upon fusion with an avian cell, indicating that there are host-specific factors present within avian cells that promote activity (Mehle & Doudna, 2008; Moncorge *et al.*, 2010). Specific cellular factors have been implicated in determining host-range, for example the DEAD box RNA helicase 17 (DDX17) which when down regulated in human cells inhibited a PB2-627K RdRP, but increased activity of a PB2-627E RdRP (Bortz *et al.*, 2011). Further work is required to fully understand the role of host-specific cellular factors in the adaptation of influenza A viruses.

1.6.3 Approaches to study interactions between the viral transcription/replication machinery and the host cell

In recent years a number of different approaches have been carried out with the aim of identifying cellular factors that are required for influenza virus replication. The dawn of RNAi-based genomics and advancement in protein mass spectrometry techniques has greatly facilitated progress in this area. A number of interactions between viral proteins and cellular proteins have been reported (Figure 1.8), although many still remain elusive and it is anticipated that future emerging data in this field will contribute to elucidating molecular mechanisms of influenza virus replication.

A number of laboratories have expended much time and effort in the search for novel host factors involved in the influenza virus life-cycle using genome-wide approaches including RNAi. RNAi is a regulatory mechanism in which double-stranded RNA molecules are used to direct homology-dependent suppression of gene expression (Fire *et al.*, 1998). This powerful technology has been extensively used in molecular cell biology for the systematic study of gene functions and it has been used in approaches to identify host factors that are involved in influenza virus replication. Four genome-wide RNAi screens (Brass *et al.*, 2009; Hao *et al.*, 2008; Karlas *et al.*, 2010; Konig *et al.*, 2010) have been employed to date and in a different approach one laboratory combined RNAi technology with yeast two-hybrid and transcriptional gene profiling in order to identify host factors (Shapira *et al.*, 2009). A further large-scale screen has been carried out using random homozygous gene perturbation (RHGP) which relies on the generation of a library of mammalian cell clones by random insertion of a lentiviral-

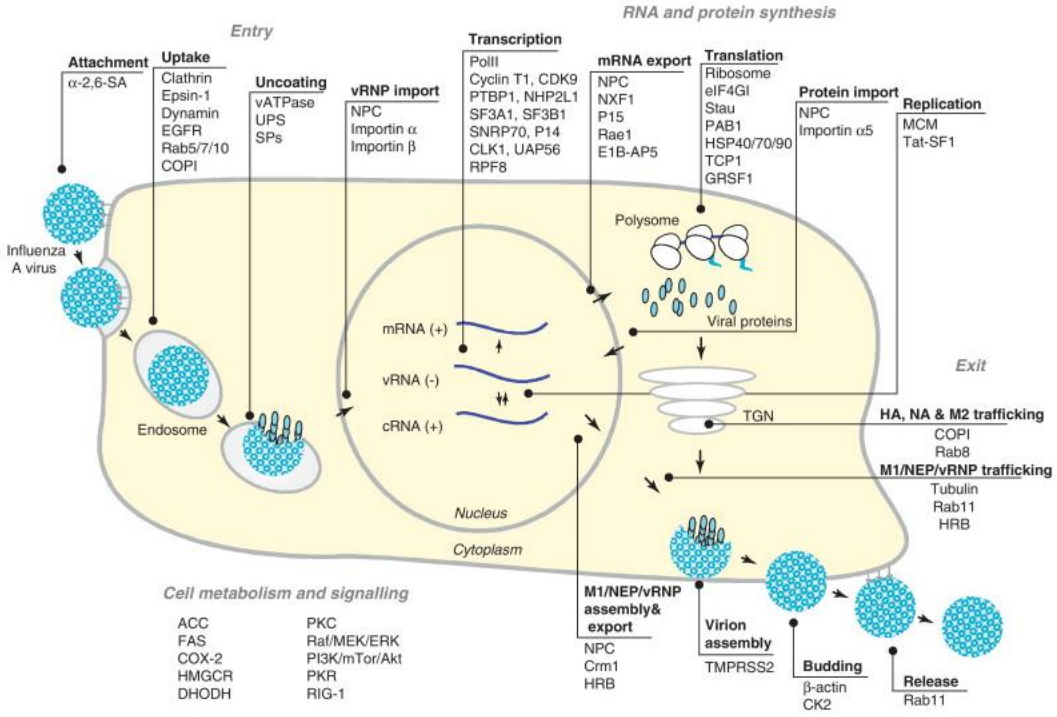


Figure 1.8 Influenza A virus life-cycle and cellular factors. Schematic of the influenza A virus life-cycle highlighting a number of cellular factors that have been shown to be important for virus replication at each stage of the virus life-cycle. From Müller *et al*., 2012.

based genetic element into random loci within the genome that can lead to overexpression or knockout of host genes (Sui *et al.*, 2009). Subsequent infection and identification of resistant clones can lead to the identification of host factors that are required for viral replication. Meta-analyses of these genome-wide screens identified a total of 1,449 human genes (including 110 human orthologs of *Drosophila* genes) with possible roles in the virus life-cycle. However, limited overlap was observed among these studies (de Chassey *et al.*, 2012; Watanabe *et al.*, 2010). The limited overlap between studies has been attributed to differences in experimental design and execution of the screens. For example, non-authentic influenza viruses (e.g. viruses that possess reporter genes) and cells that are non-permissive for infection were used. Furthermore, the criteria that were used to identify host factors differed between screens and most of the identifications were not validated or functionally assessed. A number of smaller RNAi based screens have also been performed which has led to the identification of specific cellular factors which were subsequently validated, and in some cases the role of the identified protein was investigated (Bortz *et al.*, 2011; Su *et al.*, 2013; Zhou *et al.*, 2014). A major drawback with these approaches is that they fail to inform about specific stages of the virus life-cycle at which particular cellular factors are critical. Furthermore, these methods do not distinguish between factors that are required for virus replication by directly interacting with a viral component such as the transcription/replication machinery and those factors that can contribute to virus replication indirectly.

Other techniques have been used with the aim of identifying host factors that interact with the viral transcription/replication machinery. These include a yeast two-hybrid

screen (Tafforeau *et al.*, 2011), complementation assays (Munier *et al.*, 2013) and affinity-purification mass spectrometry (AP-MS) (Bradel-Tretheway *et al.*, 2011; Fislova *et al.*, 2010; Jorba *et al.*, 2008; Mayer *et al.*, 2007). Yeast-two hybrid and complementation assays are similar in that they rely on the read out of a reporter gene if bait and prey proteins come into close physical proximity, and therefore these approaches aim to identify physical associations between viral and host proteins. Similarly, AP-MS approaches aim to identify proteins that form a physical complex and co-purify with a bait protein. However, these different approaches have been limited by either the number of cellular factors that can be cloned and screened, as in the case of yeast two-hybrid and complementation assays, or the identifications of interaction partners of the viral transcription/replication machinery by mass spectrometry were not performed in the context of the infected cell. A significant advance would be to elucidate physical interactions that occur between the viral transcription/replication machinery and cellular proteins in the context of an infected cell.

Despite some of the limitations of these approaches a number of cellular factors have been identified as significant players in the life-cycle of influenza virus. Figure 1.8 illustrates examples of cellular proteins that have been shown to be important at the various stages of the influenza virus life-cycle. Some of these cellular proteins have been shown to be important for regulating viral RdRP activity and for efficient transcription and replication of the viral genome. For example, the MCM complex, which functions as a DNA replication fork helicase, has been shown to play a significant role in influenza virus genome replication by promoting the association between nascent cRNA and the viral RdRP during the transition from the initiation to

elongation phase of RNA synthesis, therefore stabilising elongating complexes and stimulating cRNA synthesis (Kawaguchi & Nagata, 2007). A general transcription factor, Tat-SF1, was found to interact with NP and facilitate the formation of RNA-NP complexes, suggesting that Tat-SF1 may function as a molecular chaperone for RNP assembly (Naito *et al.*, 2007). Similarly a helicase, UAP56, has been proposed to act as an NP molecular chaperone and prevent the formation of double-stranded RNA in the assembly of RNP complexes (Momose *et al.*, 2001; Wisskirchen *et al.*, 2011). Host factors have also been proposed to bind directly to the viral RdRP and modulate polymerase activity, for example the molecular chaperone Hsp90 was found to interact with the PB2 subunit of the RdRP and it was shown to stimulate RNA synthesis in a concentration-dependent manner *in vitro* (Momose *et al.*, 2002).

Although numerous advances have been made in the identification of cellular factors that support viral replication, many host-virus interactions remain to be discovered. Furthermore, extensive validation and a systematic assessment of the functional roles of the identified cellular factors have been lacking.

1.7 Thesis objectives and outline

The segmented negative-sense vRNA genome of influenza virus is replicated and transcribed by the viral RdRP. The aim of this thesis was to understand the role of viral and cellular factors in the regulation of the influenza virus RdRP with a view to

elucidating the fundamental molecular biology of viral RNA synthesis in influenza virus infected cells.

The basic molecular requirements for vRNA replication (vRNA→cRNA→vRNA) are unknown and therefore one aim of the thesis was to dissect the requirements for viral RNA synthesis at each stage of vRNA replication. The development of an RNA-based affinity purification method for the isolation of viral RNP complexes from infected cells (Chapter 3) allowed the genomic vRNP and the replicative intermediate cRNP to be isolated separately. This was the first isolation of the genomic replicative intermediate of a negative-strand RNA virus. The molecular architecture of the cRNP complex was studied by electron microscopy giving important insight into this previously uncharacterised component of the vRNA replication machine. Importantly, this advance enabled the molecular requirements for vRNA replication to be elucidated *in vitro* (Chapter 4). It was discovered that vRNA synthesis by the cRNP-associated RdRP requires activation by a *trans*-activating RdRP.

In order to understand the role of host factors in the regulation of the viral RdRP and in viral RNA synthesis a study of the interactome of the viral transcription/replication machinery in the context of an infected cell was performed using affinity-purification mass spectrometry (Chapter 5). Identification of cellular serine/threonine phosphatase 6 as an interaction partner of the viral transcription/replication machinery by mass spectrometry led to validation of the interaction and assessment of the functional role that this cellular factor plays in RNA synthesis (Chapter 6). This cellular factor was

found to interact directly with the viral RdRP and act as a positive regulatory factor that is required for efficient viral RNA synthesis and virus growth.

Chapter 2: Materials and Methods

2.1 Materials

2.1.1 General reagents

General chemical reagents were all AnalaR grade and purchased from New England Biolabs, Roche, GE Healthcare Life Sciences, Millipore, Invitrogen Life Technologies, Sigma-Aldrich, Thermo Scientific, Stratagene, Agilent Technologies, Geneflow, VWR International, QIAGEN, Bio-Rad and Promega. The sources of all special reagents are indicated separately.

2.1.2 Enzymes

Restriction endonucleases were supplied by New England Biolabs, Thermo Scientific or Roche. T4 Polynucleotide Kinase (PNK) was purchased from Thermo Scientific; Tobacco Etch Virus (AcTEV) protease from Invitrogen; Pfu Turbo from Stratagene; RNase A from Sigma-Aldrich; Ligation High from Toyobo Life Science; Calf intestinal alkaline phosphatase (CIP) and RNasin ribonuclease inhibitor from Promega.

2.1.3 Radiochemicals

Radiochemicals were all obtained from PerkinElmer (UK) Ltd. at the following specific activities:

[α-^{32}P]CTP	~3000 Ci/mmol (10 mCi/ml)
[α-^{32}P]UTP	~3000 Ci/mmol (10 mCi/ml)
[α-^{32}P]GTP	~3000 Ci/mmol (10 mCi/ml)
[γ-^{32}P]ATP	~6000 Ci/mmol (10 mCi/ml)

2.1.4 Synthetic oligodeoxyribonucleotides and oligoribonucleotides

Synthetic oligodeoxyribonucleotides and oligoribonucleotides were purchased from Sigma-Aldrich.

2.1.5 Antibodies

The rabbit polyclonal anti-NP antibody was a kind gift from Otto Haller (University of Freiburg, Germany). The rabbit polyclonal anti-PA, anti-PB2 and anti-RdRP antibodies were kind gifts from Tao Deng, Simon Carr and Mónica Martínez-Alonso (Sir William Dunn School of Pathology, University of Oxford), respectively. The mouse monoclonal anti-NP antibody (Ab128193) was purchased from Abcam. The anti-PPP6C (A300-844A) and anti-PPP6R3 (A300-972A) rabbit polyclonal antibodies were purchased from Bethyl Laboratories. The rabbit polyclonal anti-Actin antibody (A2066) was purchased from Sigma-Aldrich. The mouse monoclonal anti-$His_{6\times}$ antibody (04905318001) was purchased from Roche.

2.1.6 Bacteria and bacterial culture medium

Escherichia coli strain DH5α was purchased from Invitrogen. *Escherichia coli* strain BL21 (DE3) was purchased from New England Biolabs. Bacterial culture media 2×YT (16 g bacto-tryptone, 10 g yeast extract, and 5 g NaCl per litre), luria broth (LB) (10 g bacto-tryptone, 5 g yeast extract, and 10 g NaCl per litre) and nutrient agar plates with or without ampicillin were supplied by the departmental media service of the Sir William Dunn School of Pathology. If required, ampicillin was added to culture media to give a final concentration of 100 μg/ml.

2.1.7 Cell culture media

Minimal Essential Medium (MEM) and Dulbecco's Modified Eagle Medium, Foetal Calf Serum (FCS) and Phosphate Buffered Saline (PBS) were all purchased from Sigma-Aldrich. TrypLE Express dissociation reagent, L-glutamine and Penicillin-Streptomycin were purchased from Invitrogen. Insect-XPRESS protein-free insect cell medium was purchased from Lonza Group Ltd.

2.1.8 Cell lines

Human Embryonic Kidney 293T (HEK 293T) cells, Madin-Darby Bovine Kidney epithelial (MDBK) cells, human adenocarcinoma alveolar basal epithelial (A549) cells and *Spodoptera frugiperda* (Sf9) cells were obtained from the Cell Bank of the Sir William Dunn School of Pathology (University of Oxford).

The HEK 293T-PP7CP stable cell line was produced under the selection of hygromycin-B (Roche). For this purpose, 30 µg of pcDNA-PP7CP-$His_{6\times}$ was transfected using Lipofectamine-2000 (Invitrogen) according to the manufacturer's instructions into approximately 4 $\times 10^6$ HEK 293T cells in 10 cm dishes. After 48 h, cells were replated into 15 cm dishes containing DMEM supplemented with 10% FCS and hygromycin-B (500 µg/ml). Stable clone selection occurred in the presence of hygromycin-B (500 µg/ml) for approximately 30 d. Stable colonies resistant to

hygromycin-B were picked and recultured and protein expression was confirmed by Western blotting using an anti-$His_{6\times}$ antibody.

2.1.9 Viruses

Influenza A/WSN/33 (H1N1) virus stocks were a gift from Peter Palese (Icahn School of Medicine at Mount Sinai, New York, USA). The recombinant MultiBac baculovirus expressing influenza A virus RdRP was a kind gift from Narin Hengrung (Sir William Dunn School of Pathology, University of Oxford).

2.1.10 Plasmids

The protein expression plasmids pcDNA-PB1, pcDNA-PB2, pcDNA-PA, pcDNA-NP and pcDNA3A have been described previously (Fodor *et al.*, 2002), as have the pPOLI-PB1, pPOLI-PB2, pPOLI-PA, pPOLI-HA, pPOLI-NP, pPOLI-NA, pPOLI-M and pPOLI-NS vRNA transcription plasmids (Fodor *et al.*, 1999).

The pcDNA-PB1a plasmid has been described previously (Vreede *et al.*, 2004).

The pcDNA-PB1-TAP, pcDNA-PB2-TAP and pcDNA-PA-TAP constructs have been described previously (Deng *et al.*, 2005; Fodor & Smith, 2004).

The pETZZ-tev-PP7CP plasmid has been described previously (Hogg & Collins, 2007) and was a kind gift from J. Robert Hogg (National Heart, Lung, and Blood Institute, National Institutes of Health, Bethesda, USA).

The pHW2000-PB2-Strep plasmid has been described previously (Rameix-Welti *et al.*, 2009) and was a kind gift from Martin Schwemmle (University of Freiburg, Germany).

The pGEX-6P1-GST, pGEX-6P1-GST-PPP6C, pGEX-4T1-GST-PPP6R1, pGEX-4T1-GST-PPP6R2 and pGEX-GST-4T1-PPP6R3 *Escherichia coli* expression plasmids have been described previously (Douglas *et al.*, 2010) and were a kind gift from Susan P. Lees-Miller (University of Calgary, Canada).

2.2 Cloning

2.2.1 Plasmid construction

The pPOLI-NA-PP7-cRNA and pPOLI-NA-PP7-vRNA plasmids were constructed by PCR mutagenesis of the pPOLI-NA plasmid to introduce a unique XbaI restriction site with primers shown in Table 2.1. The PCR reaction was carried out using 100 ng of template plasmid, 25 pmol of each primer, 200 μM of each dNTP and 1.25 U Pfu Turbo in 1 × Pfu turbo reaction buffer, and incubated in a thermocycler at 95°C for 30 s denaturing, 60°C for 30 s annealing and 72°C for 16 min for elongation, for a total of 30 cycles. Following PCR mutagenesis, a small volume of the total reaction was

analysed by agarose gel electrophoresis to confirm that the PCR reaction was successful. The remaining PCR product was subsequently digested with DpnI and transformed into *E. coli* DH5α to generate the pPOLI-NA-XbaI plasmid. The pPOLI-NA-XbaI plasmid was digested with XbaI and treated with CIP. Two pre-annealed complementary oligonucleotides (Table 2.1) were subsequently ligated into the digested plasmid using Ligation High and the reaction was transformed into *E. coli* DH5α.

The pPOLI-NS-PP7-cRNA and pPOLI-NS-PP7-vRNA plasmids were constructed by digesting the pPOLI-NS plasmid with NcoI and then treating with CIP. Two pre-annealed complementary oligonucleotides (Table 2.1) were subsequently ligated into the digested plasmid using Ligation High and the reaction was transformed into *E. coli* DH5α.

The pcDNA-PP7CP-$His_{6\times}$ plasmid was constructed in two stages, firstly by PCR amplification of the PP7CP open reading frame from the pETZZ-tev-PP7CP plasmid using primers shown in Table 2.1., followed by insertion of a $His_{6\times}$-tag into the pcDNA-PP7CP plasmid. The PCR reaction was carried out using 1 ng of template plasmid, 25 pmol of each primer, 200 μM of each dNTP and 1.25 U Pfu Turbo in 1 × Pfu turbo reaction buffer, and incubated in a thermocycler at 95°C for 30 s denaturing, 57°C for 30 s annealing and 72°C for 1 min for elongation, for a total of 30 cycles. Following PCR amplification, a small volume of the total reaction was analysed by agarose gel electrophoresis to confirm that the PCR reaction was successful. The remaining PCR product was subsequently digested with KpnI and NotI. The pcDNA3A plasmid was simultaneously digested and treated with CIP. The digested pcDNA3A

plasmid was subsequently isolated by agarose gel electrophoresis and the digested pcDNA3A and PCR product were ligated using Ligation High and the reaction was transformed into *E. coli* DH5α to generate the pcDNA-PP7CP plasmid. The pcDNA-PP7CP plasmid was digested with KpnI and NotI and treated with CIP. Two pre-annealed complementary oligonucleotides (Table 2.1) were subsequently ligated into the digested plasmid using Ligation High and the reaction was transformed into *E. coli* DH5α to generate the pcDNA-PP7CP-$His_{6\times}$ plasmid.

The pcDNA-PP7-Strep plasmid was constructed by digestion of the pcDNA-PP7CP-$His_{6\times}$ plasmid with XbaI and NotI and the digest was treated with CIP. The digested plasmid was isolated by agarose gel electrophoresis and two pre-annealed complementary oligonucleotides (Table 2.1) were ligated into the digested plasmid using Ligation High and the ligation reaction was transformed into *E. coli* DH5α.

The pcDNA-PB2-Strep plasmid was constructed by PCR amplifying the PB2-Strep open reading frame from the pHW2000-PB2-Strep plasmid using the primers shown in Table 2.1. The PCR reaction was carried out using 1 ng of template plasmid, 25 pmol of each primer, 200 μM of each dNTP and 1.25 U Pfu Turbo in 1 × Pfu turbo reaction buffer, and incubated in a thermocycler at 95°C for 30 s denaturing, 60°C for 30 s annealing and 72°C for 3 min for elongation, for a total of 30 cycles. The PCR product and the pcDNA3A plasmid were digested with KpnI and NotI and the digested pcDNA3A plasmid was treated with CIP. The digested plasmid was isolated by agarose gel electrophoresis and the digested pcDNA3A and PCR product were ligated using Ligation High and the reaction was transformed into *E. coli* DH5α.

The pcDNA-PB1-Strep plasmid was constructed by digestion of the pcDNA-PB1-TAP plasmid with XbaI and NotI. The digested plasmid was treated with CIP and isolated by agarose gel electrophoresis. Two pre-annealed complementary oligonucleotides (Table 2.1) were ligated into the digested plasmid using Ligation High and the ligation reaction was transformed into *E. coli* DH5α.

The pcDNA-PA-Strep plasmid was constructed by digestion of the pcDNA-PA-TAP plasmid with XbaI and NotI and the digest was treated with CIP. The digested plasmid was isolated by agarose gel electrophoresis and two pre-annealed complementary oligonucleotides (Table 2.1) were ligated into the digested plasmid using Ligation High and the ligation reaction was transformed into *E. coli* DH5α.

Table 2.1 Sequences of primers used for cloning described in section 2.2.

Plasmid	Oligodeoxyribonucleotides
pPOLI-NA-XbaI	5′-GGCAGCATTACCTCTAGAGTTGTTGC-3′ 5′-GCAACAACTCTAGAGGTAATGCTGCC-3′
pPOLI-NA-PP7-cRNA	5′-CTAGTAAGGAGTTTATATGGAAACCCTTAT-3′ 5′-CTAGATAAGGGTTTCCATATAAACTCCTTA-3′
pPOLI-NA-PP7-vRNA	5′-CTAGGTAAGGAGTTTATATGGAAACCCTTA-3′ 5′-CATGTAAGGGTTTCCATATAAACTCCTTAC-3′
pPOLI-NS-PP7-cRNA	5′ CTAGGTAAGGAGTTTATATGGAAACCCTTA-3′ 5′-CATGTAAGGGTTTCCATATAAACTCCTTAC-3′
pPOLI-NS-PP7-vRNA	5′-CATGGCTAAGGGTTTCCATATAAACTCCTTAGT-3′ 5′-CATGACTAAGGAGTTTATATGGAAACCCTTAGC-3′
pcDNA-PP7CP	5′-ATATGGTACCGCCGCCACCATGGCCAAAACCATCGTT-3′ 5′-ATATGCGGCCGCGAACGGCCCAGCGGCAC-3′
pcDNA-PP7CP-$His_{6\times}$	5′-GGCCGCAAGATTATGATATTCCAACTACTCTGGAAGTTCTGT TCCAGGGGCCCGATTATGATATTCCAACTACTCACCACCACCA CCACCACTGA-3′ 5′-CTAGATCAGTGGTGGTGGTGGTGGTGAGTAGTTGGAATAT CATAATCGGGCCCCTGGAACAGAACTTCCAGAGTAGTTGGAAT ATCATAATCTT-3′
pcDNA-PP7-Strep	5′-ATATGCGGCCGCTTTGGAGCCACCCGCAGTTCGAGAAAGG TGGAGGTTCCGGAGGTGGATCGGGAGGTGGATCGTGGAGCC ACCCGCAGTTCGAAAAATAGTCTAGAATA-3′ 5′-TATTCTAGACTATTTTTCGAACTGCGGGTGGCTCCACGATC CACCTCCCGATCCACCTCCGGAACCTCCACCTTTCTCGAACTG CGGGTGGCTCCAAAGCGGCCGCATAT-3′
pcDNA-PB2-Strep	5′-ATATGGTACCGCCGCCACCATGGAAAGAATAAAAGAA-3′ 5′-ATATGCGGCCGCCTATTTTTCGAACTGCGG-3′
pcDNA-PB1-Strep	5′-GGCCGCAAGCGCTTGGAGCCACCCGCAGTTCGAGAAAGG TGGAGGTTCCGGAGGTGGATCGGGAGGTGGATCGTGGAGCC ACCCGCAGTTCGAAAAATAGT-3′ 5′-CTAGACTATTTTTCGAACTGCGGGTGGCTCCACGATCCACC TCCCGATCCACCTCCGGAACCTCCACCTTTCTCGAACTGCGG GTGGCTCCAAGCGCTTGC-3′
pcDNA-PA-Strep	5′-GGCCGCAAGCGCTTGGAGCCACCCGCAGTTCGAGAAAGG TGGAGGTTCCGGAGGTGGATCGGGAGGTGGATCGTGGAGCC ACCCGCAGTTCGAAAAATAGT-3′ 5′-CTAGACTATTTTTCGAACTGCGGGTGGCTCCACGATCCACC TCCCGATCCACCTCCGGAACCTCCACCTTTCTCGAACTGCGG GTGGCTCCAAGCGCTTGC-3′

2.2.2 Transformation into competent *E. coli*

Chemically competent *E. coli* DH5α cells were thawed on ice and 20 µl of cells were incubated with DNA for 30 min. Cells were heated to 42˚C for 45 s and immediately transferred to ice for a further 2 min. After the addition of 280 µl of S.O.C. medium

(Sigma) the cells were incubated for 60 min at 37°C in a shaking incubator. Cells were spread onto agar plates containing 100 µg/ml ampicillin and the plates were incubated at 37°C overnight. Cells that had not been incubated with DNA were used as a negative control.

2.2.3 Plasmid preparation and sequencing

Bacterial colonies were picked and used to inoculate 2 ml cultures of LB medium supplemented with 100 µg/ml ampicillin. Inoculates were incubated in a shaking incubator overnight at 37°C. The cells were pelleted and plasmid DNA was extracted using a QIAprep spin miniprep kit (QIAGEN) according to the manufacturer's instructions. The plasmid DNA was eluted in 50 µl of ddH_2O.

For large-scale preparation of plasmid DNA, 100 ml cultures of LB medium supplemented with 100 µg/ml ampicillin were inoculated with 100 µl of overnight culture and incubated in a shaking incubator overnight at 37°C. The cells were pelleted and plasmid DNA was extracted using a QIAfilter maxiprep kit (QIAGEN) according to the manufacturer's instructions. The plasmid DNA was dissolved in ddH_2O to a final concentration of 1 mg/ml.

Plasmid DNA was sequenced by Source Bioscience LifeSciences (Oxford) using Sanger sequencing. Plasmids were sent for sequencing at concentrations of 100 ng/µl with primers at 3.2 pmol/µl.

2.3 Eukaryotic cell culture

HEK 293T cells were maintained in DMEM supplemented with 10% FCS. A549 cells and MDBK cells were maintained in MEM supplemented with 2 mM L-glutamine and 10% FCS. Mammalian cells were maintained in humidified incubators at 37°C, 5% CO_2. Cells were passaged at a one in ten dilution and were removed from tissue culture flasks by trypsinisation using TrypLE Express dissociation reagent. *Spodoptera frugiperda* (Sf9) cells were propagated at 28°C in Insect-XPRESS supplemented with 1% Penicillin-Streptomycin. When required, a viable cell count was performed using a haemocytometer cell counting chamber viewed under a light microscope, after dilution of the cell sample with an equal volume of 0.4% trypan blue in PBS.

2.4 Virus culture and handling

2.4.1 Reverse genetics

Wild-type and recombinant influenza A/WSN/33 (H1N1) viruses were rescued using the twelve plasmid-based reverse genetics rescue system (Fodor *et al.*, 1999). HEK 293T cells were grown in 3.5 cm dishes and transfected with 1 µg of each of the four protein expression plasmids pcDNA-PB1, pcDNA-PB2, pcDNA-PA and pcDNA-NP and the eight vRNA pPOLI plasmids to express the eight vRNA segments using Lipofectamine-2000 transfection reagent (Invitrogen) according to the manufacturer's

instructions. Cells were incubated at 37ºC, 5% CO_2 in DMEM (10% FCS). 24 h post-transfection the cells were rinsed with PBS and the medium was replaced with low serum DMEM (0.5% FCS) and the cells were incubated for a further 48 h at 37ºC, 5% CO_2. Amplification of viruses for viral stocks was carried out by applying virus-containing medium to 80% confluent monolayers of MDBK cells in 75 cm^2 cell culture flasks for 1 h at room temperature, applying fresh MEM supplemented with 0.5% FCS and 2 mM L-glutamine and incubating the cells for 72 h. Viral stocks were centrifuged briefly at 4,000 × *g* to remove cellular debris and supernatants were stored at –80ºC. Viral production and titre was assessed by performing plaque assays.

2.4.2 Plaque assay

Influenza A viruses were serially diluted in MEM supplemented with 0.5% FCS and 2 mM L-glutamine. MDBK cells were rinsed with PBS and infected as monolayers in 6-well plates with 200 µl of virus for 1 h at room temperature. After aspiration of the virus solution, 2 ml of agarose solution (2% agarose in PBS plus an equal volume of MEM supplemented with 0.5% FCS and 2 mM L-glutamine) was overlaid and allowed to set. The 6-well plates were incubated at 37°C, 5% CO_2 for 72 h p.i. when the agarose was removed and the plaques were stained using 2 ml of 0.2% Coomassie Brilliant Blue dye in 7.5% glacial acetic acid and 50% methanol.

2.4.3 Infection of eukaryotic cells with influenza A virus

Viruses were diluted in the appropriate cell culture media supplemented with 0.5% FCS to the desired multiplicity of infection (MOI). Cell monolayers were infected in appropriately sized dishes for 1 h at room temperature. The virus solution was aspirated and replaced with the appropriate cell culture media supplemented with 0.5% FCS to cover the cells. Cells were harvested at indicated time points. For cells that were treated with PPP6C siRNAs, cells were transfected twice prior to infection (see section 2.12). Where cycloheximide (CHX) was used, DMEM was also supplemented with 100 μg/ml of the drug.

2.4.4 Growth curve analysis

Growth curve analysis was performed by infecting 80% confluent MDBK cells in 3.5 cm dishes at a MOI of 0.001 with influenza A viruses and harvesting the supernatant every 12 h p.i. for 72 h. Viral titres were determined by plaque assay.

2.5 RNA analyses

2.5.1 RNP reconstitution assay

RNP reconstitution assays were performed in approximately 1 $\times 10^6$ HEK 293T cells in 3.5 cm dishes by transfection of 1 ug of each of the relevant plasmids using Lipofectamine-2000 (Invitrogen) in 1.5 ml of DMEM supplemented with 10% FCS. Cells were harvested at 48 h post-transfection.

2.5.2 TRIzol extraction of RNA

Unless otherwise indicated, RNA was extracted from cells and samples using TRIzol reagent (Invitrogen) according to the manufacturer's instructions. Briefly, cells or sample were resuspended in an appropriate volume of TRIzol reagent and incubated for 5 min at room temperature. Chloroform was added at a volume of one fifth of TRIzol reagent, followed by centrifugation at 17,000 × *g* for 15 min. The clear upper liquid layer was then transferred to a clean microcentrifuge tube and an equal volume of isopropanol was added, followed by centrifugation at 17,000 × *g* for 15 min. Where indicated, RNA was precipitated in the presence of 10 µg of tRNA from *E. coli* MRE 600 (Roche). The RNA pellet was washed in 70% ethanol and dissolved in an appropriate volume of ddH_2O, before being stored at –20°C.

2.5.3 Primer extension analyses

Segment-specific oligodeoxyribonucleotides were used to detect viral NA RNAs ([5'-TGGACTAGTGGGAGCATCAT-3'] detecting vRNA and [5'-TCCAGTATGGTTTTGATTTCCG-3'] detecting mRNA and cRNA) and NS RNAs ([5'-TGATTGAAGAAGTGAGACACAG-3'] detecting vRNA and [5'-CGCTCCACTATTTGCTTTCC-3'] detecting mRNA and cRNA). The primer detecting cellular 5S rRNA (5'-TCCCAGGCGGTCTCCCATCC-3') was included as an internal control when required.

2.5.3.1 ^{32}P labelling of oligodeoxyribonucleotides

Oligodeoxyribonucleotides were labelled in a 10 µl reaction by incubating 1 pmol of primer with 10 µCi γ-^{32}P-ATP (PerkinElmer) and 2.5 U of PNK (Roche) in 1× kinase buffer A (Roche). The reaction was incubated for 1 h at 37°C. Excess γ-^{32}P-ATP was removed using a QIAGEN nucleotide removal kit, according to the manufacturer's instructions. Radiolabeled oligodeoxyribonucleotides were eluted in 30 µl of ddH_2O and stored at –20°C.

2.5.3.2 Primer extension assay

RNA samples were analysed by primer extension as previously described (Robb *et al.*, 2009). Briefly, RNA was mixed with an excess of two ^{32}P-labelled oligodeoxyribonucleotides in 5 µl and denatured by heating to 95°C for 3 min. The mixture was immediately cooled on ice and transferred to 50°C prior to the addition of 5 µl of a 2 × transcription mix (2× First Strand buffer [Invitrogen], 20 mM dithiothreitol [DTT], 1 mM dNTP mix [Fermentas] and 50 U of SuperScript III [Invitrogen]), also heated to 50°C. After 1 h of incubation, the reaction was heated to 70°C for 10 min to stop the reaction. 8 µl of 90% formamide (90% formamide [Sigma], 10 mM EDTA, 0.001% bromophenol blue and xylene cyanol) was added prior to heating at 95°C for 3 min.

2.5.4 Polyacrylamide gel electrophoresis (PAGE)

DNA products from primer extension assays or RNA products from *in vitro* transcription assays were analysed on polyacrylamide gels (acrylamide:bisacrylamide, 19:1) (ProtoGel, National Diagnostics) in 7 M urea and 1× TBE (90 mM Tris, 90 mM orthoboric acid and 2.5 mM ETDA), respectively. Gels were polymerised by the addition of ammonium persulfate (APS) to 0.2% and TEMED (*N*,*N*,*N′*,*N′*-Tetramethylethylenediamine) to 0.02%. The gels were run at 1200 V in 1× TBE buffer. Bands were detected by autoradiography and quantitation was performed using

phosphor Fujifilm imaging plates and a Fujifilm FLA-5000 fluorescent image analyser. Data were analysed using Aida software (Raytest).

2.6 Sodium dodecyl sulphate polyacrylamide gel electrophoresis (SDS-PAGE)

2.6.1 Gel electrophoresis of proteins

A discontinuous PAGE system cast in a 'mini-protean' protein gel apparatus (Bio-Rad) was used for gel electrophoresis of all proteins. Resolving gels contained 8–13% acrylamide (acrylamide:bisacrylamide, 29:1) in 375 mM Tris-HCl (pH 8.8) and 0.1% SDS and the stacking gel contained 3.2% acrylamide (acrylamide:bisacrylamide, 29:1) in 125 mM Tris-HCl (pH 6.8) and 0.1% SDS. Polymerisation of the gels was carried out by the addition of APS and TEMED to a final concentration of 0.2% and 0.02%, respectively.

Protein samples were mixed with an equal volume of 2× Laemmli buffer (125 mM Tris-HCl [pH 6.8], 4% SDS, 20% glycerol, 10% β-mercaptoethanol and 0.01% bromophenol blue) and heated at 99°C for 5 min. Samples were then loaded onto the gel and run at 120 V in SDS-PAGE running buffer (25 mM Tris, 250 mM glycine and 0.1% SDS) at room temperature. A pre-stained protein marker ‘Precision plus protein all blue standards’ (Bio-Rad) was run in parallel.

2.6.2 Western blotting

Separated proteins were transferred to nitrocellulose membrane (GE Healthcare Life Sciences) in transfer buffer (30 mM Tris, 20 mM glycine, 10% methanol), at 100 V at 4°C. The nitrocellulose blot was then blocked in 2.5% non-fat milk in PBS (0.1% Tween-20) for 1 h at room temperature. The blot was then incubated with the indicated antibodies diluted in 2.5% non-fat milk in PBS (0.1% Tween-20) for 1 h at room temperature or at 4°C overnight on a rotating wheel. Blots were washed three times in PBS (0.1% Tween-20) (10 min for each wash), then incubated for 1 h with an appropriate secondary antibody conjugated to horseradish peroxidase (HRP). Blots were then washed a further three times in PBS (0.1% Tween-20) (10 min for each wash). Subsequently the blots were developed by chemiluminescence using either Immobilon Western chemiluminescent HRP substrate (Millipore) or Amersham ECL Western blotting system (Amersham Biosciences). Blots were incubated for 1 min with the chemiluminescent reagent, drained, covered in acetate and exposed to X-ray film (Super RX Fuji Medical X-Ray film, Kodak). Data were analysed using densitometry and Aida software (Raytest).

2.6.3 Silver and Coomassie staining of proteins

For silver-staining, proteins separated by SDS-PAGE were transferred to a clean plastic dish and fixed in 50% methanol and 10% acetic acid for 10 min. The fixed gel was then sensitised in 50% methanol and 2.5% sensitizer from the SilverXpress silver staining kit

(Invitrogen) prior to washing three times in dH_2O. The gel was then stained and developed according to the manufacturer's instructions. For Coomassie staining, proteins separated by SDS-PAGE were transferred to a clean plastic dish and washed three times with dH_2O (10 min washes) and stained with Coomassie Brilliant Blue (SimplyBlue SafeStain; Invitrogen) according to the manufacturer's instructions.

2.7 Isolation of viral ribonucleoprotein (RNP) complexes by RNA-based affinity purification

Approximately 3×10^7 HEK 293T-PP7CP cells were seeded into 15 cm dishes and cultured for 48 h in DMEM supplemented with 10% FCS and hygromycin-B (500 µg/ml) at 37°C, 5% CO_2. Alternatively, approximately 3×10^7 HEK 293T cells were transfected with pcDNA-PP7CP-$His_{6\times}$ using Lipofectamine-2000 according to the manufacturer's instructions and incubated for 48 h in DMEM supplemented with 10% FCS at 37°C, 5% CO_2. Cells were rinsed with PBS and infected at an MOI of 5 for 1 h at room temperature with wild-type or PP7-tagged influenza A/WSN/33 viruses and incubated for a further 6–9 h in DMEM supplemented with 0.5% FCS at 37°C, 5% CO_2. 6–9 h p.i. cells were collected by centrifugation at 200 × *g* for 5 min at 4°C and washed with ice cold PBS. Cells were collected by centrifugation at 200 × *g* for 5 min at 4°C, flash-frozen and stored at –80°C.

Cells were thawed on ice and lysed in 4 ml of Tris lysis buffer (50 mM Tris-HCl [pH 8.0], 200 mM NaCl, 33% glycerol, 20 mM imidazole, 0.5% Igepal CA-630 [Sigma], 1

mM DTT, 1× complete EDTA-free protease inhibitor cocktail [Roche]) by rotation for 1 h at 4°C and then the soluble and insoluble fractions were separated by centrifugation at 17,000 × *g* for 5 min at 4°C. The soluble fraction was diluted 1:5 with Ni-NTA binding buffer (20 mM Tris-HCl [pH 8.0], 200 mM NaCl, 20 mM imidazole, 1 mM $MgCl_2$ and 1× complete EDTA-free protease inhibitor cocktail) and incubated with 4 ml Ni-NTA agarose (QIAGEN) for 2 h by rotation at 4ºC. Ni-NTA agarose was washed extensively with Ni-NTA wash buffer (20 mM Tris-HCl [pH 8.0], 200 mM NaCl, 40 mM imidazole, 1 mM $MgCl_2$, 0.1% Igepal CA-630, 10% glycerol, 1× phenylmethanesulfonylfluoride [PMSF]) and PP7CP-bound RNPs were eluted in 5 ml of Ni-NTA elution buffer (20 mM Tris-HCl [pH 8.0], 200 mM NaCl, 250 mM imidazole, 1 mM $MgCl_2$, 0.1% Igepal CA-630, 10% glycerol, 1× complete EDTA-free protease inhibitor cocktail) for 2 h at 4°C by rotation. Eluates were subsequently analysed for proteins by SDS-PAGE and silver-staining and RNA was extracted and analysed for by primer extension using NA-specific primers. Eluates were concentrated to 1 ml using Amicon Ultra-4 (100K MWCO) centrifugation devices (Millipore) prior to density gradient centrifugation.

RNPs were isolated by ultracentrifugation on a discontinuous glycerol gradient (1 ml each of 70%, 50%, 40%, and 33%) in 50 mM Tris-HCl (pH 8.0), 200 mM NaCl and 1 mM $MgCl_2$. The gradients were centrifuged at 192,000 × *g* (45,000 rpm) in a Beckman SW55Ti rotor for 4 h at 4°C. Fractions of approximately 300 µl were collected dropwise from the bottom of the tube. Fractions were analysed for RNA by primer extension using NA-specific primers. Proteins were analysed by SDS-PAGE and silver staining and Western blotting using polyclonal antibodies directed against PB2 and NP.

Fractions enriched with RNPs were pooled and used for electron microscopy and *in vitro* activity assays.

2.8 Recombinant influenza virus RdRP purification

Recombinant influenza A virus RdRP with a protein-A tag on the PB2 subunit was expressed using the Multibac system in Sf9 insect cells (Bieniossek *et al.*, 2008). 1L Sf9 cell suspension cultures at 1.2 $\times 10^6$ cells/ml were infected with recombinant baculovirus at an MOI of 1 and incubated for 72 h at 27°C. Infected Sf9 cells were harvested by centrifugation at 800 × *g* for 15 min at 4°C and lysed by continuous sonication for 90 s with a Soniprep 150 (MSE) at 10 microns amplitude in lysis buffer (50 mM Tris-HCl [pH 8.0], 500 mM NaCl, 10% glycerol, 0.05% octylthioglucoside, 1× complete EDTA-free protease inhibitor cocktail [Roche] and 100 μg/ml RNase A). The lysate was clarified by centrifugation at 35,000 × *g* for 45 min at 4°C and the supernatant was incubated with washed IgG Sepharose (GE Healthcare Life Sciences, approximately 2 ml bead slurry per litre of original culture) for 3 h at 4ºC. After binding, the beads were washed extensively with 50 mM Tris-HCl (pH 8.0), 500 mM NaCl, 10% glycerol and 0.05% octylthioglucoside. The recombinant RdRP was released using AcTEV protease (150 U/ml of IgG Sepharose) (Invitrogen) at 4ºC overnight in 50 mM Tris-HCl (pH 8.0), 500 mM NaCl, 10% glycerol, 0.05% octylthioglucoside and 2.5 mM reduced glutathione. Released recombinant protein was subsequently analysed by SDS-PAGE and Coomassie Brilliant Blue staining.

Recombinant influenza A/WSN/33 virus RdRP expressed in mammalian cells was prepared by transiently transfecting approximately 2 $\times 10^7$ HEK 293T cells with 60 µg of each of the RdRP expression plasmids (pcDNA-PA, pcDNA-PB2-TAP and pcDNA-PB1 for wild-type RdRP or pcDNA-PB1a for active site mutant RdRP) using Lipofectamine-2000 (Invitrogen) according to the manufacturer's instructions. Cells were incubated for 48 h in DMEM supplemented with 10% FCS at 37°C, 5% CO_2 prior to collection by centrifugation at 200 × *g* for 5 min at 4°C. Cells were then washed with ice cold PBS and pelleted by centrifugation at 200 × *g* for 5 min at 4°C and then lysed in 2 ml of Tris lysis buffer (50 mM Tris-HCl [pH 8.0], 200 mM NaCl, 33% glycerol, 0.5% Igepal CA-630, 1 mM DTT, 1× complete EDTA-free protease inhibitor cocktail) by rotation for 1 h at 4°C. The soluble and insoluble fractions were separated by centrifugation at 17,000 × *g* for 5 min at 4°C and the soluble fraction was diluted 1:5 with binding buffer (20 mM Tris-HCl [pH 8.0], 150 mM NaCl, and 1× complete EDTA-free protease inhibitor cocktail) and incubated with 400 µl of IgG Sepharose (GE Healthcare Life Sciences) for 2 h by rotation at 4°C. IgG Sepharose was washed extensively with wash buffer (20 mM Tris-HCl [pH 8.0], 150 mM NaCl, 0.1% Igepal CA-630, 10% glycerol and 1× PMSF) and the RdRP was released by cleavage overnight at 4°C with 20 U of AcTEV (Invitrogen) in 500 µl of cleavage buffer (10 mM Tris-HCl [pH 8.0], 150 mM NaCl, 0.1% Igepal CA-630, 10% glycerol, 1 mM DTT, 1× complete EDTA-free protease inhibitor cocktail). AcTEV was removed by binding the eluate to 100 µl Ni-NTA agarose for 30 min at 4°C by rotation and centrifuging at 17,000 × *g* for 5 min at 4°C. The supernatant was concentrated to 50 µl using Amicon Ultra-4 (100K MWCO) centrifugation devices (Millipore) and stored at 4°C. Mock

samples as negative controls were prepared by processing HEK 293T cells transfected with empty vector (pcDNA3A) as described above.

2.9 *In vitro* activity assays

RNP activity was assessed in a 20 µl reaction mixture containing 10 µl of purified RNPs, incubated for 16 h at 30°C with 1 mM ATP, 0.5 mM of each CTP, GTP, and UTP (Amersham), 5 mM $MgCl_2$, 2 mM DTT and 5 U RNasin, with 360 ng β-globin mRNA (Sigma) or 0.5 mM ApG (Sigma) as indicated. Where indicated, 500 ng of purified recombinant influenza virus RdRP expressed in Sf9 cells or 40 ng of wild-type or PB1a mutant RdRP expressed in mammalian HEK 293T cells was included. Transcription products were extracted using TRIzol reagent (Invitrogen) according to the manufacturer's instructions and precipitated with isopropanol in the presence of 10 µg of tRNA from *E. coli* MRE 600 (Roche) prior to analysis by NA gene-specific primer extension and 6% PAGE in 7M urea.

Alternatively, RNP activity was assessed in a 10 µl reaction mixture containing 5 µl of purified RNPs incubated for 2 h at 30°C with 1 mM ATP, 0.5 mM GTP and 0.16 µM of [α-^{32}P]UTP for cRNPs or 0.16 µM of [α-^{32}P]CTP for vRNPs, 0.5 mM ApG, 5 mM $MgCl_2$, 2 mM DTT and 5 U RNasin, with 10 ng of wild-type RdRP, PB1a active site mutant RdRP or mock purified sample. RNA was extracted by adding an equal volume of phenol/chloroform 1:1 (pH 4.3) and vortexing for 5 min at room temperature before centrifuging at 17,000 × *g* for 20 min at 4°C. RNA was precipitated from the aqueous

fraction by adding 5 volumes of acetone/ethanol 3:1 in the presence of 10 µg of tRNA from *E. coli* MRE 600 and incubating for 30 min at –20°C prior to centrifuging at 17,000 × *g* for 20 min at 4°C. The RNA pellet was washed in ice cold 70% ethanol before dissolving in 10 µl formamide (90% formamide, 10 mM EDTA, 0.001% bromophenol blue and 0.001% xylene cyanol) and heating to 95°C for 3 min and cooling directly on ice before being analysed by 20% PAGE containing 7 M urea.

Activity of purified recombinant RdRP polymerase was assessed using an [α-^{32}P]GTP incorporation assay as previously described (Brownlee & Sharps, 2002). Briefly, 1.5 µl of purified polymerase and 15 pmol of each of 5′ end (15 nt [5′-AGUAGAAACAAGGCC-3′]) and 3′ end (14 nt [5′-GGCCUGCUUUUGCU-3′]) promoter templates were incubated in a 3 µl reaction mixture for 2 hours at 30°C with 1 mM ATP, 0.5 mM CTP, 0.5 mM UTP and 0.1 µM [α-^{32}P]GTP, 0.5 mM ApG, 5 mM $MgCl_2$, 2 mM DTT and 5 U RNasin. After 2 hours, 10 µl formamide was added (90% formamide, 10 mM EDTA, 0.001% bromophenol blue and 0.001% xylene cyanol) and heated to 95°C for 3 min and cooling directly on ice before being analysed by 20% PAGE containing 7 M urea.

2.10 Strep-tag affinity-purifications

To purify PB2-Strep complexes by Strep-tag affinity-chromatography (Schmidt & Skerra, 2007), infections were carried out with PB2-Strep or WT virus at an MOI of 5 using approximately 4 ×10^7 HEK 293T cells in two 15 cm dishes. Alternatively,

transfections were carried out using Lipofectamine-2000 (Invitrogen) with 60 µg of each of the indicated pcDNA plasmids (180 µg total) using approximately 2 ×10^7 HEK 293T cells in two 15 cm dishes. At 7 h p.i. or 48 h post-transfection cells were harvested, washed in ice cold phosphate-buffered saline (PBS) and pelleted at 450 × *g* for 5 min at 4°C. Lysates were prepared by incubating cells on a rotating wheel for 1 h at 4°C in lysis buffer (50 mM Tris-HCl [pH 8.0], 200 mM NaCl, 33% glycerol, 0.5% Igepal CA-630 and 1 mM DTT with 1× complete EDTA-free protease inhibitor cocktail [Roche]). The soluble fraction was separated by centrifugation at 17,000 × *g* for 5 min at 4°C, diluted 1:5 with binding buffer (20 mM Tris-HCl [pH 8.0], 200 mM NaCl and 1× complete EDTA-free protease inhibitor cocktail) and incubated overnight at 4°C with 200 µl of washed 50% suspension Strep-Tactin Superflow high capacity resin (IBA GmbH). The resin was washed extensively with wash buffer (20 mM Tris-HCl [pH 8.0], 150 mM NaCl, 1 mM EDTA, 0.1% Igepal CA-630, 10% glycerol and 1 mM PMSF), and proteins were eluted in 2 ml of elution buffer (20 mM Tris-HCl pH 8.0, 150 mM NaCl, 1 mM EDTA, 0.1% Igepal CA-630, 10% glycerol, 1× complete EDTA-free protease inhibitor cocktail and 2 mM *d*-desthiobiotin [IBA GmbH]) for 2 h on a rotating wheel at 4°C. Eluates were concentrated using Amicon Ultra-4 (3 kDa MWCO) centrifugation devices prior to analysing by SDS-PAGE and silver staining or primer extension analysis using NA-specific primers or mass spectrometry.

2.11 GST-pulldown assay

GST, GST-PPP6C, GST-PPP6R1, GST-PPP6R2, and GST-PPP6R3 were expressed in *E. coli* strain BL21 (DE3) by isopropyl β-D-1-thiogalactopyranoside (IPTG) induction at a concentration of 0.1 mM overnight at 21ºC. Cells were harvested by centrifugation at 5000 × *g* for 20 min at 4ºC. Cell pellets were resuspended in lysis buffer (20 mM Tris-HCl [pH 8.0], 150 mM NaCl, 1 mM $MgCl_2$, 10% glycerol, 1× complete EDTA-free protease inhibitor cocktail and 0.25 mg/ml lysozyme) and sonicated for 5 min (30 s on/off) with a Soniprep 150 (MSE) at 10 microns amplitude. The lysate was clarified by centrifugation at 35,000 × *g* for 30 min at 4ºC and the supernatant was incubated with 100 µl of washed glutathione Sepharose (GE Healthcare Life Sciences) for 3 h at 4ºC. After binding, the beads were washed extensively with 20 mM Tris-HCl (pH 8.0), 200 mM NaCl, 1 mM $MgCl_2$, 10% glycerol, 0.1% Igepal CA-630 and 1 mM PMSF. Beads were then incubated for 2 h at 4°C with 40 µg of recombinant RdRP in a total volume of 1 ml in 20 mM Tris-HCl (pH 8.0), 200 mM NaCl, 1 mM $MgCl_2$, 10% glycerol, 0.1% Igepal CA-630 and 1× complete EDTA-free protease inhibitor cocktail. After binding, the beads were washed extensively with 20 mM Tris-HCl (pH 8.0), 200 mM NaCl, 1 mM $MgCl_2$, 10% glycerol, 0.1% Igepal CA-630 and 1 mM PMSF. Recombinant proteins were at eluted at room temperature for 15 min in 250 µl of 50 mM Tris-HCl (pH 8.0), 200 mM NaCl, 10 mM reduced glutathione, 1 mM $MgCl_2$, 10% glycerol and 1× complete EDTA-free protease inhibitor cocktail. Eluates were analysed by SDS-PAGE, Coomassie Brilliant Blue staining and Western blotting with an anti-RdRP antibody.

2.12 RNA interference of PPP6C

Small interfering RNAs (siRNAs; Sigma) were designed using the Dharmacon siDESIGN center. Three independent siRNA duplexes with 3′ dTT overhangs were designed against the PPP6C gene (accession: NM_001123369) with different starting positions 239 (siPPP6C1 [5′-GGACAAGTATGTGGAAATA-3′]), 494 (siPPP6C2 [5′-TCATGAGAGTAGACAGATA-3′]) and 875 (siPPP6C3 [5′-GCACGAAGGCTATAAATTT-3′]). To knockdown PPP6C, HEK 293T cells or A549 cells were transfected in suspension or as a monolayer, respectively, with 0.18 nmol/ml of siRNA using Lipofectamine-2000 (Invitrogen) according to the manufacturer's instructions. The AllStars negative control siRNA (QIAGEN) was used as a negative control. The transfection was repeated 24 h later on the cell monolayers and the cells were incubated for a further 24 h prior to infection. After two consecutive transfections with siRNAs, HEK 293T and A549 cells in 24-well dishes were resuspended in PBS and the cell viability was determined using a CellTiter-Glo luminescent assay (Promega) according to the manufacturer's instructions. PPP6C protein levels were determined by densitometry of Western blots with an anti-PPP6C polyclonal antibody.

2.13 Mass spectrometry

2.13.1 Sample preparation and mass spectrometry

Affinity-purified samples from infected cells were prepared for mass spectrometry by boiling in 2× Laemmli buffer and running a short distance into a polyacrylamide gel (Thermo Scientific) to remove detergent and salts. The entire sample was then excised from the gel with a clean scalpel. Samples were submitted to the Central Proteomics Facility (Sir William Dunn School of Pathology, University of Oxford) for tryptic digestion and mass spectrometry analyses. Samples were run on a Thermo LTQ XL Orbitrap or a Thermo Q Exactive Orbitrap mass spectrometer.

2.13.2 Analyses of mass spectrometry

Data files were converted from .RAW to .MGF using ProteoWizard (Chambers *et al.*, 2012). For data that was generated by the Thermo LTQ XL Orbitrap files were analysed using Mascot (Matrix Science, London, UK) by searching peptide spectral matches against a custom database that concatenated the proteome of the influenza A/WSN/33 virus with that of *Homo sapiens*, with common contaminants and decoy sequences. Tolerance was set at 20 ppm for MS and 0.6 Da for MS/MS. Carbamidomethylation of cysteine was set as a fixed modification, and methionine oxidation was set as a variable modification. Positive identifications were accepted with a confidence interval of 95%

or greater and two unique peptides. For data that was generated by the Thermo Q Exactive Orbitrap mass spectra were analysed using the Central Proteomics Facilities Pipeline (CPFP) (Trudgian *et al.*, 2010). Data from experimental replicates were merged. Peptide spectral matches were made to custom databases that concatenated the sequence of the tagged PB2-Strep protein, with the proteomes of *Homo sapiens* and of the influenza A/WSN/33 virus, as well as common contaminants and decoy sequences. The viral proteome in the database was expanded to include hypothetical as well as experimentally confirmed proteins, as previously described (Hutchinson *et al.*, 2012). For the identification of peptides, CPFP uses iProphet (Shteynberg *et al.*, 2011) to combine searches made with Mascot (Matrix Science, London, UK), OMSSA (Geer *et al.*, 2004) and X!TANDEM (Craig & Beavis, 2004), with peptide identifications validated using PeptideProphet (Keller *et al.*, 2002). Combined protein identifications were assigned using ProteinProphet (Nesvizhskii *et al.*, 2003) with a 1% false discovery rate (FDR). Searches were made for peptides with up to two missed cleavages, with carbamidomethylation of cysteine as a fixed modification and oxidation of methionine and deamidation of glutamine and asparagine as variable modifications. A minimum of 2 peptides were required to make positive protein identifications. Label-free protein quantitation was performed using spectral index normalized quantitation (SINQ) in CPFP (Trudgian *et al.*, 2011). Common contaminants, keratins, serum albumin and decoy sequences were manually removed from the data before further processing. To control for non-specific binding, proteins were identified which were present in all three experiments in both the PB2-Strep and WT samples (93 proteins from the 619 identified). The median intensity of this set of proteins was used to normalise protein abundance, and the mean abundance of each protein in the PB2-Strep and WT samples

was then calculated (missing data did not contribute to the means). The majority of the proteins consistently found in both the WT and PB2-Strep samples had an abundance in the PB2-Strep sample that was within 10-fold of their abundance in the WT sample after normalisation. Proteins that did not increase at least 10-fold in abundance in the PB2-Strep sample when compared to WT were therefore excluded from further analyses. Finally, for each PB2-Strep sample protein abundance was normalised by the amount of PB2-Strep present.

To construct an interaction network, protein-protein interactions were taken from STRING (Search Tool for the Retrieval of Interacting Genes/Proteins) version 9.1 (http://string-db.org) on 10/06/2014 (Jensen *et al.*, 2009) and illustrated using Cytoscape version 3.1.0. (Lopes *et al.*, 2010). Gene Ontology analysis was performed using the PANTHER (Protein ANalysis THrough Evolutionary Relationships) classification system (Mi *et al.*, 2013).

2.14 Microscopy

2.14.1 Electron microscopy and image processing

A 5 µl aliquot of purified RNPs were applied to glow-discharged 200 mesh carbon-formvar copper grids and grids were stained with 2% uranyl acetate. Images were taken on CCD (UltraScan 4000SP, Gatan) with a transmission electron microscope (Tecnai

F30, FEI) operated at 200 kV and at 39,000× nominal magnification. Contrast transfer function estimation and phase flipping was carried out using XMIPP (http://xmipp.cnb.csic.es/) (Scheres *et al.*, 2008). Images were down-sampled by a factor of two, resulting in a pixel size of 6.08 Å/pixels. In total, 529 images were taken resulting in a dataset of 2,456 cRNP particles. Extracted particles (150×150 pixels) were subjected to simultaneous alignment and classification in Relion (http://www2.mrc-lmb.cam.ac.uk/relion/) (Scheres, 2012). The approximate coordinates of the termini were defined in the selected class averages and 2,456 corresponding sub-images (80×80 pixels) were extracted from the original micrographs. Sub-images were aligned and classified using the in-plane rotation angle of the central filament (psi) as prior information. To derive final class-average images of the RdRP and NP-RNA loop ends, particles assigned to either group were subjected to further 2D classification. Class averaging was performed by Juha Huiskonen (Division of Structural Biology, University of Oxford) as a collaboration.

2.14.2 Indirect immunofluorescence and confocal microscopy analysis

To analyse the cellular localisation of viral NP in infected cells that were knockdown for PPP6C or negative control cells, A549 cells on 13 mm cover glasses in 24-well plates were infected with WT virus at an MOI of 1. At 0, 4, 6 and 8 h p.i. cells were washed with PBS and fixed with 4% paraformaldehyde in 250 mM HEPES (pH 7.5) for 15 min at room temperature. Cells were permeabilized with 0.5% Triton X-100 in PBS for 15 min at room temperature, washed with PBS and subsequently blocked in

blocking PBS containing 1% bovine serum albumin, 0.2% porcine gelatine (Sigma) and 0.1% Tween-20 overnight at 4ºC. Indirect immunofluorescence was performed using a mouse monoclonal anti-NP antibody at a 1:500 dilution in blocking PBS for 1 h at room temperature. Coverslips were washed extensively with PBS before labelling with a Cy3-conjugated anti-mouse secondary antibody (Jackson ImmunoResearch Laboratories) at a 1:500 dilution in blocking PBS for 1 h at room temperature. Coverslips were washed extensively with PBS prior to mounting in Mowiol (Calbiochem) containing 1 µg/ml 4′,6′-diamidino-2-phenylindole (DAPI; Sigma). Cells were imaged on an Olympus Fluoview FV1000 confocal laser scanning microscope, using a 60×/1.35 Oil UPlanSApo objective for detailed imaging and a 40×/1.30 Oil UPlan FLN objective to capture four images in a random field of view from each sample for scoring. Images were processed using ImageJ and scored using the Cell Counter plugin.

Chapter 3: RNA-based affinity purification of influenza virus ribonucleoproteins

3.1 Introduction

Influenza viruses are negative-strand RNA viruses belonging to group V of the Baltimore classification system (Baltimore, 1971). This group of viruses comprise several significant human, animal and plant pathogens that have considerable health and economic impact globally. Notable examples of negative-strand RNA viruses that cause disease in humans are rabies virus, mumps virus, measles virus and respiratory syncytial virus, as well as the haemorrhagic fever-causing Ebola and Lassa viruses. Negative-strand RNA viruses are characterised by a single-stranded negative-sense viral RNA (vRNA) genome that is transcribed into mRNA and replicated via complementary RNA (cRNA) intermediate by a virally-encoded RNA-dependent RNA

polymerase (RdRP) (Morin *et al.*, 2013). Biochemical studies have shown that genomic vRNA molecules of influenza viruses are assembled into viral ribonucleoprotein complexes (vRNPs) that contain single-stranded vRNA that is encapsidated by viral nucleoprotein (NP) and is bound at the 5′ and 3′ ends by the viral RdRP. Once a full-length complementary cRNA has been synthesised using vRNA as a template, this cRNA is believed to assemble with viral RdRP and NP into a complementary ribonucleoprotein complex (cRNP) for the synthesis of multiple copies of progeny vRNPs, which subsequently serve for secondary rounds of transcription, genome amplification or are exported from the nucleus for packaging into progeny virions (Fodor, 2013; Resa-Infante *et al.*, 2011). Although a cRNP complex that is analogous to a vRNP complex has long been assumed to serve as a replicative intermediate for influenza virus genome replication, such cRNP complexes of influenza virus, or indeed of any negative-strand RNA virus, have not been isolated and studied. This shortcoming can be attributed to the technical difficulties of separating the cRNP from vRNP during purification of ribonucleoprotein complexes from infected cells. Furthermore, the level of cRNA accumulation in an infected cell is 10 to 100-fold lower compared to vRNA levels (Hay *et al.*, 1977; Kawakami *et al.*, 2011). The separate isolation of cRNP and vRNP complexes from infected cells for functional, structural and proteomic studies would advance our understanding of the molecular mechanisms of genome replication. Previous studies of viral RNP complexes has relied on the isolation of virion-derived vRNPs, or the purification of the viral RdRP from transfected or infected cells, which results in a mixed population of RNPs with vRNPs representing the majority of the population (Arranz *et al.*, 2012; Coloma *et al.*, 2009; Martin-Benito *et al.*, 2001; Moeller *et al.*, 2012). Therefore, previous biochemical studies have been unable to

distinguish between cRNP and vRNP complexes and consequently, cRNP complexes remain uncharacterised both structurally and functionally, greatly hampering our understanding of an essential component in the replication of the influenza virus genome. Revealing the fundamental differences between cRNP and vRNP function is of great importance in understanding how the synthesis of mRNA, cRNA and vRNA by the viral RdRP is regulated. Therefore, the aim of this chapter is to develop a method for the separate isolation of cRNP and vRNP complexes from infected cells for subsequent functional, structural and proteomic analyses with a view to heightening our understanding of the role of cellular and viral factors in the molecular biology of influenza virus genome replication.

3.2 Rationale and strategy for the insertion of an RNA tag into the influenza virus genome

The separate isolation of viral RNP complexes from infected cells that are assumed to contain the same protein components necessitates the development of an entirely RNA-based strategy for RNP affinity purification. Several strategies for RNA-based affinity purification of RNP complexes have been reported in the literature. Early attempts relied on the hybridisation of biotinylated complementary oligonucleotides to a target RNA (Lingner & Cech, 1996). This method, however, has technical limitations that are imposed by the requirement for the binding of the oligonucleotide to an accessible single-stranded stretch of RNA within the RNP. It was reasoned that such a single-stranded stretch of RNA would be unlikely to be accessible within the context of a viral

RNP due to encapsidation by oligomeric NP. Instead a more feasible approach would rely on the formation of an accessible secondary RNA structure, or RNA tag, within the RNP complex for the binding to a specific ligand. There is an increasing body of evidence that the packaging of eight individual vRNP complexes into nascent virions is driven by *cis*-acting packaging signals in the form of secondary RNA structures that protrude from the surface of the RNP (Gerber *et al.*, 2014; Hutchinson *et al.*, 2010). These hairpin structures form unique networks of direct intermolecular RNA-RNA interactions between different vRNP segments. Therefore, it was reasoned that an RNA hairpin that is bound with high affinity by a ligand could be a suitable RNA tagging strategy. Existing RNA tags can be classified into two categories depending on whether they are naturally occurring or whether they were developed by SELEX (systematic evolution of ligands by exponential enrichment) (Srisawat & Engelke, 2002; Tuerk & Gold, 1990). Examples of naturally occurring RNA tags include bacteriophage RNA translational operator motifs that are bound by the coat proteins of the *Pseudomonas aeruginosa* PP7 and the *Escherichia coli* MS2 bacteriophages (Lim & Peabody, 2002; Stockley *et al.*, 1995). Conversely, a number of RNA aptamers have been developed *in vitro* bind to small molecules such as streptomycin or tobramycin (McKeague & Derosa, 2012). A fundamental distinction between the use of a protein or a non-protein ligand is the ability to express a protein within the cell in which the tagged RNP assembles. Conversely, the use of a small molecule such as tobramycin would require the binding to the tagged RNA after cell lysis. As it was unknown as to whether a secondary RNA structure would remain stable within a viral RNP complex in the absence of its ligand, a strategy that relies on the binding of a ligand *in vivo* was preferred. Therefore, a methodology that relies on the pre-expression of protein ligand

of an RNA tag within a cell was favoured. The aim was to firstly insert an RNA tag into a single gene segment within the influenza virus genome that would allow the specific purification of positive-sense or negative-sense RNA depending on the orientation of the tag and then to generate recombinant viruses containing this RNA tag by reverse genetics. Recombinant viruses harbouring an RNA tag could then be used to infect cells that express a bacteriophage coat protein that binds to the RNA tag with high affinity. It should be noted that the insertion of an RNA tag into the cRNA sense results not only in cRNA that is tagged, but also results in tagged mRNA. Both viral RNA species are positive sense and the RNA tag, therefore, would be recognised in mRNA as well as in cRNA. The PP7 RNA (PP7) that binds to its cognate PP7 coat protein (PP7CP) was selected on the basis that a previous study had successfully purified a small nuclear RNP (snRNP) complex containing a PP7 RNA tag in the cellular 7SK RNA (Hogg & Collins, 2007). Furthermore, the binding affinity of the PP7CP for RNA (K_d = ~1 nM) is an order of magnitude greater than MS2 binding to RNA (K_d = ~10–20 nM) (Lim *et al.*, 2001; Stockley *et al.*, 1995). The PP7CP-RNA co-crystal structure (Figure 3.1) shows that RNA recognition by PP7CP is reliant on the formation of an extended β-sheet surface that forms upon dimerisation, providing a flexible scaffold that recognises RNA with high specificity (Chao *et al.*, 2008).

As the 5′ and 3′ non-coding regions (NCRs) of genomic RNAs contain sequences that are necessary for vRNP incorporation into progeny virions (Gerber *et al.*, 2014; Hutchinson *et al.*, 2010), coding regions of the influenza A/WSN/33 virus genome were selected for the insertion of the PP7 RNA tag. Altering the NCRs within the genome could result in the occlusion of a tagged RNP segment from incorporation into virions,

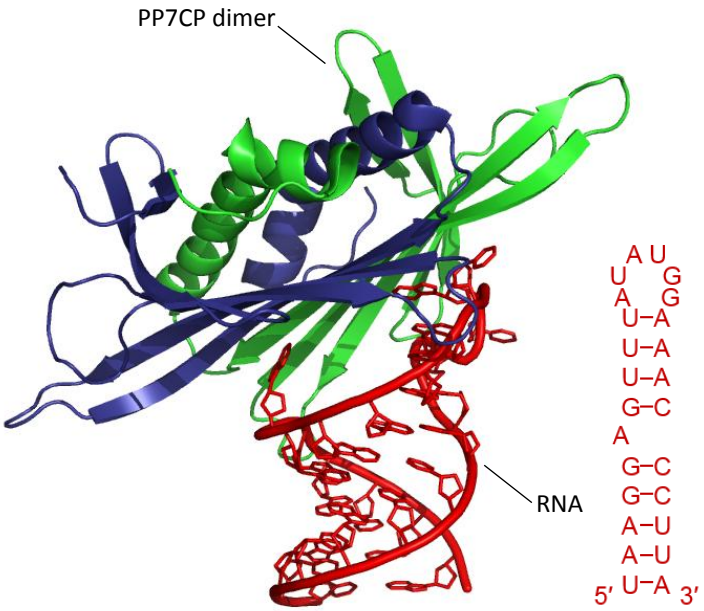


Figure 3.1 Co-crystal structure of the PP7CP protein in complex with its translational operator RNA. PP7CP-RNA complex is shown as a cartoon, with the RNA hairpin (red) binding to a dimer of PP7 (blue and green) across an extended β-sheet surface that is formed by the PP7CP dimer. From Chao *et al*., 2008. PDB code: 2QUX.

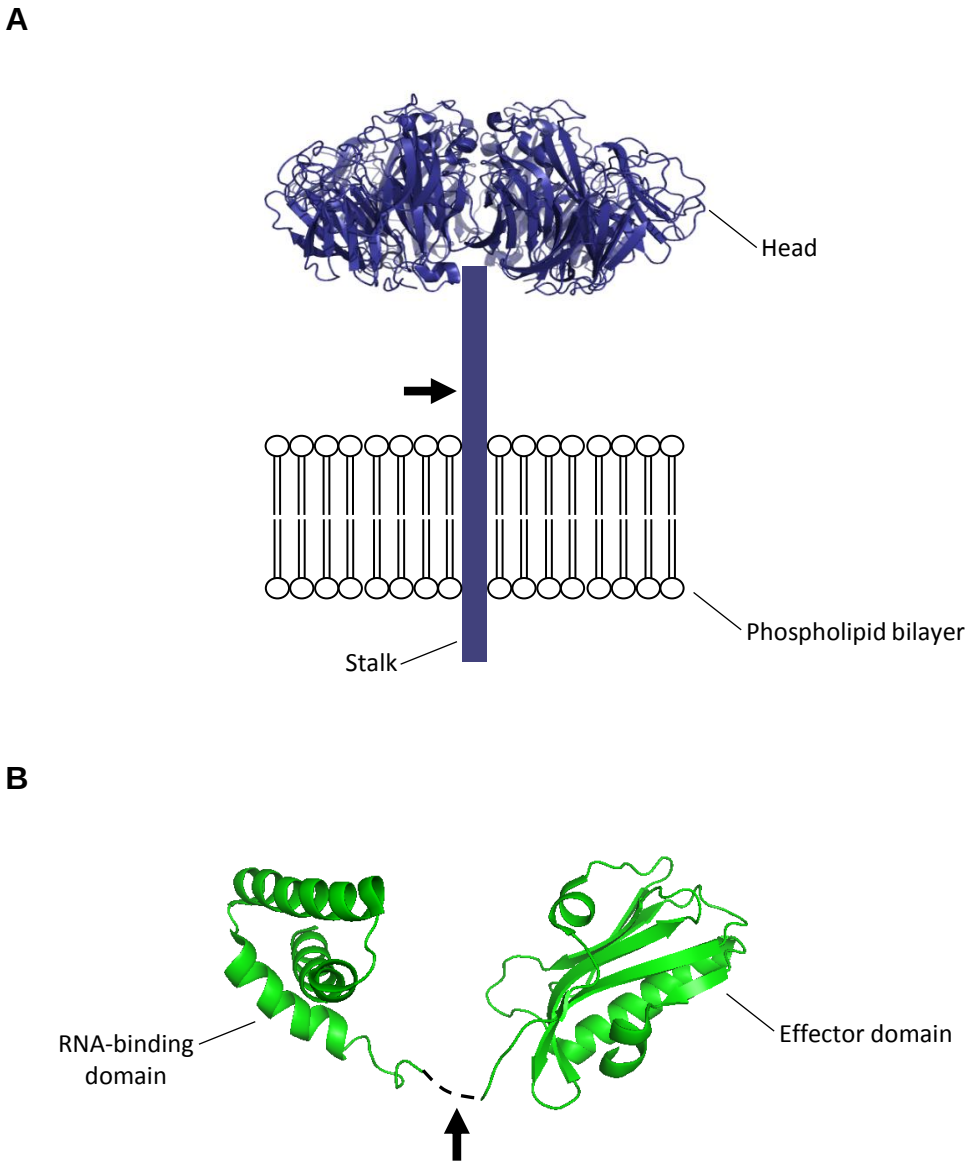


Figure 3.2 Insertion of PP7 RNA into regions of plasticity in the influenza A/WSN/33 virus genome. (A) PP7 RNA was inserted at a position corresponding to Y56 in the stalk region of the NA glycoprotein and (B) at a position that corresponds to M81 in the linker region between the RNA binding domain and effector domain of NS1. Crystal structures were obtained from Russell *et al*., 2006 for NA (PDB code: 2HTY) and Bornholdt & Prasad, 2008 for NS1 (PDB code: 3F5T).

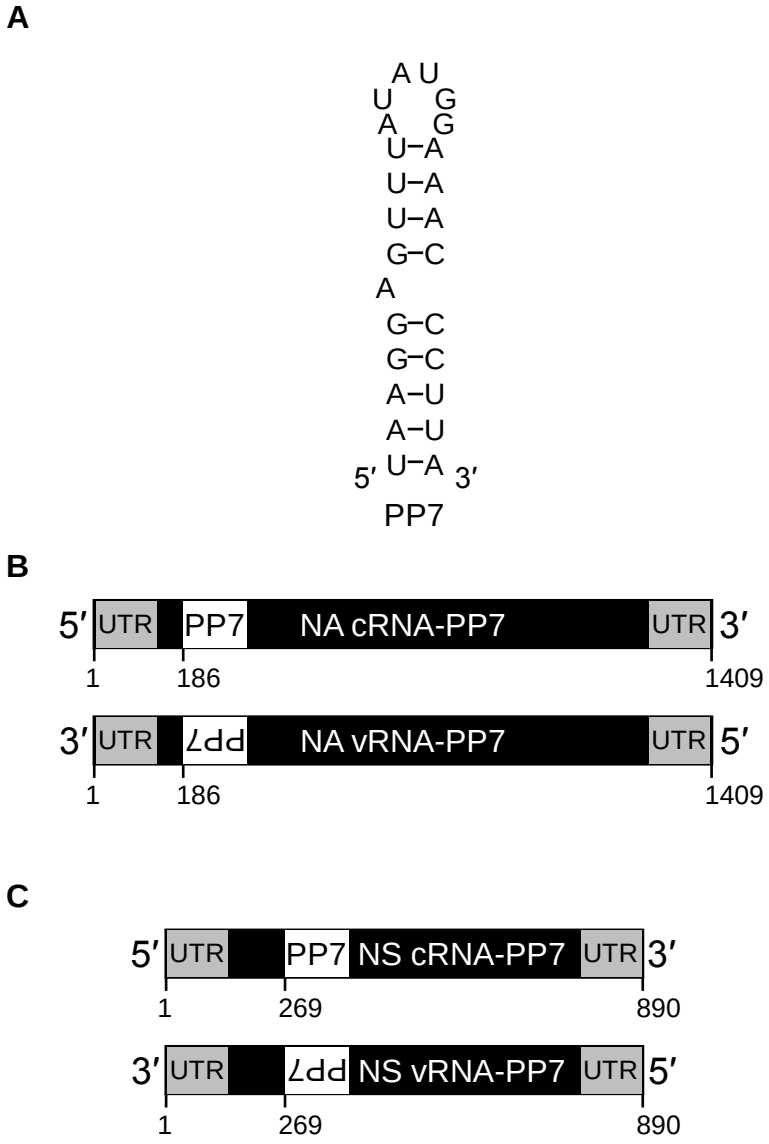


Figure 3.3 Introduction of a PP7 RNA into the genome of influenza A/WSN/33 virus to allow RNA-affinity purification of cRNA or vRNA. (A) Sequence of the PP7 RNA tag and the predicted secondary RNA structure for PP7CP RNA binding as described in Lim and Peabody (2002). (B) Position of the PP7 RNA in the neuraminidase (NA) gene. (C) Position of the PP7 RNA in the non-structural (NS) gene. Untranslated terminal sequences (UTR), the NA ORF (black box), and the PP7 RNA tag are shown.

preventing the generation of recombinant influenza viruses. Regions of the influenza virus genome were selected on the basis of genomic plasticity, defined as positions of potential mutability without impairment of viral protein function and thus, virus replication. Two regions were selected for insertion; the region of NA gene that encodes the stalk and the flexible linker between the RNA-binding and effector domains in the NS1 protein (Figure 3.2 and 3.3). The NA stalk was selected for insertion as previous reports had shown that relatively large insertions and deletions at this position in the genome do not affect the neuraminidase function in replication-competent viruses (Castrucci & Kawaoka, 1993; Luo *et al.*, 1993; Munier *et al.*, 2010; Sorrell *et al.*, 2010). The flexible linker within the NS1 protein was chosen because this region of the protein had been unresolved in the crystal structure and is of unknown function (Bornholdt & Prasad, 2008; Hale *et al.*, 2008). Furthermore, one study had reported the insertion of a tetracysteine motif for biarsenical fluorescent labelling of the NS1 protein (Li *et al.*, 2010). For these reasons, it seemed plausible that the insertion of an RNA tag at this location would not radically affect the function of the NS1 protein and consequently, would not diminish viral fitness.

3.3 Accumulation of tagged viral RNAs in RNP reconstitution assays

To investigate whether the insertion of an RNA tag into the NA or NS gene segments had an effect on transcription or replication by the viral RdRP, viral mRNA, cRNA and vRNA species were analysed by a primer extension assay after the reconstitution of recombinant vRNP complexes in transfected cells (Fodor *et al.*, 2002; Robb *et al.*,

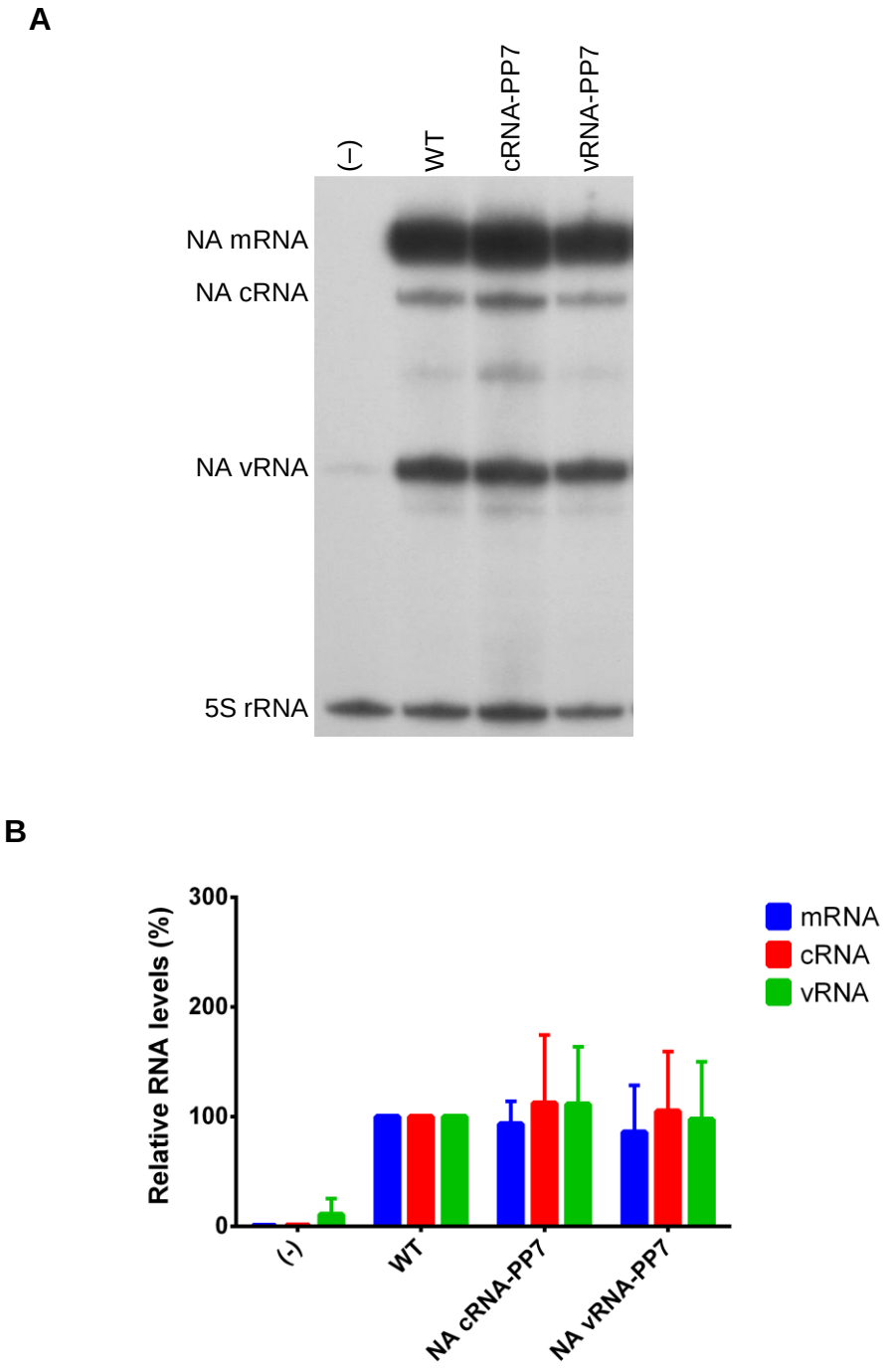
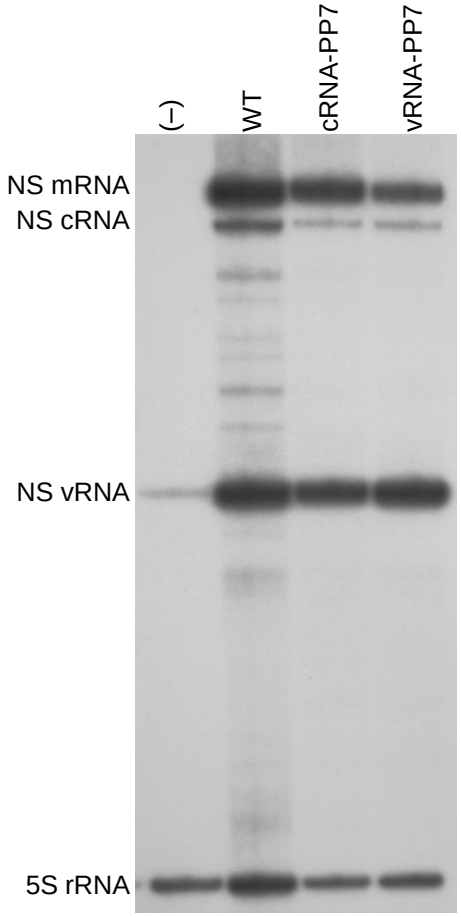


Figure 3.4 Primer extension analyses of NA viral RNA species containing a PP7 RNA tag. HEK 293T cells were transfected with plasmids expressing NP and the viral RdRP proteins PB1, PB2 and PA. Either WT or PP7-tagged NA vRNA expressing vectors were co-transfected. The PB1 plasmid was replaced with an empty plasmid as a negative control. RNA was isolated 48 hours post-transfection and (A) analysed by primer extension using radiolabeled primers for positive sense (mRNA and cRNA) and negative sense (vRNA) NA-specific viral RNAs. Primer extension analysis of 5S rRNA was used as a control. (B) Quantitative analyses of three repeats. RNA levels represent the mean and the error bars represent SDs from three biological repeats.

A


(–)
WT
cRNA-PP7
vRNA-PP7
NS mRNA
NS cRNA
NS vRNA
5S rRNA

B

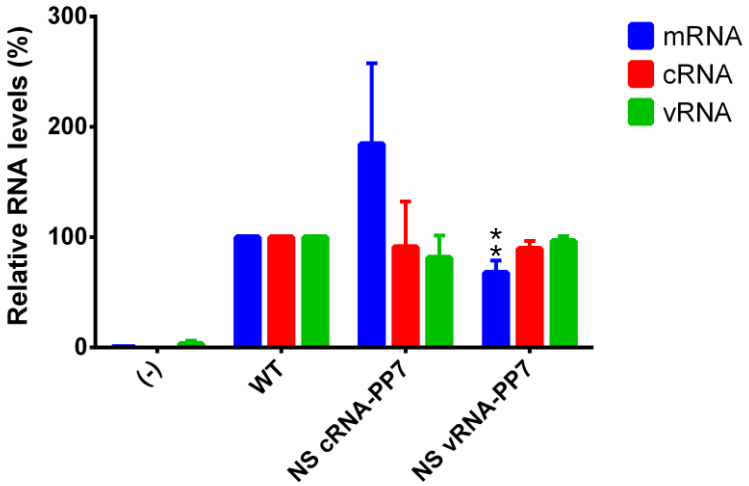

Relative RNA levels (%)
300
200
100
0
mRNA
cRNA
vRNA
**
(-)
WT
NS cRNA-PP7
NS vRNA-PP7

Figure 3.5 Primer extension analyses of NS viral RNA species containing a PP7 RNA tag. HEK 293T cells were transfected with plasmids expressing NP and the viral polymerase proteins PB1, PB2 and PA. Either WT or PP7-tagged NS vRNA expressing vectors were co-transfected. The PB1 plasmid was replaced with an empty plasmid as a negative control. RNA was isolated 48 hours post-transfection and (A) analysed by primer extension using radiolabeled primers for positive sense (mRNA and cRNA) and negative sense (vRNA) NS-specific viral RNAs. Primer extension analysis of 5S rRNA was used as a control. (B) Quantitative analyses of three repeats. RNA levels represent the mean and the error bars represent SDs from three biological repeats. Asterisks indicate a significant difference from WT (** $P < 0.01$, based on a one-sample Student's *t*-test).

2009). In this assay pcDNA plasmids that express viral RdRP subunits and NP are co-transfected into cells along with a pPOLI plasmid that generates a vRNA template for the reconstitution of a vRNP segment. HEK 293T cells were co-transfected with PB1, PB2, PA and NP pcDNA expression plasmids with one of the pPOLI-NA-cRNA-PP7, pPOLI-NA-vRNA-PP7, pPOLI-NS-cRNA-PP7 or pPOLI-NS-vRNA-PP7 plasmids. Wild-type (WT) pPOLI-NA or pPOLI-NS plasmids were used as positive controls and a pcDNA-PB1 plasmid was omitted as a negative control. After 48 hours post transfection (h p.t.), total RNA was isolated and primer extension analyses were performed using NA or NS segment-specific radiolabeled primers. Levels of NA RNAs that contain a PP7 RNA tag were not significantly different to levels of WT NA RNAs (Figure 3.4). Accumulation of NS segment RNAs containing a tag was also comparable to WT (Figure 3.5). It was concluded that the insertion of a PP7 RNA tag into the NA and NS genes did not significantly affect the transcription and replication of the these segments and therefore it was concluded that these constructs were suitable for attempting to generate recombinant influenza A viruses by reverse genetics.

3.4 Generation of recombinant influenza A viruses containing a PP7 RNA tag in the NA or NS gene segments

In order to generate recombinant influenza A viruses that contain a PP7 RNA tag in the positive-sense or negative-sense RNAs of the NA and NS genes, the plasmid-based reverse genetics technology was employed (Fodor *et al.*, 1999; Neumann *et al.*, 1999). In this technique the generation of infectious recombinant virus is achieved through the

reconstitution of all eight individual genomic vRNP segments within a single cell which consequently results in generation of infectious virus. The eight individual negative-sense genomic vRNAs are transcribed from pPOLI plasmids, in addition to the viral RdRP and NP proteins being expressed from pcDNA plasmids. Accordingly, each of the pPOLI-NA-cRNA-PP7, pPOLI-NA-vRNA-PP7, pPOLI-NS-cRNA-PP7 or pPOLI-NS-vRNA-PP7 plasmids was co-transfected with the seven remaining pPOLI plasmids and pcDNA plasmids into HEK 293T cells. The WT pPOLI-NA and pPOLI-NS plasmids were used as a positive control to generate WT virus. As a negative control the pPOLI-PB1 plasmid was replaced with the empty pPOLI-SapI-Rib plasmid. After amplification of recovered virus from HEK 293T cells on MDBK cells, virus growth was assessed using a plaque assay on MDBK cells. As expected, WT virus was rescued as indicated by the presence of viral plaques (Figure 3.6A). Recombinant viruses NA-cRNA-PP7, NA-vRNA-PP7, NS-cRNA-PP7 and NS-vRNA-PP7 were also rescued with a comparable plaque phenotype to WT virus, indicating that the introduction of a PP7 RNA tag into the NA and NS genes does not affect the generation of recombinant virus and that these viruses are able to undergo multiple replication cycles (Figure 3.6A).

Next, the growth properties of the recombinant influenza A/WSN/33 NA-cRNA-PP7, NA-vRNA-PP7, NS-cRNA-PP7 and NS-vRNA-PP7 viruses were compared to WT virus over the course of 72 h (Figure 3.6B). MDBK cells were infected at an MOI of 0.001 with either WT virus or recombinant viruses and viral supernatants were collected at 12, 24, 36, 48, 60 and 72 h p.i.. Virus titres were determined by plaque assay on MDBK cells. As expected, WT virus titres peaked at approximately 1.2×10^7

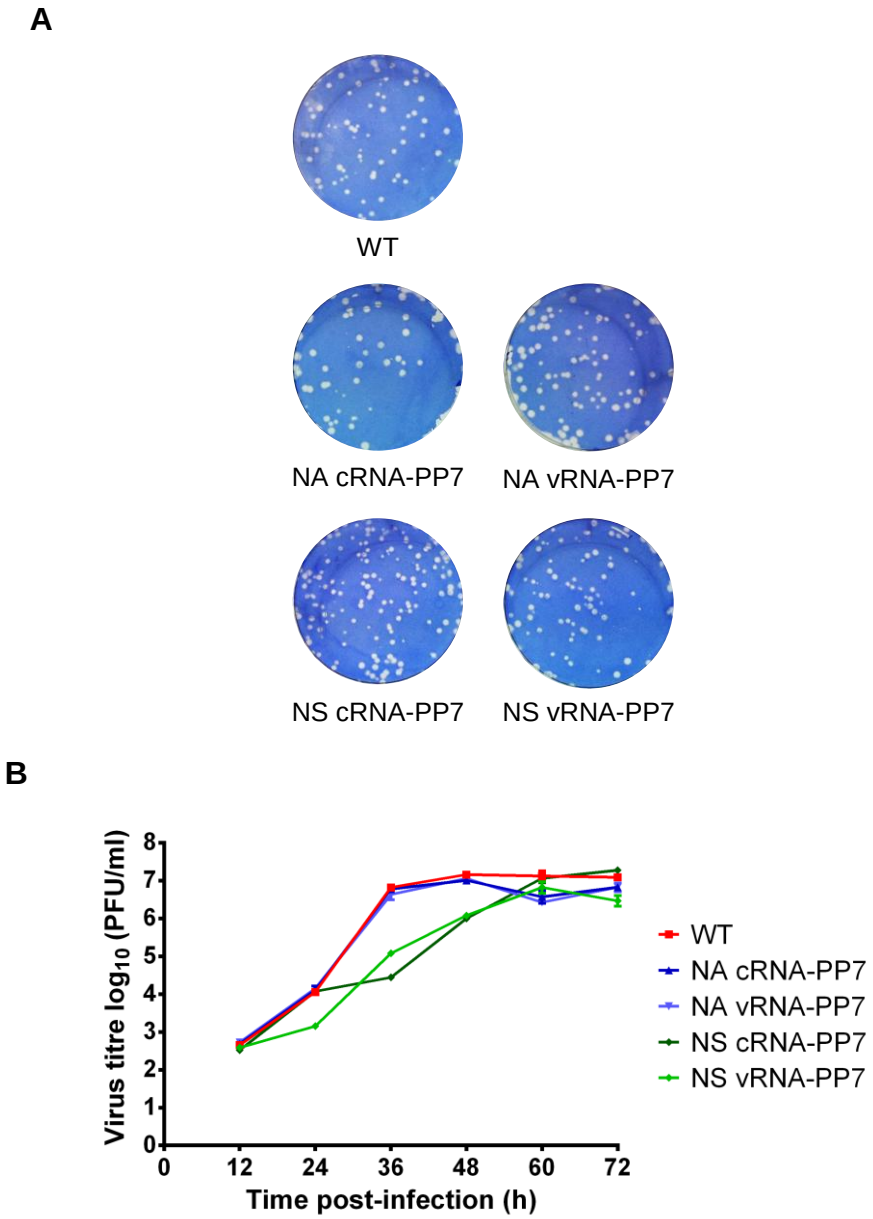


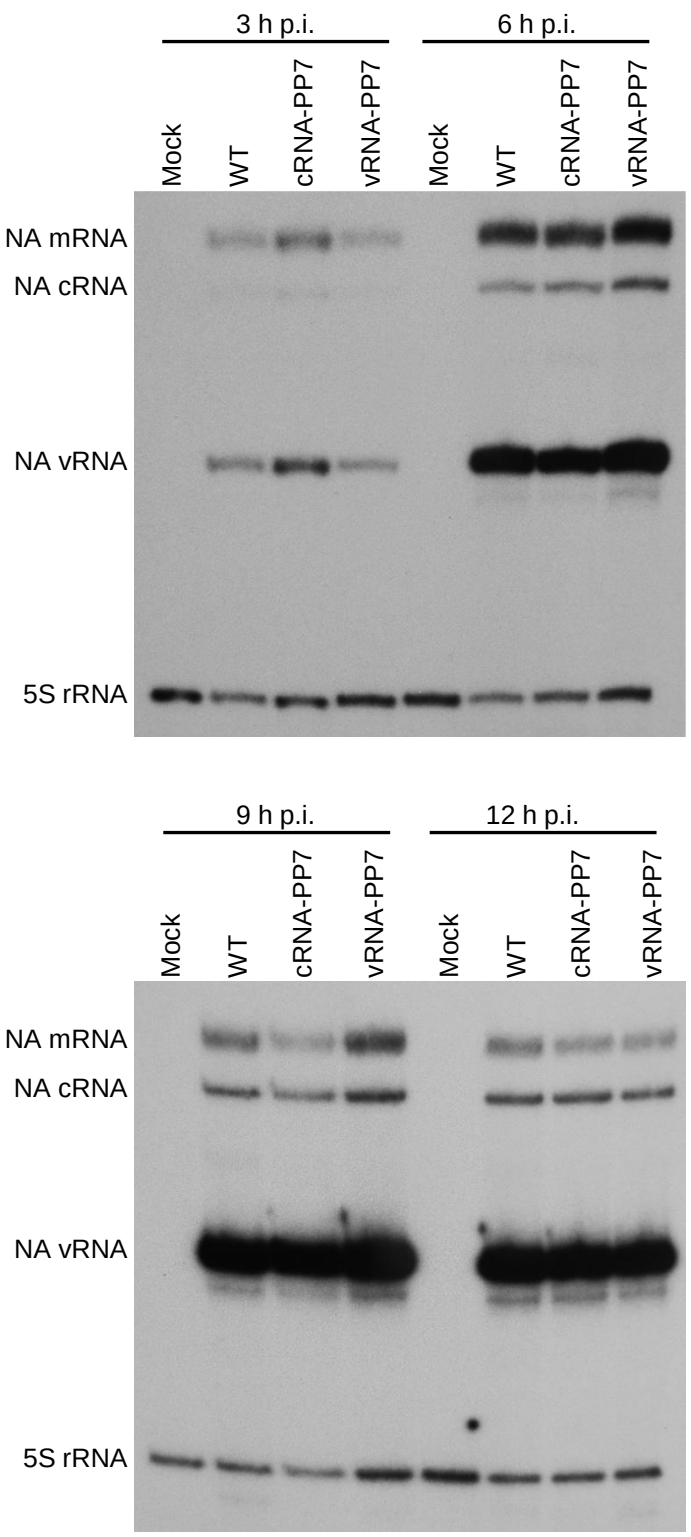
Figure 3.6 Generation of recombinant influenza A/WSN/33 viruses containing a PP7 RNA tag in the NA or NS genes. (A) Plaque phenotype of wild-type (WT) virus and viruses that contain a PP7 RNA tag in the NA and NS genes with the PP7 RNA in the positive-sense or negative sense. MDBK cells were infected for 72 h prior to staining with Coomassie Brilliant Blue. (B) Growth kinetics of WT virus and recombinant viruses. MDBK cells were infected at an MOI of 0.001 and at the indicated time points cell supernatants were collected and virus titres were determined by plaque assay on MDBK cells.

PFU/ml at 48 h p.i.. NA-cRNA-PP7 and NA-vRNA-PP7 recombinant viruses exhibited similar growth properties to that of WT virus, with comparable maximal virus titres at 48 h p.i.. However, NS-cRNA-PP7 and NS-vRNA-PP7 viruses exhibited significantly reduced growth properties compared to WT, NA-cRNA-PP7 and NA-vRNA-PP7 viruses with a 1–2.5 log reduction in virus titre at 36–48 h p.i.. However, final titres of NS-cRNA-PP7 and NS-vRNA-PP7 viruses were comparable to WT virus. These results show that insertion of a PP7 RNA tag into the stalk-encoding region of the NA gene does not significantly affect the multi-cycle growth kinetics of influenza virus. Insertion of a PP7 RNA tag into the linker-encoding region of NS1 attenuates the growth of influenza virus, indicating that the insertion of this tag affects the function of the NS1 protein, which impacts upon viral fitness. Therefore, further experiments in the development of an RNA-based RNP affinity purification strategy used the WT, NA cRNA-PP7 and NA vRNA-PP7 viruses only.

3.5 Accumulation of viral RNAs containing a PP7 RNA tag in infected cells

The isolation of viral RNP complexes that contain a tagged RNA relies on the efficient accumulation of this RNA in infected cells. In order to investigate the accumulation of viral RNAs that contain a PP7 RNA tag during the course of an infection, viral NA mRNA, cRNA and vRNA were analysed by NA segment-specific primer extension (Figure 3.7A and 3.7B). HEK 293T cells were mock infected or infected with WT, NA cRNA-PP7 or NA vRNA-PP7 influenza A/WSN/33 viruses at an MOI of 1 and total

A


3 h p.i.
6 h p.i.
Mock
WT
cRNA-PP7
vRNA-PP7
Mock
WT
cRNA-PP7
vRNA-PP7
NA mRNA
NA cRNA
NA vRNA
5S rRNA
9 h p.i.
12 h p.i.
Mock
WT
cRNA-PP7
vRNA-PP7
Mock
WT
cRNA-PP7
vRNA-PP7
NA mRNA
NA cRNA
NA vRNA
5S rRNA

B

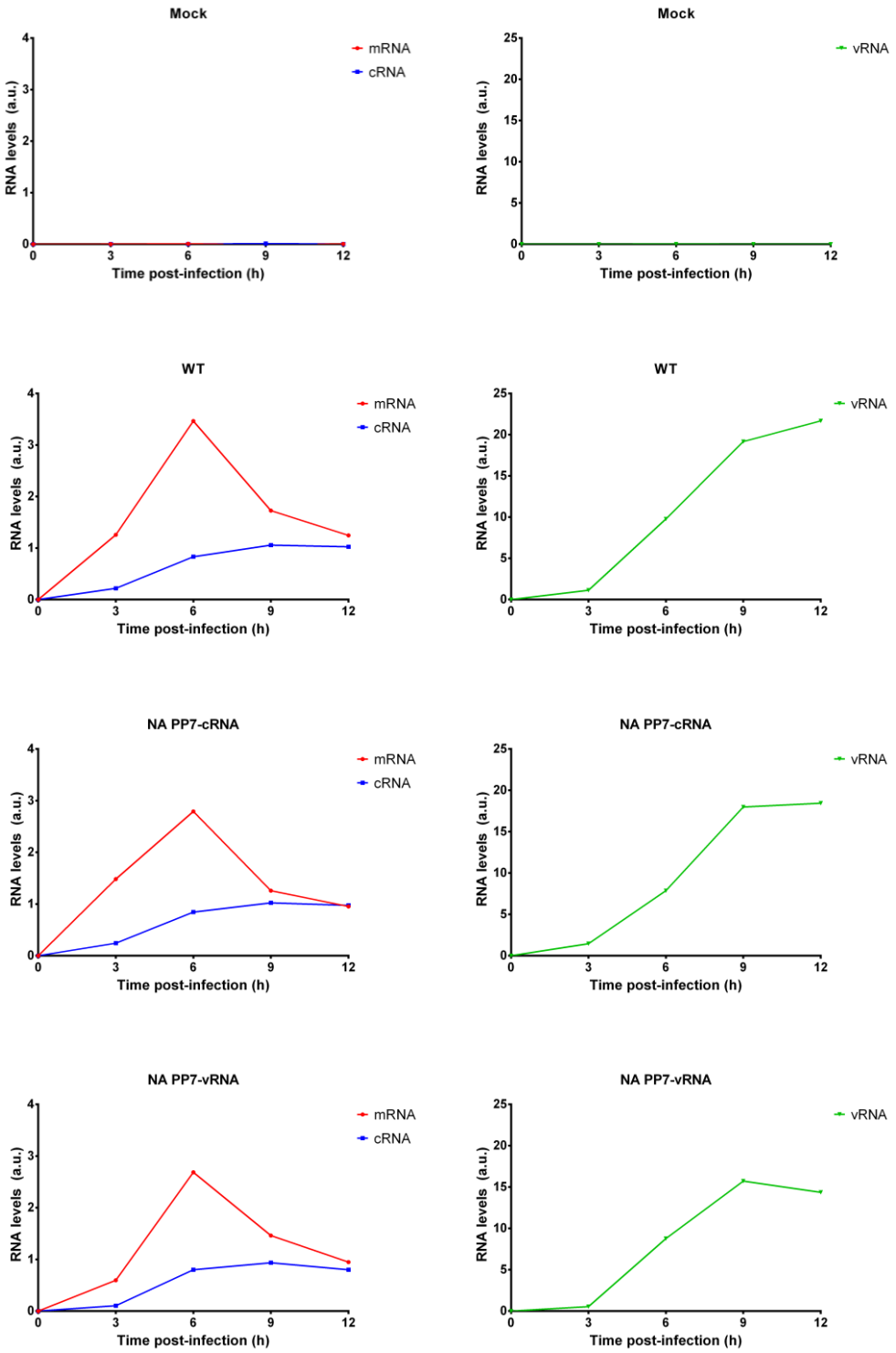

Mock
mRNA
cRNA
RNA levels (a.u.)
Time post-infection (h)
Mock
vRNA
RNA levels (a.u.)
Time post-infection (h)
WT
mRNA
cRNA
RNA levels (a.u.)
Time post-infection (h)
WT
vRNA
RNA levels (a.u.)
Time post-infection (h)
NA PP7-cRNA
mRNA
cRNA
RNA levels (a.u.)
Time post-infection (h)
NA PP7-cRNA
vRNA
RNA levels (a.u.)
Time post-infection (h)
NA PP7-vRNA
mRNA
cRNA
RNA levels (a.u.)
Time post-infection (h)
NA PP7-vRNA
vRNA
RNA levels (a.u.)
Time post-infection (h)

Figure 3.7 Accumulation of viral RNAs in cells infected with influenza A/WSN/33 viruses with a PP7 RNA tag in the NA gene. HEK 293T cells were infected at an MOI of 1 with wild-type (WT) virus or viruses that contain a PP7 RNA tag the NA gene. Cells were harvested at the indicated time points post-infection and RNA was extracted. (A) RNA was analysed by primer extension using radiolabeled primers for positive sense (mRNA and cRNA) and negative sense (vRNA) NA-specific viral RNAs. Primer extension analysis of 5S rRNA was used as a control. (B) Quantitative analysis of viral RNA accumulation representing a single analysis of two independent experiments. a.u. represents arbitrary units.

RNA was isolated at 0, 3, 6, 9 and 12 h p.i.. As anticipated, viral mRNA accumulation peaked at 4–6 h p.i. in WT virus infected cells, with a comparable level of NA mRNA accumulation being observed in cells that were infected with the NA cRNA-PP7 and NA vRNA-PP7 recombinant viruses. NA cRNA accumulation was comparable in all virus infected cells. The presence of a PP7 RNA tag did not affect the accumulation of vRNA in recombinant virus infected cells compared to WT virus infected cells. These analyses of the viral RNA accumulation show that the presence of a PP7 RNA tag does not diminish viral RNA accumulation, indicating that these recombinant viruses could be suitable for isolating RNP complexes from infected cells using RNA-based affinity purification.

3.6 Generation of a stable cell line that expresses the coat protein of the *Pseudomonas aeruginosa* PP7 bacteriophage

The isolation of viral RNP complexes that contain a PP7 RNA tag relies on the binding of the coat protein of the *Pseudomonas aeruginosa* PP7 bacteriophage (PP7CP) to that tag. Therefore, a HEK 293T stable cell line that expresses PP7CP fused to a $His_{6\times}$-tag for Ni-NTA affinity purification was generated. HEK 293T cells were transfected with a pcDNA plasmid that encodes both PP7CP fused to a $His_{6\times}$-tag and hygromycin phosphotransferase that confers hygromycin-B resistance to transfected cells. Transfected cells were cultured in the presence of hygromycin-B at a concentration that is toxic to non-resistant cells for approximately 30 days, at which point, colonies of clones were picked and recultured prior to analysing for the expression of PP7CP.

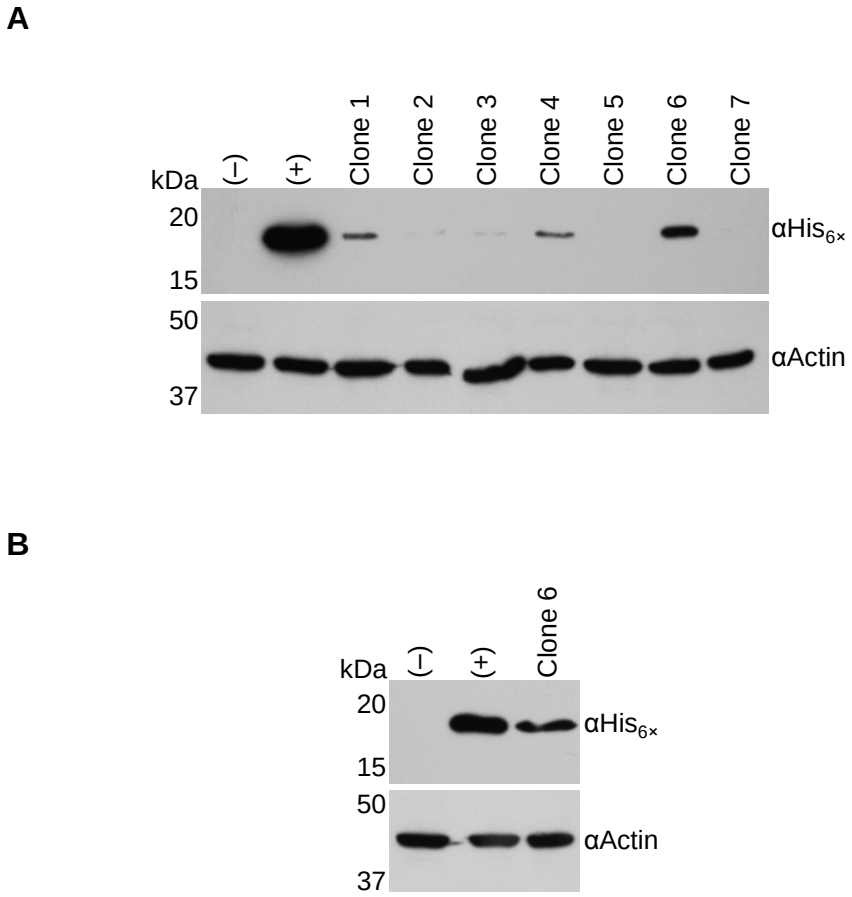


Figure 3.8 Generation of a HEK 293T cell line that stably expresses PP7CP. HEK 293T cells were transfected with a pcDNA plasmid that expresses both PP7CP fused to a $His_{6\times}$-tag and also hygromycin phosphotransferase that confers hygromycin-B resistance. Cells were cultured in hygromycin-B for approximately 30 days and stable clones that were resistant to hygromycin-B were picked, recultured and then assayed for protein expression. (A) Western blot analyses of initial cultures derived from resistant colonies using an anti-$His_{6\times}$-tag antibody. Cells that were untransfected (–) or transfected (+) with pcDNA-PP7CP-$His_{6\times}$ were used as a negative or positive control, respectively. Actin levels were monitored as a loading control. (B) Western blot analyses using an anti-$His_{6\times}$-tag antibody of cells derived from the 'Clone 6' colony after a further 30 days of passage in the presence of hygromycin-B. Cells that were untransfected (–) or transfected (+) with pcDNA-PP7CP-$His_{6\times}$ were used as a negative or positive control, respectively. Actin levels were monitored as a loading control.

Analysis of protein expression showed that PP7CP levels were variable between hygromycin-B resistant clones (Figure 3.8A). Cell lysate from an equivalent number of cells that had been untransfected or transfected with the pcDNA PP7CP expression vector was used as negative or positive control, respectively. The clone with the highest level of PP7CP expression was passaged for a further 30 days prior to protein expression analysis, which showed that PP7CP DNA had been stably integrated into the chromosomal DNA (Figure 3.8B).

3.7 Purification of influenza virus cRNP and vRNP complexes separately from infected cells

To purify PP7-tagged viral RNAs HEK 293T-PP7CP cells were infected at an MOI of 5 with the NA cRNA-PP7 or NA vRNA-PP7 viruses. Cells were also infected with WT virus as a negative control. At 7 h p.i. cells were lysed and PP7CP was purified using Ni-NTA chromatography. Total RNA was isolated from input sample and from the eluates, and the RNA was analysed in a primer extension assay using NA segment-specific primers (Figure 3.9A). The 5S rRNA was monitored as a control. These analyses showed that target viral NA cRNP and vRNP complexes were separated with high specificity using RNA-based affinity chromatography; on average, 20.0% of total cRNA and 11.8% of the total vRNA from cell lysates could be purified. However, only 3.2% of total mRNA could be recovered in the purification process (Figure 3.9B). Analyses of the purification eluates showed that PP7CP had been purified, however, many non-specific cellular proteins were present (Figure 3.10). In order to further

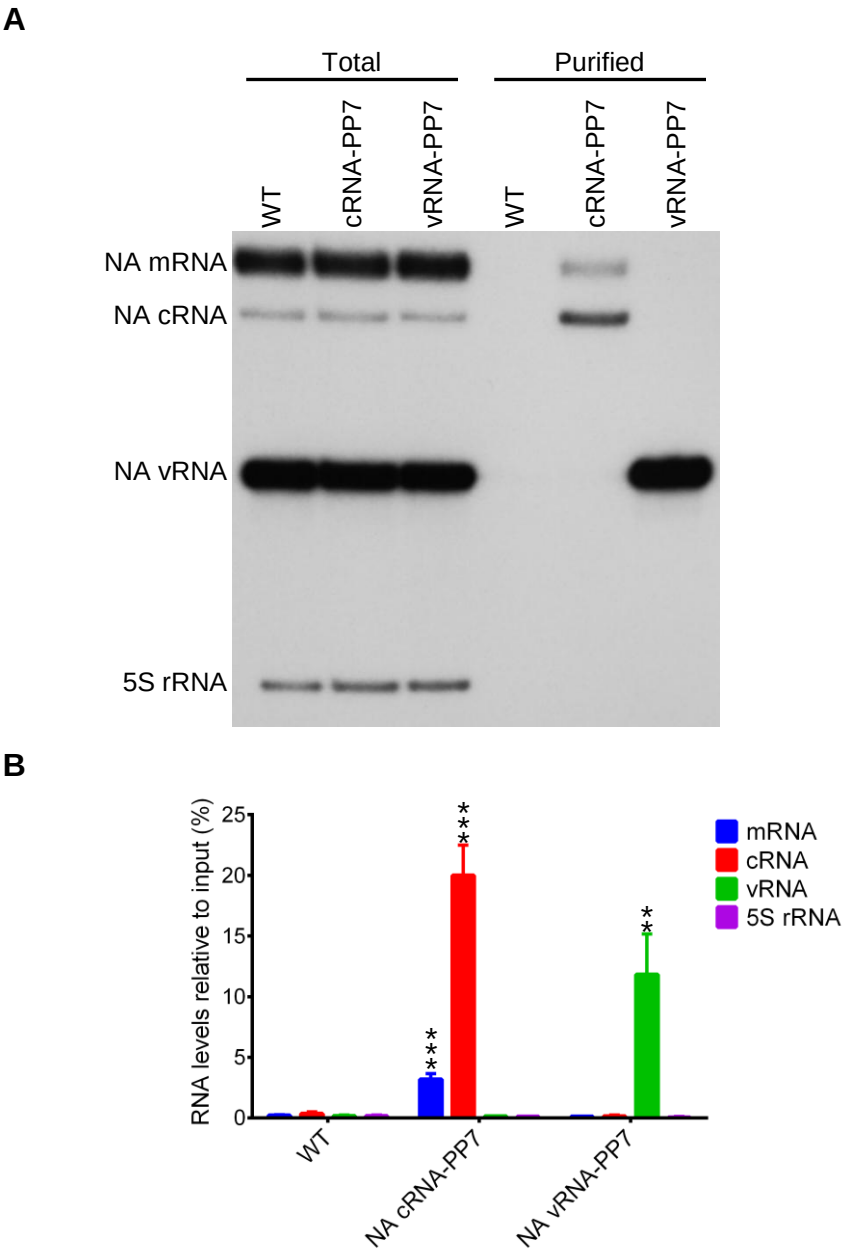


Figure 3.9 RNA-based affinity purification of tagged RNA from cells infected with influenza A/WSN/33 viruses with a PP7 RNA tag in the NA gene. HEK 293T-PP7CP cells were infected at an MOI of 5 with viruses that contain a PP7 RNA tag in the cRNA or vRNA orientations of the NA gene. Cells were also infected with wild-type (WT) virus as a negative control. At 7 h p.i. tagged RNA was purified by Ni-NTA chromatography of PP7CP. (A) Primer extension analyses of total and purified RNA using NA segment-specific primers for detecting positive sense (mRNA and cRNA) and negative sense (vRNA) RNAs. Primer extension analysis of 5S rRNA was used as a control. Ten times more sample of purified RNA was analysed relative to total RNA. (B) Quantitation of primer extension analyses of purified RNA. RNA levels represent the mean and the error bars represent standard deviations from three biological repeats. Asterisks indicate a significant difference from WT (** $P < 0.01$, *** $P < 0.001$, based on a two-sample Student's *t*-test).

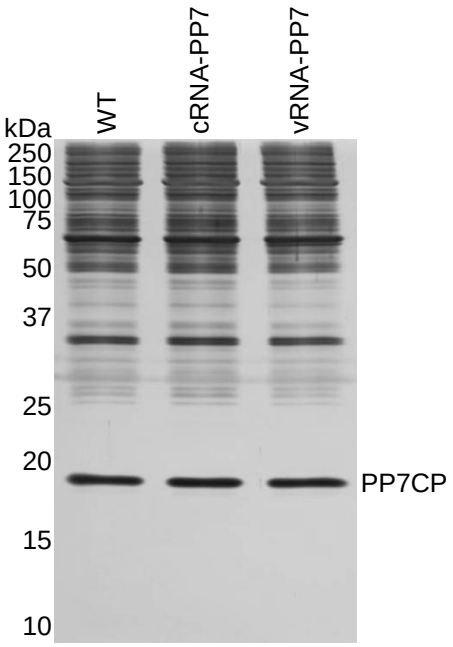


Figure 3.10 Ni-NTA affinity purification of PP7CP from infected cells. HEK 293T-PP7 cells were infected at an MOI of 5 with influenza A/WSN/33 viruses that contain a PP7 RNA tag in the cRNA or vRNA orientations of the NA gene. Cells were also infected with wild-type (WT) virus as a negative control. At 7 h p.i. tagged RNA was purified by Ni-NTA affinity purification of PP7CP and proteins were analysed by SDS-PAGE and silver staining.

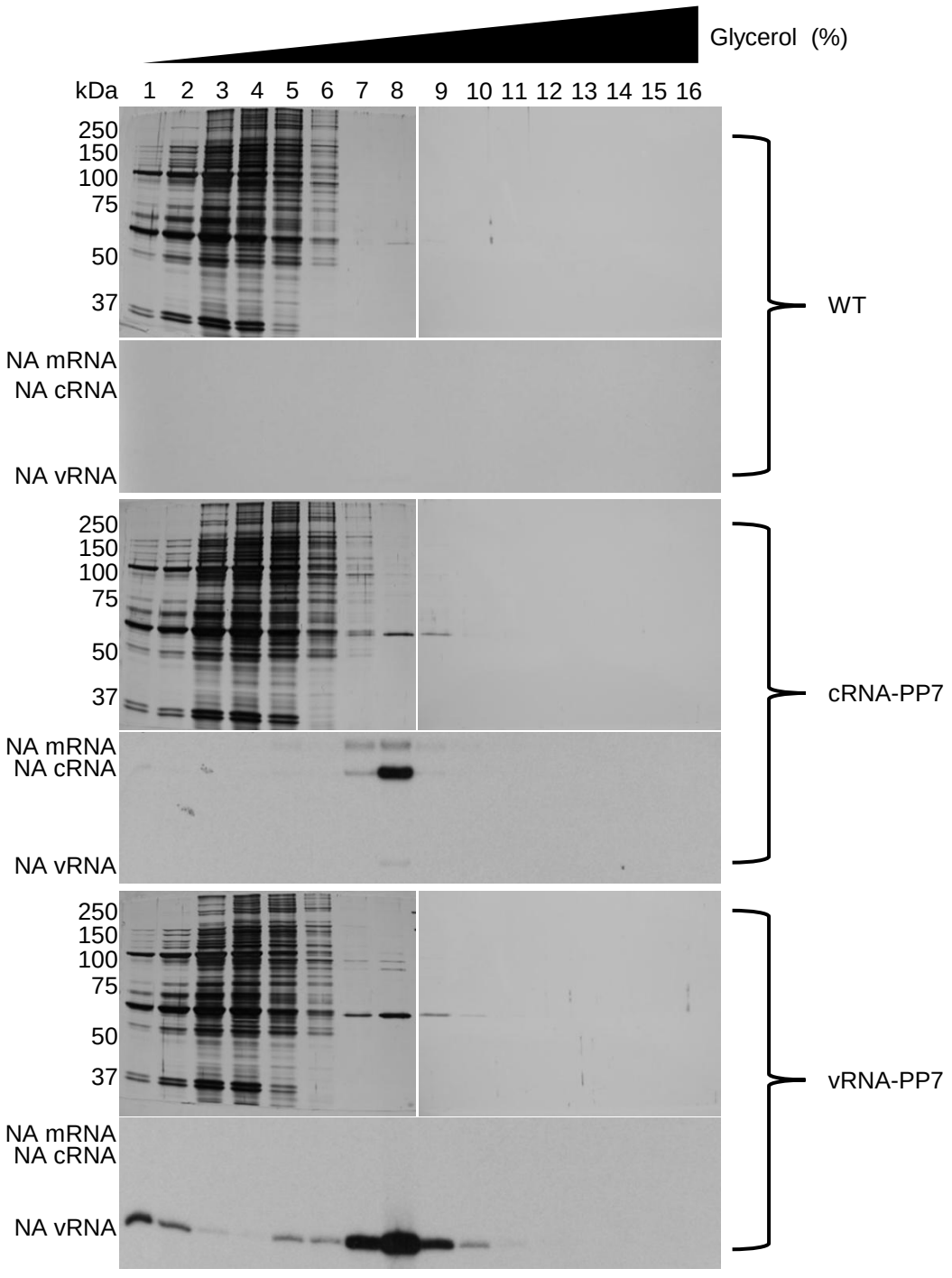

Glycerol (%)
kDa 1 2 3 4 5 6 7 8 9 10 11 12 13 14 15 16
250
150
100
75
50
37
NA mRNA
NA cRNA
NA vRNA
WT
cRNA-PP7
vRNA-PP7

Figure 3.11 Isolation of NA cRNP and vRNP complexes by density gradient ultracentrifugation. RNA-affinity purified material obtained from cells infected with WT, NA cRNA-PP7 or NA vRNA-PP7 influenza A/WSN/33 viruses was fractionated on glycerol gradients and fractions were analysed by SDS-PAGE and staining with silver (upper panels). RNA isolated from the fractions was analysed by NA-specific primer extension (lower panels) for detecting positive sense (mRNA and cRNA) and negative sense (vRNA) RNAs.

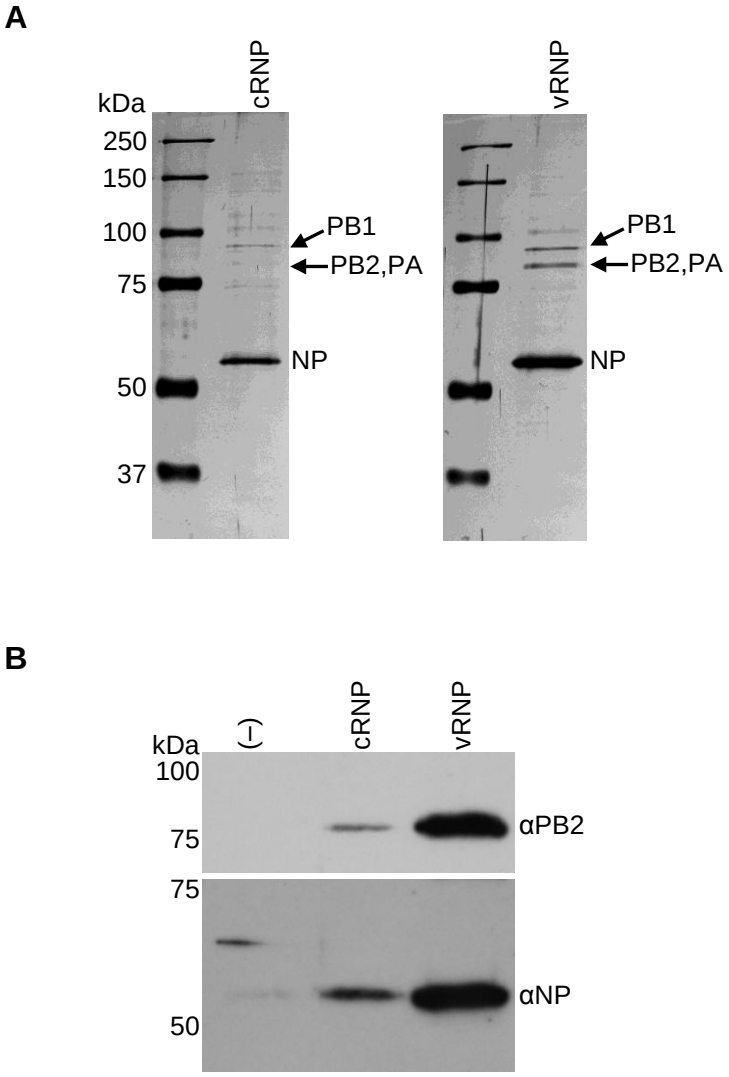


Figure 3.12 Analyses of isolated NA cRNP and vRNP complexes by SDS-PAGE. NA cRNP and vRNP complexes that were isolated by RNA-based affinity purification and density gradient centrifugation from cells infected with NA cRNA-PP7 or NA vRNA-PP7 influenza A/WSN/33 viruses were analysed by SDS-PAGE. (A) SDS-PAGE and silver staining analysis of isolated cRNPs and vRNPs. (B) SDS-PAGE and Western blot analyses using PB2 and NP antibodies of cRNPs and vRNPs. The equivalent position from the density gradient of mock purified RNPs from wild-type (–) infected cells was analysed as a negative control.

purify cRNP and vRNP complexes, the eluates were subjected to density gradient centrifugation through a glycerol gradient. The eluate sample from cells infected with WT virus was used as a negative control. The glycerol gradients were then fractionated prior to RNA and protein analyses. Total RNA was isolated from each fraction and analysed in a primer extension assay using NA segment-specific primers and the proteins in each fraction were analysed by SDS-PAGE and silver staining (Figure 3.11). Viral NP and RdRP co-migrated with viral RNA through the gradient. As expected, viral RNA was not detected in the negative control gradient. These analyses showed that viral RNP complexes could be isolated due to the difference in density between the RNPs and contaminating cellular proteins. Isolated cRNP and vRNP complexes were further analysed by Western blotting with NP and PB2 antibodies (Figure 3.12), confirming the presence of the viral RdRP and NP within the RNP complex. These data demonstrate that RNA-based affinity purification allows the separate isolation of influenza virus cRNPs and vRNPs from infected cells and that sufficient flexibility is inherent within these RNP complexes for the formation of secondary RNA structures that are not eliminated as a result of encapsidation by NP.

3.8 Discussion

The aim of this chapter was to develop a methodology that would permit the separate isolation of cRNP and vRNP complexes from influenza virus infected cells. A cRNP replicative intermediate for negative-strand RNA virus genome replication has never been isolated, and consequently, this essential component of genome replication in

many virus families has remained elusive and consequently, uncharacterised both functionally and structurally. In the absence of a methodology to separately isolate the cRNP and vRNP of influenza virus, it has been impossible to gain a complete overview of the molecular architecture of the viral transcription and replication machinery. Many questions concerning how the viral RdRP is regulated during replication and transcription of the viral genome remain unanswered. Moreover, it is unknown how the viral RdRP is differentially regulated on cRNA and vRNA templates. The separate isolation of the cRNP and vRNP of influenza virus would allow the role of specific viral and cellular factors in viral RNA synthesis to be addressed. For example, functional and structural studies of these RNPs could help elucidate the fundamental differences in the molecular biology between vRNA synthesis carried out by the cRNP and mRNA and cRNA synthesis by the vRNP.

The specific purification of cRNP and vRNP complexes required the development of an entirely RNA-based affinity purification strategy. This approach relied on the introduction of an accessible RNA tag within the target RNPs. The translational operator RNA from the *Pseudomonas aeruginosa* PP7 bacteriophage (Chao *et al.*, 2008; Hogg & Collins, 2007; Lim *et al.*, 2001) was inserted into the stalk-encoding region of the NA gene and the flexible linker-encoding region of NS1. The insertion of the PP7 RNA resulted in the extension of the polypeptide by 10 amino acids in these domains. Viruses were generated that contain a tag in these regions of the genome, with the NA viruses displaying no significant reduction in replication properties. These data corroborate previous studies that had reported that this region of the genome can tolerate additions and deletions without affecting neuraminidase function (Castrucci &

Kawaoka, 1993; Luo *et al.*, 1993; Munier *et al.*, 2010; Sorrell *et al.*, 2010). Interestingly, the NS viruses exhibited a reduced growth phenotype. The length of the flexible linker between the RNA binding domain and the effector domain in the NS1 protein has been proposed to modulate affinity of NS1 for dsRNA by influencing the positioning and spacing of RNA binding domain dimers in a model of dsRNA sequestration that relies on cooperative oligomerisation of NS1 (Bornholdt & Prasad, 2008). In this model, the presence of dsRNA within a cell results in the formation of a tubular structure that encases the dsRNA within a central tunnel. Therefore, perturbation of the spacing in this tubular structure caused by an increase in length in the linker region could interfere with the sequestration of dsRNA and therefore, heighten the cellular innate immune response, resulting in a reduction in virus growth.

It was unknown as to whether a secondary structure formed by an RNA tag would remain stable within a viral RNP complex due the encapsidation of the RNA by NP, which could result in the disruption of the RNA structure. Results in this chapter show that an RNA tag present within viral RNPs is accessible to the PP7CP protein, providing the first direct experimental evidence that sufficient flexibility exists within viral RNPs for secondary RNA structures to form and that these secondary RNA structures do not prevent read-through by the viral RdRP. In recent electron microscopy structural studies of the influenza virus vRNP, the vRNA was modelled to follow a positively charged pathway of basic patches on the surface of the helical NP oligomer (Arranz *et al.*, 2012; Moeller *et al.*, 2012). The ability of the PP7 RNA tag to form within an RNP structure provides evidence that RNA is able to deviate from these basic patches and protrude from the surface of NP. Such secondary RNA structures have been

proposed to play a major role in the selective packaging of the vRNA genome into budding virions (Gerber *et al.*, 2014; Hutchinson *et al.*, 2010). A number of electron tomography, biochemical assays and reverse genetics techniques have been used to build a model in which an intermolecular network of RNA-RNA interactions between vRNP segments forms, leading to the observed 7+1 arrangement of vRNPs within budding virions (Fournier *et al.*, 2012; Noda *et al.*, 2006; Noda *et al.*, 2012).

Intriguingly, viral mRNA was purified with a significantly lower efficiency than cRNA or vRNA (Figure 3.9). This unexpected finding suggests that the PP7 RNA is less accessible to PP7CP binding in the NA mRNPs, likely reflecting the association of viral mRNAs with a plethora of cellular factors that are involved in their processing, nuclear export and translation (York & Fodor, 2013). It is unknown as to whether secondary RNA structures could form in RNPs of other negative-strand RNA viruses. In contrast to influenza virus vRNPs, the RNA of the majority of negative-strand RNA virus RNPs is more resistant to digestion with endonucleases, suggesting tighter packaging of RNA within these complexes compared to RNA within influenza virus RNPs (Ruigrok *et al.*, 2011).

In conclusion, the principal advancement in this chapter was the isolation of the replicative intermediate of influenza virus. The presented approach for isolating viral RNP complexes represents a powerful method for understanding how influenza vRNA replication works. Furthermore, such an approach could be applied to other RNA viruses to yield mechanistic insights into the molecular biology of other important pathogens.

3.9 Summary

- An RNA tag from the *Pseudomonas aeruginosa* PP7 bacteriophage was inserted into the NA and NS genes of the influenza A/WSN/33 virus genome for the isolation of cRNA or vRNA depending on the orientation of the tag.
- The stalk region of the NA glycoprotein and the flexible linker domain of the NS1 protein were selected for insertion of the PP7 RNA tag.
- The presence of an RNA tag did not significantly reduce the accumulation of viral RNAs in an RNP reconstitution assay.
- Recombinant viruses were recovered that contain a PP7 RNA tag in the NA and NS genes.
- Recombinant viruses that contained a tag in the NA gene did not exhibit reduced growth properties, however, viruses that contained a tag in the NS gene had attenuated growth properties.
- Viral NA segment cRNP and vRNP complexes containing the viral RdRP and NP were isolated separately by RNA-based affinity purification from infected HEK 293T cells that stably express the coat protein of *Pseudomonas aeruginosa* PP7 bacteriophage.
- The principal advancement of this chapter was the isolation of a replicative intermediate cRNP of a negative-strand RNA virus for the first time.

Chapter 4: Characterisation of the complementary ribonucleoprotein of influenza virus

4.1 Introduction

Once genomic vRNPs have been delivered into the cytoplasm after the fusion of virion and endosomal membranes, vRNP entry into the host cell nucleus is mediated by the α/β-importin machinery (Martin & Helenius, 1991; Oneill *et al.*, 1995). Upon entry into the nucleus, the vRNA genome is transcribed into mRNA and replicated by the viral RdRP. Transcription is initiated by the viral RdRP binding to 7-methylguanylate cap structures of pre-mRNAs (Guilligay *et al.*, 2008). Subsequent endonucleolytic cleavage of the pre-mRNA then proceeds to generate a 5′ capped RNA that is used as a primer to copy the vRNA template (Dias *et al.*, 2009; Yuan *et al.*, 2009). Polyadenylation is achieved by the viral RdRP reiteratively stuttering on a stretch of uridine residues at the 5′ end of the vRNA (Poon *et al.*, 2000; Poon *et al.*, 1999). The replication of vRNA

proceeds in two stages (Fodor, 2013; Resa-Infante *et al.*, 2011). Firstly, the viral RdRP synthesises a full-length positive-sense cRNA (vRNA→cRNA). This cRNA does not have a 5′ cap or a 3′ poly(A) tail, therefore the viral RdRP requires a different mode of initiation and termination that is distinct to mRNA synthesis. Initiation is thought to occur *de novo*, as evidenced by the presence of a 5′ triphosphate. The newly synthesised cRNA is then used as a template by the viral RdRP for the synthesis of multiple copies of vRNA (cRNA→vRNA), which are assembled into vRNP complexes with viral RdRP and NP. While much has been learned about the basic molecular biology of genome replication, many of the structural and mechanistic differences between vRNA and cRNA synthesis are not well understood. It has been a mystery as to whether a structured double-helical cRNP complex that is analogous to the vRNP catalyses vRNA synthesis within infected cells. There have been a number of biochemical and genetic studies that suggest the cRNP and vRNP are not structurally equivalent. It has been reported that cRNA and vRNA promoters interact with different regions of the viral RdRP (Gonzalez & Ortin, 1999a; b), and that the initiation of cRNA and vRNA synthesis is carried out by distinct mechanisms (Deng *et al.*, 2006; Vreede *et al.*, 2008; Zhang *et al.*, 2010). Moreover, temperature-sensitive NP mutants have been described that are differentially defective in cRNA or vRNA synthesis, suggesting that cRNP and vRNP complexes are structurally and functionally distinct (Mena *et al.*, 1999; Thierry & Danos, 1982). Another major difference between the function of the viral RdRP on a cRNA or vRNA template is the ability of the viral RdRP to cap-snatch. It is believed that the viral RdRP is unable to cap-snatch on a cRNA template (Cianci *et al.*, 1995; Honda *et al.*, 2001; Rao *et al.*, 2003; Zhirnov *et al.*, 2007). Gaining in-depth knowledge of the structure of the cRNP could help to address questions concerning the

fundamental differences between RNA synthesis that is carried out by the viral RdRP on cRNA and vRNA templates. Although high-resolution structures of vRNPs have been determined by means of electron microscopy (Arranz *et al.*, 2012; Coloma *et al.*, 2009; Moeller *et al.*, 2012), the cRNP had not previously been isolated, and therefore structural information of this essential component of viral replication has been elusive. In this chapter, electron microscopy and single particle analysis of the cRNP is performed to reveal the overall molecular architecture of the cRNP.

In this chapter it was also sought to define the molecular requirements for genome replication (vRNA→cRNA→vRNA). The precise detail of the molecular biology of RNA synthesis during vRNA replication is poorly defined and in some cases, controversial. Therefore, a detailed understanding of the viral and cellular factors that are required at each stage of vRNA replication is essential for understanding this process. A number of important questions have remained unanswered as to whether RNA synthesis is carried out in *cis* or *trans* by the viral RdRP on cRNA and vRNA templates. It has been proposed that vRNA synthesis is carried out in *trans* by a viral RdRP that is distinct from the RdRP that is part of the cRNP complex (Jorba *et al.*, 2009; Moeller *et al.*, 2012). The involvement of a small viral RNA (svRNA) has also been proposed to regulate this *trans*-acting polymerase (Perez *et al.*, 2010; Perez *et al.*, 2012; Umbach *et al.*, 2010). It has also been proposed that RNA synthesis is carried out in *trans* on a vRNA template (Moeller *et al.*, 2012), while other studies conclude that this event is unlikely (Vreede & Brownlee, 2007; Vreede *et al.*, 2004). Other viral factors including NEP and NS1 are also thought to be involved in the regulation of RNA synthesis (Marion *et al.*, 1997; Robb *et al.*, 2009). The separate isolation of the

cRNP and vRNP from infected cells therefore permits the molecular requirements for genome replication to be defined in *in vitro* assays. Accordingly, a further aim of this chapter is to dissect the molecular requirements for cRNA and vRNA synthesis.

4.2 Influenza virus cRNP exhibits a double-helical arrangement

In order to study the molecular architecture and organisation of the influenza virus cRNP, purified complexes were studied by negative stain electron microscopy. The purified cRNP appeared as ribbon-like closed superhelical structures, comparable to the structure of the purified vRNP (Figure 4.1 and Figure 4.2A). The filamentous cRNP complexes had a median length of 72 nm (n = 231), in agreement with the length of influenza virus vRNP segments of an intermediate length in nucleotides (Compans *et al.*, 1972). A gallery of 2,456 cRNP images was obtained, revealing that the filaments were highly flexible. Two-dimensional (2D) class averaging was performed to gain a more complete view of the structural features of the cRNP. The flexible nature of the cRNP resulted in disorder in the 2D class averaging, particularly at the termini (Figure 4.2B). In order to gain insight into the structural features of the central filament and the termini, these regions were classified separately in the averaging. The central filament class averages revealed the presence of repeating triangular structural motifs, consistent with a double-helical arrangement of NP (Figure 4.2C). The termini were classified and then these averages were split into two groups, comprising either arrowhead-shaped (Figure 4.2D) or looped structures (Figure 4.2E). These termini were interpreted to correspond to different side views of the viral RdRP and the NP loops, respectively.

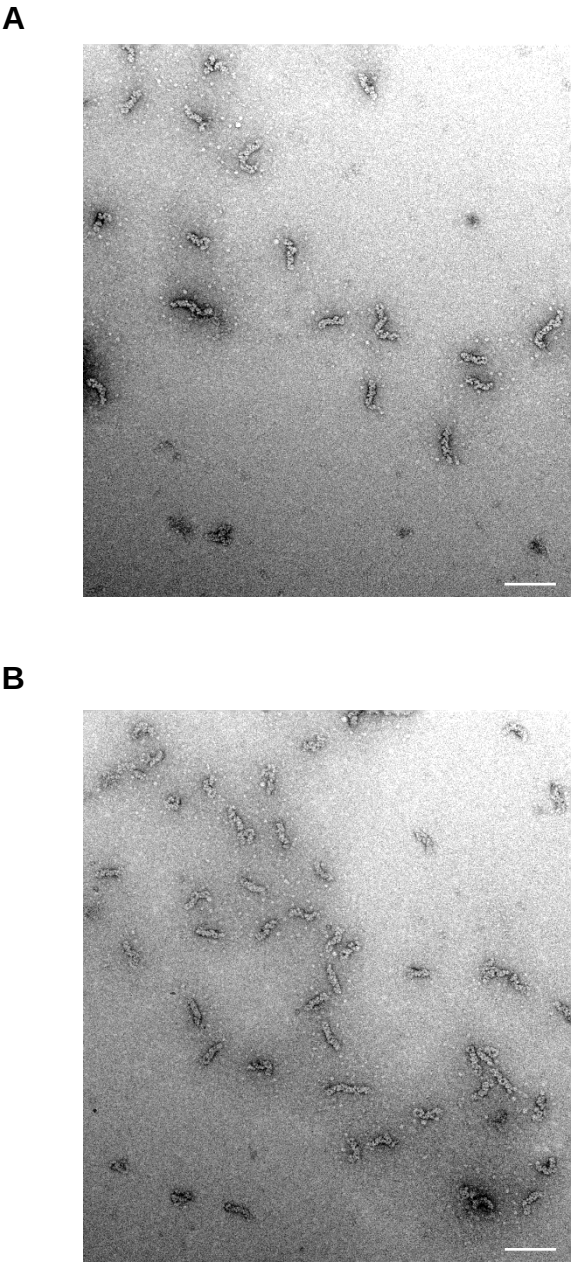


Figure 4.1 Negative stain electron microscopy of purified influenza A virus cRNP and vRNP complexes. Examples of electron micrographs obtained from negative-stained samples of (A) cRNP and (B) vRNP complexes that were isolated by RNA-based affinity purification and density gradient centrifugation. Scale bars, 100 nm.

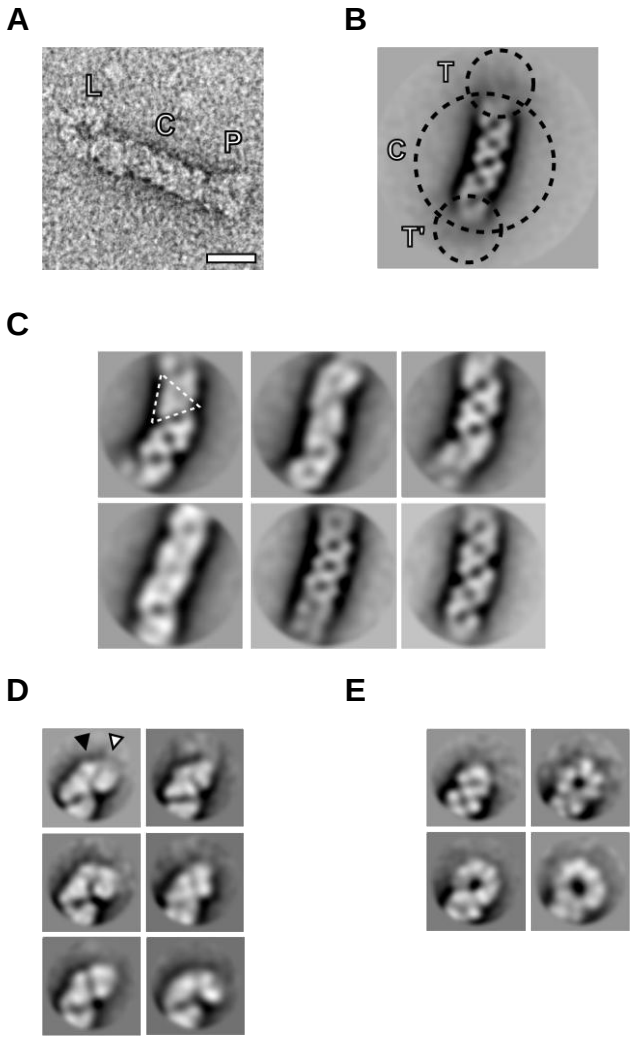


Figure 4.2 Molecular architecture of the influenza A virus cRNP. (A) A single cRNP complex extracted from an electron micrograph. NP loop end (L), central helical filament (C) and RdRP end (P) are labelled. Scale bar, 20 nm. (B) Two-dimensional class averages of cRNP complexes. Two termini (T and T′) were not resolved in initial class averages. Further classification focussed on sub-images of the termini and the central filament (C). (C) Class averages of the central filament show variation due to different displays of orientation around the filament long axis and variable curvature of the filament. Dependent on the orientation, repeating triangular structural motifs were visible (triangle). (D) Two-dimensional class averages of the termini representing different side views. Two globular densities, that putatively correspond to a large (white triangle) and small (black triangle) structural feature of the RdRP are indicated. (E) Two-dimensional class averages of loop side views show variation in loop diameter and the number of NP monomers present in the loop. The scale of B–E is identical as in A.

Sample preparation and electron microscopy was performed by Ashley York, while two-dimensional class averaging was performed by Juha T. Huiskonen as a collaboration.

The viral RdRP structure exhibited a small and larger domain that adopted different angles relative to the central filament (Figure 4.2D). The terminus that contained the NP loop had a varying diameter (~14–23 nm), corresponding to three to seven NP protomers in the loop, suggesting a degree of flexibility at this terminus (Figure 4.2E).

4.3 Isolated vRNPs, but not cRNPs, can synthesise RNA *in vitro*

The separate isolation of the cRNP and vRNP from infected cells permitted the basic molecular requirements for RNA synthesis for each of these complexes to be determined and compared in *in vitro* activity assays. Viral RNAs were detected using a primer extension assay that analyses the 5′ end of the templates and products using NA segment-specific radiolabeled primers. In the absence of ribonucleoside triphosphates (rNTPs), as anticipated neither cRNP nor vRNP can synthesise RNA (Figure 4.3). As demonstrated by the synthesis of *de novo* initiated cRNA, vRNPs are able to replicate. This replication activity of the vRNP is greatly enhanced in the presence of an ApG dinucleotide primer that aligns to the 3′ of the vRNA template. The addition of β-globin mRNA resulted in cap-snatching and synthesis of viral mRNA. In stark contrast to the vRNP, the cRNP did not synthesise detectable amounts of vRNA *de novo*, or in the presence of the ApG dinucleotide that is complementary to the 3′ end of the cRNA (Figure 4.3).

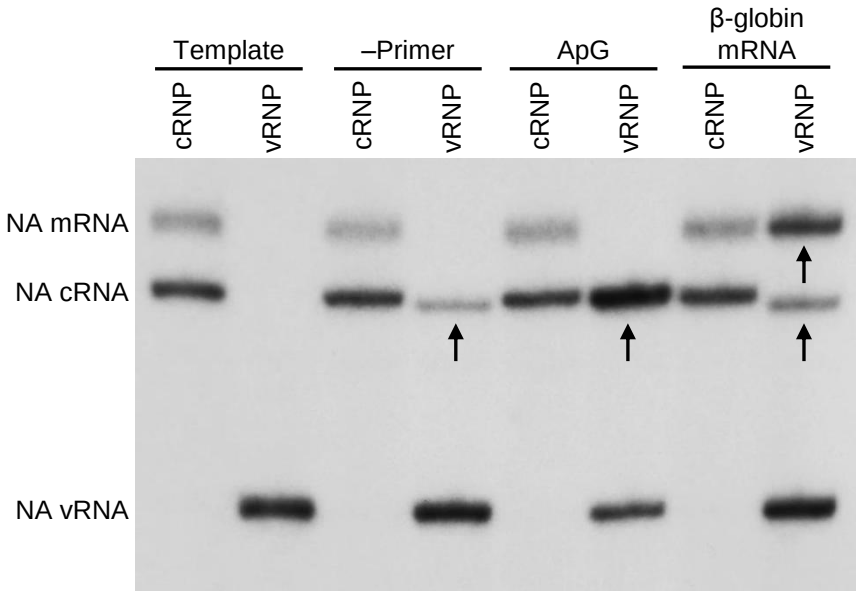


Figure 4.3 RNA synthesis activity of isolated cRNP and vRNP *in vitro*. *In vitro* activity assays of purified NA cRNPs and vRNPs in the absence of rNTPs as a negative control to indicate template RNA (Template) or in the presence of rNTPs but absence of primer (–Primer), presence of ApG dinucleotide primer (ApG) or capped RNA (β-globin mRNA). Templates and transcription products were analysed by primer extension using primers specific for positive sense (mRNA and cRNA) or negative sense (vRNA) NA-specific viral RNAs. Small arrows indicate products of vRNP activity.

4.4 A *trans*-activating RdRP is required for vRNA synthesis

A previous study had carried out experiments *in vivo* using polymerase complexes that are defective in transcription and replication to propose a model whereby a viral RdRP that is not part of the cRNP complex acts in *trans* on the cRNA template to synthesise vRNA (Jorba *et al.*, 2009). It was therefore hypothesised that the inactivity of the cRNP observed *in vitro* was due to the absence of a viral RdRP that can act in *trans*. In order to test this hypothesis, recombinant influenza virus RdRP was purified from *Spodoptera frugiperda* (Sf9) cells (Appendix A) and included in *in vitro* activity assays. Viral RNAs were detected using a primer extension assay that analyses the 5′ end of the templates and products using NA segment-specific radiolabeled primers. In the absence of rNTPs, RNA synthesis was not detected (Figure 4.4). In the absence of recombinant viral RdRP, as expected the vRNP was able to synthesise cRNA and the cRNP was inactive. When recombinant RdRP was added to the cRNP in this assay vRNA synthesis was observed, with a shorter product likely representing vRNA initiated internally at position 4 on the cRNA promoter, consistent with the previously proposed internal initiation model of vRNA synthesis. These products were confirmed to be specific for vRNA as they were not detected in the absence of a vRNA-specific radiolabeled primer (Figure 4.4). An increase of 4.1-fold in vRNA signal was observed in the presence of added viral RdRP compared to the absence of added RdRP. These results strongly suggest that RNA synthesis on a cRNA template is performed by viral RdRP in *trans*.

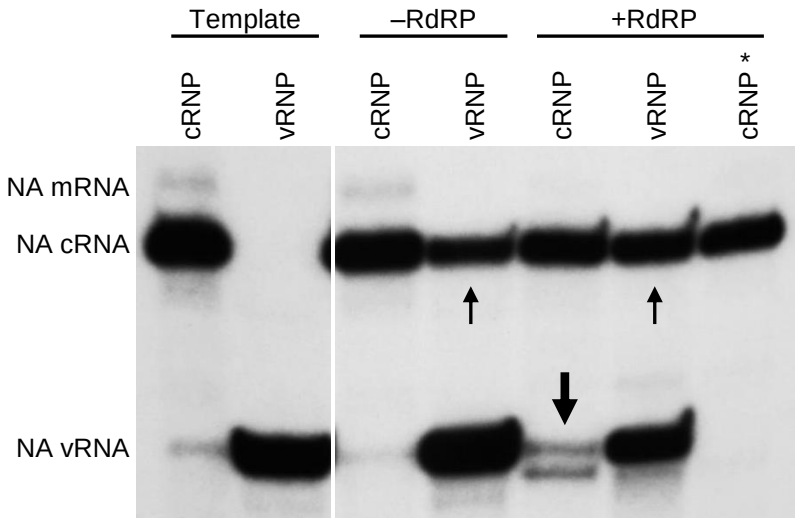


Figure 4.4 A *trans*-activating RdRP is required for vRNA synthesis. Analyses of viral RNAs in an *in vitro* activity assay of purified NA cRNPs and vRNPs. Assays were performed in the absence of rNTPs as a negative control to indicate template RNA (Template) or in the presence of rNTPs and ApG dinucleotide primer without (–RdRP) or with (+RdRP) added recombinant influenza A virus RdRP purified from *Spodoptera frugiperda* (Sf9) cells. Templates and transcription products were analysed by primer extension using primers specific for positive sense (mRNA and cRNA) or negative sense (vRNA) NA-specific viral RNAs. cRNP * denotes primer extension analysis in the absence of vRNA-specific primer. Small arrows indicate products of vRNP activity and a large arrow indicates products of cRNP activity that form a doublet. Note that the weak vRNA-specific signals observed in the Template and –RdRP cRNP lanes represent small amounts of vRNA that co-purify with cRNPs.

4.5 A *trans*-activating RdRP acts cooperatively with the resident RdRP, which carries out vRNA synthesis

In order to determine whether the added recombinant RdRP acts in *trans* in agreement with a previously proposed model (Jorba *et al.,* 2009), or whether the added RdRP has an uncharacterised function for supporting the cRNP-associated RdRP to act in *cis*, recombinant wild-type RdRP (RdRP) and PB1 active-site mutant ($RdRP^{PB1a}$) were purified from HEK 293T cells (Appendix A) and included in *in vitro* activity assays. Viral RNAs were detected using a primer extension assay that analyses the 5′ end of the templates and products using NA segment-specific radiolabeled primers. In the absence of rNTPs, RNA synthesis was not detected (Figure 4.5). In the absence of ApG, as expected, the vRNP was able to *de novo* initiate cRNA synthesis. In the presence of ApG and in the absence of added WT RdRP the vRNP was able to synthesise increased levels of cRNA, however, vRNA was not detected, confirming that the cRNP is inactive in the absence of soluble RdRP. The addition of WT RdRP resulted in the synthesis of vRNA as expected, however unexpectedly, the addition of $RdRP^{PB1a}$ to the cRNP also resulted in the synthesis of vRNA products (Figure 4.5). A 3.1-fold and a 2.8-fold increase in vRNA was detected over background for WT RdRP and $RdRP^{PB1a}$, respectively. These results suggested that the added recombinant RdRP does not act in *trans*, but acts cooperatively with the cRNP-associated RdRP which acts as a replicase in *cis*.

To examine this result further, an alternative *in vitro* assay was used to investigate RNP activity. In this assay, purified RNPs are incubated in the presence of [α^{32}P]-rNTPs and

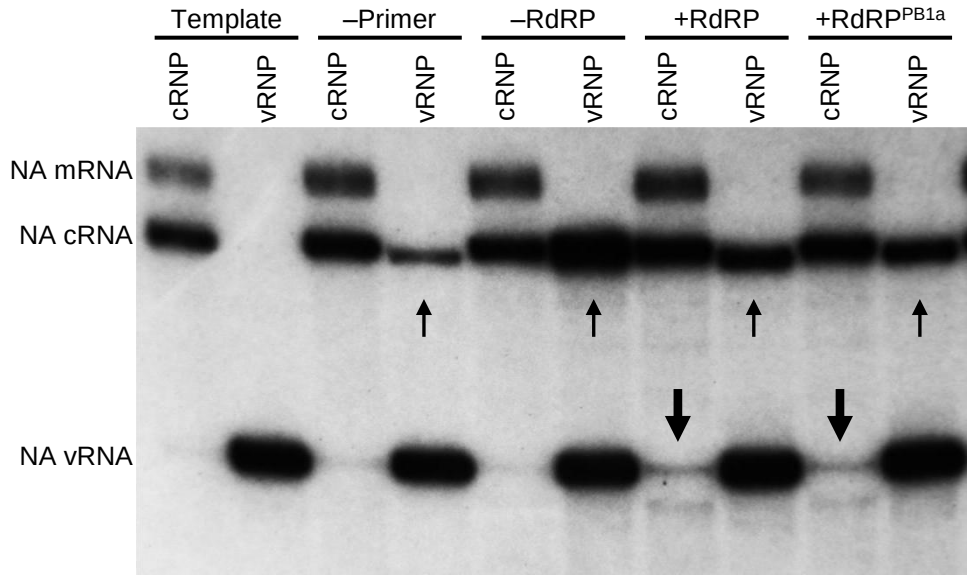


Figure 4.5 An RNA synthesis mutant RdRP activates cRNP activity. Analyses of viral RNAs in an *in vitro* activity assay of purified NA cRNPs and vRNPs. Assays were performed in the absence of rNTPs as a negative control to indicate template RNA (Template), in the presence of rNTPs without a dinucleotide primer (–Primer), or with added recombinant (+RdRP) or active site mutant (+RdRP^{PB1a}) influenza A virus RdRP purified from transfected HEK 293T cells. Templates and transcription products were analysed by primer extension using primers specific for positive sense (mRNA and cRNA) or negative sense (vRNA) NA-specific viral RNAs. Small arrows indicate products of vRNP activity and large arrows indicate products of cRNP activity that form a doublet.

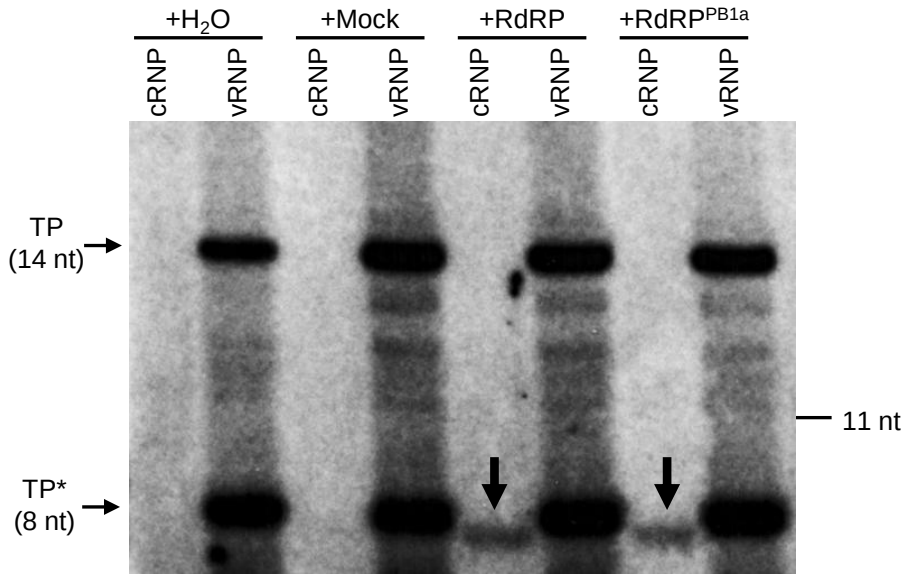


Figure 4.6 A *trans*-activating RdRP is required for cRNP activity. The activity of purified cRNPs and vRNPs was assessed in an *in vitro* [α-^{32}P]NTP incorporation assay in the presence of ApG primer and water (+H_2O), mock polymerase (+Mock), wild-type (+RdRP) or active site mutant (+RdRP^{PB1a}) RdRP purified from transfected HEK 293T cells. TP (14 nt) denotes the expected transcription product derived from the vRNA template and TP* (8 nt) denotes a premature termination product due to limiting CTP concentrations. The 8 nt product of cRNP activity is indicated by large arrows.

the products of replication can be detected directly. To analyse vRNP activity, reactions were set up leaving out UTP, expecting a product of 14 nt in length as the first ATP in the template occurs at position 15. Analogously, to analyse the activity of the cRNP reactions were set up leaving out CTP, expecting a product of 8 nt in length. Consistent with the previous finding, the cRNP was active only in the presence of an added recombinant RdRP, regardless of whether this RdRP was WT or a PB1 active-site mutant (Figure 4.6). Taken together, these results strongly suggest that the RdRP present within the purified cRNP complex requires a *trans*-activating RdRP to perform RNA synthesis in *cis* on the cRNA template.

4.6 Discussion

The isolation of the cRNP and vRNP separately from influenza virus infected cells permitted the visualisation and characterisation of the cRNP for the first time. The data presented in this chapter revealed that this replicative intermediate of influenza virus genome replication exists as an individual structured complex. It was observed that the cRNP complex has three major domains, a central filament and two distinct termini. One terminus formed a loop structure that was composed of NP molecules. The opposite terminus contained a structure that was interpreted to be the viral RdRP, on the basis of analogy to previously published vRNP structures (Arranz *et al.*, 2012; Moeller *et al.*, 2012). The central filament exhibited a double helical arrangement that is facilitated by NP-NP interactions, similar to the reported vRNP structure (Arranz *et al.*, 2012; Moeller *et al.*, 2012). A varying diameter of the loop at the terminus of the cRNP

was observed, with three to seven NP molecules being present within this loop. This varying diameter is consistent with the previous reports that the loop-end of a vRNP comprises five to eight NP molecules in one study (Moeller *et al.*, 2012) and three in another study (Arranz *et al.*, 2012). In contrast to previous studies which analysed a mixture of vRNP complexes with varying lengths, in this study the NA segment cRNP, with a defined length, was analysed. The ability for the cRNP complex to contain loop structures containing different numbers of NP molecules implies that there is flexibility within the complex for unwinding within the central filament, or for different degrees of winding at the loop-end of the filament. The terminus that contained the viral RdRP exhibited a small and a large structural feature. This small structural feature could correspond to the C-terminus of PA, while the larger feature could possibly correspond to PB1, PB2 and the N-terminus of PA, as had been reported in previous EM studies of the viral RdRP within the vRNP (Moeller *et al.*, 2012). Higher resolution techniques (e.g. cryo-EM) will be required to address whether a different of a similar arrangement of the viral RdRP subunits exist within the cRNP compared to the vRNP.

The separate isolation of the cRNP and the vRNP also permitted the characterisation of RNP function in activity assays *in vitro*. This approach consequently allowed the model of genome replication for influenza viruses to be advanced. Previous studies of influenza virus RNP function had led to the proposal that replication of the vRNA genome on a cRNA template is performed by a *trans*-acting polymerase (Jorba *et al.*, 2009). In this previous study, genetic *trans*-complementation assays were performed *in vivo* using mutant viral RdRPs that are either defective in transcription or replication. The authors concluded that a replication-defective vRNP could become replication-

competent in the presence of a mutant viral RdRP that is transcription-defective. In contrast to this model, the data presented in this study of cRNP function strongly suggests that replication (cRNA→vRNA) is performed by a viral RdRP that is associated with the purified cRNP complex in *cis*, and that a *trans*-activating RdRP is required to activate vRNA synthesis. This model of *trans*-activation is supported by two major findings. Firstly, the cRNP had no detectable activity in vRNA synthesis assays and vRNA synthesis activity could be gained by the addition of a recombinant viral RdRP in *trans*. Secondly, the addition of a mutant RdRP that contains a mutation in the PB1 active site, abolishing RNA synthesis activity (Vreede *et al.*, 2004), had the same effect as adding WT RdRP, demonstrating that RNA synthesis is performed by the resident cRNP-associated RdRP in *cis*. A *trans*-activating viral RdRP, however, is required for activation of RNA synthesis by the resident RdRP. This model could be disputed due to the possibility that there is an exchange of the WT and mutant viral RdRP at the cRNA promoter, such that the WT RdRP could then act in *trans* on the template. Although this possibility cannot be excluded, previous data showed that the binding of viral RdRP to the promoter cannot be outcompeted by a pre-expressed RdRP (Jorba *et al.*, 2009; Vreede & Brownlee, 2007), suggesting that an exchange is unlikely to occur.

The precise role of the *trans*-activating RdRP is currently unknown, but it could be speculated that the *trans*-activating RdRP could provide structural support to the resident RdRP, or it could induce a conformational change in the resident RdRP that enables the catalysis of nucleotide polymerisation. It is plausible that this is facilitated by the formation of a quaternary structure between viral RdRPs. Indeed, it has been

proposed that the influenza virus RdRP oligomerises, possibly through interactions between PB1 and PB2 subunits (Digard *et al.*, 1989; Jorba *et al.*, 2008). It is often assumed that enzymes function as isolated soluble entities, however, within cells many macromolecular processes occur in large complexes that are immobilised to a particular subcellular structure. Nucleic acid synthesis is often associated with large, immobilised complexes (Cook, 1999; 2010), examples of which can be found in positive-strand RNA virus biology, including members of the *Picornaviridae*, *Flaviviridae* and *Coronaviridae*. Viral RNA synthesis in these virus families occurs on the surface of membranous structures in the cytoplasm, with the involvement of catalytically inactive RdRPs. By analogy, vRNA synthesis that occurs within influenza virus infected cells could occur in association to a nuclear macromolecular complex that is partially recapitulated *in vitro* by the addition and subsequent oligomerisation of viral RdRP. Specific examples of cooperation and oligomerisation between viral RdRPs has been reported to be required for viral RNA synthesis in poliovirus (Lyle *et al.*, 2002), hepatitis C virus (Wang *et al.*, 2002) and Sendai virus (Smallwood *et al.*, 2002). Also, the HIV-1 reverse transcriptase DNA polymerase functions as a dimeric complex of the p66 subunit and a processed product p51 (Jacobo-Molina *et al.*, 1993; Kohlstaedt *et al.*, 1992). Together with results in this chapter, these findings suggest that oligomerisation-driven stimulation of RdRP activity is a common theme across virus genera. Whether the oligomerisation of viral RdRPs plays an architectural role, required for the reorganisation of RNA structural motifs or the rearrangement of the active site of the *cis*-acting RdRP, remains unknown. It should be noted that the purified vRNP is able to synthesise cRNA *in vitro* in the absence of recombinant viral RdRP. These data strongly oppose a model that cRNA synthesis occurs in *trans* as has been previously

proposed (Moeller *et al.*, 2012), and is fully compatible with the observations that vRNPs isolated from virions are able to produce cRNA *in vitro* and that vRNPs introduced into cycloheximide-treated cells by infecting virions can also synthesise cRNA (Vreede & Brownlee, 2007; Vreede *et al.*, 2004).

The proposal of a model of vRNA synthesis that relies on the *trans*-activation of a viral RdRP is an important step towards understanding the molecular mechanisms of influenza virus genome replication. However, many questions remain unanswered. For example, in functional *in vitro* activity assays described in this chapter the cRNP synthesises relatively lower levels of RNA compared to the vRNP *in vitro*. This finding does not reconcile with the observation that vRNA accumulates to higher levels than cRNA within infected cells for subsequent genome packaging into budding virions (Hay *et al.*, 1977). It has been proposed that viral and host factors are involved in the regulation of viral RNA synthesis, and therefore, the absence of specific factors could explain the difference in RNA levels observed. The viral NEP protein has been described to be a significant player in genome replication by up-regulating the accumulation of replication products (Robb *et al.*, 2009), and therefore the absence of NEP could account for the observed difference. Furthermore, svRNAs have been proposed to act as an allosteric enhancer of replication, possibly through an interaction with a putative RNA binding cleft in the PA subunit of the RdRP (Perez *et al.*, 2010; Perez *et al.*, 2012). It is plausible that svRNAs could bind to the PA subunit of a *trans*-activating or a *cis*-acting viral RdRP to promote vRNA synthesis. The presence of NP may also be required for efficient vRNA synthesis, however, NP was not required for efficient cRNA synthesis in the analogous vRNP activity assay. Moreover, NP has been

shown to be entirely dispensable for replication on short viral RNA-like templates *in vivo*, suggesting that NP represents an elongation factor for the viral RdRP. Regulatory host factors are believed to have an important role in the replication of the viral genome (Matsuoka *et al.*, 2013; Nagata *et al.*, 2008), and therefore their absence *in vitro* may account for inefficient vRNA synthesis. For example, the minichromosome maintenance (MCM) complex has been proposed to be a replication-specific stimulatory factor in the *de novo* initiation of RNA synthesis by the viral RdRP (Kawaguchi & Nagata, 2007).

In conclusion, electron microscopy, single particle analysis and functional *in vitro* assays yielded important insight into the structural organisation of the replicative intermediate of influenza virus. The cRNP was found to have a comparable organisation to the vRNP complex, with a double helical arrangement and defined termini containing a loop at one terminus and the viral RdRP at the opposite. This work provides an important framework for further structural analyses in order to elucidate potential differences that could help to explain the distinct mechanistic dissimilarities between these two components of the vRNA replication molecular machinery. In this chapter, a model of vRNA synthesis that relies on the *trans*-activation of the cRNA-associated RdRP was proposed, advancing previous models that had advocated a role for a *trans*-acting RdRP in vRNA synthesis.

4.7 Summary

- 2D single particle analysis was used to gain structural insight into the cRNP.
- Three major domains in the cRNP were observed. A central filament with a double helical arrangement and two termini. One terminus contains a loop structure while the opposite terminus contains the viral RdRP that exhibits two structural features.
- vRNPs, but not cRNPs, are able to synthesise RNA in the absence of recombinant RdRP in *in vitro* activity assays.
- cRNP requires the presence of a *trans*-activating RdRP for the synthesis of vRNA.

Chapter 5: Interactome of the influenza virus transcription/replication machinery

5.1 Introduction

Viruses are obligate intracellular parasites that have been compelled by evolutionary processes to encode a minimal number of proteins for the completion of an infectious life-cycle, in order to infect naïve hosts and to persist in nature. This is particularly exemplified by RNA viruses, the genomes of which are generally smaller than the genomes of DNA viruses and therefore they greatly rely on the exploitation and subversion of host cellular proteins, structures and pathways to facilitate virus replication (Holmes, 2013). Transcription and replication of the influenza A virus genome is performed by the virally-encoded RdRP, a major determinant of species tropism, pathogenicity and a key player in the adaptation of avian influenza A viruses to

mammalian hosts. These characteristics of the viral RdRP are thought to be governed by numerous interactions with cellular factors (Cauldwell *et al.*, 2014; Manz *et al.*, 2013). It is therefore of great importance to understand the relationship between the viral transcription/replication machinery and host cellular factors in order to understand how the host cell can influence the function of the viral transcription/replication machinery and *vice versa*. Insight into the molecular biology of these relationships could help elucidate how viral RdRP function is regulated by cellular factors. Moreover, it could lead to novel antiviral strategies and has the potential to identify host-specific interactions that would act as a barrier to pandemic emergence.

The purpose of this chapter is to identify the interactome of the influenza A virus replication/transcription machinery within the context of an infected cell, with a view to discovering cellular proteins that are involved in the regulation of viral RdRP function. Interactomics is the study of the complete set of physical interactions that occur between molecules within a cell (Collura & Boissy, 2007; Sanchez *et al.*, 1999). Affinity-purification mass spectrometry (AP-MS) approaches have been instrumental in identifying these physical associations and therefore it was sought to isolate the viral RNP and RdRP complexes from infected cells for the purpose of identifying co-purifying host factors by liquid-chromatography and tandem mass spectrometry (LC-MS/MS). This approach complements previous studies that have aimed to identify critical cellular factors that are involved in the virus life-cycle, including a number of genome-wide screens (Hao *et al.*, 2008; Karlas *et al.*, 2010; Konig *et al.*, 2010; Shapira *et al.*, 2009; Sui *et al.*, 2009). Although informative, these genome-wide screens have failed to identify specific stages of the virus life-cycle at which particular cellular

factors are critical. Furthermore, these methods do not distinguish between factors that are required for virus replication by directly interacting with a viral component and those factors that can contribute to virus replication indirectly. Additional techniques have been employed with the aim of identifying host factors that interact with the viral transcription/replication machinery, including yeast two-hybrid screens (Shapira *et al.*, 2009; Tafforeau *et al.*, 2011), complementation assays (Munier *et al.*, 2013) and AP-MS (Bradel-Tretheway *et al.*, 2011; Fislova *et al.*, 2010; Jorba *et al.*, 2008; Mayer *et al.*, 2007). However, these studies have been limited by either the number of cellular factors that can be cloned and screened or because the identifications were not carried out in the context of the infected cell. Furthermore, these approaches have not been able to distinguish between cellular factors that interact differentially with the cRNP and the vRNP. Therefore, in order to identify the cellular interactome of the virus transcription/replication machinery within the context of the infected cell two approaches would be employed. Firstly to perform LC-MS/MS on isolated cRNPs and vRNPs from infected cells, taking advantage of the RNA-based affinity purification strategy presented in chapter one. A further approach is to perform LC-MS/MS on the viral RdRP isolated from infected cells. In employing these strategies it is the aim to identify components of the interactome that can be studied further in order to gain a greater understanding of viral RdRP function.

5.2 Isolation of influenza A virus cRNP and vRNP complexes and the identification of co-purifying cellular factors

In order to identify cellular factors that interact with cRNP and vRNP complexes these complexes were isolated from infected cells. The RNA-based affinity purification strategy for the isolation of RNPs presented in chapter one was used to isolate viral RNPs for LC-MS/MS analyses. The approach presented in chapter one, however, uses a density gradient centrifugation step in order to isolate a homogenous population of cRNPs and vRNPs that could exclude RNPs that are in association with specific cellular factors. Indeed, in SDS-PAGE and silver stain analyses of RNPs isolated by density gradient centrifugation there were few additional bands that correspond to cellular proteins, indicating that the majority of RNPs isolated using this method were not associated with host factors. Therefore, a two-step affinity purification strategy of cRNP and vRNP complexes was devised that relies firstly on the separation of positive-sense and negative-sense RNA by RNA-based affinity purification, followed by the isolation of the viral RdRP by Strep-tag affinity purification. The Strep-tag is a small polypeptide tag that exhibits intrinsic reversible affinity for Strep-Tactin, an engineered streptavidin that allows highly selective purification of Strep-tag fusion proteins under physiological conditions (Schmidt & Skerra, 2007). For this second step of affinity purification, a Strep-tag was introduced to the C-terminus of the PB2 subunit (PB2-Strep) which would allow the purification of the viral RdRP (Figure 5.1), as has been previously described (Rameix-Welti *et al.*, 2009). Recombinant influenza A/WSN/33 viruses that encode a PB2-Strep protein and contain a PP7 RNA tag in the positive-sense or the negative-sense of the NA gene were generated by reverse genetics (Fodor



Figure 5.1 Schematic representation of the PB2-Strep gene encoding a PB2 protein fused to a Strep-tag at the C-terminus. The PB2 open reading frame is fused to a Strep-tag and flanked by 5′ and 3′ non-coding regions (NCRs) indicated by black lines. The terminal 109 nt of the PB2 ORF are duplicated after the indicated stop codon. Underlined amino acid sequences correspond to the Strep-tag.

et al., 1999; Neumann *et al.*, 1999). The pPOLI-NA-cRNA-PP7 or pPOLI-NA-vRNA-PP7 plasmids were co-transfected into HEK 293T cells with the pHW2000-PB2-Strep plasmid and the six remaining pPOLI plasmids. The pcDNA plasmids expressing NP and the viral RdRP proteins were also co-transfected. WT plasmids were used as a positive control. As a negative control the pPOLI-PB1 plasmid was replaced with the empty pPOLI-SapI-Rib plasmid. After amplification of recovered virus from HEK 293T cells on MDBK cells, virus growth was assessed using a plaque assay on MDBK cells. As expected, WT virus was rescued as indicated by the presence of viral plaques (Figure 5.2A). Recombinant viruses PB2-Strep-NA-cRNA-PP7 and PB2-Strep-NA-vRNA-PP7 were also rescued with a comparable plaque phenotype to WT virus, indicating that the introduction of a C-terminal Strep-tag to PB2 and a PP7 RNA tag into the NA gene does not affect the generation of recombinant virus and that these viruses are able to undergo multiple replication cycles (Figure 5.2A).

Next, the growth properties of the recombinant influenza A/WSN/33 PB2-Strep-NA-cRNA-PP7 and PB2-Strep-NA-vRNA-PP7 viruses were compared to WT virus over the course of 72 h (Figure 5.2B). MDBK cells were infected at an MOI of 0.001 with either WT virus or recombinant viruses and aliquots of growth medium were collected at 12, 24, 36, 48, 60 and 72 h p.i.. Virus titres were determined by plaque assay on MDBK cells. As expected, WT virus titres peaked at approximately 5.3×10^7 PFU/ml at 48 h p.i.. PB2-Strep-NA-cRNA-PP7 and PB2-Strep-NA-vRNA-PP7 recombinant viruses exhibited similar growth curve properties to that of WT virus, with comparable maximal virus titres at 48 h p.i.. These results show that the introduction of a C-terminal Strep-tag to PB2 and a PP7 RNA tag into the NA gene does not significantly affect the multi-cycle growth kinetics of influenza virus.

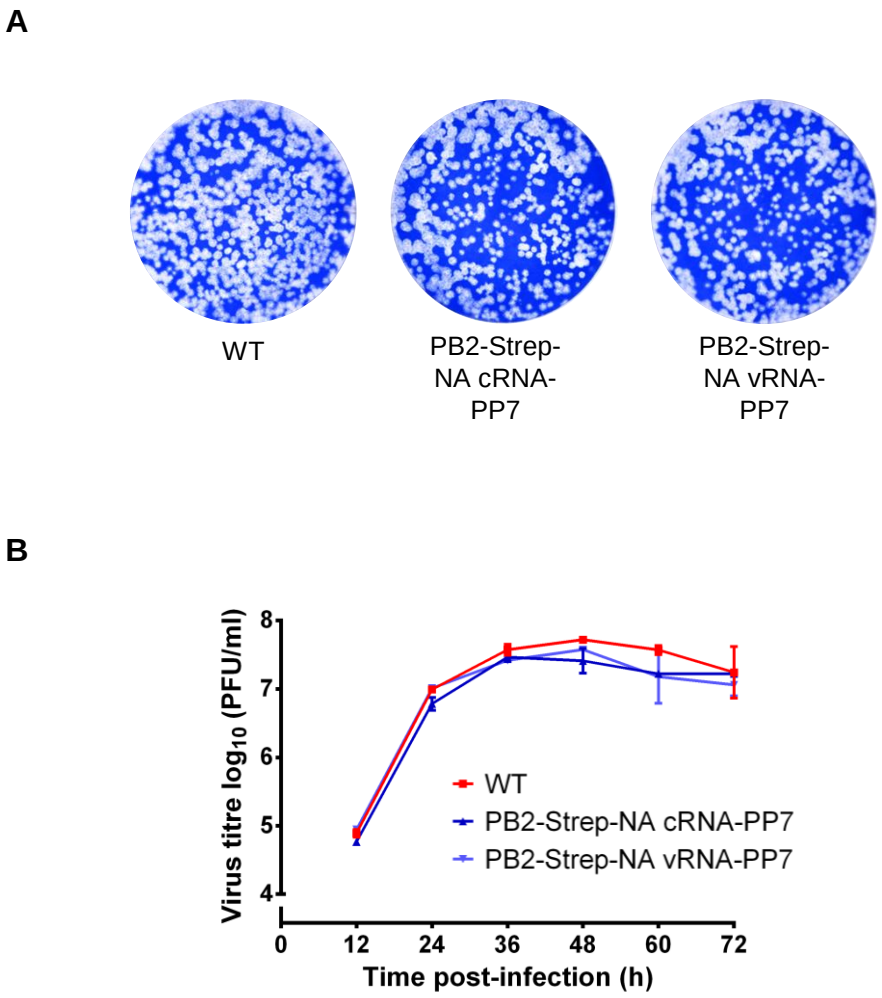
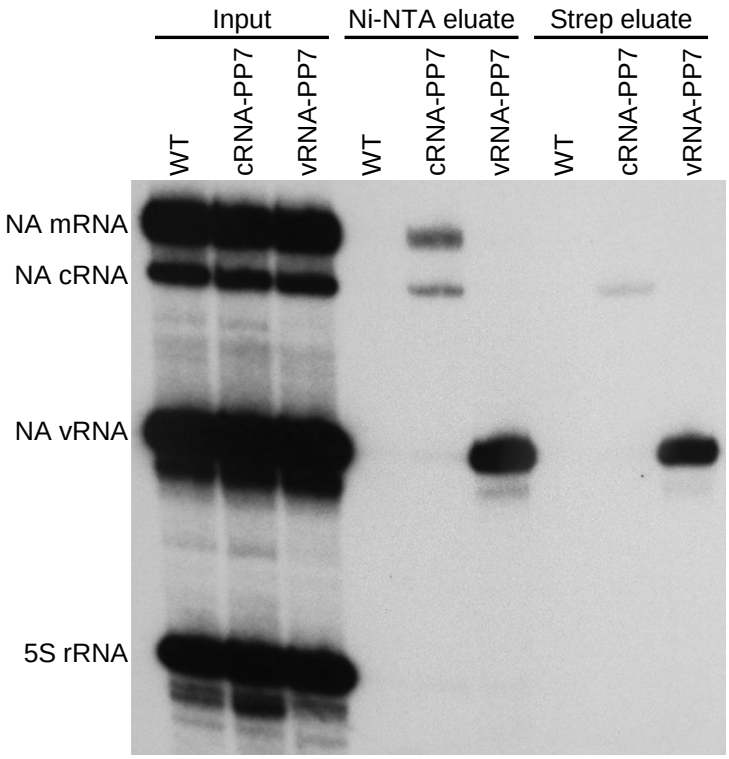


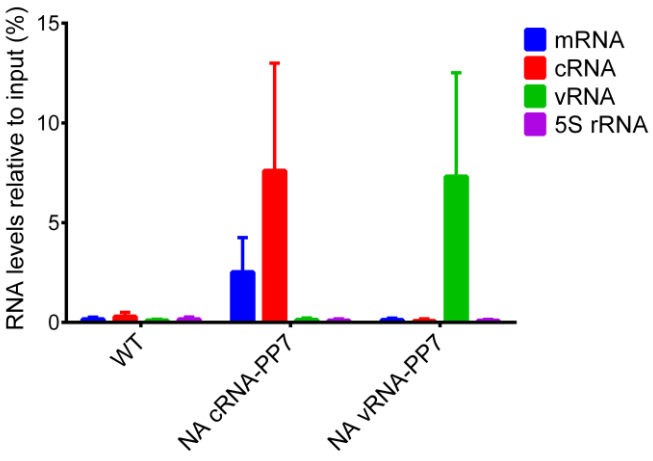
Figure 5.2 Generation of recombinant influenza A/WSN/33 viruses containing a PB2-Strep subunit and a PP7 RNA tag in the NA gene. (A) Plaque phenotype of wild-type (WT) virus and viruses that contain a PP7 RNA tag in the cRNA or vRNA orientation of the NA with a PB2-Strep RdRP subunit. MDBK cells were infected for 72 h prior to staining with Coomassie Brilliant Blue. (B) Growth kinetics of WT virus and recombinant viruses. MDBK cells were infected at an MOI of 0.001 and at the indicated time points cell supernatants were collected and virus titres were determined by plaque assay on MDBK cells.

To isolate cRNP and vRNP complexes for LC-MS/MS analyses HEK 293T-PP7CP cells were infected at an MOI of 5 with the PB2-Strep-NA cRNA-PP7 or PB2-Strep-NA vRNA-PP7 viruses. Cells were also infected with WT virus as a negative control. At 7 h p.i. cells were lysed and PP7CP was purified using Ni-NTA chromatography. PB2-Strep was subsequently purified from the Ni-NTA eluate by Strep-tag affinity purification. Total RNA was isolated from the input sample, Ni-NTA chromatography eluate and the Strep-tag affinity purification eluate, and the RNA was analysed in a primer extension assay using NA segment-specific primers (Figure 5.3A). The 5S rRNA was monitored as a control. These analyses showed that, as expected, target NA cRNP and vRNP complexes are separated with high specificity using RNA-based affinity chromatography. Approximately 7.5% of total cRNA and vRNA was purified (Figure 5.3B). However, in the second step of affinity purification using the Strep-tag on PB2, only approximately 0.4% of total cRNA and vRNA was recovered. SDS-PAGE and silver staining analyses of the Strep-tag affinity purification eluates revealed the presence of protein bands that correspond to the viral RdRP and NP, with a number of bands that correspond to co-purifying cellular proteins (Figure 5.4). Viral RdRP and NP bands were absent in the WT negative control indicating that RNP complexes were specifically purified. Western blot analyses using PB2, PA and NP specific antibodies showed that PB2 and PA levels were equivalent between the samples that contained cRNP and vRNP complexes, however, the levels of NP were considerably lower in the sample that contained the cRNP (Figure 5.5). It was therefore concluded that the majority of the viral RdRP that was purified was not associated with RNA in the form of an RNP, but was free trimeric RdRP.

A


Input
Ni-NTA eluate
Strep eluate
WT
cRNA-PP7
vRNA-PP7
WT
cRNA-PP7
vRNA-PP7
WT
cRNA-PP7
vRNA-PP7
NA mRNA
NA cRNA
NA vRNA
5S rRNA

B


RNA levels relative to input (%)
15
10
5
0
mRNA
cRNA
vRNA
5S rRNA
WT
NA cRNA-PP7
NA vRNA-PP7

C

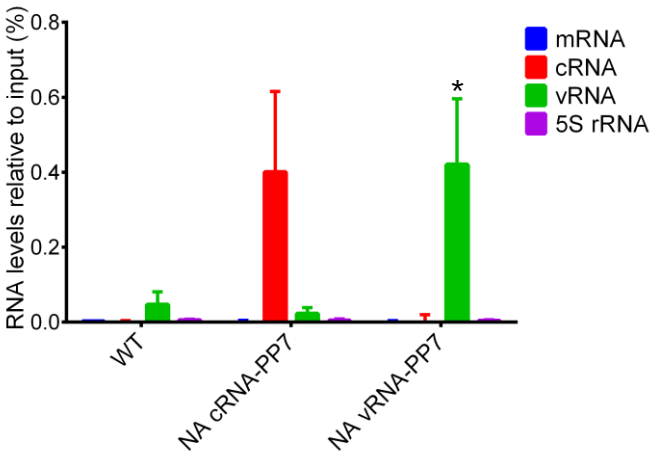


Figure 5.3 Two-step affinity purification of cRNP and vRNP complexes from influenza A/WSN/33 virus infected cells with a PP7 RNA tag in the NA gene and a PB2-Strep RdRP subunit. HEK 293T-PP7CP cells were infected at an MOI of 5 with viruses that have a PB2-Strep RdRP subunit and that also contain a PP7 RNA tag in the cRNA or vRNA orientations of the NA gene. Cells were also infected with wild-type (WT) virus as a negative control. At 7 h p.i. tagged RNA was purified by Ni-NTA chromatography of PP7CP and subsequently PB2-Strep was purified by Strep-tag affinity chromatography. (A) Primer extension analyses of total and purified RNA using NA segment-specific primers for detecting positive sense (mRNA and cRNA) and negative sense (vRNA) RNAs. Primer extension analysis of 5S rRNA was used as a control. Ten times and one hundred times more sample of Ni-NTA and Strep-tag affinity purified RNA was analysed relative to total RNA, respectively. (B) Quantitation of primer extension analyses of Ni-NTA purified RNA. RNA levels represent the mean and the error bars represent standard deviations from three biological repeats. (C) Quantitation of primer extension analyses of Strep-tag purified RNA. RNA levels represent the mean and the error bars represent standard deviations from three biological repeats. Asterisks indicate a significant difference from WT (* $P < 0.05$, based on a two-sample Student's *t*-test).

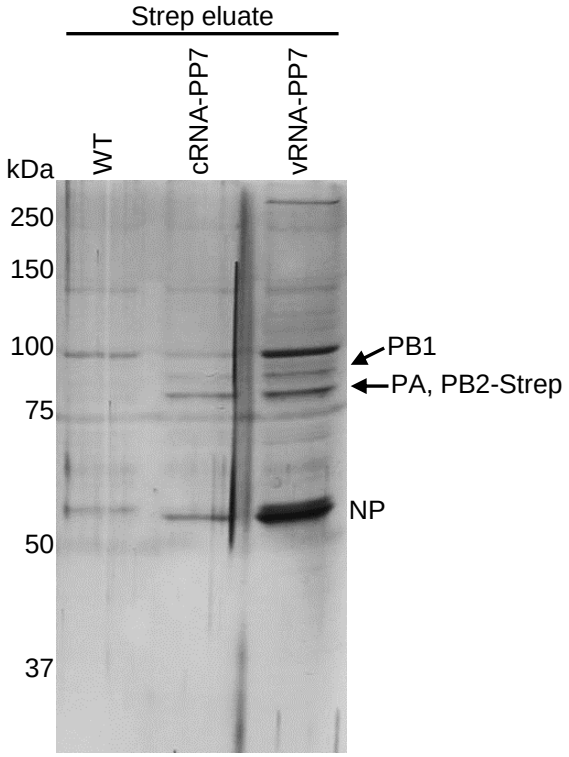


Figure 5.4 Analysis of RNP complexes isolated by two-step affinity purification. HEK 293T-PP7CP cells were infected at an MOI of 5 with viruses that have a PB2-Strep RdRP subunit and that also contain a PP7 RNA tag in the cRNA or vRNA orientations of the NA gene. Cells were also infected with wild-type (WT) virus as a negative control. At 7 h p.i. tagged RNA was purified by Ni-NTA chromatography of PP7CP and subsequently PB2-Strep was purified by Strep-tag affinity chromatography. Purified RNP complexes were analysed by SDS-PAGE and silver staining.

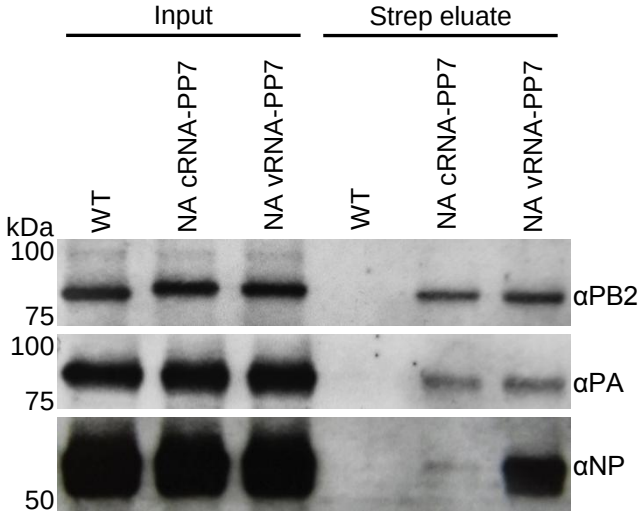


Figure 5.5 Western blot analyses of RNP complexes isolated by two-step affinity purification. HEK 293T-PP7CP cells were infected at an MOI of 5 with viruses that have a PB2-Strep RdRP subunit and that also contain a PP7 RNA tag in the cRNA or vRNA orientations of the NA gene. Cells were also infected with wild-type (WT) virus as a negative control. At 7 h p.i. tagged RNA was purified by Ni-NTA chromatography of PP7CP and subsequently PB2-Strep was purified by Strep-tag affinity chromatography. Purified RNP complexes were analysed by SDS-PAGE and Western blotting with PB2, PA and NP specific polyclonal antibodies.

Mass spectrometry analyses were employed to identify co-purifying cellular proteins. Three independent purifications were carried out and the samples were submitted to the Central Proteomics Facility (Sir William Dunn School of Pathology, University of Oxford) for peptide and protein identifications using a Thermo LTQ XL Orbitrap mass spectrometer. Peptide and protein identifications were analysed using Mascot (Perkins *et al.*, 1999). Protein identifications with a *P*-value less than 0.05 ($P < 0.05$) were considered statistically significant identifications. A subtractive analysis was performed, whereby proteins that were identified in the negative control sample (WT) were excluded from further analyses. Assignments made to decoy proteins, used to calculate false discovery rates, and the contaminants trypsin, serum albumin and keratins were also excluded. Mass spectrometry of the isolated cRNP complexes revealed that low numbers of peptides that derived from viral RdRP subunits and NP had been detected, corresponding to relatively low percentage sequence coverage of these viral proteins (Table 5.1). On one occasion it was not possible to detect any peptides from the PB1 and PA proteins. Similarly, mass spectrometry of purified vRNP complexes identified relatively few peptides belonging to the viral RdRP and NP proteins (Table 5.2). These results reflect the low purification efficiency of two-step affinity purification of RNP complexes. A total of 119 and 96 cellular factors were found to co-purify with cRNP and vRNP complexes, respectively, isolated by two-step affinity purification (Appendices C and D). However, minimal overlap of protein identifications was observed between three biological repeats (Figure 5.6).

Table 5.1 A summary of mass spectrometry data of influenza virus RdRP subunit and NP proteins detected in samples of cRNP complexes isolated by two-step affinity purification.

	Protein	***Mascot Score***[a]	***Peptide Spectrum Matches***	***Peptide Sequences***	***% Sequence Coverage***
Experiment 1	PB1	38	2	2	7.3
	PB2-Strep	169	7	6	14.2
	PA	59	2	2	6.6
	NP	208	11	9	26.7
Experiment 2	PB1	N/A	N/A	N/A	N/A
	PB2-Strep	229	16	16	24.5
	PA	205	11	10	17.2
	NP	286	15	15	38.6
Experiment 3	PB1	N/A	N/A	N/A	N/A
	PB2-Strep	34	1	1	3.6
	PA	N/A	N/A	N/A	N/A
	NP	34	1	1	3.6

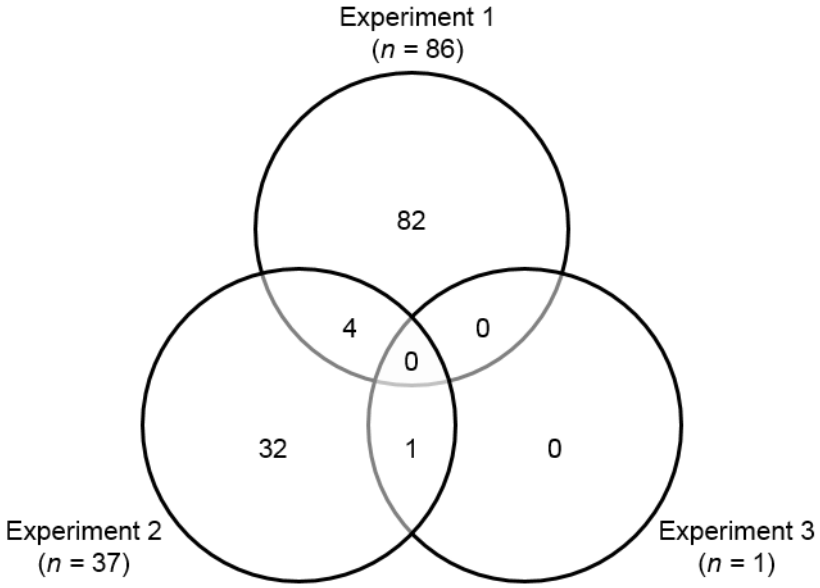
[a]-$10 \times \log_{10}(P)$, where P is the absolute probability

Table 5.2 A summary of mass spectrometry data of influenza virus RdRP subunit and NP proteins detected in samples of vRNP complexes isolated by two-step affinity purification.

	Protein	***Mascot Score***[a]	***Peptide Spectrum Matches***	***Peptide Sequences***	***% Sequence Coverage***
Experiment 1	PB1	102	2	2	9.8
	PB2-Strep	147	5	5	10.4
	PA	86	5	5	14.8
	NP	669	38	27	62.9
Experiment 2	PB1	36	3	3	6.5
	PB2-Strep	131	7	7	12.4
	PA	61	3	3	5.2
	NP	362	20	15	46.4
Experiment 3	PB1	69	6	6	13.9
	PB2-Strep	456	22	21	34.7
	PA	206	14	13	28.4
	NP	489	40	24	48.4

[a]-$10 \times \log_{10}(P)$, where P is the absolute probability

A



B

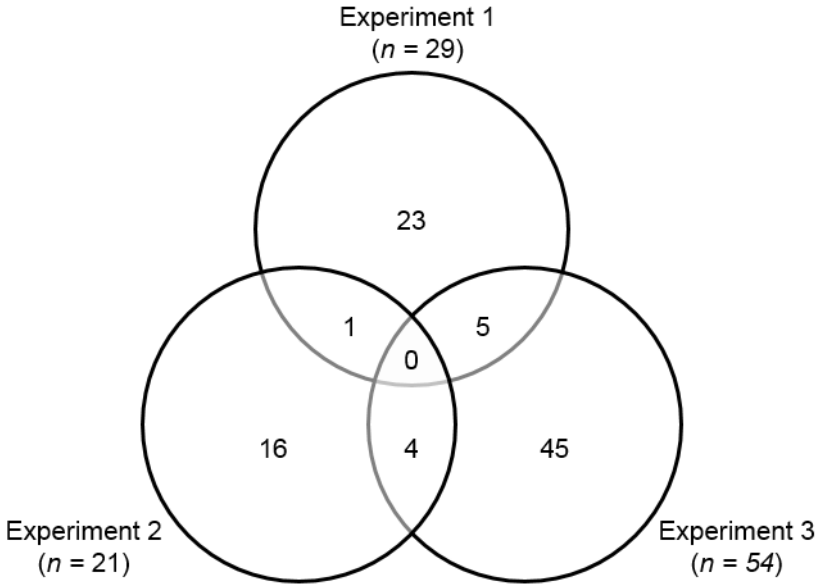


Figure 5.6 Identification of cellular factors that co-purify with RNP complexes isolated by two-step Ni-NTA and Strep-tag affinity purification. Venn diagrams representing cellular proteins identified by mass spectrometry of (A) cRNP and (B) vRNP complexes isolated by two-step affinity purification from infected HEK 293T cells, highlighting the number of identifications that overlap between three independent biological repeats.

5.3 Isolation of influenza A virus RdRP complexes and the associated interactome from infected cells

As an alternative strategy for identifying the interactome of the influenza virus transcription and replication machinery, one-step Strep-tag affinity purification of the viral RdRP from infected cells was performed. A recombinant influenza A/WSN/33 virus that encodes a PB2-Strep protein was generated by reverse genetics. The pHW2000-PB2-Strep plasmid was transfected into HEK 293T cells with the seven remaining pPOLI plasmids for the synthesis of the eight vRNAs of the influenza virus genome. Four pcDNA plasmids expressing the NP and the viral RdRP proteins were co-transfected for the expression of viral RdRP and NP. WT pPOLI-PB2 plasmid was used as a positive control. As a negative control the pPOLI-PB1 plasmid was replaced with the empty pPOLI-SapI-Rib plasmid. After amplification of recovered virus from HEK 293T cells on MDBK cells, virus growth was assessed using a plaque assay on MDBK cells. As expected, WT virus was rescued as indicated by the presence of viral plaques (Figure 5.7A). Recombinant PB2-Strep virus was also rescued with a comparable plaque phenotype to WT virus, confirming that the presence of a C-terminal Strep-tag does not affect the generation of recombinant virus and that this virus is able to undergo multiple replication cycles (Figure 5.7A). The growth properties of the recombinant PB2-Strep virus over the course of 72 h were found to be indistinguishable from WT virus, confirming that the C-terminal Strep-tag does not affect multi-cycle replication of influenza virus (Figure 5.7B).

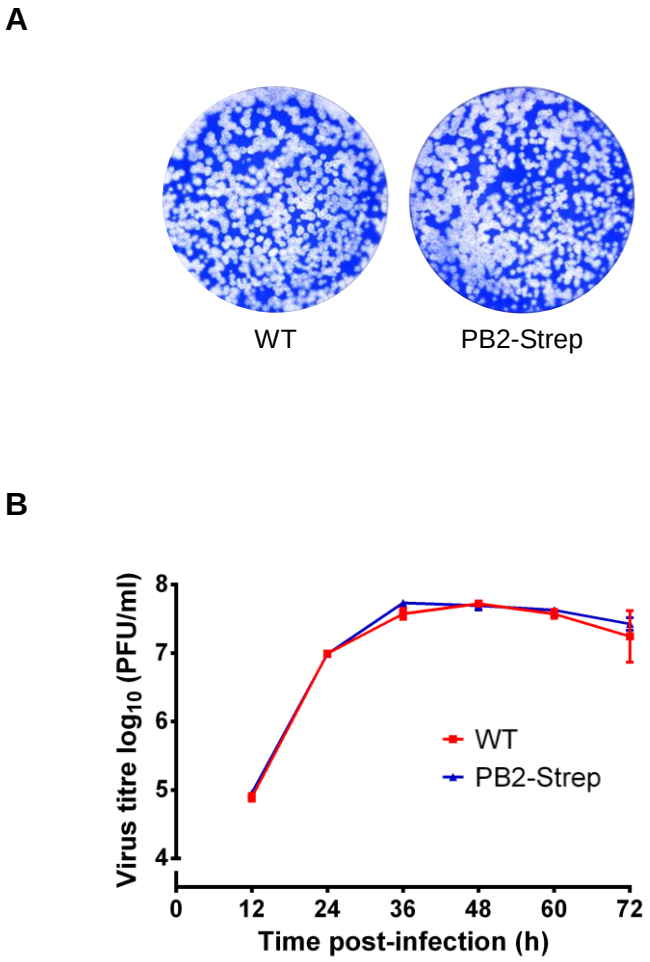


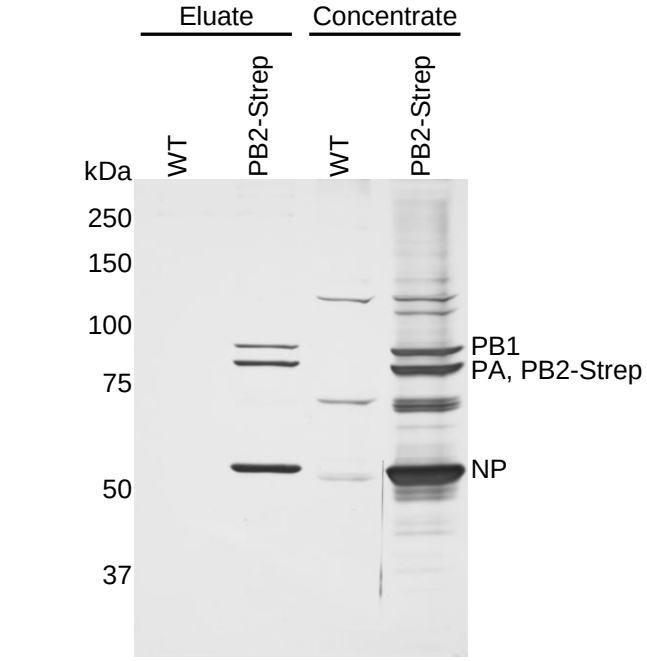
Figure 5.7 Characterisation of a recombinant influenza A virus encoding a PB2-Strep RdRP subunit. (A) Plaque phenotype of wild-type (WT) and PB2-Strep virus. MDBK cells were infected for 72 h prior to staining with Coomassie Brilliant Blue. (B) Growth kinetics of WT virus and PB2-Strep virus. MDBK cells were infected at an MOI of 0.001 and at the indicated time points cell supernatants were collected and virus titres were determined by plaque assay on MDBK cells.

In order to isolate viral RdRP complexes from infected cells for mass spectrometry analyses, HEK 293T cells were infected with the PB2-Strep virus or WT virus (negative control) at an MOI of 5. Whole cell lysates were prepared 7 h p.i. and PB2-Strep complexes were affinity purified. PB2-Strep complexes were eluted and analysed by SDS-PAGE and silver staining and RNA was analysed by primer extension analyses using NA segment-specific primers. SDS-PAGE and silver staining analysis revealed that viral RdRP-containing complexes were isolated from cells infected with the PB2-Strep virus, but not when the cells were infected with WT virus (Figure 5.8A). Concentration of the eluates revealed a number of cellular proteins co-purifying with PB2-Strep that were absent in the WT negative control (Figure 5.8A). Analyses of the viral RNAs showed that viral cRNA and vRNA, but not viral mRNA or the highly abundant 5S rRNA, were isolated using PB2-Strep affinity-purification (Figure 5.8B). Approximately 7% and 6% of total cRNA and vRNA, respectively, was isolated from infected cells using PB2-Strep affinity-purification (Figure 5.8C). These data illustrate that viral RdRP and RNP complexes had been specifically isolated from infected cells.

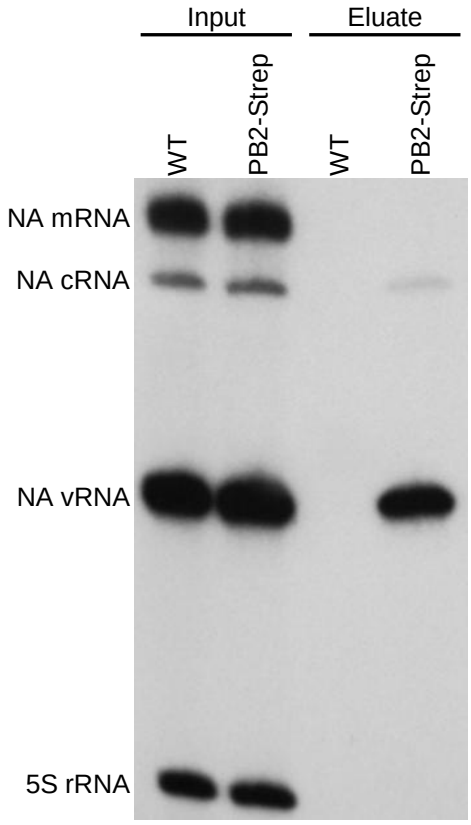
5.4 Identification of the interactome of the influenza A virus replication machinery by mass spectrometry

Mass spectrometry analyses were employed to identify co-purifying cellular proteins. Three independent purifications were carried out and the samples were submitted to the Central Proteomics Facility (Sir William Dunn School of Pathology, University of Oxford) for peptide and protein identifications using a Thermo Q Exactive Orbitrap

A


Eluate
Concentrate
WT
PB2-Strep
WT
PB2-Strep
kDa
250
150
100
75
50
37
PB1
PA, PB2-Strep
NP

B


Input
Eluate
WT
PB2-Strep
WT
PB2-Strep
NA mRNA
NA cRNA
NA vRNA
5S rRNA

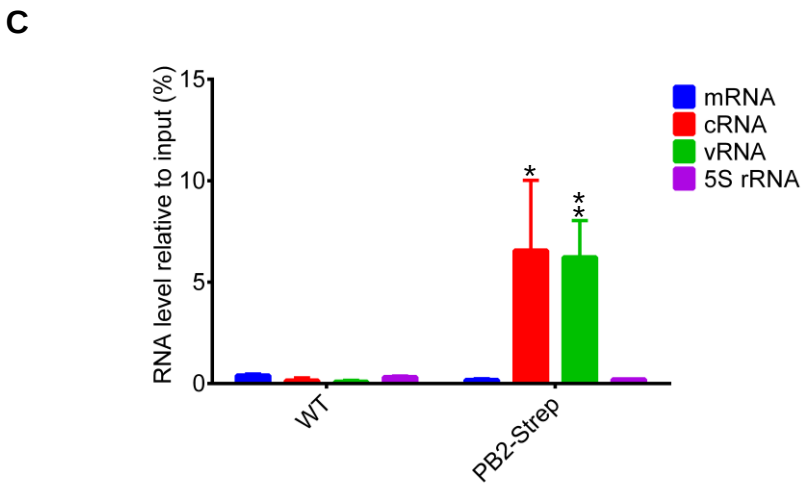


Figure 5.8 Isolation of influenza A virus RdRP from infected HEK 293T cells. HEK 293T cells were infected with WT virus (negative control) or PB2-Strep virus at an MOI of 5 for 7 h. PB2-Strep complexes were purified by Strep-tag affinity-purification from cell lysates. (A) Purified proteins were analysed by SDS-PAGE and silver staining. (B) Viral RNAs isolated from total cell lysates or purified material were analysed by primer extension using radiolabeled primers for positive sense (mRNA and cRNA) and negative sense (vRNA) NA-specific viral RNAs. Primer extension analysis of 5S rRNA was used as a control. Ten times more sample of co-purified RNA was analysed relative to total RNA. (C) Quantitation of primer extension analyses of co-purified RNA. RNA levels represent the mean and the error bars represent SDs from three biological repeats. Asterisks indicate a significant difference from WT (* $P < 0.05$, ** $P < 0.01$, based on a two-sample Student's *t*-test).

mass spectrometer. Proteins were quantified using spectral index normalised quantitation (SINQ), a label-free method which uses the intensities of the peptide fragment ions to measure protein abundance (Appendix E) (Trudgian *et al.*, 2011). Background binding was determined by identifying proteins purified from cells infected with WT virus and identifications were normalised to PB2-Strep abundance. Assignments made to decoy proteins, used to calculate false discovery rates, and the contaminants trypsin, serum albumin and keratins were also excluded (Appendix F).

As expected, the viral RdRP subunits and NP were the most abundant proteins in three separate experiments (Table 5.3 and Appendix F). All three RdRP subunits were detected at approximately similar levels, consistent with the purification of RdRP trimers. However, there was an excess of approximately one third of PB2-Strep, indicating that not all of the PB2-Strep purified was incorporated into trimeric RdRPs. The ratio of NP to PB2-Strep was 8. Each NP is thought to bind approximately 24 nt of RNA (Ortega *et al.*, 2000; Ye *et al.*, 2006), so even for the shortest segment of the viral genome (890 nt) this would not be sufficient for all of the purified RdRPs to be incorporated into RNPs. Assuming equimolar binding of all eight genome segments (with an average length of 1,700 nt per vRNP, and hence an average binding capacity of 71 copies of NP), approximately 1 in 9 of the PB2-Strep proteins analysed could be part of an RNP. It was therefore concluded that the samples contained a mixture of RNPs, free trimeric RdRPs, and free PB2-Strep polymerase subunits.

In addition to these viral proteins, 171 cellular proteins were specifically purified. The abundance of these proteins varied over approximately four orders of magnitude

Table 5.3 A summary of SINQ data of influenza virus RdRP subunit and NP proteins detected.

Protein	*Mean SINQ Score*	*(+/–)*[a]	*N*[b]
NP	8.08	2.18	3
PB2-Strep	1		3
PA	0.79	0.03	3
PB1	0.60	0.10	3

[a]SD
[b]Number of experiments in which the protein was identified.

(Appendix F). The majority of these proteins could be identified reproducibly (Figure 5.9), with reproducible observations more likely for the more abundant proteins (Appendix F). The most abundant of the interacting host proteins was the Hsp70 molecular chaperone, which is clearly visible by SDS-PAGE and silver-staining (Figure 5.8A, 5.10 and Appendix B). Other categories of particularly abundant protein are shown in Figure 5.10 and Appendix B. These include the chaperonin containing TCP1 complex (CCT), nuclear import factors such as importin-5 (RanBP5) and importin-α3, -α4, -α5 and -α7, ubiquitin and ubiquitin ligases, cytoskeletal proteins (in particular tubulin), ribosomal proteins, mitochondrial proteins, phosphatases and kinases. Most of the bound proteins could interact with at least one of the other bound proteins, suggesting that complexes of interacting proteins may have been purified (Figure 5.10). Consistent with this, the eight subunits of the chaperonin CCT were purified in approximately equal quantities (Figure 5.10). Gene Ontology (GO) enrichment analysis was performed using PANTHER (Protein Analysis THrough Evolutionary Relationships) to map the GO terms for molecular function and subcellular distribution of the viral RdRP interactome (Mi *et al.*, 2013). Over 40% of the interactome had the catalytic activity GO term associated to it, with hydrolases and transferases being the most represented GO terms within this category (Figure 5.11). The next significant molecular function GO term was binding, with over half of these binding proteins being involved in nucleic acid binding, of which the majority are involved in RNA binding.

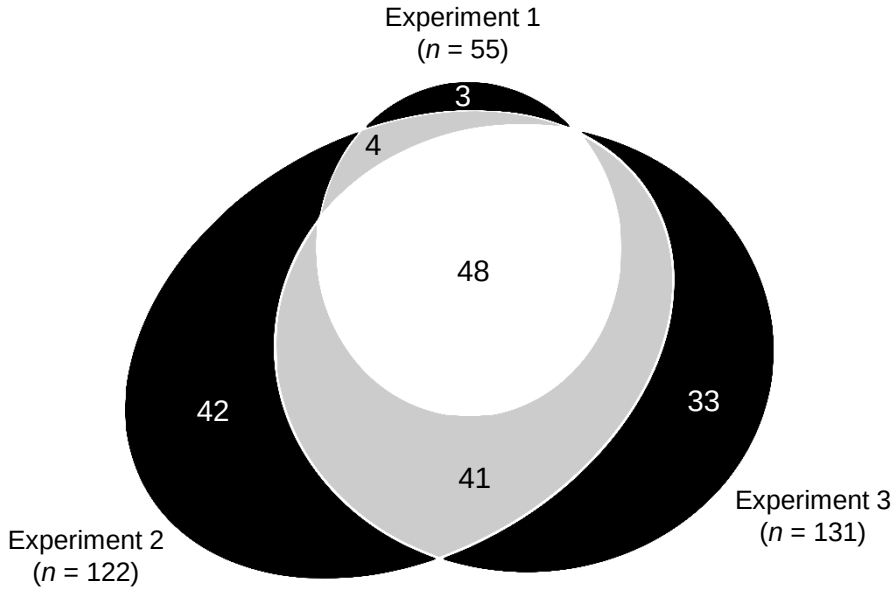


Figure 5.9 Identification of cellular factors that co-purify with PB2-Strep isolated by one-step Strep-tag affinity purification. Venn diagram representing 171 cellular proteins identified by affinity-purification mass spectrometry of PB2-Strep complexes isolated from infected HEK 293T cells, highlighting the number of identifications that overlap between three independent biological repeats.

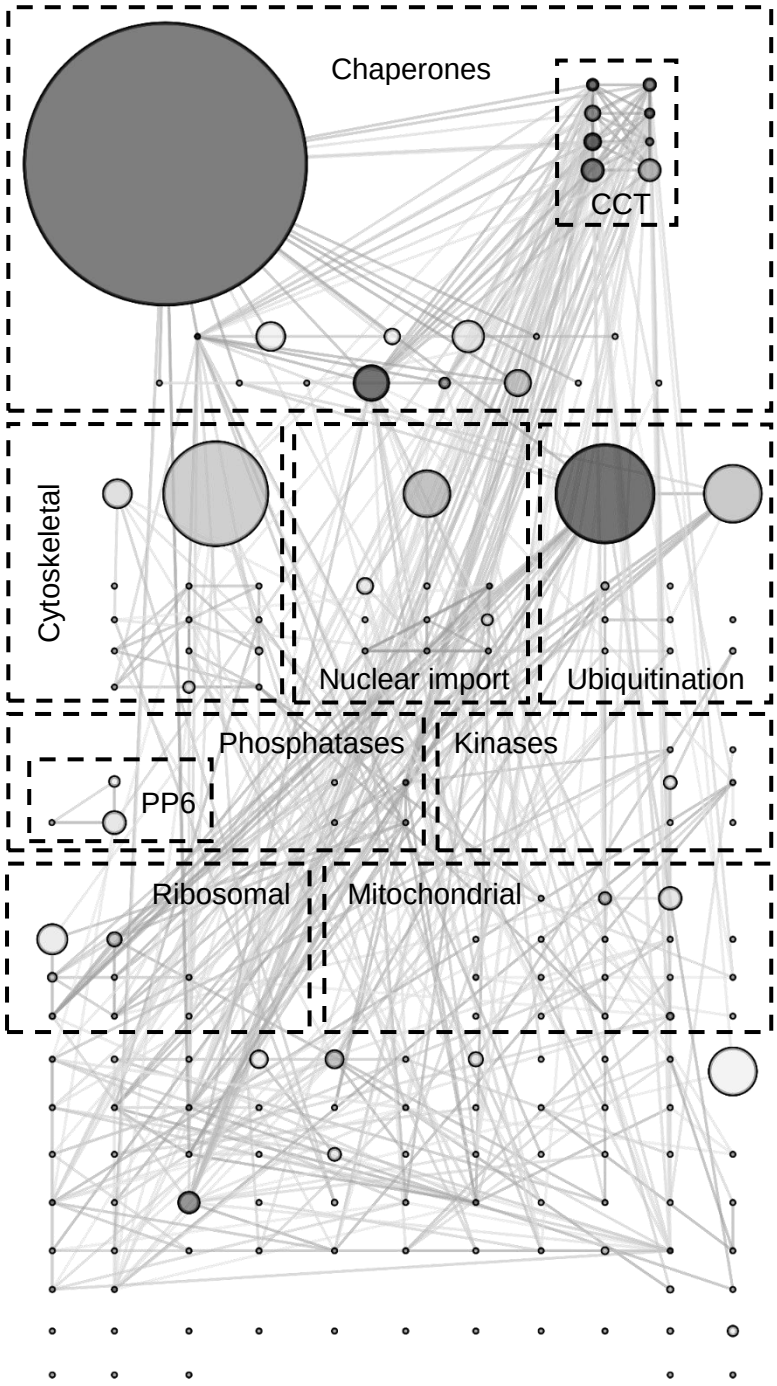


Figure 5.10 Interaction network of cellular proteins in the viral transcription/replication machinery interactome. Abundant proteins have been manually sorted into the indicated categories. The shading of nodes indicates their connectivity in the network, with darker shading for highly-connected nodes. The size of nodes is proportional to protein abundance in the sample, an indication of each protein's likelihood of being bound to the transcription/replication machinery. For clarification, no node has an area less than one fortieth of the largest node.

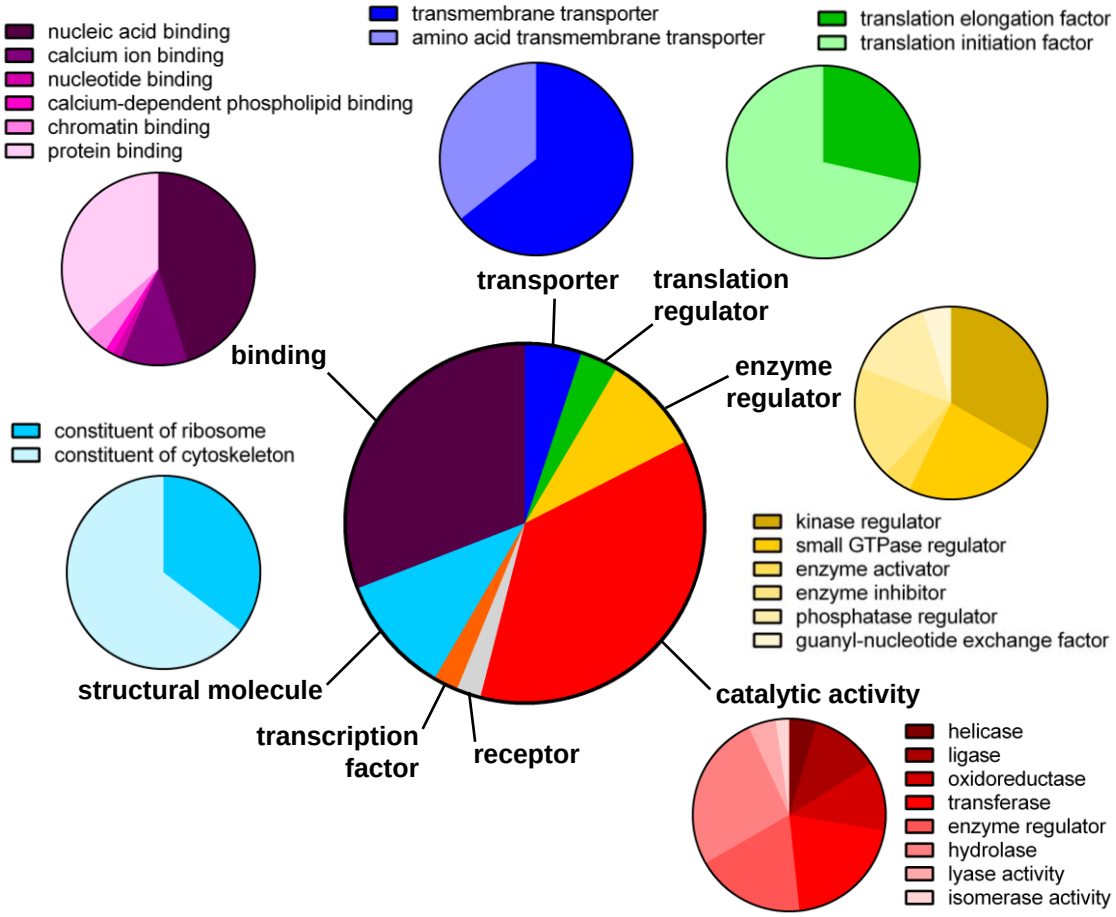


Figure 5.11 Gene Ontology (GO) analysis of cellular proteins in the viral transcription/replication machinery interactome. The 171 identified cellular proteins were subjected to PANTHER gene list analysis to gain an overview of the molecular functions of the interactome. Note that a single protein may be associated with many terms.

5.5 Discussion

An in-depth understanding of the physical interactions that occur between viral proteins and cellular proteins within an infected cell is necessary for elucidating the molecular mechanisms that underlie virus replication. During infection the influenza virus transcription/replication machinery makes numerous interactions with the host cell (Matsuoka *et al.*, 2013; Muller *et al.*, 2012; Shaw, 2011; Watanabe *et al.*, 2010). Following infection, vRNPs from virions enter the host cell nucleus and recruit host factors to enable them to transcribe and replicate their vRNA. Subsequently, new viral RdRP subunits are translated in the cytoplasm and must be imported into the nucleus for trimer assembly and incorporation into RNPs. This requires the viral RdRP to interface with molecular chaperones and the host nuclear import machinery (Geller *et al.*, 2012; Hutchinson & Fodor, 2012; Resa-Infante & Gabriel, 2013). While many interactions between the viral transcription/replication machinery and the host cell have been reported, and some of the molecular biology of these interactions has been elucidated, a full description of the cellular proteins interacting with the viral transcription/replication machinery in an infected host is lacking. Furthermore, much of the mechanistic detail and the roles of previously identified host-pathogen interactions is not understood.

In this chapter, an AP-MS approach was employed with the aim of identifying the cellular interactome of the influenza virus transcription and replication machinery, with a view to understanding how viral RdRP function is regulated in infected cells. Viral RNP complexes and the viral RdRP were isolated from infected cells, in contrast to

previous studies that had isolated the viral RdRP from transfected cells (Bradel-Tretheway *et al.*, 2011; Fislova *et al.*, 2010; Jorba *et al.*, 2008; Mayer *et al.*, 2007). RNA-based affinity purification offers a powerful technology to isolate and identify the cellular interactome of cRNP and vRNP complexes. Detection of cellular factors that form part of cRNP and vRNP complexes could give important insight into how viral RNA synthesis is regulated on vRNA and cRNA templates. RNP complexes isolated by RNA-based affinity purification and density gradient centrifugation are homogenous in nature, with few co-purifying host proteins being detected by SDS-PAGE and silver staining. To isolate RNP complexes and associated cellular factors the method was advanced to include a second affinity purification step that uses a Strep-tag on the C-terminus of PB2, as has previously been described (Rameix-Welti *et al.*, 2009). Recombinant viruses were generated that encode a PB2-Strep protein and also contain a PP7 RNA tag in the NA gene in the region that encodes the NA stalk to allow the purification of cRNA or vRNA depending on the orientation of the tag. These viruses exhibited similar growth kinetics to WT virus, demonstrating that the presence of these two tags did not affect viral fitness. Viral cRNP and vRNP complexes were able to be isolated with high specificity using this two-step affinity purification approach, however, due to the inefficiency of purification, low numbers of viral RdRP and NP peptides were detected by mass spectrometry. Due to a low yield of RNP recovery, it was not possible to identify cellular factors with significant reproducibility.

As an alternative strategy for identifying components of the cellular interactome of the influenza virus transcription/replication machinery, viral PB2-containing complexes were isolated from infected cells by Strep-tag affinity purification of PB2. This

approach yielded a quantity of viral RdRP complexes that was amenable to mass spectrometry analyses for the aim of identifying co-purifying cellular factors. SDS-PAGE and silver staining analyses of the purified protein complexes revealed that PB1, PB2-Strep, PA and NP proteins could be efficiently purified from PB2-Strep virus infected cells, but not from WT virus infected cells. Concentration of the protein samples revealed the presence of many cellular proteins that had co-purified with PB2-Strep from PB2-Strep virus infected cells, but not from WT virus infected cells. Mass spectrometry and SINQ analyses of purified PB2-Strep sample showed that PB1, PB2-Strep, PA and NP proteins were the most abundant within the samples in each repeat. SINQ analyses of purified viral proteins and primer extension analyses of viral RNAs that had co-purified with PB2-Strep showed that a mixture of cRNPs, vRNPs, trimeric RdRP and monomeric PB2-Strep had purified, representing components of the viral transcription/replication machinery at different stages of the virus life-cycle. In contrast, viral mRNA was not found to co-purify with PB2-Strep, confirming that the viral RdRP does not stably associate with viral mRNA and the viral RdRP is unlikely to form a stable component of viral mRNPs (Bier *et al.*, 2011; York & Fodor, 2013). Quantitative analyses of co-purifying host factors using SINQ revealed 171 cellular factors that co-purified with the viral transcription/replication machinery from infected cells. The majority of proteins that had co-purified were reproducible between three independent biological repeats. These data show that many cellular factors that associate with complexes containing PB2-Strep can be isolated from infected cells, with high reproducibility, suggesting that these identifications could be important for virus replication.

This study is the first to use the relative abundance of co-purifying cellular proteins to assess the probability that they are bound to the influenza virus transcription/replication machinery in infected cells. Most of the abundant cellular proteins could be placed into eight major categories: chaperones, cytoskeletal proteins, importins, proteins involved in ubiquitination, kinases and phosphatases, mitochondrial proteins and ribosomal proteins. This interactome was subjected to GO term analysis, revealing that interaction-partners of the viral RdRP have a range of molecular functions. For example, a significant number of identified proteins are RNA-binding proteins. Considering the RNA-binding functions of the viral RdRP in transcription and replication of the viral genome (Krug & Fodor, 2013; Resa-Infante *et al.*, 2011) and the reported association of the viral RdRP with cellular DNA-dependent RNA polymerase II and chromatin (Chase *et al.*, 2011; Engelhardt *et al.*, 2005), it is plausible that many of these factors are involved in viral RNA synthesis.

Within the interactome of the viral transcription and replication machinery the most abundant protein that was detected was the Hsp70 protein chaperone. Hsp70 family members have been reported to interact with PB1 and PB2 subunits of the viral RdRP, with an inhibitory role for Hsp70 being described in the nuclear export of vRNP complexes by preventing their association to M1 (Hirayama *et al.*, 2004; Watanabe *et al.*, 2006). Hsp70 has also been described to down-regulate RNA synthesis by the viral RdRP (Li *et al.*, 2011), however, this was not observed in an independent study (Momose *et al.*, 2002). Furthermore, a recent study described a modulatory function for Hsp70 with both a stimulatory and an inhibitory effect on RdRP activity (Manzoor *et al.*, 2014). A number of DnaJ/Hsp40 proteins were also found within the interactome.

This family of proteins act primarily by stimulating the ATPase activity of Hsp70 chaperones (Qiu *et al.*, 2006), indicating that Hsp70 is likely to be involved in the folding, assembly or disassembly viral RdRP complexes. A number of additional molecular chaperones were present in the interactome, including Hsp90 and members of the chaperonin containing TCP1 complex (CCT). Hsp90 has been shown to interact with PB1 and PB2 and stimulate viral RNA synthesis *in vitro* (Momose et al., 2002) and it has been observed that Hsp90 chaperones PB2 during nuclear import (Naito *et al.*, 2007). Members of the CCT chaperonin have been proposed to aid in the folding of PB2 for its incorporation into a trimeric RdRP (Fislova *et al.*, 2010). The high abundance of molecular chaperones in the interactome reflects the importance of proper protein folding, proteome integrity and proteostasis for biological function of viral proteins.

Nuclear transport proteins were also enriched in the interactome. Unlike the majority of RNA viruses, influenza viruses have adopted a replication cycle in which their genomes are transcribed and replicated in the nuclei of infected cells (Herz *et al.*, 1981; Jackson *et al.*, 1982). Consequently, influenza virus has evolved to exploit cellular nuclear import and export pathways for accessing various cellular functions that are compartmentalised by the nuclear envelope (Hutchinson & Fodor, 2012). The most abundant of the nuclear transport machinery that was found in the interactome was importin-5 (RanBP5), a member of the importin-β family. Once viral RdRP subunits have been synthesised in the cytoplasm they are imported into the nucleus for trimer assembly. The current accepted model for nuclear import of viral RdRP subunits is the formation of a PB1-PA dimer in the cytoplasm which is then imported by RanBP5

(Deng *et al.*, 2006; Fodor & Smith, 2004; Hutchinson *et al.*, 2011). The PB2 subunit is recognised by importin-α isoforms and is imported into the nucleus by the classical α/β-importin pathway (Gabriel *et al.*, 2011; Resa-Infante *et al.*, 2008; Tarendeau *et al.*, 2007). Once PB1-PA dimer has entered the nucleus, RanBP5 disassociates due to the association with Ran-GTP and it is assumed to be exported to the cytoplasm. Subsequently, PB1-PA forms a complex with viral promoters and PB2 (Deng *et al.*, 2006; Deng *et al.*, 2005). Intriguingly, the presence of RanBP5 in the interactome is not compatible with this model of nuclear import and assembly of the viral RdRP, since PB2 monomer, PB1-PB2 dimer and the trimeric RdRP was reported not to bind to RanBP5 efficiently (Deng *et al.*, 2006). Although it is clear that RanBP5 plays a role in PB1-PA nuclear import, the complete mechanism of import remains unclear. In addition to RanBP5, the importin-α3, -α4, -α5 and -α7 proteins were present in the interactome, which is likely to reflect the use of the α/β-importin pathway for nuclear import of PB2, NP and vRNP complexes (Gabriel *et al.*, 2011; Hutchinson & Fodor, 2012; Martin & Helenius, 1991; Oneill *et al.*, 1995; Tarendeau *et al.*, 2007). Nevertheless, a non-canonical function for importin-α proteins has been proposed to play a direct role in viral transcription/replication and in the assembly of vRNP complexes that is independent of nuclear import function (Hudjetz & Gabriel, 2012; Resa-Infante *et al.*, 2008).

Among the cytoskeletal proteins identified, tubulins, the major constituents of microtubules, were found to be the most abundant. Treatment of infected cells with the microtubule-depolymerizing agent nocodazole results in the loss of vRNP transport to the plasma membrane, which has been attributed to microtubule-dependent vesicular

transport of vRNP complexes from the nucleus (Amorim *et al.*, 2011). It was shown that vRNP complexes on their journey from the nucleus to the plasma membrane first associate with the microtubule organising centre (MTOC) where they form a complex with Rab11 on recycling endosomes, which subsequently traffic to the apical plasma membrane for virion assembly and egress (Amorim *et al.*, 2011; Bruce *et al.*, 2010; Jo *et al.*, 2010; Lakdawala *et al.*, 2014). The abundance of tubulin in the interactome is likely to reflect the microtubule-dependence of viral cargo trafficking during infection.

A number of mitochondrial proteins were present in the interactome. PB2 contains an N-terminal mitochondrial-targeting signal and has been shown to accumulate in the mitochondria of infected cells. PB2 was found to associate with the mitochondrial antiviral signaling protein (MAVS) and suppress IFN-β production (Carr *et al.*, 2006; Graef *et al.*, 2010; Iwai *et al.*, 2010). A previous AP-MS study of the viral RdRP in transfected cells recognised an association of PA with over thirty mitochondrial proteins (Bradel-Tretheway *et al.*, 2011). In particular, a strong association was reported with apoptosis-inducing factor (AIFM1). AIFM1 was also present in the PB2-Strep interactome, suggesting a potential role or the regulation of apoptosis by the viral RdRP. The promotion of apoptosis in infected cells has been proposed to enhance pathogenicity in mice. In particular, a small 87-amino acid pro-apoptotic protein encoded in the second open reading frame (+2) of PB1 (PB1-F2) has been shown to localise to the inner and outer membranes of mitochondria and induce apoptosis by perturbation of mitochondrial morphology, loss of the mitochondrial membrane potential and cytochrome *c* release (Chen *et al.*, 2001; Zamarin *et al.*, 2005; Zamarin *et al.*, 2006). The presence of a number of mitochondrial proteins in the interactome could

imply that uncharacterised associations exist between mitochondria and the viral transcription/replication machinery for the control of innate immune responses and apoptosis.

The interactome has the potential to contribute important insights into regulatory post-translational modification of the viral transcription/replication machinery. A number of components of the ubiquitination pathway were identified, including an E1 ubiquitin-activating enzyme and a number of E3 ubiquitin ligases. Ubiquitination is a post-translational modification in which an 8 kDa ubiquitin peptide is covalently attached to lysine residues on a target protein, orchestrated by the concerted actions of E1 ubiquitin-activating enzymes, E2 ubiquitin-conjugating enzymes and E3 ubiquitin ligases (Kerscher *et al.*, 2006). Ubiquitination of a target protein can occur as a single ubiquitin (monoubiquitination), or as ubiquitinated chains through sequential rounds of ubiquitination (polyubiquitination). Critical roles for polyubiquitination in proteasomal degradation and turnover of target proteins is well characterised and influenza virus proteins have been shown to be polyubiquitinated for degradation by the 26S proteasome (Di Pietro *et al.*, 2013; Finley, 2009; Liu *et al.*, 2012; Su *et al.*, 2013a). For example, the IFN-inducible antiviral protein TRIM22 has been shown to target NP for degradation in order to curtail virus replication (Di Pietro *et al.*, 2013), and polyubiquitination has been shown to regulate uncoating of influenza virus from endosomes (Su *et al.*, 2013a; Widjaja *et al.*, 2010). Indeed, components of the 26S proteasome are present in the interactome. Conversely, non-degradative roles of ubiquitination have been described in the regulation of intramolecular autoinhibition, intracellular localisation and trafficking, transcription, macromolecular complex

assembly and immune responses (Bienko *et al.*, 2010; Hoeller *et al.*, 2006; Pavri *et al.*, 2006; Su *et al.*, 2013b). Viral NP is reversibly monoubiquitinated, which has been shown to regulate RNA binding (Liao *et al.*, 2010). The ubiquitination enzymes present in the interactome could therefore be involved in a targeted response by the innate immune system to down regulate virus replication. In addition, the function of the viral transcription and replication machinery could be regulated by reversible monoubiquitination.

Additional evidence of regulatory post-translational modification of viral proteins by cellular proteins exists in the interactome. A number of kinases and phosphatases were found to co-purify with PB2-Strep. Regulatory phosphorylation of proteins has been shown to affect the function of proteins manifold, including modulation of enzymatic activity, protein stability, subcellular distribution and protein-protein interactions (Cohen, 2000; Tarrant & Cole, 2009). The influenza virus RdRP and NP are phosphorylated in infected cells (Almond & Felsenreich, 1982; Arrese & Portela, 1996; Hutchinson *et al.*, 2012; Kistner *et al.*, 1985; Mahmoudian *et al.*, 2009; Perales *et al.*, 2000; Sanz-Ezquerro *et al.*, 1998), however, elucidating the importance of sites of phosphorylation is a challenging and emerging field. Nevertheless, the conservation of phosphorylation sites between influenza A and B viruses and the structural context in which they have been identified has led to hypotheses that phosphorylation in the viral RdRP and NP can regulate nuclear localisation and protein oligomerisation (Chenavas *et al.*, 2013; Hutchinson *et al.*, 2012). Kinase activity has been shown to be essential for influenza virus replication and treatment of cells with protein kinase inhibitors has been shown to interfere with different stages in the virus life-cycle including nuclear import,

transcription, translation, nuclear export and viral egress (Hui & Nayak, 2002; Kumar *et al.*, 2011; Kurokawa *et al.*, 1990; Pleschka *et al.*, 2001; Root *et al.*, 2000). These effects can be attributed to perturbation in the phosphorylation status of host proteins (Haidari *et al.*, 2011; Shin *et al.*, 2007), but altered phosphorylation of viral proteins has been shown to have direct effects on viral protein function (Chenavas *et al.*, 2013; Hutchinson *et al.*, 2012; Reuther *et al.*, 2014). The most abundant regulator of phosphorylation in the interactome is serine/threonine-protein phosphatase 6 (PP6) in which three individual subunits were identified. The revelation that phosphatases and kinases that are present within in interactome could imply a role for regulatory phosphorylation of viral proteins in influenza virus replication.

5.6 Summary

- Affinity purification mass spectrometry was employed to identify cellular factors that interact with the influenza virus transcription/replication machinery.
- Viral cRNP and vRNP complexes were isolated from infected cells using a two-step affinity purification strategy which relies on RNA-based affinity purification and Strep-tag affinity purification of the viral RdRP, however, due to inefficiency in the isolation of these complexes it was not possible to reproduce identifications of co-purifying cellular factors.
- Isolation of the PB2 subunit of the viral RdRP from infected cells using single-step Strep-tag affinity purification was used as an alternative strategy to identify

cellular factors that interact with the influenza virus transcription/replication machinery.

- 171 cellular factors were identified to co-purify with the influenza virus transcription/replication machinery from infected cells.
- Most of the abundant cellular proteins could be placed into eight major categories: chaperones, cytoskeletal proteins, importins, proteins involved in ubiquitination, kinases and phosphatases, mitochondrial proteins and ribosomal proteins.

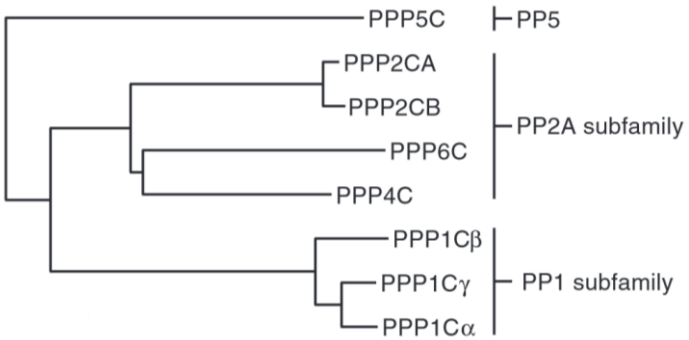
Chapter 6: Protein phosphatase 6 is required for efficient replication of influenza virus

6.1 Introduction

The interactome of the influenza A virus transcription/replication machinery presented in Chapter 5 serves as a basis for the elucidation of the molecular mechanisms that underlie virus replication. The identification and subsequent characterisation of *bona fide* interactions between the viral RdRP and cellular proteins can elucidate mechanisms and molecular control of viral RNA synthesis and polymerase function during the virus life-cycle. Three individual subunits of cellular serine/threonine-protein phosphatase 6 (PP6) were identified to co-purify with the viral RdRP from infected cells. PP6 is an enzyme that catalyses the liberation of phosphate groups from serine or threonine residues by hydrolysing phosphoric acid monoesters into a phosphate ion and a free

hydroxyl group on the targeted residue (Bastians & Ponstingl, 1996). Serine/threonine-specific phosphatases can be divided into the PPM family of metallo-dependent phosphatases or the phosphoprotein phosphatases (PPP), the latter of which PP6 is a member (Shi, 2009). The PPP family of phosphatases can be further classified into subfamilies according to sequence conservation between the different catalytic subunits (Figure 6.1A). PP6 belongs to the PP2A subfamily in which multimeric holoenzyme complexes are formed by catalytic subunits associating with a great variety of regulatory subunits to define substrate specificity (Barr *et al.*, 2011; Shi, 2009). The PP2A subfamily of phosphatases typically possess a catalytic subunit, a scaffolding subunit and a regulatory subunit (Figure 6.1B). PP6 is a heterotrimer composed of a catalytic subunit (PPP6C), an ankyrin repeat domain scaffolding subunit (Ankrd28) and a regulatory subunit that contains a SIT4 phosphatase-associated protein (SAPS) domain (Stefansson *et al.*, 2008). Three individual regulatory subunits of PP6 have been identified (PPP6R1, PPP6R2 and PPP6R3) (Stefansson *et al.*, 2008). The ability of catalytic subunits of PP2A subfamily phosphatases to form a complex with a variety of regulatory subunits allows the relatively small number of catalytic subunits to form a range of functionally distinct holoenzyme complexes that each has unique substrate specificities, regulatory properties and subcellular localisations (Shi, 2009). PP6 is a significant regulator of a number of cellular processes including the DNA damage response (Douglas *et al.*, 2010; Hammond *et al.*, 2013; Hosing *et al.*, 2012; Shen *et al.*, 2011; Zhong *et al.*, 2011), mitosis and the regulation of cell cycle progression (Barr *et al.*, 2011; Bastians & Ponstingl, 1996; Stefansson & Brautigan, 2007; Stefansson *et al.*, 2008; Zeng *et al.*, 2010), cell signaling (Dai *et al.*, 2013; Kajino *et al.*, 2006), pre-mRNA splicing (Kamoun *et al.*, 2013) and vesicular trafficking (Bhandari *et al.*, 2013).

A



B

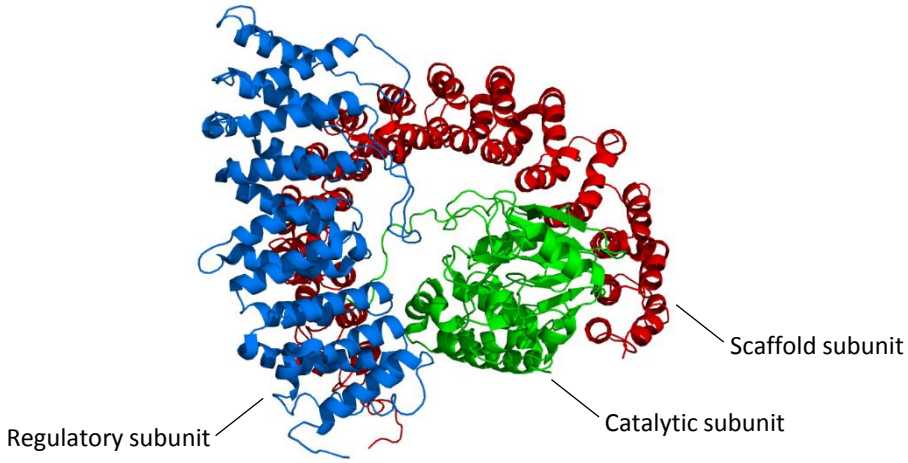


Figure 6.1 PP6 is a distinct member of the PP2A subfamily of the PPP phosphatases. (A) Eight human PPP family catalytic subunits fall within the PP5, PP2A and PP1 subfamilies, based on amino acid conservation. Figure adapted from Barr *et al*., 2011. (B) Structure of the PP2A holoenzyme. PP2A forms a heterotrimer composed of the catalytic subunit (green), the scaffold subunit (red) and a regulatory subunit (blue) that determines substrate specificity. From Cho & Xu, 2007. PDB code: 2IAE.

The formation of a protein-protein complex between PP6 and the viral RdRP within infected cells could imply that a functional relationship of biological importance exists between these viral and cellular proteins. The proteomes of influenza viruses have been reported to undergo a variety of post-translational modifications, including phosphorylation. The phosphorylation of proteins within eukaryotic cells on serine, threonine or tyrosine residues is frequently detected and has been shown to affect protein function in a myriad of ways, including modulation of enzymatic activity, half-life, subcellular localisation and protein-protein interactions (Cohen, 2000; Tarrant & Cole, 2009). The proteins encoded by influenza viruses have long been known to be phosphorylated (Almond & Felsenreich, 1982; Arrese & Portela, 1996; Gregoriades *et al.*, 1984; Gregoriades *et al.*, 1990; Hale *et al.*, 2009; Holsinger *et al.*, 1995; Hsiang *et al.*, 2012; Kistner *et al.*, 1985; Mahmoudian *et al.*, 2009; Mitzner *et al.*, 2009; Perales *et al.*, 2000; Richardson & Akkina, 1991; Sanz-Ezquerro *et al.*, 1998; Whittaker *et al.*, 1995), with a recent study identifying numerous novel sites of phosphorylation in the influenza virus proteome (Hutchinson *et al.*, 2012). Understanding the significance of these sites of phosphorylation is a challenging and emerging field. However, their conservation between influenza A and B viruses and their structural context has led to numerous hypotheses for regulatory phosphorylation in regulating virus entry and egress, nuclear localisation and protein oligomerisation (Chenavas *et al.*, 2013; Hutchinson *et al.*, 2012). Phosphoserines and phosphothreonines can be detected in all three subunits of the heterotrimeric RdRP (Hutchinson *et al.*, 2012; Mitzner *et al.*, 2009; Perales *et al.*, 2000; Sanz-Ezquerro *et al.*, 1998), and therefore it is plausible that PP6 could modulate the phosphorylation status of the viral RdRP with consequential functional importance. Therefore, the aim of this chapter is to confirm and characterise

the interaction between the viral RdRP and PP6, and to understand the overall biological significance of this relationship in the context of the infected cell.

6.2 PP6 co-purifies with viral RdRP complexes from infected cells

The interactome of the viral RdRP contained three individual subunits of the cellular phosphatase PP6. The catalytic PPP6C subunit and the regulatory PPP6R3 subunit of PP6 were present in all three data sets, with an alternative regulatory subunit, PPP6R1, present in datasets 2 and 3 (Table 6.1 and Appendix E). By molar abundance PPP6C comprised approximately 1.53% of the interactome, with PPP6R3 and PPP6R1 comprising approximately 0.78% and 0.12% respectively (Appendix F). Western blotting confirmed that PPP6C and PPP6R3 co-purified with viral RdRP complexes from HEK 293T cells infected with PB2-Strep virus, but did not co-purify from cells infected with WT virus (negative control) (Figure 6.2), demonstrating that PP6 is a specific and reproducible interaction partner of the viral RdRP.

6.3 PB1 and PB2 subunits of the viral RdRP interact directly with a regulatory subunit of PP6

In order to address the specificity of the interaction of PP6 with the viral RdRP, individual polymerase subunits, trimeric RdRP or PB1-PA dimer were purified from HEK 293T cells transfected with mammalian expression plasmids encoding a Strep-

Table 6.1 A summary of PP6 subunit identifications from mass spectrometry of the influenza virus transcription/replication machinery interactome.

	Protein	***Peptide Spectrum Matches***	***Peptide Sequences***	***% Sequence Coverage***
Experiment 1	PPP6C	13	10	47.5
	PPP6R3	6	6	9.6
Experiment 2	PPP6C	18	9	35.4
	PPP6R1	9	8	17.1
	PPP6R3	31	21	28.1
Experiment 3	PPP6C	26	12	37.0
	PPP6R1	3	3	4.2
	PPP6R3	38	23	34.0

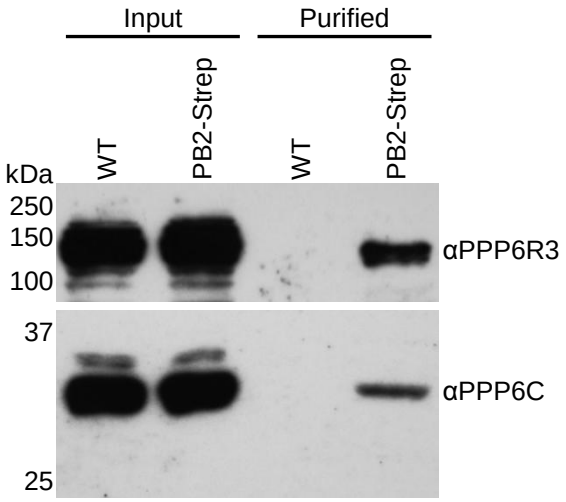


Figure 6.2 PP6 co-purifies with PB2 from infected cells. SDS-PAGE and Western blot analyses of total cell lysate and Strep-tag affinity purified material from WT virus and PB2-Strep virus infected HEK 293T cells using PPP6R3 (upper panel) and PPP6C (lower panel) specific antibodies.

tagged polymerase subunit. Cells were transfected with an empty expression vector or a mammalian expression vector encoding the coat protein of the *Pseudomonas aeruginosa* bacteriophage PP7 (PP7CP) fused to Strep-tag (PP7CP-Strep) to control for background binding of PP6 to Strep-Tactin beads or the Strep-tag, respectively. To analyse for co-purification of PP6, Western blotting was performed using antibodies specific to PPP6C and PPP6R3. PP6 did not co-purify from the negative control cells transfected with an empty vector or the PP7CP-Strep expression vector, or with PA-Strep in the absence of other RdRP subunits. However, PP6 co-purified with PB1-Strep, PB2-Strep, trimeric PB2-PB1-PA-Strep and a PB1-PA-Strep dimer, indicating that PP6 could interact with PB1 and PB2, both individually and as part of the RdRP complex (Figure 6.3).

To determine whether the interaction between the viral RdRP and PP6 was direct an *in vitro* GST pull down assay was performed. N-terminally GST-tagged PPP6C, PPP6R1, PPP6R2 and PPP6R3 subunits of PP6 or GST alone (negative control) were individually expressed in *E. coli*. After cell lysis the lysate was incubated with glutathione Sepharose beads and, after washing, the beads were incubated with viral RdRP purified from *Spodoptera frugiperda* (Sf9) cells. After a further washing step, the GST fusion proteins were eluted and Western blotting was performed using an antibody specific to the viral RdRP. Viral RdRP was not detected when GST was expressed alone, but GST-tagged PP6 subunits could pull down RdRP *in vitro*, indicating that their interaction was direct. GST-tagged PP6C could only pull down a small quantity of RdRP, but relatively large amounts of RdRP were pulled down by all three GST-tagged

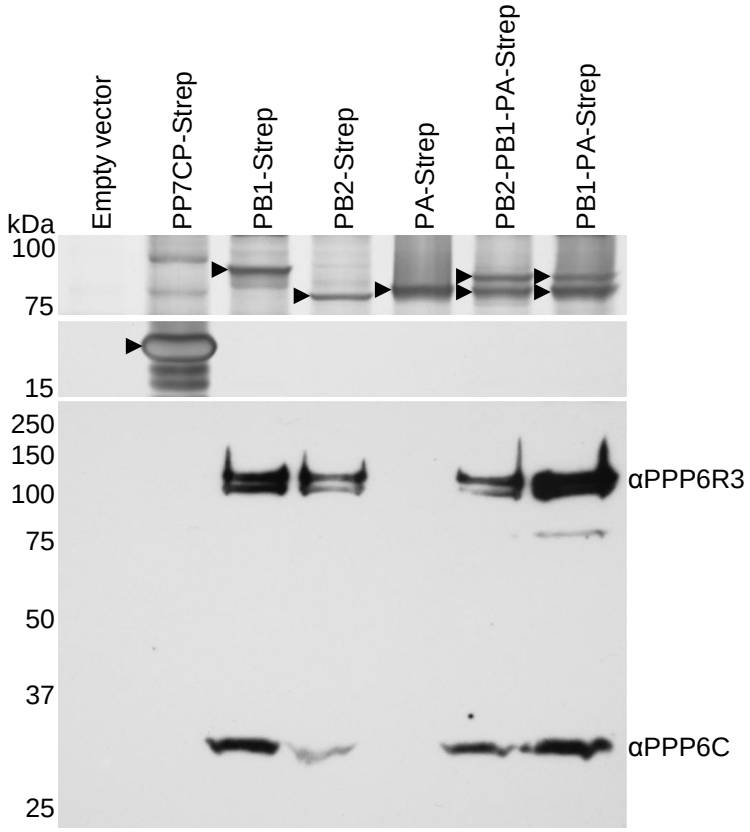


Figure 6.3 PP6 co-purifies with complexes containing PB1 and PB2 from transfected cells. SDS-PAGE and silver staining analyses (upper panels) and Western blot analyses (lower panel) using PPP6R3 and PPP6C antibodies of purified Strep-tagged viral RdRP polymerase subunits or negative control samples. Samples are from HEK 293T cells transfected with the plasmids that express the indicated proteins. Black arrowheads indicate Strep-tagged proteins.

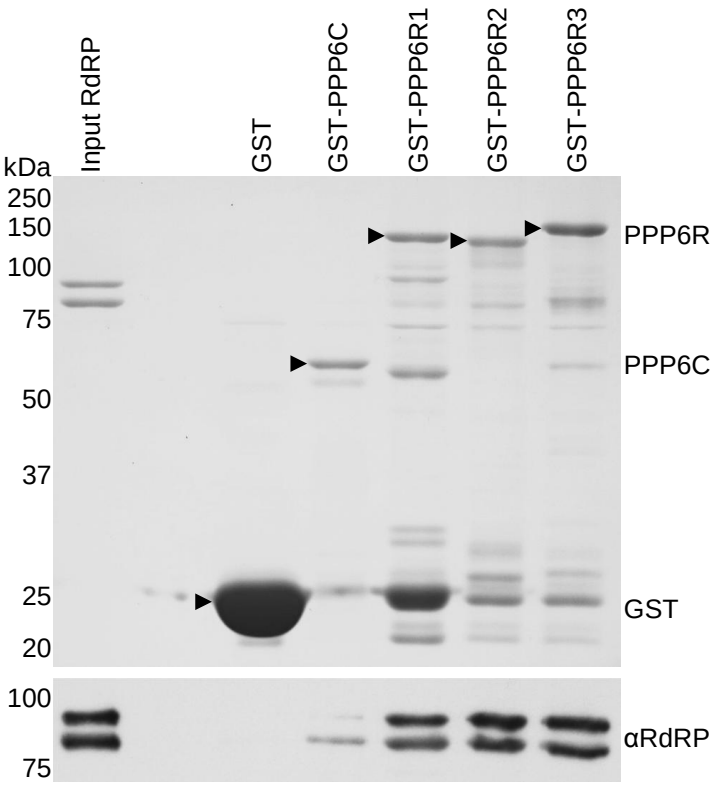


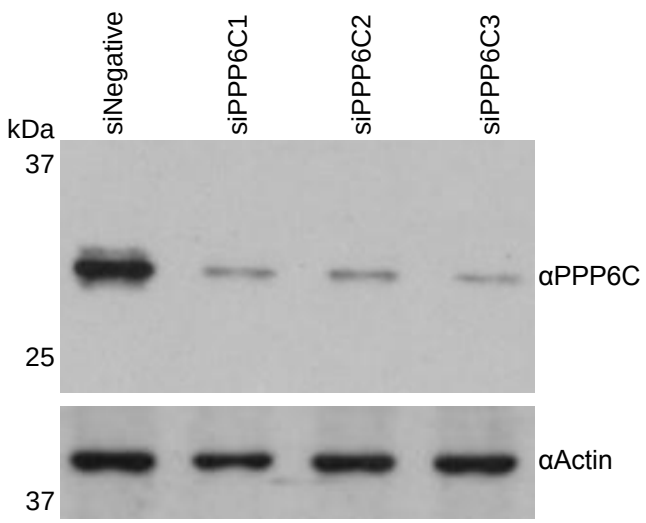
Figure 6.4 PP6 interacts directly with the heterotrimeric influenza virus RdRP. GST-pulldown assay whereby GST, GST-PPP6C, GST-PPP6R1, GST-PPP6R2 and GST-PPP6R3 were expressed separately in *E. coli* and immobilised on glutathione Sepharose beads. Recombinant influenza A virus RdRP purified from *Spodoptera frugiperda* (Sf9) cells was incubated with immobilised GST-tagged proteins. Bound material was analysed by SDS-PAGE and staining with Coomassie Brilliant Blue (upper panel) and Western blot analysis with an RdRP antibody (lower panel). Black arrowheads indicate the position of full-length GST-tagged proteins. For Western blotting, the input sample was diluted 10-fold.

PP6 regulatory subunits (Figure 6.4). Thus, the catalytic and regulatory subunits of PP6 interact directly with the PB1 and PB2 subunits of the viral RdRP.

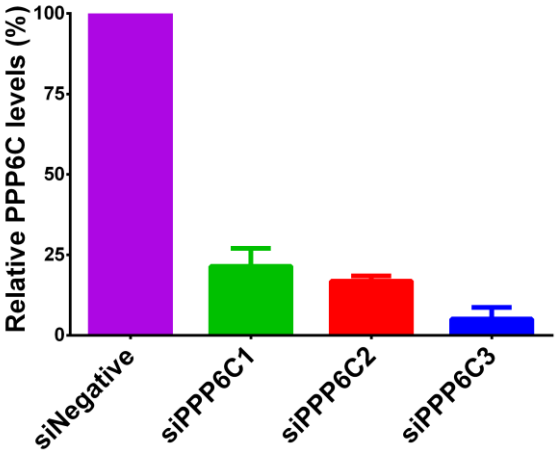
6.4 Down regulation of PPP6C significantly attenuates influenza A virus replication

To assess the biological significance of PP6 in the influenza A virus life-cycle, siRNA-mediated knockdown of the PP6 catalytic subunit was performed and growth of influenza A virus was assessed in knockdown cells. Three independent siRNAs specific for the PPP6C subunit, targeting the mRNA transcript at different positions (Figure 6.5A), were transfected independently into HEK 293T cells (siPPP6C1, siPPP6C2 and siPPP6C3), alongside AllStars negative control siRNA (siNegative). Cell lysates were analysed for the levels of PPP6C by Western blotting (Figure 6.6A). siRNA treatment resulted in reduction of PPP6C protein levels to 5–20% (Figure 6.6B). To ensure that the same number of viable cells were infected for each siRNA treatment, a quantitative luminescent cell viability assay based on the levels of ATP, an indicator of metabolically active cells, was performed on HEK 293T cells transfected with siPPP6C1, siPPP6C2, siPPP6C3 or the negative control siRNA (Figure 6.5B). The results show that the numbers of viable cells were comparable. To investigate the effect of PPP6C knockdown on the virus life-cycle, cells that were knocked down for PPP6C and control cells were infected with WT virus at an MOI of 0.001 and virus growth kinetics were measured (Figure 6.6C). At 12 h p.i. there was no significant difference between control and knockdown cells, but at all subsequent time points there was

A


siNegative
siPPP6C1
siPPP6C2
siPPP6C3
kDa
37
25
37
αPPP6C
αActin

B


Relative PPP6C levels (%)
100
75
50
25
0
siNegative
siPPP6C1
siPPP6C2
siPPP6C3

C

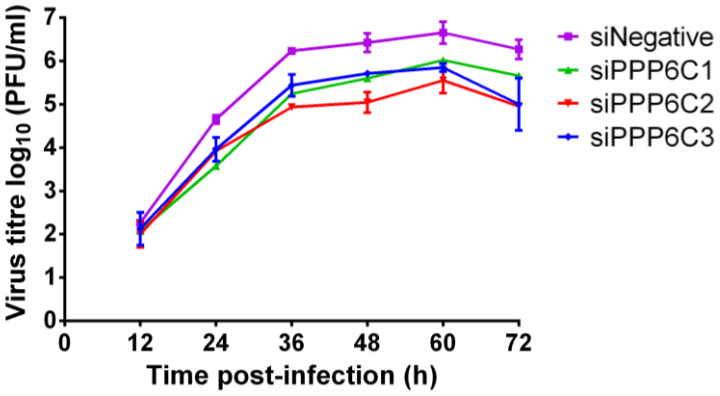


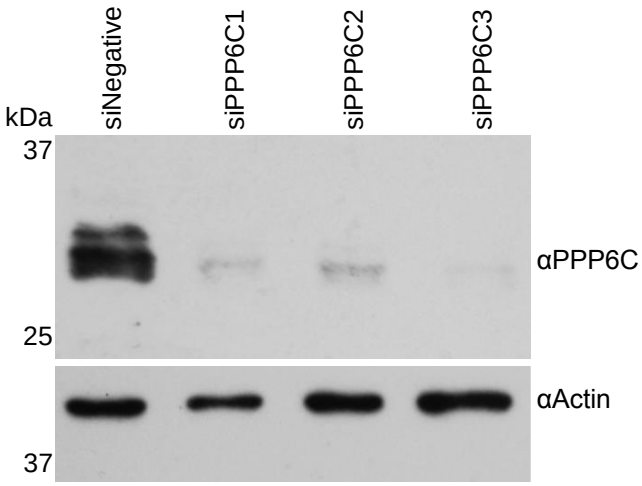
Figure 6.6 Effect of PPP6C knockdown in HEK 293T cells on influenza A virus growth. (A) Western blot analysis of PPP6C in HEK 293T cells treated with PPP6C-targeting siRNAs (siPPP6C1, siPPP6C2 and siPPP6C3) or a negative control siRNA (siNegative). PPP6C (upper panel) was detected with a PPP6C-specific antibody. Actin (lower panel) was used as a loading control. (B) Quantitation of Western blot analyses of the knockdown of PPP6C. PPP6C levels were normalised to the levels of actin and expressed as a percentage of PPP6C levels in cells treated with siNegative. PPP6C levels represent the mean and error bars represent SD from three biological repeats. (C) Growth curves of WT virus in PPP6C knockdown or control cells. Cells were treated with the indicated siRNAs and infected at an MOI of 0.001. At the indicated time points post-infection, cell supernatants were collected and virus titres were determined by plaque assay on MDBK cells.

approximately a 10-fold reduction in virus accumulation in PPP6C-knockdown cells, indicating an important role for PP6 in the influenza A virus life-cycle.

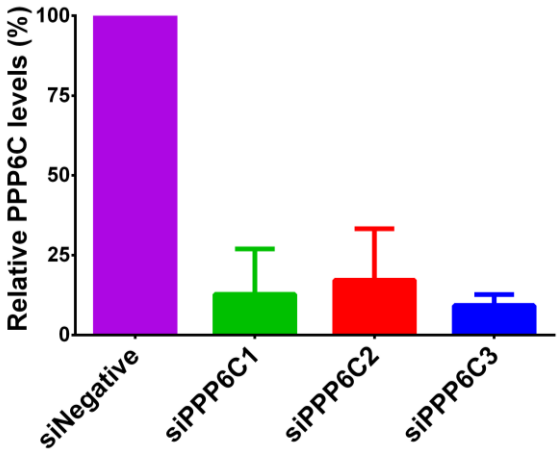
6.5 Down regulation of PPP6C reduces viral RNA accumulation in influenza A virus infected cells

In order to investigate the mechanisms that resulted in approximately 10-fold reduction of virus growth in PPP6C knockdown cells, viral RNA accumulation was assessed in PPP6C knockdown cells at 0, 6 and 8 h p.i.. HEK 293T cells were transfected with three independent siRNAs that target PPP6C or a control siRNA. Levels of PPP6C protein in cell lysates were assessed by Western blotting (Figure 6.7A). siRNA treatment resulted in reduction of PPP6C protein levels to 9–17% (Figure 6.7B). Cells were infected at an MOI of 1 and RNA was isolated from infected cells at 0, 6 and 8 h p.i.. Primer extension analyses using NA segment-specific primers showed that there was a significant reduction in mRNA, cRNA and vRNA accumulation compared to control cells at 6 h p.i. (Figure 6.7C and 6.7D), however, at 8 h p.i. a significant reduction in cRNA and vRNA accumulation was only observed with the PPP6C-targetting siRNA that gave the greatest reduction in PPP6C levels (siPPP6C3), and no significant reduction was observed for viral mRNA accumulation (Figure 6.7C and 6.7E). These data suggest that RNA accumulation is significantly delayed in PPP6C knockdown cells. In order to assess whether the requirement of PP6 for efficient viral RNA synthesis takes place at a stage of the influenza A virus life-cycle that precedes primary transcription, PPP6C knockdown or negative control cells were infected or

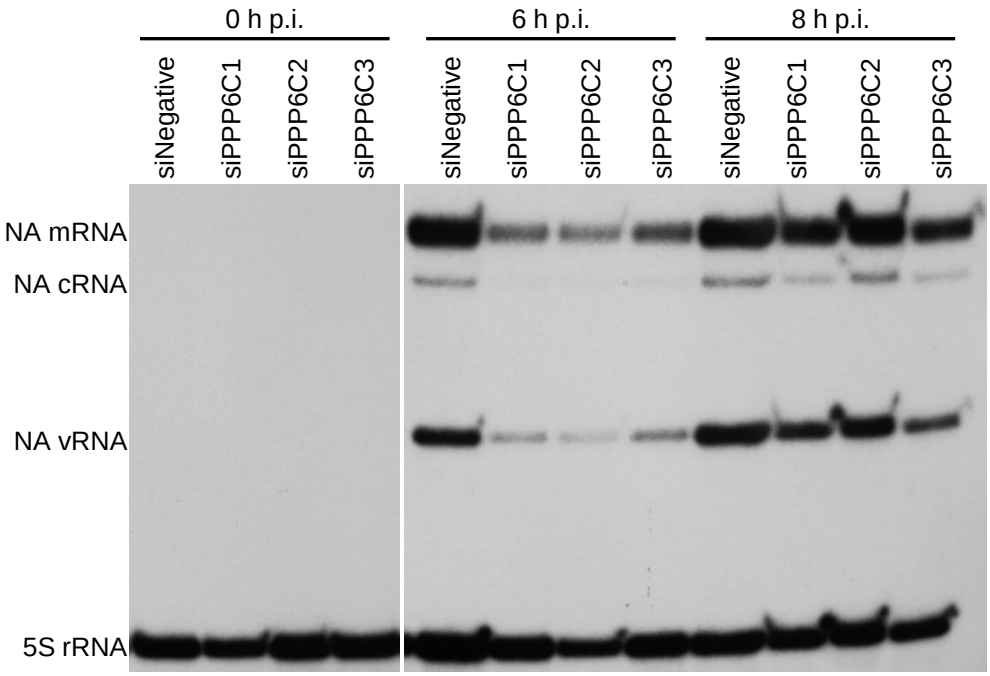
A


siNegative
siPPP6C1
siPPP6C2
siPPP6C3
kDa
37
25
37
αPPP6C
αActin

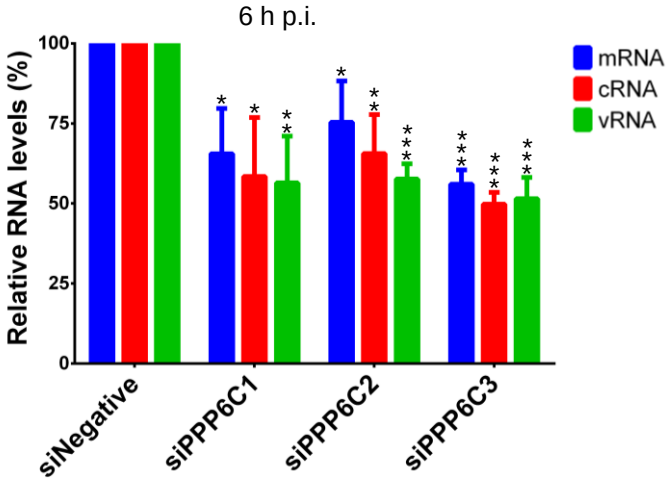
B


Relative PPP6C levels (%)
100
75
50
25
0
siNegative
siPPP6C1
siPPP6C2
siPPP6C3

C


0 h p.i.
6 h p.i.
8 h p.i.
siNegative
siPPP6C1
siPPP6C2
siPPP6C3
siNegative
siPPP6C1
siPPP6C2
siPPP6C3
siNegative
siPPP6C1
siPPP6C2
siPPP6C3
NA mRNA
NA cRNA
NA vRNA
5S rRNA

D


6 h p.i.
Relative RNA levels (%)
100
75
50
25
0
mRNA
cRNA
vRNA
siNegative
siPPP6C1
siPPP6C2
siPPP6C3

E

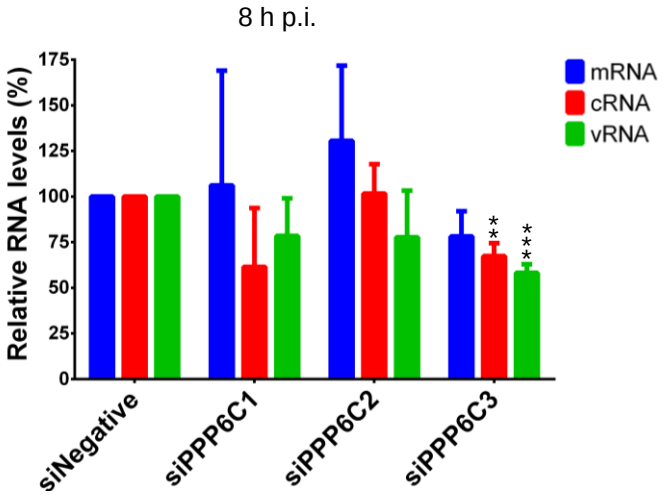
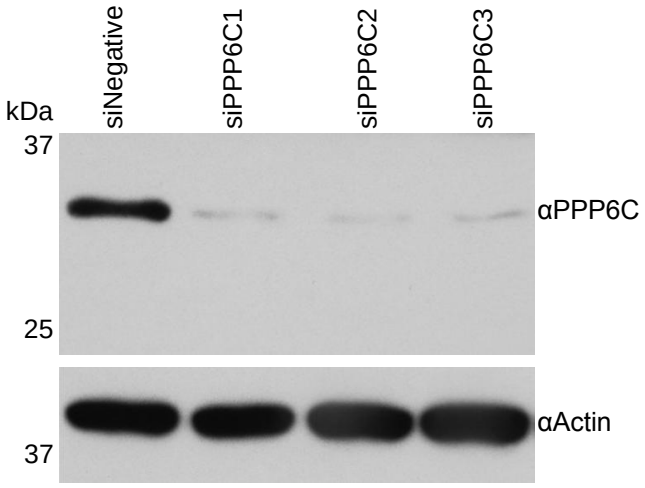
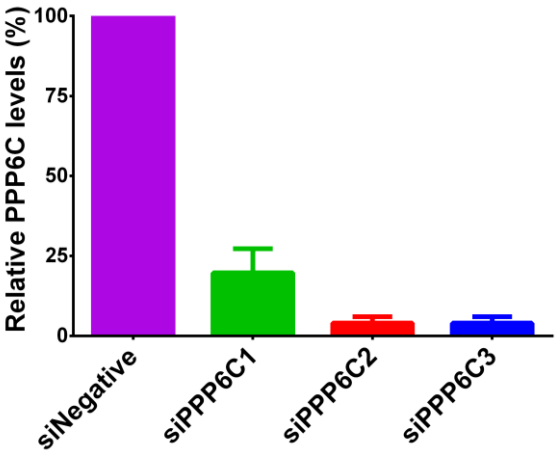


Figure 6.7 Effect of PPP6C knockdown in HEK 293T cells on the accumulation of viral RNAs. (A) Western blot analysis of PPP6C in HEK 293T cells treated with PPP6C-targeting siRNAs (siPPP6C1, siPPP6C2 and siPPP6C3) or a negative control siRNA (siNegative). PPP6C (upper panel) was detected with a PPP6C-specific antibody. Actin (lower panel) was used as a loading control. (B) Quantitation of Western blot analyses of the knockdown of PPP6C. PPP6C levels were normalised to the levels of actin and expressed as a percentage of PPP6C levels in cells treated with siNegative. PPP6C levels represent the mean and error bars represent SD from three biological repeats. (C) Primer extension analysis of viral NA segment-specific mRNA, cRNA and vRNA in PPP6C knockdown or control cells. Cells were treated with the indicated siRNAs and infected at an MOI of 1. At the indicated time points post-infection RNA was extracted from infected cells and viral RNAs were analysed by primer extension using radiolabeled primers for positive sense (mRNA and cRNA) and negative sense (vRNA) NA-specific viral RNAs. 5S rRNA was used as a loading control. (D) Quantitation of primer extension analyses. RNA levels represent the mean, and the error bars represent SDs from three biological repeats. Asterisks indicate a significant difference from 100% (* $P < 0.05$, ** $P < 0.01$, *** $P < 0.001$, based on a one-sample Student's *t*-test).

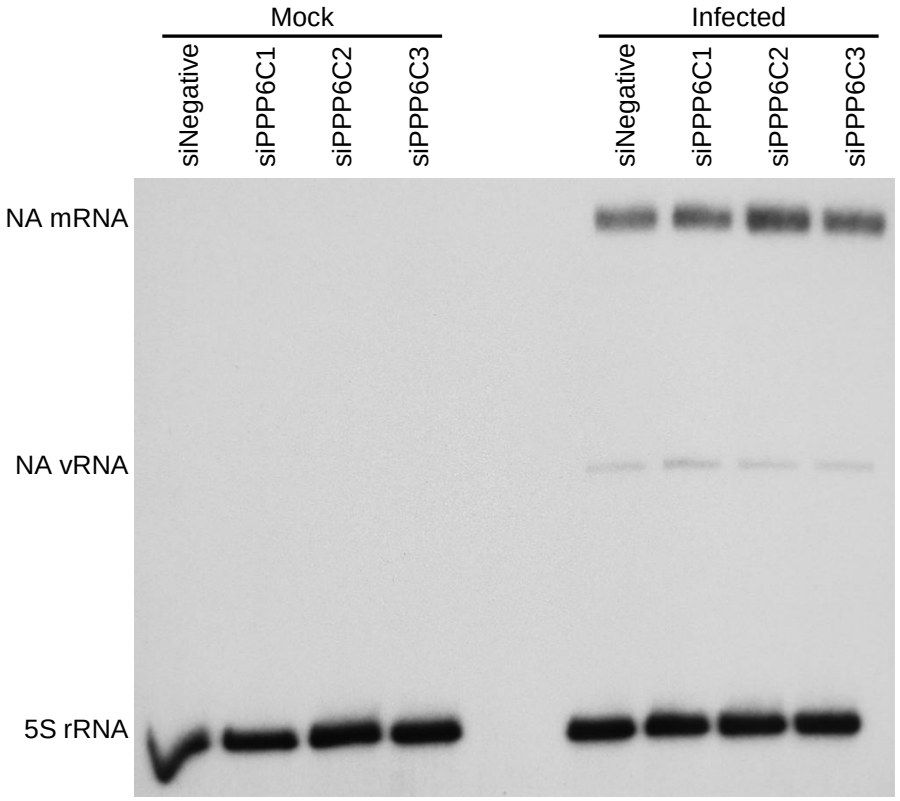
A


siNegative
siPPP6C1
siPPP6C2
siPPP6C3
kDa
37
25
37
αPPP6C
αActin

B


Relative PPP6C levels (%)
100
75
50
25
0
siNegative
siPPP6C1
siPPP6C2
siPPP6C3

C


Mock
Infected
siNegative
siPPP6C1
siPPP6C2
siPPP6C3
siNegative
siPPP6C1
siPPP6C2
siPPP6C3
NA mRNA
NA vRNA
5S rRNA

D

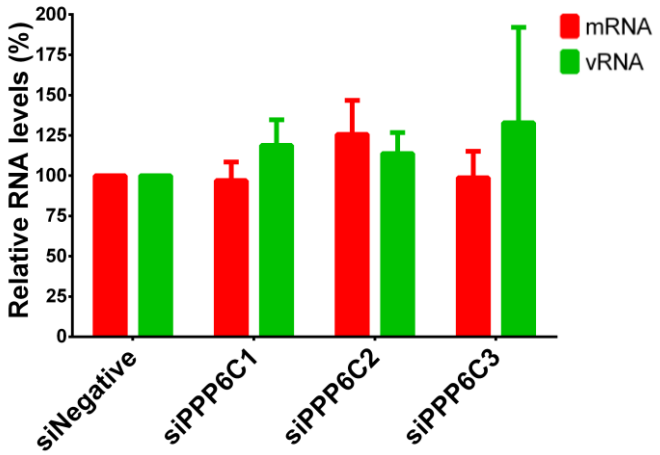

Relative RNA levels (%)
200
175
150
125
100
75
50
25
0
mRNA
vRNA
siNegative
siPPP6C1
siPPP6C2
siPPP6C3

Figure 6.8 Effect of PPP6C knockdown in HEK 293T cells on primary transcription by parental vRNPs. (A) Western blot analysis of PPP6C in HEK 293T cells treated with PPP6C-targeting siRNAs (siPPP6C1, siPPP6C2 and siPPP6C3) or a negative control siRNA (siNegative). PPP6C (upper panel) was detected with a PPP6C-specific antibody. Actin (lower panel) was used as a loading control. (B) Quantitation of Western blot analyses of the knockdown of PPP6C. PPP6C levels were normalised to the levels of actin and expressed as a percentage of PPP6C levels in cells treated with siNegative. PPP6C levels represent the mean and error bars represent SD from three biological repeats. (C) Primer extension analysis of viral NA segment-specific mRNA, cRNA and vRNA in PPP6C knockdown or control cells. Cells were treated with the indicated siRNAs and mock infected or infected at an MOI of 10 in the presence of cycloheximide (100 μg/ml). At 6 h p.i. RNA was extracted from infected cells and viral RNAs were analysed by primer extension using radiolabeled primers for positive sense (mRNA and cRNA) and negative sense (vRNA) NA-specific viral RNAs. 5S rRNA was used as a loading control. (D) Quantitation of primer extension analyses. RNA levels represent the mean, and the error bars represent SDs from three biological repeats.

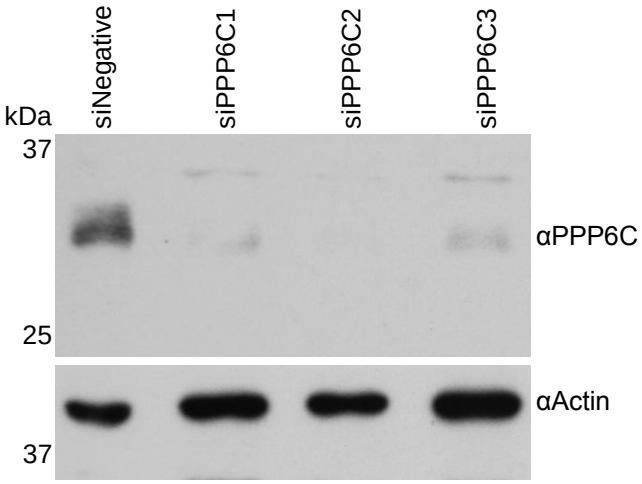
mock infected at an MOI of 10 in the presence of cycloheximide (CHX), an inhibitor of protein synthesis in eukaryotic cells, and the levels of viral mRNA were analysed. Knockdown of PPP6C was confirmed by Western blotting (Figure 6.8A) and quantitation showed that siRNA treatment resulted in reduction of PPP6C protein levels to 4–19% (Figure 6.8B). At 6 h p.i., RNA was extracted from the infected cells and primer extension analyses using NA segment-specific primers showed that levels of primary transcription were not significantly different in knockdown cells compared to negative control cells (Figure 6.8C and 6.8D). This result indicates that the requirement of PP6 for efficient viral RNA accumulation is at a stage of the viral life-cycle after nuclear import of genomic vRNPs and primary transcription has occurred. Taken together, these data strongly suggest that the phosphatase activity of PP6 is required for efficient viral RNA accumulation after primary transcription and consequently, virus growth in infected cells.

6.6 Reduced nuclear export of vRNPs is observed in PPP6C knockdown cells infected with influenza A virus

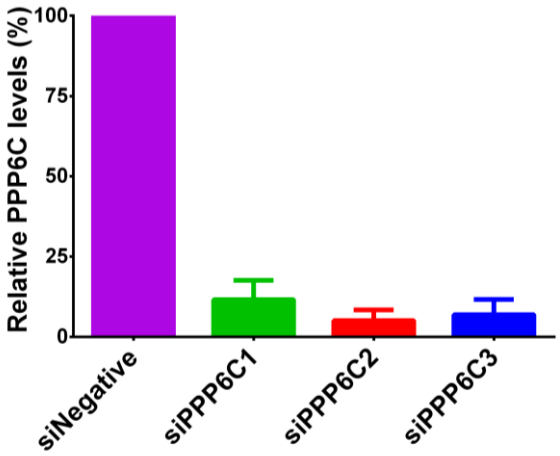
To further understand the reduction of influenza A virus growth in PPP6C knockdown cells, the nuclear export of vRNPs was compared in human alveolar basal epithelial (A549) cells with or without PPP6C knockdown. Levels of PPP6C protein were reduced to 5–11% compared to negative control cells (Figure 6.9A and 6.9B). To assess the viability of A549 cells treated with PPP6C-targeting siRNAs, a quantitative luminescent cell viability assay based on the quantitation of ATP levels was performed.

Luminescence levels were not significantly different in PPP6C knockdown cells compared to negative control cells (Figure 6.5B). The cellular localisation of viral NP was determined in PPP6C knockdown or negative control cells infected at an MOI of 1 with WT virus at 0, 4, 6 and 8 h p.i.. The cellular localisation of NP was scored in infected knockdown or negative control cells from random fields of view in three biological replicas. As anticipated, at 0 h p.i. NP signal was absent in infected cells (Figure 6.9C). At 4 h p.i., an expected phenotype of nuclear NP staining was observed in 100% of infected cells for both the knockdown and negative control treatments, confirming that significant vRNP export is not undertaken at this time point (Figure 6.9D). At 6 h p.i., an average of 30% of negative control cells showed a nucleocytoplasmic NP phenotype, representing the nuclear export of vRNPs that had occurred in these infected cells. However, on average, only 6%, 7% and 11% of the PPP6C knockdown cells treated with the three different siRNAs showed nucleocytoplasmic NP localisation (Figure 6.9E and 6.9G). At 8 h p.i., the average number of infected negative control cells that had a nucleocytoplasmic NP localisation increased to 71%. However, the average number of infected knockdown cells with a nucleocytoplasmic NP localisation reached only 44%, 49% and 45% for each PPP6C siRNA, respectively (Figure 6.9F and 6.9G). These results demonstrate that when the levels of the catalytic subunit of PP6 are reduced in infected cells there is a marked delay in the nuclear export of vRNPs, indicating that PP6 is required for the efficient completion of the virus life-cycle.

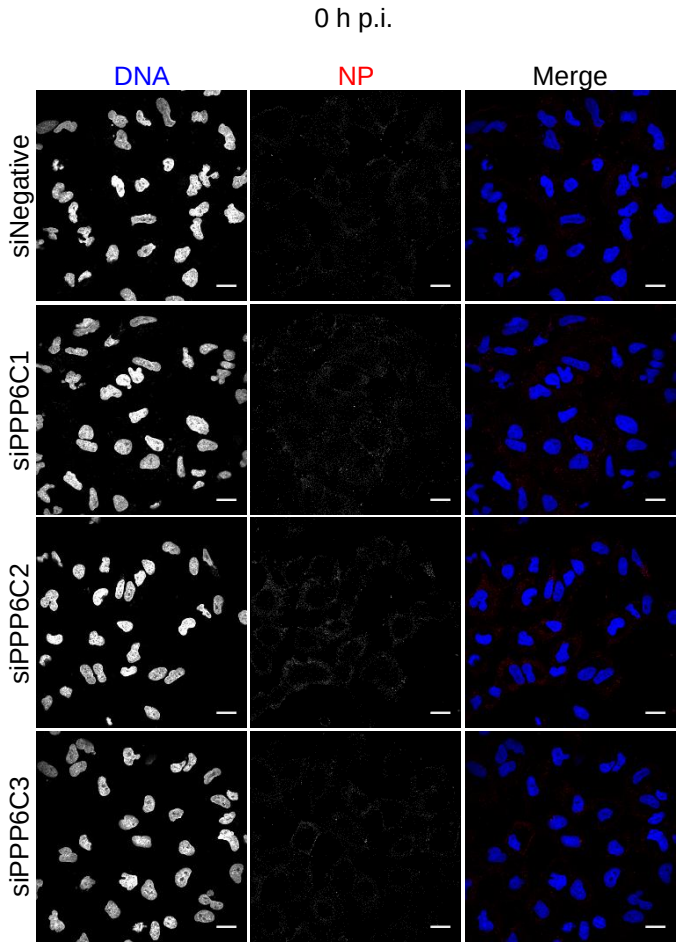
A


siNegative
siPPP6C1
siPPP6C2
siPPP6C3
kDa
37
25
37
αPPP6C
αActin

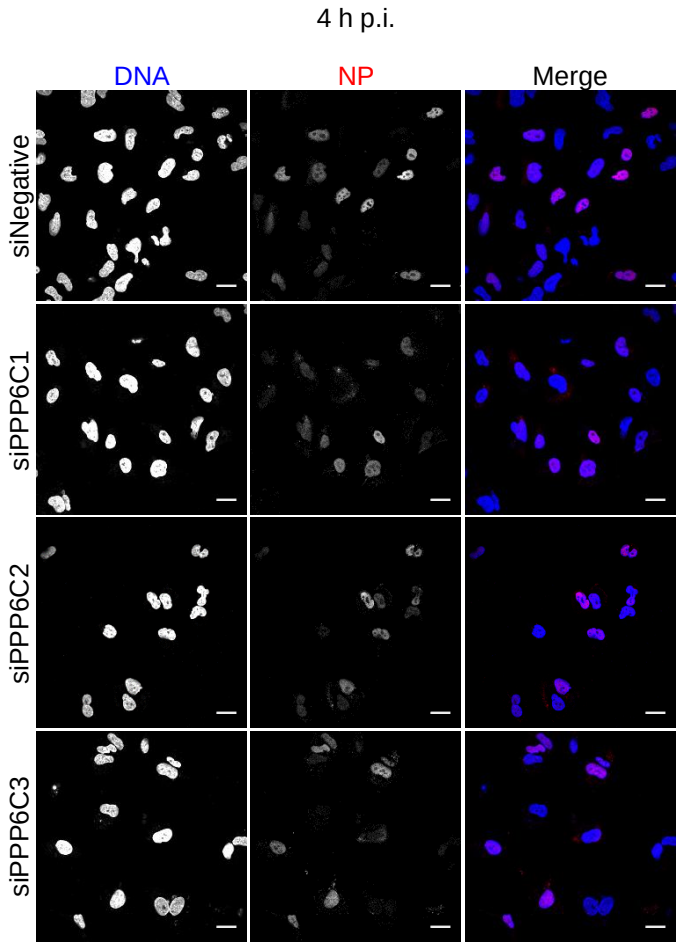
B


Relative PPP6C levels (%)
100
75
50
25
0
siNegative
siPPP6C1
siPPP6C2
siPPP6C3

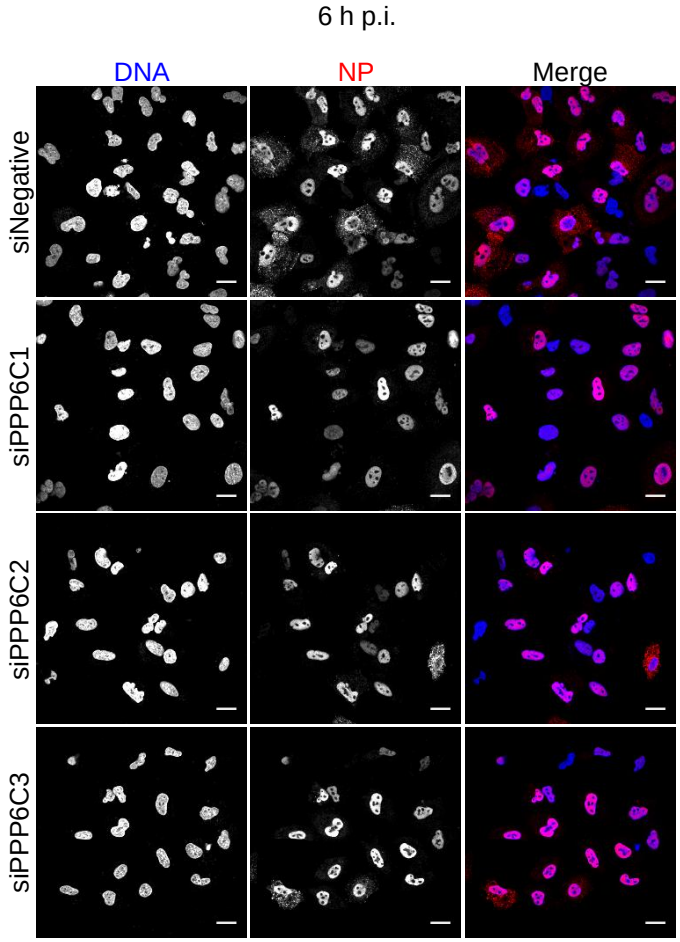
C



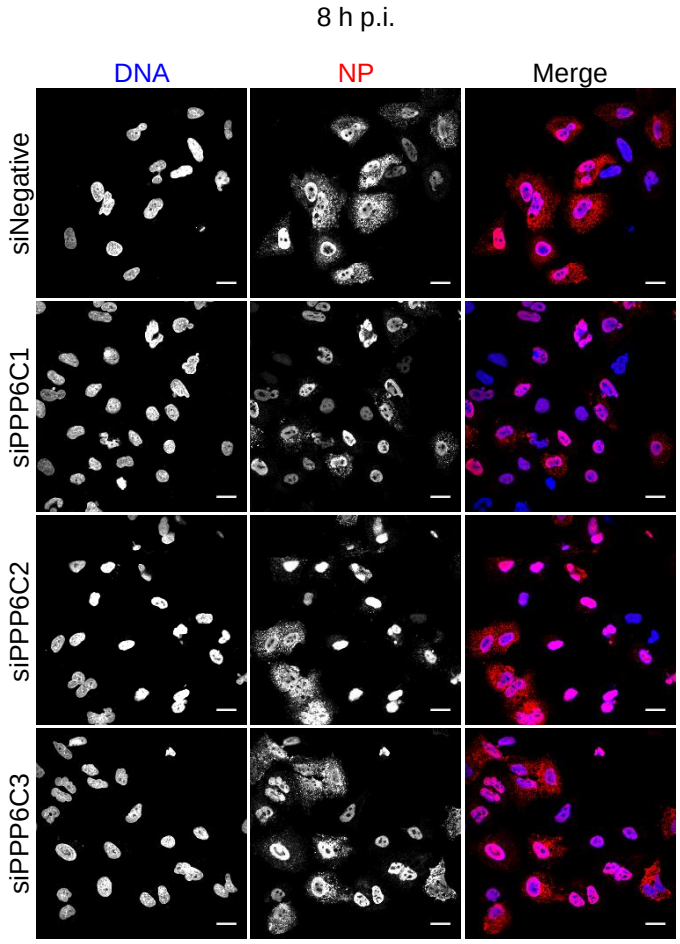
D



E



F



G

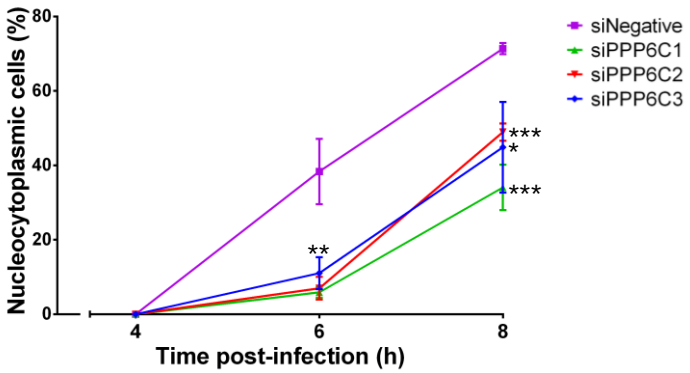


Figure 6.9 Effect of PPP6C knockdown on NP nucleocytoplasmic distribution in influenza A virus infected A549 cells. (A) Western blot analysis of PPP6C in HEK 293T cells treated with PPP6C-targeting siRNAs (siPPP6C1, siPPP6C2 and siPPP6C3) or a negative control siRNA (siNegative). PPP6C (upper panel) was detected with a PPP6C-specific antibody. Actin (lower panel) was used as a loading control. (B) Quantitation of Western blot analyses of the knockdown of PPP6C. PPP6C levels were normalised to the levels of actin and expressed as a percentage of PPP6C levels in cells treated with siNegative. PPP6C levels represent the mean and error bars represent SD from three biological repeats. (C–F) Confocal microscopy of the nucleocytoplasmic distribution of NP in infected PPP6C knockdown cells. A549 cells treated with the indicated siRNAs were infected at an MOI of 1. NP was detected by indirect immunofluorescence using a monoclonal NP antibody and confocal microscopy at the indicated time points p.i.. Representative images of NP localisation are shown. Scale bars, 20 µm. (G) Percentage of infected cells with a nucleocytoplasmic NP localisation at each time point. Percentage represents the mean and the error bars represent SDs from three biological repeats. Asterisks indicate a significant difference from siNegative (* $P < 0.05$, ** $P < 0.01$, *** $P < 0.001$, based on a two-sample Student's *t*-test).

6.7 Discussion

This chapter focuses on the role of the cellular phosphatase PP6 in the regulation of the influenza virus RdRP. PP6 was identified as a component of the viral transcription/replication interactome in Chapter 5 and subsequent characterisation of this interaction and functional experiments presented in this chapter revealed PP6 to act as a positive regulator of influenza virus replication. PP6 is a member of the PP2A subfamily of phosphoprotein phosphatases that reverse the activity of kinases through the dephosphorylation of specific serine or threonine residues (Bastians & Ponstingl, 1996; Shi, 2009). The catalytic subunits of the PP2A subfamily of phosphatases interact with a variety of regulatory subunits and it is the regulatory subunits within the PP6 holoenzyme that define substrate specificity (Barr *et al.*, 2011; Shi, 2009). The PP6 heterotrimeric holoenzyme is composed of a catalytic subunit and a further two subunits: the ankyrin repeat domain 28 scaffold protein (Ankrd28) and one of the PPP6R1, PPP6R2 or PPP6R3 regulatory subunits (Stefansson *et al.*, 2008). PPP6C, PPP6R1 and PPP6R3 were detected by mass spectrometry as co-purifying with the viral RdRP. However, Ankrd28 was not detected in the mass spectrometry. This absence could be explained by a proposed model of PP6 holoenzyme assembly in which Ankrd28 is not required for the interaction between the catalytic and regulatory subunits of PP6 (Stefansson *et al.*, 2008).

To validate the identification of PP6 as an interaction partner of the viral RdRP by mass spectrometry, Western blot analyses confirmed that PP6 co-purified with the viral RdRP from infected cells. PP6 was shown to interact with monomeric PB1 and PB2,

dimeric PB1-PA and with the trimeric RdRP in mammalian cells. It had previously been reported in a proteomics study that the PPP6C subunit of PP6 interacted with a PB1-PA dimer in transiently transfected cells, however, this interaction was not studied further (Bradel-Tretheway *et al.*, 2011). It was then determined that the interaction between PP6 and the viral RdRP is direct, mediated by the regulatory subunit of PP6, consistent with the substrate specificity of PP2A phosphatases being defined by their regulatory subunits. These findings show that PP6 directly binds to the PB1 and PB2 subunit of the viral RdRP via regulatory subunit substrate recognition. Although there is no high resolution structural information available for the PP6 holoenzyme, the crystal structure of the PP2A holoenzyme shows that a substrate-binding groove within the regulatory subunit is located in close proximity to the active site of the catalytic subunit, supporting the view that the regulatory subunits are responsible for target specificity and the positioning of the phosphorylated substrate close to the catalytic centre for dephosphorylation (Xu *et al.*, 2008). PP6 binds to PB1 and PB2 subunits of the viral RdRP, suggesting that it could dephosphorylate PB1 or PB2.

All three subunits of the viral RdRP have been found to be phosphorylated (Hutchinson *et al.*, 2012; Mahmoudian *et al.*, 2009; Mitzner *et al.*, 2009; Sanz-Ezquerro *et al.*, 1998) and PP6 could be involved in the regulation of the phosphorylation status of the viral RdRP. One example of where the phosphorylation status of the viral RdRP could have a function is the regulation of subunit binding to components of the importin pathway. The structure of the C-terminus of PB2 in complex with importin-α5 reveals that S742, a residue that can be phosphorylated (Hutchinson *et al.*, 2012), is positioned close to two basic residues on the surface of importin-α5 (Tarendeau *et al.*, 2007). The

phosphorylation status of S742 could therefore regulate PB2 binding to importin-α, offering a mechanism of the regulation of its nuclear import as has previously been hypothesised (Hutchinson *et al.*, 2012). The PB1 subunit of the viral RdRP has been shown to be phosphorylated at position T223, in the proximity of a nuclear localisation signal (NLS) and a region that is believed to be involved in promoter binding, indicating a potential role in regulating cellular localisation of PB1, or RNA binding (Gonzalez & Ortin, 1999a; b; Hutchinson *et al.*, 2012; Hutchinson *et al.*, 2011; Jung & Brownlee, 2006; Mukaigawa & Nayak, 1991).

As PP6 interacts directly with PB1 and PB2 they represent the most obvious substrates. However, it is possible that PP6 could dephosphorylate another viral or host protein in close proximity to PB1 or PB2. The viral RdRP forms a compact structure (Arranz *et al.*, 2012; Moeller *et al.*, 2012; Resa-Infante *et al.*, 2010) and therefore it is conceivable that PA could be dephosphorylated. PA has been shown to be phosphorylated at positions S224/S225, in an unstructured region linking the PA endonuclease and C-terminal domains (Dias *et al.*, 2009; He *et al.*, 2008; Hutchinson *et al.*, 2012; Obayashi *et al.*, 2008; Yuan *et al.*, 2009). The viral NP has also been found to be phosphorylated at multiple sites (Almond & Felsenreich, 1982; Arrese & Portela, 1996; Hutchinson *et al.*, 2012; Kistner *et al.*, 1989), and therefore it is also plausible that PP6 could bind to the viral RdRP and dephosphorylate a proximal NP molecule, for example NP within the vRNP complex, perhaps serving to regulate the oligomerisation of NP as previously proposed (Chenavas *et al.*, 2013; Hutchinson *et al.*, 2012). NEP, a viral factor for the nuclear export of genomic vRNPs and a regulator of viral RNA synthesis, has been found to be phosphorylated at position S23 to S25 (Hutchinson *et al.*, 2012; Paterson &

Fodor, 2012). NEP is known to interact with and modulate the activity of the viral RdRP (Manz *et al.*, 2012; Paterson & Fodor, 2012; Reuther *et al.*, 2014a; Robb *et al.*, 2009) and therefore it could be subjected to PP6-mediated regulatory phosphorylation. In support of this hypothesis, a recent study described a minor role for phosphorylation of NEP in controlling vRNP export and the polymerase co-factor activity in regulating RNA synthesis (Reuther *et al.*, 2014b). Further studies will be required to identify the precise substrate and residues targeted by PP6 and to determine the molecular function that dephosphorylation by PP6 plays in the influenza virus life-cycle.

The biological significance of PP6 in the influenza A virus life-cycle was assessed in functional experiments in which the catalytic subunit of PP6 was knocked down in infected cells. Knockdown of PP6 resulted in a 10-fold reduction in virus growth, signifying the importance of PP6 in influenza virus infection. The mechanism leading to reduction in virus growth was dissected further by analysing RNA synthesis and export of vRNPs from the nucleus in knockdown cells. In the case of PPP6C knockdown, viral RNA accumulation was significantly down regulated, and nuclear-export of vRNPs was significantly reduced. These findings show that PP6 is a positive regulatory factor for efficient viral RNA synthesis, which consequently affect vRNP nuclear-export and virus growth in infected cells. However, these experiments do not exclude the possibility that PP6 also plays an additional, indirect role in the virus life-cycle, independent of binding to the viral RdRP. PP6 has been shown to have important role in a number of cellular processes, including the DNA damage response and the repair of double strand breaks (Douglas *et al.*, 2010; Hammond *et al.*, 2013; Hosing *et al.*, 2012; Shen *et al.*, 2011; Zhong *et al.*, 2011), mitosis and cell division (Bastians &

Ponstingl, 1996; Stefansson & Brautigan, 2007; Zeng *et al.*, 2010), vesicular trafficking (Bhandari *et al.*, 2013), splicing (Kamoun *et al.*, 2013) and signalling events (Dai *et al.*, 2013; Kajino *et al.*, 2006). Thus, it is possible that PP6 silencing perturbs the virus life-cycle progression by affecting cellular processes that rely on PP6 function. However, the fact that PP6 interacts directly with the viral RdRP suggests that it plays a direct role in regulating the post-translational modification of the viral proteome.

In summary, the identification of components of the cellular interactome of the influenza A virus RdRP provides the basis for subsequent dissection of the role of cellular factors in the regulation of the viral RdRP. One of the identified factors, cellular phosphatase PP6, was shown to be essential for efficient completion of the influenza A virus life-cycle as revealed by siRNA-mediated knockdown resulting in the inhibition of viral RNA synthesis, vRNP nuclear export and viral growth. These findings highlight the significance of regulatory phosphorylation in influenza virus biology.

6.8 Summary

- PPP6C, PPP6R1 and PPP6R3 subunits of PP6 were identified as components of the viral transcription/replication machinery cellular interactome, as determined by mass spectrometry.
- PP6 was confirmed to co-purify with the viral RdRP from infected cells.
- PP6 interacts directly with PB1 and PB2 subunits of the viral RdRP via a regulatory subunit.

- Knockdown of the catalytic subunit of PP6 resulted in significant reduction in virus growth by 10-fold.
- RNA accumulation of mRNA, cRNA and vRNA was markedly reduced when PPP6C was down regulated in infected cells.
- A significant delay in vRNP nuclear export was observed when PPP6C was knocked down in infected cells.

Chapter 7: Summary and Discussion

7.1 Introduction

This thesis examines the fundamental biology of viral RNA synthesis by the influenza virus RdRP. In particular, the role of viral and host factors were investigated. Two approaches were taken in this thesis to study the role of viral and cellular factors in the regulation of the viral RdRP. Firstly, the minimal requirements for genome replication (vRNA→cRNA→vRNA) by the viral RdRP were investigated. This required the isolation of cRNP and vRNP complexes separately from infected cells, enabling RdRP activity within these RNP complexes to be assessed independently *in vitro*. Secondly, a more general approach was taken that involved tagging of the viral RdRP to identify novel cellular factors associated with the viral transcription/replication machinery. A

cellular phosphatase was found to interact with the viral RdRP and act as a positive regulatory factor in influenza virus replication. This discussion will summarise the findings from this study.

7.2 Isolation of influenza virus RNP complexes by RNA-based affinity purification

Replication of the influenza virus genome by the viral RdRP begins with the synthesis of a full-length complementary RNA that is used in turn as a template for the synthesis of multiple copies of genomic RNA, which are subsequently packaged into virions. As both cRNA and vRNA interact with the viral RdRP and NP, the separate isolation of ribonucleoprotein complexes that contain either cRNA or vRNA necessitated the development of an entirely RNA-based isolation strategy. To this end, a translational operator RNA from the *Pseudomonas aeruginosa* PP7 was inserted into influenza A/WSN/33 (H1N1) virus genome in the region that encodes the NA stalk. The PP7 RNA was inserted into the genome such that NA mRNA and cRNA was tagged, or NA vRNA was tagged. The insertion of the PP7 RNA into the viral genome increased the NA gene by 30 nt and increased the stalk length of the NA glycoprotein by 10 amino acids. Recombinant viruses were generated by reverse genetics and these viruses exhibited similar growth properties to wild-type virus in cell culture. This finding is consistent with the observation that neuraminidase activity and virus growth is not affected by relatively large insertions and deletions in the stalk region of the NA glycoprotein (Castrucci & Kawaoka, 1993; Luo *et al.*, 1993; Munier *et al.*, 2010;

Sorrell *et al.*, 2010). Indeed, growth of influenza A/WSN/33 virus in cell culture has been shown to be unaffected even after the deletion of the entire NA stalk (Castrucci & Kawaoka, 1993). In the same study, virus growth was unaffected when the stalk length was increased by 28 amino acids in length. However, NA stalk length has been shown to affect the ability of an influenza A virus to replicate efficiently *in vivo*. Stalk length has been proposed to act as a barrier of transmission from avian to mammalian hosts. For example, short stalk length of NA is selected for when influenza A viruses adapt to gallinaceous hosts (Blumenkrantz *et al.*, 2013; Hossain *et al.*, 2008; Munier *et al.*, 2010; Sorrell *et al.*, 2010; Zhou *et al.*, 2009). Alternatively, the PP7 RNA tag was also inserted into the linker region between the RNA binding and effector domain of the NS1 protein. Although recombinant viruses were generated, these viruses containing a PP7 RNA tag at this position within the genome exhibited reduced growth properties, indicating that the extension of the linker region in the NS1 protein significantly impacted multi-cycle replication of the virus. The length of the linker in the NS1 protein has been hypothesised to affect the ability of NS1 protein to sequester dsRNA in a model that relies on cooperative oligomerisation of NS1 (Bornholdt & Prasad, 2008). Therefore, the reduced growth phenotype that was observed when a PP7 RNA tag was inserted into the linker region could reduce the ability of NS1 to sequester RNA, leading to heightening of the cellular innate immune response, resulting in a reduction in virus growth.

Using the recombinant viruses that contain a PP7 RNA tag in NA viral RNAs, cRNP complexes and vRNP complexes were separately isolated from infected cells. Importantly, this provides the first direct evidence that secondary RNA structures are

able to form within these complexes without being melted by viral NP. Secondary RNA structures within vRNP complexes have been proposed to facilitate the selective packaging of vRNA segments into nascent virions (Gerber *et al.*, 2014; Hutchinson *et al.*, 2010). This finding supports previous electron tomography, biochemical and reverse genetics studies that have led to this proposal (Fournier *et al.*, 2012a; Fournier *et al.*, 2012b; Gavazzi *et al.*, 2013; Noda *et al.*, 2006; Noda *et al.*, 2012). Viral mRNP complexes were also purified, but with a lower efficiency. This unexpected observation suggests that secondary RNA structures are less accessible in NA mRNP complexes, likely reflecting the association of viral mRNAs with a plethora of cellular factors that are involved in their processing, nuclear export and translation (York & Fodor, 2013). Further optimisation of RNA-based affinity purification, with a view to specifically isolating viral mRNP complexes, could lead to deeper knowledge and understanding of the protein occupancy of viral mRNA, providing valuable insight into the biogenesis, nuclear export and translation of viral mRNP complexes.

7.3 Molecular architecture of the influenza virus cRNP complex

Isolation of the influenza virus cRNP complex from infected cells permitted visualisation of this essential component of viral RNA replication machinery for the first time. Negative-stain electron microscopy was carried out in order to investigate the molecular architecture of the cRNP complex. The complex adopted a structure that is analogous to previously reported vRNP complexes (Arranz *et al.*, 2012; Moeller *et al.*, 2012). The complex contained a central double-helical filament with two distinct

termini. One terminus contained a loop structure that was composed of a varying number of NP molecules. The opposite terminus contained a structure that was interpreted to be the viral RdRP, on the basis of analogy to previously published vRNP structures. The terminus that was assumed to harbour the viral RdRP contained a small and large structural feature, which had been observed in previously reported cryo-electron microscopy vRNP and viral RdRP structures (Arranz *et al.*, 2012; Moeller *et al.*, 2012). These findings suggest that the viral RdRP adopts a similar conformation in cRNP and vRNP complexes. Further studies of cRNP and vRNP complexes using high resolution cryo-electron microscopy are required in order to ascertain whether any structural dissimilarities exist between the viral RdRP in these complexes. Elucidating any potential differences in viral RdRP structure in these complexes could help in understanding the differences in function of the viral RdRP that has been observed on viral cRNA and vRNA templates.

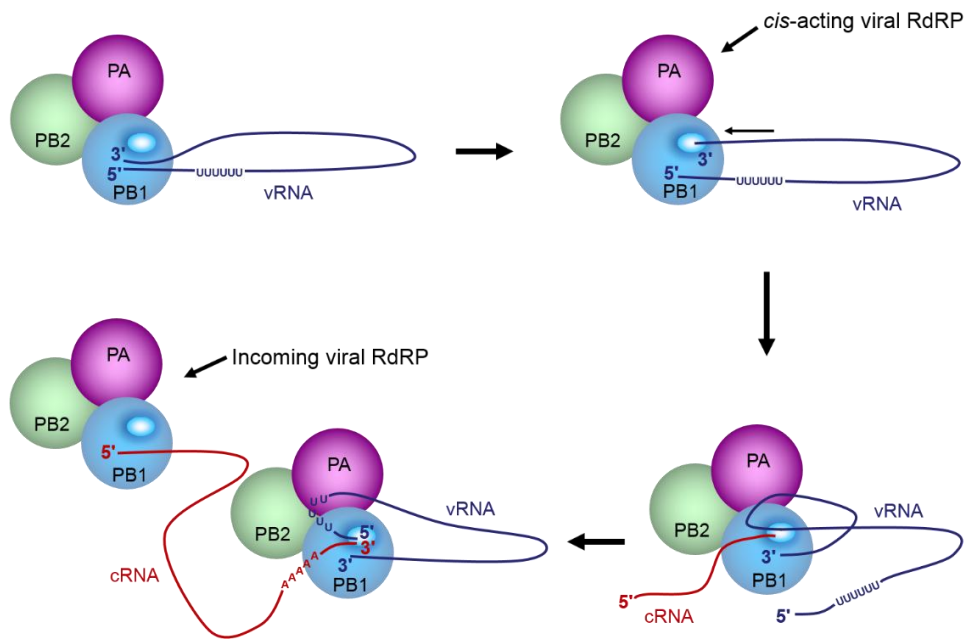
7.4 A *trans*-activation model of vRNA synthesis

The separate isolation of cRNP and vRNP complexes from infected cells enabled the minimal requirements of vRNA replication (vRNA→cRNA→vRNA) to be studied *in vitro*. The viral RdRP within isolated vRNP complexes was shown to be able to synthesise cRNA in the absence of added viral or cellular factors. This observation is in agreement that vRNP complexes isolated from virions are able to synthesise cRNA *in vitro* (Vreede & Brownlee, 2007). Furthermore, this observation is in agreement with a stabilisation model of cRNA synthesis (Vreede *et al.*, 2004). It had been previously

reported that the viral RdRP within vRNP complexes introduced into cells by infection are able to synthesise cRNA in the absence of protein translation, as observed in cells treated with cycloheximide. This activity relied on the presence of pre-expressed NP and inactive viral RdRP for stabilisation and protection of cRNA. Taken together with the results presented in Chapter 4, the minimal requirements for cRNA synthesis (vRNA→cRNA) are the vRNP complex, with the viral RdRP acting in *cis* on the vRNA template (Figure 7.1). In contrast, isolated cRNP complexes were only able to synthesise vRNA (cRNA→vRNA) in the presence of additional RdRP, regardless of whether the viral RdRP included in the *in vitro* assay had enzymatic activity or not. This led to the proposal of a *trans*-activation model of vRNA synthesis (Figure 7.1). In this model, a second *trans*-activating RdRP oligomerises with a *cis*-acting RdRP for activity. This *trans*-activation model of vRNA synthesis is in contradiction to a *trans*-acting model of vRNA synthesis whereby a *trans*-acting viral RdRP synthesises vRNA on the cRNA template (Jorba *et al.*, 2009). In the study that led to the proposal of this model, a vRNP complex containing a replication mutant viral RdRP was co-transfected into cells with plasmids that express a transcription mutant viral RdRP, after which vRNA synthesis was observed. It was therefore concluded that replication (cRNA→vRNA) occurs in *trans*. It could be possible that both models are correct and that a *trans*-activating RdRP is required for initial vRNA synthesis, while the bulk of vRNA synthesis is performed in *trans*.

The precise role of the *trans*-activating RdRP that has been proposed in this thesis is currently unknown, however, it could be speculated that a *trans*-activating RdRP plays an architectural role and is required to provide structural support to the *cis*-acting RdRP.

A


vRNA→cRNA
PA
PB2
PB1
3'
5'
vRNA
cis-acting viral RdRP
Incoming viral RdRP
cRNA

B

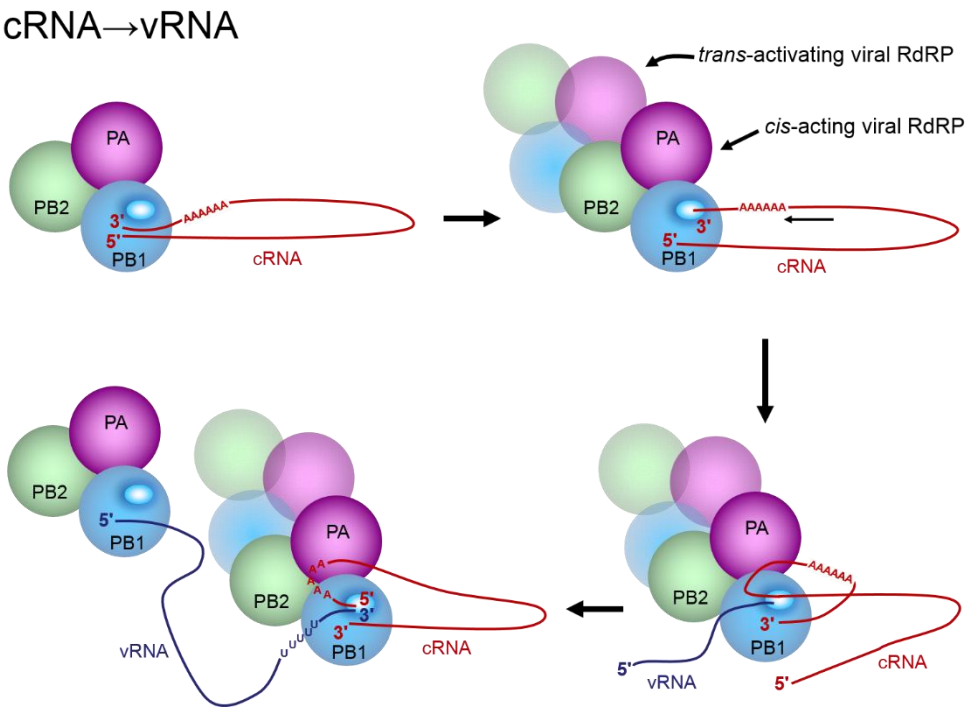

cRNA→vRNA
PA
PB2
PB1
3'
5'
cRNA
vRNA
trans-activating viral RdRP
cis-acting viral RdRP

Figure 7.1 Model for influenza A virus genome replication. In vRNP and cRNP complexes the viral RdRP, consisting of the PB1, PB2 and PA subunits, is bound to the partially complementary 5′ and 3′ termini of vRNA and cRNA segments. The oligomeric nucleoprotein that encapsidates the viral RNA has been omitted for simplicity. (A) Replication of vRNA to cRNA (vRNA→cRNA) is performed by the vRNP-associated RdRP in *cis*. Replication is initiated by the *cis*-acting RdRP binding to GTP in the active site in the PB1 subunit, directed by the penultimate residue in the 3′ end of the vRNA for the generation of pppApG that is extended (not shown). The vRNA template is threaded through the active site in PB1, copying the entire length of the vRNA. The nascent cRNA is bound by a second incoming RdRP at the 5′ end. (B) Replication of cRNA to vRNA (cRNA→vRNA), performed by the cRNP-associated RdRP in *cis*, requires a *trans*-activating RdRP. A *trans*-activating RdRP oligomerises with the cRNP-associated RdRP. The cRNP-associated RdRP synthesises pppApG, directed by positions 4 and 5 of the 3′ end of the cRNA, which realign to positions 1 and 2 for subsequent elongation (not shown). The cRNA template is threaded through the active site in the PB1 subunit. The nascent cRNA is bound by a second incoming RdRP at the 5′ end.

It is also plausible that a *trans*-activating RdRP could act as an allosteric inducer of vRNA synthesis by causing a conformational change in the RdRP, such as the rearrangement of the active site or the reorganisation of RNA structural motifs. The formation of a quaternary structure between influenza virus RdRPs has been reported previously. It has been proposed that the influenza virus RdRP oligomerises through interactions between PB1 and PB2 subunits (Digard *et al.*, 1989; Jorba *et al.*, 2008). Atomic resolution structural information is required in order to fully understand how the viral RdRP oligomerises and how vRNA synthesis could be activated by oligomerisation.

The role of oligomeric RdRP in RNA synthesis is not exclusive to influenza viruses. Nucleic acid synthesis is often associated with large, immobilised complexes (Cook, 1999; 2010), examples of which can be found in a number of virus families, particularly in positive-strand RNA viruses, including members of the *Picornaviridae*, *Flaviviridae* and *Coronaviridae*. Viral RNA synthesis in cells infected by members of these virus families occurs in association with specific cellular structures, such a membranous structures and requires the involvement of viral RdRPs that are catalytically inactive. It is therefore plausible that vRNA synthesis by the influenza virus RdRP requires the involvement of catalytically inactive RdRPs, perhaps in association with a specific nuclear substructure, or within a particular nuclear microenvironment that is distinct from cRNA synthesis. It is possible that the addition of inactive viral RdRP to cRNP complexes results in the formation of a structure that recapitulates, or partially recapitulates the scenario that results in vRNA synthesis in infected cells.

Although the minimal requirements for influenza virus genome replication have been proposed in this thesis, a number of additional factors are involved in viral RNA synthesis in influenza virus infected cells. For example, the viral NEP protein has been shown to be a significant regulator of genome replication, by up-regulating the accumulation of replication products (Robb *et al.*, 2009). A further example is the involvement of svRNAs. It has been proposed that svRNAs act as an allosteric enhancer of replication, possibly through an interaction with a putative RNA binding cleft in the PA subunit of the RdRP (Perez *et al.*, 2010; Perez *et al.*, 2012). The presence of NP has also been shown to be required for efficient viral RNA synthesis, acting as an elongation factor (Turrell *et al.*, 2013). Regulatory host factors are believed to have an important role in the replication of the viral genome (Matsuoka *et al.*, 2013; Nagata *et al.*, 2008). Further work is required to understand how viral and cellular factors act in concert to achieve efficient genome replication in infected cells.

7.5 Identification of cellular factors that interact with the viral replication/transcription machinery

Identification of cellular factors that interact with the viral RdRP could help elucidate previously unchartered molecular mechanisms of viral RNA synthesis. During infection the influenza virus transcription/replication machinery makes numerous interactions with the host cell (Matsuoka *et al.*, 2013; Shaw, 2011; Watanabe *et al.*, 2010). The results presented in Chapter 5 provide the first quantitative analysis of cellular factors that interact with the viral transcription/replication machinery. Furthermore, this work is

the first study to identify the transcription/replication machinery interactome in the context of infected cells. The affinity-purification mass spectrometry approach that was employed to isolate viral RNP and viral RdRP complexes from infected cells relied on the introduction of a Strep-tag to the PB2 subunit of the viral RdRP (Rameix-Welti *et al.*, 2009). Label-free quantitative mass spectrometry revealed a total of 171 reproducible cellular factors that were found to co-purify with complexes containing PB2-Strep from infected cells. The most abundant of these host proteins were chaperones, cytoskeletal proteins, importins, proteins involved in ubiquitination, kinases and phosphatases, mitochondrial and ribosomal proteins. The presented interactome provides an important starting point towards unravelling the molecular mechanisms of viral RNA synthesis and regulation of the viral RdRP. Accordingly, the role of cellular phosphatase PP6 was investigated due to its relatively high abundance in the interactome.

7.6 Cellular PP6 interacts with the viral RdRP and acts a positive regulatory factor in influenza virus replication

The PP6 heterotrimeric holoenzyme has been proposed to be composed of the catalytic subunit PPP6C, Ankrd28 and one of regulatory subunits PPP6R1, PPP6R2 or PPP6R3 (Stefansson *et al.*, 2008). PPP6C, PPP6R1 and PPP6R3 were identified by mass spectrometry as interactors of the viral transcription/replication machinery. The influenza virus RdRP and NP are known to be phosphorylated in infected cells (Almond & Felsenreich, 1982; Arrese & Portela, 1996; Hutchinson *et al.*, 2012; Kistner

et al., 1985; Mahmoudian *et al.*, 2009; Perales *et al.*, 2000; Sanz-Ezquerro *et al.*, 1998). Kinase activity has been shown to be essential for influenza virus replication (Hui & Nayak, 2002; Kumar *et al.*, 2011; Kurokawa *et al.*, 1990; Pleschka *et al.*, 2001; Root *et al.*, 2000), however, the role of phosphatases has not been studied in the context of influenza virus infection. The biological significance of PP6 in the influenza virus life-cycle was assessed by functional experiments in which the catalytic subunit of PP6 was knocked down in infected cells. These experiments showed that knockdown of the catalytic subunit resulted in significant attenuation of virus growth. Moreover, viral RNA synthesis was significantly attenuated, which resulted in a delay of export of vRNP complexes from the nucleus. It was established that PP6 interacted with monomeric PB1 and PB2, dimeric PB1-PA and with the trimeric RdRP in mammalian cells. PP6 was found to interact directly with the trimeric viral RdRP *in vitro*. In this assay, the regulatory subunits of PP6 pulled down the viral RdRP. The catalytic subunit also bound to the viral RdRP, however, this interaction was considerably weaker. It was therefore concluded that the interaction was mediated by PB1 and/or PB2 of the viral RdRP, and a regulatory subunit of PP6.

Although the precise target substrate and residue for PP6 were not determined, the most obvious targets are residues within the PB1 and PB2 subunits. Both of these subunits have been found to be phosphorylated (Hutchinson *et al.*, 2012). The phosphorylation site that was detected in the PB2 subunit falls within a region of PB2 for which there is an atomic structure. The PB2 C-terminus/importin-α5 co-crystal revealed that the S742 phosphorylation site is in juxtaposition with two basic residues on the surface of the importin (Tarendeau *et al.*, 2007), suggesting that phosphorylation could be playing a

role in regulating binding to importin-α. The PB1 subunit of the viral RdRP can be phosphorylated at position T223. This is close to a NLS and a region that is thought to be involved in promoter binding, indicating a potential role in regulating the cellular localisation or RNA binding of PB1 (Gonzalez & Ortin, 1999a; b; Hutchinson *et al.*, 2012; Hutchinson *et al.*, 2011; Jung & Brownlee, 2006; Mukaigawa & Nayak, 1991). It is plausible that due to the compact structure of the viral RdRP (Area *et al.*, 2004; Coloma *et al.*, 2009; Resa-Infante *et al.*, 2010; Torreira *et al.*, 2007), the PA subunit could be dephosphorylated. PA has been shown to be phosphorylated at S224/S225 (Hutchinson & Fodor, 2012), however, a function of this region of PA has yet to be described. The viral NP can also be phosphorylated at multiple sites (Almond & Felsenreich, 1982; Arrese & Portela, 1996; Chenavas *et al.*, 2013; Hutchinson *et al.*, 2012; Kistner *et al.*, 1989), and therefore PP6 may bind to the viral RdRP and dephosphorylate a proximal NP molecule within an assembling RNP complex, perhaps serving to regulate the oligomerisation of NP as has been previously proposed (Chenavas *et al.*, 2013; Hutchinson *et al.*, 2012). It is possible that PP6 may bind to the viral RdRP to dephosphorylate another viral protein, or a cellular factor to regulate their activity. The viral NEP protein has been found to be phosphorylated at a position between S23 and S25 (Hutchinson *et al.*, 2012). As NEP is known to interact with and modulate the activity of the viral RdRP for up-regulation of replication products (Manz *et al.*, 2012; Paterson & Fodor, 2012; Reuther *et al.*, 2014a; Robb *et al.*, 2009), it could be subject to PP6-mediated regulatory dephosphorylation. A recent study described a minor role for phosphorylation of NEP in controlling vRNP export and the polymerase co-factor activity in regulating RNA synthesis (Reuther *et al.*, 2014b) in support of this theory. Further studies are required to identify the precise substrate and residues

targeted by PP6 and to determine the molecular function that dephosphorylation by PP6 plays in the influenza virus life-cycle.

Chapter 8: References

Air, G. M. & Laver, W. G. (1989). The neuraminidase of influenza virus. *Proteins* **6**, 341-356.

Ali, A., Avalos, R. T., Ponimaskin, E. & Nayak, D. P. (2000). Influenza virus assembly: effect of influenza virus glycoproteins on the membrane association of M1 protein. *J Virol* **74**, 8709-8719.

Almond, J. W. (1977). A single gene determines the host range of influenza virus. *Nature* **270**, 617-618.

Almond, J. W. & Felsenreich, V. (1982). Phosphorylation of the nucleoprotein of an avian influenza virus. *J Gen Virol* **60**, 295-305.

Amorim, M. J., Bruce, E. A., Read, E. K., Foeglein, A., Mahen, R., Stuart, A. D. & Digard, P. (2011). A Rab11- and microtubule-dependent mechanism for cytoplasmic transport of influenza A virus viral RNA. *J Virol* **85**, 4143-4156.

Amorim, M. J., Read, E. K., Dalton, R. M., Medcalf, L. & Digard, P. (2007). Nuclear export of influenza A virus mRNAs requires ongoing RNA polymerase II activity. *Traffic* **8**, 1-11.

Area, E., Martin-Benito, J., Gastaminza, P., Torreira, E., Valpuesta, J. M., Carrascosa, J. L. & Ortin, J. (2004). 3D structure of the influenza virus polymerase complex: Localization of subunit domains. *P Natl Acad Sci USA* **101**, 308-313.

Arranz, R., Coloma, R., Chichon, F. J., Conesa, J. J., Carrascosa, J. L., Valpuesta, J. M., Ortin, J. & Martin-Benito, J. (2012). The structure of native influenza virion ribonucleoproteins. *Science* **338**, 1634-1637.

Arrese, M. & Portela, A. (1996). Serine 3 is critical for phosphorylation at the N-terminal end of the nucleoprotein of influenza virus A/Victoria/3/75. *J Virol* **70**, 3385-3391.

Azzeh, M., Flick, R. & Hobom, G. (2001). Functional analysis of the influenza A virus cRNA promoter and construction of an ambisense transcription system. *Virology* **289**, 400-410.

Bae, S. H., Cheong, H. K., Lee, J. H., Cheong, C., Kainosho, M. & Choi, B. S. (2001). Structural features of an influenza virus promoter and their implications for viral RNA synthesis. *Proc Natl Acad Sci U S A* **98**, 10602-10607.

Baltimore, D. (1971). Expression of animal virus genomes. *Bacteriological reviews* **35**, 235-241.

Barr, F. A., Elliott, P. R. & Gruneberg, U. (2011). Protein phosphatases and the regulation of mitosis. *J Cell Sci* **124**, 2323-2334.

Barrett, T., Wolstenholme, A. J. & Mahy, B. W. (1979). Transcription and replication of influenza virus RNA. *Virology* **98**, 211-225.

Bastians, H. & Ponstingl, H. (1996). The novel human protein serine/threonine phosphatase 6 is a functional homologue of budding yeast Sit4p and fission yeast ppe1, which are involved in cell cycle regulation. *J Cell Sci* **109 (Pt 12)**, 2865-2874.

Baudin, F., Bach, C., Cusack, S. & Ruigrok, R. W. (1994). Structure of influenza virus RNP. I. Influenza virus nucleoprotein melts secondary structure in panhandle RNA and exposes the bases to the solvent. *EMBO J* **13**, 3158-3165.

Baudin, F., Petit, I., Weissenhorn, W. & Ruigrok, R. W. (2001). In vitro dissection of the membrane and RNP binding activities of influenza virus M1 protein. *Virology* **281**, 102-108.

Beaton, A. R. & Krug, R. M. (1981). Selected host cell capped RNA fragments prime influenza viral RNA transcription in vivo. *Nucleic Acids Res* **9**, 4423-4436.

Beaton, A. R. & Krug, R. M. (1986). Transcription antitermination during influenza viral template RNA synthesis requires the nucleocapsid protein and the absence of a 5' capped end. *Proc Natl Acad Sci U S A* **83**, 6282-6286.

Bergmann, M. & Muster, T. (1995). The relative amount of an influenza A virus segment present in the viral particle is not affected by a reduction in replication of that segment. *J Gen Virol* **76 (Pt 12)**, 3211-3215.

Bhandari, D., Zhang, J., Menon, S., Lord, C., Chen, S., Helm, J. R., Thorsen, K., Corbett, K. D., Hay, J. C. & Ferro-Novick, S. (2013). Sit4p/PP6 regulates ER-to-Golgi traffic by controlling the dephosphorylation of COPII coat subunits. *Molecular biology of the cell* **24**, 2727-2738.

Bieniossek, C., Richmond, T. J. & Berger, I. (2008). MultiBac: multigene baculovirus-based eukaryotic protein complex production. *Curr Protoc Protein Sci* **Chapter 5**, Unit 5 20.

Bienko, M., Green, C. M., Sabbioneda, S., Crosetto, N., Matic, I., Hibbert, R. G., Begovic, T., Niimi, A., Mann, M., Lehmann, A. R. & Dikic, I. (2010). Regulation of Translesion Synthesis DNA Polymerase eta by Monoubiquitination. *Molecular Cell* **37**, 396-407.

Bier, K., York, A. & Fodor, E. (2011). Cellular cap-binding proteins associate with influenza virus mRNAs. *J Gen Virol* **92**, 1627-1634.

Biswas, S. K., Boutz, P. L. & Nayak, D. P. (1998). Influenza virus nucleoprotein interacts with influenza virus polymerase proteins. *J Virol* **72**, 5493-5501.

Biswas, S. K. & Nayak, D. P. (1994). Mutational analysis of the conserved motifs of influenza A virus polymerase basic protein 1. *J Virol* **68**, 1819-1826.

Blaas, D., Patzelt, E. & Kuechler, E. (1982). Identification of the cap binding protein of influenza virus. *Nucleic Acids Res* **10**, 4803-4812.

Blumenkrantz, D., Roberts, K. L., Shelton, H., Lycett, S. & Barclay, W. S. (2013). The short stalk length of highly pathogenic avian influenza H5N1 virus neuraminidase limits transmission of pandemic H1N1 virus in ferrets. *J Virol* **87**, 10539-10551.

Bornholdt, Z. A. & Prasad, B. V. (2008). X-ray structure of NS1 from a highly pathogenic H5N1 influenza virus. *Nature* **456**, 985-988.

Bortz, E., Westera, L., Maamary, J., Steel, J., Albrecht, R. A., Manicassamy, B., Chase, G., Martinez-Sobrido, L., Schwemmle, M. & Garcia-Sastre, A. (2011). Host- and strain-specific regulation of influenza virus polymerase activity by interacting cellular proteins. *mBio* **2**.

Boulay, F., Doms, R. W., Wilson, I. & Helenius, A. (1987). The influenza hemagglutinin precursor as an acid-sensitive probe of the biosynthetic pathway. *EMBO J* **6**, 2643-2650.

Bouloy, M., Plotch, S. J. & Krug, R. M. (1978). Globin mRNAs are primers for the transcription of influenza viral RNA in vitro. *Proc Natl Acad Sci U S A* **75**, 4886-4890.

Bourmakina, S. V. & Garcia-Sastre, A. (2003). Reverse genetics studies on the filamentous morphology of influenza A virus. *J Gen Virol* **84**, 517-527.

Braam, J., Ulmanen, I. & Krug, R. M. (1983). Molecular model of a eucaryotic transcription complex: functions and movements of influenza P proteins during capped RNA-primed transcription. *Cell* **34**, 609-618.

Bradel-Tretheway, B. G., Mattiacio, J. L., Krasnoselsky, A., Stevenson, C., Purdy, D., Dewhurst, S. & Katze, M. G. (2011). Comprehensive proteomic analysis of influenza virus polymerase complex reveals a novel association with mitochondrial proteins and RNA polymerase accessory factors. *J Virol* **85**, 8569-8581.

Brass, A. L., Huang, I. C., Benita, Y., John, S. P., Krishnan, M. N., Feeley, E. M., Ryan, B. J., Weyer, J. L., van der Weyden, L., Fikrig, E., Adams, D. J., Xavier, R. J., Farzan, M. & Elledge, S. J. (2009). The IFITM proteins mediate cellular resistance to influenza A H1N1 virus, West Nile virus, and dengue virus. *Cell* **139**, 1243-1254.

Brown, D. A. & Rose, J. K. (1992). Sorting of GPI-anchored proteins to glycolipid-enriched membrane subdomains during transport to the apical cell surface. *Cell* **68**, 533-544.

Brownlee, G. G. & Sharps, J. L. (2002). The RNA polymerase of influenza a virus is stabilized by interaction with its viral RNA promoter. *J Virol* **76**, 7103-7113.

Bruce, E. A., Digard, P. & Stuart, A. D. (2010). The Rab11 pathway is required for influenza A virus budding and filament formation. *J Virol* **84**, 5848-5859.

Bui, M., Whittaker, G. & Helenius, A. (1996). Effect of M1 protein and low pH on nuclear transport of influenza virus ribonucleoproteins. *Journal of Virology* **70**, 8391-8401.

Bui, M., Wills, E. G., Helenius, A. & Whittaker, G. R. (2000). Role of the influenza virus M1 protein in nuclear export of viral ribonucleoproteins. *Journal of Virology* **74**, 1781-1786.

Bullough, P. A., Hughson, F. M., Skehel, J. J. & Wiley, D. C. (1994). Structure of influenza haemagglutinin at the pH of membrane fusion. *Nature* **371**, 37-43.

Calder, L. J., Wasilewski, S., Berriman, J. A. & Rosenthal, P. B. (2010). Structural organization of a filamentous influenza A virus. *Proc Natl Acad Sci U S A* **107**, 10685-10690.

Carmody, S. R. & Wente, S. R. (2009). mRNA nuclear export at a glance. *J Cell Sci* **122**, 1933-1937.

Carr, S. M., Carnero, E., Garcia-Sastre, A., Brownlee, G. G. & Fodor, E. (2006). Characterization of a mitochondrial-targeting signal in the PB2 protein of influenza viruses. *Virology* **344**, 492-508.

Castrucci, M. R. & Kawaoka, Y. (1993). Biologic importance of neuraminidase stalk length in influenza A virus. *J Virol* **67**, 759-764.

Cauldwell, A. V., Long, J. S., Moncorge, O. & Barclay, W. S. (2014). Viral determinants of influenza A virus host range. *J Gen Virol* **95**, 1193-1210.

Chambers, M. C., Maclean, B., Burke, R., Amodei, D., Ruderman, D. L., Neumann, S., Gatto, L., Fischer, B., Pratt, B., Egertson, J., Hoff, K., Kessner, D., Tasman, N., Shulman, N., Frewen, B., Baker, T. A., Brusniak, M. Y., Paulse, C., Creasy, D., Flashner, L., Kani, K., Moulding, C., Seymour, S. L., Nuwaysir, L. M., Lefebvre, B., Kuhlmann, F., Roark, J., Rainer, P., Detlev, S., Hemenway, T., Huhmer, A., Langridge, J., Connolly, B., Chadick, T., Holly, K., Eckels, J., Deutsch, E. W., Moritz, R. L., Katz, J. E., Agus, D. B., MacCoss, M., Tabb, D. L. & Mallick, P. (2012). A cross-platform toolkit for mass spectrometry and proteomics. *Nature biotechnology* **30**, 918-920.

Chao, J. A., Patskovsky, Y., Almo, S. C. & Singer, R. H. (2008). Structural basis for the coevolution of a viral RNA-protein complex. *Nat Struct Mol Biol* **15**, 103-105.

Chase, G. P., Rameix-Welti, M. A., Zvirbliene, A., Zvirblis, G., Gotz, V., Wolff, T., Naffakh, N. & Schwemmle, M. (2011). Influenza virus ribonucleoprotein complexes gain preferential access to cellular export machinery through chromatin targeting. *PLoS Pathog* **7**, e1002187.

Chen, B. J., Leser, G. P., Jackson, D. & Lamb, R. A. (2008). The influenza virus M2 protein cytoplasmic tail interacts with the M1 protein and influences virus assembly at the site of virus budding. *J Virol* **82**, 10059-10070.

Chen, B. J., Leser, G. P., Morita, E. & Lamb, R. A. (2007). Influenza virus hemagglutinin and neuraminidase, but not the matrix protein, are required for assembly and budding of plasmid-derived virus-like particles. *J Virol* **81**, 7111-7123.

Chen, J., Lee, K. H., Steinhauer, D. A., Stevens, D. J., Skehel, J. J. & Wiley, D. C. (1998). Structure of the hemagglutinin precursor cleavage site, a determinant of influenza pathogenicity and the origin of the labile conformation. *Cell* **95**, 409-417.

Chen, W., Calvo, P. A., Malide, D., Gibbs, J., Schubert, U., Bacik, I., Basta, S., O'Neill, R., Schickli, J., Palese, P., Henklein, P., Bennink, J. R. & Yewdell, J. W. (2001). A novel influenza A virus mitochondrial protein that induces cell death. *Nat Med* **7**, 1306-1312.

Chen, Z. & Krug, R. M. (2000). Selective nuclear export of viral mRNAs in influenza-virus-infected cells. *Trends in microbiology* **8**, 376-383.

Chenavas, S., Estrozi, L. F., Slama-Schwok, A., Delmas, B., Di Primo, C., Baudin, F., Li, X., Crepin, T. & Ruigrok, R. W. (2013). Monomeric nucleoprotein of influenza A virus. *PLoS Pathog* **9**, e1003275.

Cheng, H., Dufu, K., Lee, C. S., Hsu, J. L., Dias, A. & Reed, R. (2006). Human mRNA export machinery recruited to the 5' end of mRNA. *Cell* **127**, 1389-1400.

Chou, Y. Y., Vafabakhsh, R., Doganay, S., Gao, Q., Ha, T. & Palese, P. (2012). One influenza virus particle packages eight unique viral RNAs as shown by FISH analysis. *Proc Natl Acad Sci U S A* **109**, 9101-9106.

Chua, M. A., Schmid, S., Perez, J. T., Langlois, R. A. & Tenoever, B. R. (2013). Influenza A virus utilizes suboptimal splicing to coordinate the timing of infection. *Cell Rep* **3**, 23-29.

Cianci, C., Tiley, L. & Krystal, M. (1995). Differential activation of the influenza virus polymerase via template RNA binding. *J Virol* **69**, 3995-3999.

Claas, E. C. J., Osterhaus, A. D. M. E., van Beek, R., De Jong, J. C., Rimmelzwaan, G. F., Senne, D. A., Krauss, S., Shortridge, K. F. & Webster, R. G. (1998). Human influenza A H5N1 virus related to a highly pathogenic avian influenza virus. *Lancet* **351**, 472-477.

Cohen, P. (2000). The regulation of protein function by multisite phosphorylation--a 25 year update. *Trends Biochem Sci* **25**, 596-601.

Collura, V. & Boissy, G. (2007). From protein-protein complexes to interactomics. *Sub-cellular biochemistry* **43**, 135-183.

Coloma, R., Valpuesta, J. M., Arranz, R., Carrascosa, J. L., Ortin, J. & Martin-Benito, J. (2009). The structure of a biologically active influenza virus ribonucleoprotein complex. *PLoS Pathog* **5**, e1000491.

Compans, R. W., Content, J. & Duesberg, P. H. (1972). Structure of the ribonucleoprotein of influenza virus. *J Virol* **10**, 795-800.

Connor, R. J., Kawaoka, Y., Webster, R. G. & Paulson, J. C. (1994). Receptor Specificity in Human, Avian, and Equine H2 and H3 Influenza-Virus Isolates. *Virology* **205**, 17-23.

Cook, P. R. (1999). The organization of replication and transcription. *Science* **284**, 1790-1795.

Cook, P. R. (2010). A model for all genomes: the role of transcription factories. *J Mol Biol* **395**, 1-10.

Craig, R. & Beavis, R. C. (2004). TANDEM: matching proteins with tandem mass spectra. *Bioinformatics* **20**, 1466-1467.

Cros, J. F., Garcia-Sastre, A. & Palese, P. (2005). An unconventional NLS is critical for the nuclear import of the influenza A virus nucleoprotein and ribonucleoprotein. *Traffic* **6**, 205-213.

Crow, M., Deng, T., Addley, M. & Brownlee, G. G. (2004). Mutational analysis of the influenza virus cRNA promoter and identification of nucleotides critical for replication. *J Virol* **78**, 6263-6270.

Dai, M., Terzaghi, W. & Wang, H. (2013). Multifaceted roles of Arabidopsis PP6 phosphatase in regulating cellular signaling and plant development. *Plant signaling & behavior* **8**.

Dawood, F. S., Iuliano, A. D., Reed, C., Meltzer, M. I., Shay, D. K., Cheng, P. Y., Bandaranayake, D., Breiman, R. F., Brooks, W. A., Buchy, P., Feikin, D. R., Fowler, K. B., Gordon, A., Hien, N. T., Horby, P., Huang, Q. S., Katz, M. A., Krishnan, A., Lal, R., Montgomery, J. M., Molbak, K., Pebody, R., Presanis, A. M., Razuri, H., Steens, A., Tinoco, Y. O., Wallinga, J., Yu, H., Vong, S., Bresee, J. & Widdowson, M. A. (2012). Estimated global mortality associated with the first 12 months of 2009 pandemic influenza A H1N1 virus circulation: a modelling study. *The Lancet infectious diseases* **12**, 687-695.

de Chassey, B., Meyniel-Schicklin, L., Aublin-Gex, A., Andre, P. & Lotteau, V. (2012). Genetic screens for the control of influenza virus replication: from meta-analysis to drug discovery. *Molecular bioSystems* **8**, 1297-1303.

Deng, T., Engelhardt, O. G., Thomas, B., Akoulitchev, A. V., Brownlee, G. G. & Fodor, E. (2006a). Role of ran binding protein 5 in nuclear import and assembly of the influenza virus RNA polymerase complex. *J Virol* **80**, 11911-11919.

Deng, T., Sharps, J., Fodor, E. & Brownlee, G. G. (2005). In vitro assembly of PB2 with a PB1-PA dimer supports a new model of assembly of influenza A virus polymerase subunits into a functional trimeric complex. *J Virol* **79**, 8669-8674.

Deng, T., Vreede, F. T. & Brownlee, G. G. (2006b). Different de novo initiation strategies are used by influenza virus RNA polymerase on its cRNA and viral RNA promoters during viral RNA replication. *J Virol* **80**, 2337-2348.

Desselberger, U., Racaniello, V. R., Zazra, J. J. & Palese, P. (1980). The 3' and 5'-terminal sequences of influenza A, B and C virus RNA segments are highly conserved and show partial inverted complementarity. *Gene* **8**, 315-328.

Di Pietro, A., Kajaste-Rudnitski, A., Oteiza, A., Nicora, L., Towers, G. J., Mechti, N. & Vicenzi, E. (2013). TRIM22 inhibits influenza A virus infection by targeting the viral nucleoprotein for degradation. *J Virol* **87**, 4523-4533.

Dias, A., Bouvier, D., Crepin, T., McCarthy, A. A., Hart, D. J., Baudin, F., Cusack, S. & Ruigrok, R. W. (2009). The cap-snatching endonuclease of influenza virus polymerase resides in the PA subunit. *Nature* **458**, 914-918.

Digard, P., Blok, V. C. & Inglis, S. C. (1989). Complex formation between influenza virus polymerase proteins expressed in Xenopus oocytes. *Virology* **171**, 162-169.

Douglas, P., Zhong, J., Ye, R., Moorhead, G. B., Xu, X. & Lees-Miller, S. P. (2010). Protein phosphatase 6 interacts with the DNA-dependent protein kinase catalytic subunit and dephosphorylates gamma-H2AX. *Mol Cell Biol* **30**, 1368-1381.

Duesberg, P. H. (1969). Distinct subunits of the ribonucleoprotein of influenza virus. *J Mol Biol* **42**, 485-499.

Eccles, R. (2005). Understanding the symptoms of the common cold and influenza. *The Lancet infectious diseases* **5**, 718-725.

Edinger, T. O., Pohl, M. O. & Stertz, S. (2014). Entry of influenza A virus: host factors and antiviral targets. *J Gen Virol* **95**, 263-277.

Elton, D., Medcalf, L., Bishop, K., Harrison, D. & Digard, P. (1999). Identification of amino acid residues of influenza virus nucleoprotein essential for RNA binding. *J Virol* **73**, 7357-7367.

Elton, D., Simpson-Holley, M., Archer, K., Medcalf, L., Hallam, R., McCauley, J. & Digard, P. (2001). Interaction of the influenza virus nucleoprotein with the cellular CRM1-mediated nuclear export pathway. *J Virol* **75**, 408-419.

Enami, M., Fukuda, R. & Ishihama, A. (1985). Transcription and replication of eight RNA segments of influenza virus. *Virology* **142**, 68-77.

Engelhardt, O. G. & Fodor, E. (2006). Functional association between viral and cellular transcription during influenza virus infection. *Rev Med Virol* **16**, 329-345.

Engelhardt, O. G., Smith, M. & Fodor, E. (2005). Association of the influenza A virus RNA-dependent RNA polymerase with cellular RNA polymerase II. *J Virol* **79**, 5812-5818.

Falcon, A. M., Marion, R. M., Zurcher, T., Gomez, P., Portela, A., Nieto, A. & Ortin, J. (2004). Defective RNA replication and late gene expression in temperature-sensitive influenza viruses expressing deleted forms of the NS1 protein. *J Virol* **78**, 3880-3888.

Fields, S. & Winter, G. (1982). Nucleotide sequences of influenza virus segments 1 and 3 reveal mosaic structure of a small viral RNA segment. *Cell* **28**, 303-313.

Fields, S., Winter, G. & Brownlee, G. G. (1981). Structure of the neuraminidase gene in human influenza virus A/PR/8/34. *Nature* **290**, 213-217.

Finley, D. (2009). Recognition and processing of ubiquitin-protein conjugates by the proteasome. *Annu Rev Biochem* **78**, 477-513.

Fire, A., Xu, S., Montgomery, M. K., Kostas, S. A., Driver, S. E. & Mello, C. C. (1998). Potent and specific genetic interference by double-stranded RNA in Caenorhabditis elegans. *Nature* **391**, 806-811.

Fislova, T., Thomas, B., Graef, K. M. & Fodor, E. (2010). Association of the influenza virus RNA polymerase subunit PB2 with the host chaperonin CCT. *J Virol* **84**, 8691-8699.

Flick, R. & Hobom, G. (1999). Interaction of influenza virus polymerase with viral RNA in the 'corkscrew' conformation. *J Gen Virol* **80 (Pt 10)**, 2565-2572.

Flick, R., Neumann, G., Hoffmann, E., Neumeier, E. & Hobom, G. (1996). Promoter elements in the influenza vRNA terminal structure. *RNA* **2**, 1046-1057.

Fodor, E. (2013). The RNA polymerase of influenza a virus: mechanisms of viral transcription and replication. *Acta Virol* **57**, 113-122.

Fodor, E., Crow, M., Mingay, L. J., Deng, T., Sharps, J., Fechter, P. & Brownlee, G. G. (2002). A single amino acid mutation in the PA subunit of the influenza virus RNA polymerase inhibits endonucleolytic cleavage of capped RNAs. *J Virol* **76**, 8989-9001.

Fodor, E., Devenish, L., Engelhardt, O. G., Palese, P., Brownlee, G. G. & Garcia-Sastre, A. (1999). Rescue of influenza A virus from recombinant DNA. *J Virol* **73**, 9679-9682.

Fodor, E., Pritlove, D. C. & Brownlee, G. G. (1994). The influenza virus panhandle is involved in the initiation of transcription. *J Virol* **68**, 4092-4096.

Fodor, E., Pritlove, D. C. & Brownlee, G. G. (1995). Characterization of the RNA-fork model of virion RNA in the initiation of transcription in influenza A virus. *J Virol* **69**, 4012-4019.

Fodor, E. & Smith, M. (2004). The PA subunit is required for efficient nuclear accumulation of the PB1 subunit of the influenza A virus RNA polymerase complex. *J Virol* **78**, 9144-9153.

Fournier, E., Moules, V., Essere, B., Paillart, J. C., Sirbat, J. D., Cavalier, A., Rolland, J. P., Thomas, D., Lina, B., Isel, C. & Marquet, R. (2012a). Interaction network linking the human H3N2 influenza A virus genomic RNA segments. *Vaccine* **30**, 7359-7367.

Fournier, E., Moules, V., Essere, B., Paillart, J. C., Sirbat, J. D., Isel, C., Cavalier, A., Rolland, J. P., Thomas, D., Lina, B. & Marquet, R. (2012b). A supramolecular assembly formed by influenza A virus genomic RNA segments. *Nucleic Acids Res* **40**, 2197-2209.

Gabriel, G., Klingel, K., Otte, A., Thiele, S., Hudjetz, B., Arman-Kalcek, G., Sauter, M., Shmidt, T., Rother, F., Baumgarte, S., Keiner, B., Hartmann, E., Bader, M., Brownlee, G. G., Fodor, E. & Klenk, H. D. (2011). Differential use of importin-alpha isoforms governs cell tropism and host adaptation of influenza virus. *Nature communications* **2**, 156.

Garaigorta, U. & Ortin, J. (2007). Mutation analysis of a recombinant NS replicon shows that influenza virus NS1 protein blocks the splicing and nucleo-cytoplasmic transport of its own viral mRNA. *Nucleic Acids Res* **35**, 4573-4582.

Garcia-Sastre, A., Egorov, A., Matassov, D., Brandt, S., Levy, D. E., Durbin, J. E., Palese, P. & Muster, T. (1998). Influenza A virus lacking the NS1 gene replicates in interferon-deficient systems. *Virology* **252**, 324-330.

Garten, R. J., Davis, C. T., Russell, C. A., Shu, B., Lindstrom, S., Balish, A., Sessions, W. M., Xu, X., Skepner, E., Deyde, V., Okomo-Adhiambo, M., Gubareva, L., Barnes, J., Smith, C. B., Emery, S. L., Hillman, M. J., Rivailler, P., Smagala, J., de Graaf, M., Burke, D. F., Fouchier, R. A., Pappas, C., Alpuche-Aranda, C. M., Lopez-Gatell, H., Olivera, H., Lopez, I., Myers, C. A., Faix, D., Blair, P. J., Yu, C., Keene, K. M., Dotson, P. D., Jr., Boxrud, D., Sambol, A. R., Abid, S. H., St George, K., Bannerman, T., Moore, A. L., Stringer, D. J., Blevins, P., Demmler-Harrison, G. J., Ginsberg, M., Kriner, P., Waterman, S., Smole, S., Guevara, H. F., Belongia, E. A., Clark, P. A., Beatrice, S. T., Donis, R., Katz, J., Finelli, L., Bridges, C. B., Shaw, M., Jernigan, D. B., Uyeki, T. M., Smith, D. J., Klimov, A. I. & Cox, N. J. (2009). Antigenic and genetic characteristics of swine-origin 2009 A(H1N1) influenza viruses circulating in humans. *Science* **325**, 197-201.

Gastaminza, P., Perales, B., Falcon, A. M. & Ortin, J. (2003). Mutations in the N-terminal region of influenza virus PB2 protein affect virus RNA replication but not transcription. *J Virol* **77**, 5098-5108.

Gavazzi, C., Yver, M., Isel, C., Smyth, R. P., Rosa-Calatrava, M., Lina, B., Moules, V. & Marquet, R. (2013). A functional sequence-specific interaction between influenza A virus genomic RNA segments. *Proc Natl Acad Sci U S A* **110**, 16604-16609.

Geer, L. Y., Markey, S. P., Kowalak, J. A., Wagner, L., Xu, M., Maynard, D. M., Yang, X., Shi, W. & Bryant, S. H. (2004). Open mass spectrometry search algorithm. *J Proteome Res* **3**, 958-964.

Geller, R., Taguwa, S. & Frydman, J. (2012). Broad action of Hsp90 as a host chaperone required for viral replication. *Biochim Biophys Acta* **1823**, 698-706.

Gerber, M., Isel, C., Moules, V. & Marquet, R. (2014). Selective packaging of the influenza A genome and consequences for genetic reassortment. *Trends in microbiology*.

Gonzalez, S. & Ortin, J. (1999a). Characterization of influenza virus PB1 protein binding to viral RNA: two separate regions of the protein contribute to the interaction domain. *J Virol* **73**, 631-637.

Gonzalez, S. & Ortin, J. (1999b). Distinct regions of influenza virus PB1 polymerase subunit recognize vRNA and cRNA templates. *EMBO J* **18**, 3767-3775.

Gonzalez, S., Zurcher, T. & Ortin, J. (1996). Identification of two separate domains in the influenza virus PB1 protein involved in the interaction with the PB2 and PA subunits: a model for the viral RNA polymerase structure. *Nucleic Acids Res* **24**, 4456-4463.

Graef, K. M., Vreede, F. T., Lau, Y. F., McCall, A. W., Carr, S. M., Subbarao, K. & Fodor, E. (2010). The PB2 subunit of the influenza virus RNA polymerase affects virulence by interacting with the mitochondrial antiviral signaling protein and inhibiting expression of beta interferon. *J Virol* **84**, 8433-8445.

Gregoriades, A., Christie, T. & Markarian, K. (1984). The membrane (M1) protein of influenza virus occurs in two forms and is a phosphoprotein. *J Virol* **49**, 229-235.

Gregoriades, A., Guzman, G. G. & Paoletti, E. (1990). The phosphorylation of the integral membrane (M1) protein of influenza virus. *Virus Res* **16**, 27-41.

Guilligay, D., Tarendeau, F., Resa-Infante, P., Coloma, R., Crepin, T., Sehr, P., Lewis, J., Ruigrok, R. W., Ortin, J., Hart, D. J. & Cusack, S. (2008). The structural basis for cap binding by influenza virus polymerase subunit PB2. *Nat Struct Mol Biol* **15**, 500-506.

Haidari, M., Zhang, W., Ganjehei, L., Ali, M. & Chen, Z. (2011). Inhibition of MLC phosphorylation restricts replication of influenza virus--a mechanism of action for anti-influenza agents. *PLoS One* **6**, e21444.

Hale, B. G., Knebel, A., Botting, C. H., Galloway, C. S., Precious, B. L., Jackson, D., Elliott, R. M. & Randall, R. E. (2009). CDK/ERK-mediated phosphorylation of the human influenza A virus NS1 protein at threonine-215. *Virology* **383**, 6-11.

Hale, B. G., Randall, R. E., Ortin, J. & Jackson, D. (2008). The multifunctional NS1 protein of influenza A viruses. *J Gen Virol* **89**, 2359-2376.

Hamilton, B. S., Whittaker, G. R. & Daniel, S. (2012). Influenza virus-mediated membrane fusion: determinants of hemagglutinin fusogenic activity and experimental approaches for assessing virus fusion. *Viruses* **4**, 1144-1168.

Hammond, D., Zeng, K., Espert, A., Bastos, R. N., Baron, R. D., Gruneberg, U. & Barr, F. A. (2013). Melanoma-associated mutations in protein phosphatase 6 cause chromosome instability and DNA damage owing to dysregulated Aurora-A. *J Cell Sci* **126**, 3429-3440.

Hao, L., Sakurai, A., Watanabe, T., Sorensen, E., Nidom, C. A., Newton, M. A., Ahlquist, P. & Kawaoka, Y. (2008). Drosophila RNAi screen identifies host genes important for influenza virus replication. *Nature* **454**, 890-893.

Harris, A., Cardone, G., Winkler, D. C., Heymann, J. B., Brecher, M., White, J. M. & Steven, A. C. (2006). Influenza virus pleiomorphy characterized by cryoelectron tomography. *Proc Natl Acad Sci U S A* **103**, 19123-19127.

Hatada, E., Hasegawa, M., Mukaigawa, J., Shimizu, K. & Fukuda, R. (1989). Control of influenza virus gene expression: quantitative analysis of each viral RNA species in infected cells. *Journal of biochemistry* **105**, 537-546.

Hay, A. J., Lomniczi, B., Bellamy, A. R. & Skehel, J. J. (1977). Transcription of the influenza virus genome. *Virology* **83**, 337-355.

Hay, A. J., Skehel, J. J. & McCauley, J. (1982). Characterization of influenza virus RNA complete transcripts. *Virology* **116**, 517-522.

He, X., Zhou, J., Bartlam, M., Zhang, R., Ma, J., Lou, Z., Li, X., Li, J., Joachimiak, A., Zeng, Z., Ge, R., Rao, Z. & Liu, Y. (2008). Crystal structure of the polymerase PA(C)-PB1(N) complex from an avian influenza H5N1 virus. *Nature* **454**, 1123-1126.

Heggeness, M. H., Smith, P. R., Ulmanen, I., Krug, R. M. & Choppin, P. W. (1982). Studies on the helical nucleocapsid of influenza virus. *Virology* **118**, 466-470.

Hemerka, J. N., Wang, D., Weng, Y., Lu, W., Kaushik, R. S., Jin, J., Harmon, A. F. & Li, F. (2009). Detection and characterization of influenza A virus PA-PB2 interaction through a bimolecular fluorescence complementation assay. *J Virol* **83**, 3944-3955.

Herfst, S., Schrauwen, E. J. A., Linster, M., Chutinimitkul, S., de Wit, E., Munster, V. J., Sorrell, E. M., Bestebroer, T. M., Burke, D. F., Smith, D. J., Rimmelzwaan, G. F., Osterhaus, A. D. M. E. & Fouchier, R. A. M. (2012). Airborne Transmission of Influenza A/H5N1 Virus Between Ferrets. *Science* **336**, 1534-1541.

Herz, C., Stavnezer, E., Krug, R. & Gurney, T., Jr. (1981). Influenza virus, an RNA virus, synthesizes its messenger RNA in the nucleus of infected cells. *Cell* **26**, 391-400.

Hirayama, E., Atagi, H., Hiraki, A. & Kim, J. (2004). Heat shock protein 70 is related to thermal inhibition of nuclear export of the influenza virus ribonucleoprotein complex. *J Virol* **78**, 1263-1270.

Hoeller, D., Crosetto, N., Blagoev, B., Raiborg, C., Tikkanen, R., Wagner, S., Kowanetz, K., Breitling, R., Mann, M., Stenmark, H. & Dikic, I. (2006). Regulation of ubiquitin-binding proteins by monoubiquitination. *Nat Cell Biol* **8**, 163-169.

Hofmann, P., Sprenger, H., Kaufmann, A., Bender, A., Hasse, C., Nain, M. & Gemsa, D. (1997). Susceptibility of mononuclear phagocytes to influenza A

virus infection and possible role in the antiviral response. *J Leukocyte Biol* **61**, 408-414.

Hogg, J. R. & Collins, K. (2007). RNA-based affinity purification reveals 7SK RNPs with distinct composition and regulation. *RNA* **13**, 868-880.

Holmes, E. C. (2013). Virus Evolution. In *Fields Virology*, 6th edn, pp. 286-313. Edited by D. M. Knipe & P. M. Howley. Philadelphia: Lippincott Williams and Wilkins.

Holsinger, L. J., Shaughnessy, M. A., Micko, A., Pinto, L. H. & Lamb, R. A. (1995). Analysis of the posttranslational modifications of the influenza virus M2 protein. *J Virol* **69**, 1219-1225.

Honda, A., Endo, A., Mizumoto, K. & Ishihama, A. (2001). Differential roles of viral RNA and cRNA in functional modulation of the influenza virus RNA polymerase. *J Biol Chem* **276**, 31179-31185.

Honda, A., Mizumoto, K. & Ishihama, A. (1998). Identification of the 5' terminal structure of influenza virus genome RNA by a newly developed enzymatic method. *Virus Res* **55**, 199-206.

Hosing, A. S., Valerie, N. C., Dziegielewski, J., Brautigan, D. L. & Larner, J. M. (2012). PP6 regulatory subunit R1 is bidentate anchor for targeting protein phosphatase-6 to DNA-dependent protein kinase. *J Biol Chem* **287**, 9230-9239.

Hossain, M. J., Hickman, D. & Perez, D. R. (2008). Evidence of expanded host range and mammalian-associated genetic changes in a duck H9N2 influenza virus following adaptation in quail and chickens. *PLoS One* **3**, e3170.

Hsiang, T. Y., Zhou, L. & Krug, R. M. (2012). Roles of the phosphorylation of specific serines and threonines in the NS1 protein of human influenza A viruses. *J Virol* **86**, 10370-10376.

Hsu, M. T., Parvin, J. D., Gupta, S., Krystal, M. & Palese, P. (1987). Genomic RNAs of influenza viruses are held in a circular conformation in virions and in infected cells by a terminal panhandle. *Proc Natl Acad Sci U S A* **84**, 8140-8144.

Huang, I. C., Li, W., Sui, J., Marasco, W., Choe, H. & Farzan, M. (2008). Influenza A virus neuraminidase limits viral superinfection. *J Virol* **82**, 4834-4843.

Huang, T. S., Palese, P. & Krystal, M. (1990). Determination of influenza virus proteins required for genome replication. *J Virol* **64**, 5669-5673.

Huang, X., Liu, T., Muller, J., Levandowski, R. A. & Ye, Z. (2001). Effect of influenza virus matrix protein and viral RNA on ribonucleoprotein formation and nuclear export. *Virology* **287**, 405-416.

Hudjetz, B. & Gabriel, G. (2012). Human-like PB2 627K influenza virus polymerase activity is regulated by importin-alpha1 and -alpha7. *PLoS Pathog* **8**, e1002488.

Hui, E. K. W. & Nayak, D. P. (2002). Role of G protein and protein kinase signalling in influenza virus budding in MDCK cells. *Journal of General Virology* **83**, 3055-3066.

Hutchinson, E. C., Denham, E. M., Thomas, B., Trudgian, D. C., Hester, S. S., Ridlova, G., York, A., Turrell, L. & Fodor, E. (2012). Mapping the phosphoproteome of influenza A and B viruses by mass spectrometry. *PLoS Pathog* **8**, e1002993.

Hutchinson, E. C. & Fodor, E. (2012). Nuclear import of the influenza A virus transcriptional machinery. *Vaccine* **30**, 7353-7358.

Hutchinson, E. C., Orr, O. E., Man Liu, S., Engelhardt, O. G. & Fodor, E. (2011). Characterization of the interaction between the influenza A virus polymerase subunit PB1 and the host nuclear import factor Ran-binding protein 5. *J Gen Virol* **92**, 1859-1869.

Hutchinson, E. C., von Kirchbach, J. C., Gog, J. R. & Digard, P. (2010). Genome packaging in influenza A virus. *J Gen Virol* **91**, 313-328.

Imai, M., Watanabe, T., Hatta, M., Das, S. C., Ozawa, M., Shinya, K., Zhong, G. X., Hanson, A., Katsura, H., Watanabe, S., Li, C. J., Kawakami, E., Yamada, S., Kiso, M., Suzuki, Y., Maher, E. A., Neumann, G. & Kawaoka, Y. (2012). Experimental adaptation of an influenza H5 HA confers respiratory droplet transmission to a reassortant H5 HA/H1N1 virus in ferrets. *Nature* **486**, 420-+.

Ito, T., Couceiro, J. N. S. S., Kelm, S., Baum, L. G., Krauss, S., Castrucci, M. R., Donatelli, I., Kida, H., Paulson, J. C., Webster, R. G. & Kawaoka, Y. (1998). Molecular basis for the generation in pigs of influenza A viruses with pandemic potential. *Journal of Virology* **72**, 7367-7373.

Iwai, A., Shiozaki, T., Kawai, T., Akira, S., Kawaoka, Y., Takada, A., Kida, H. & Miyazaki, T. (2010). Influenza A virus polymerase inhibits type I interferon induction by binding to interferon beta promoter stimulator 1. *J Biol Chem* **285**, 32064-32074.

Jackson, D. A., Caton, A. J., McCready, S. J. & Cook, P. R. (1982). Influenza virus RNA is synthesized at fixed sites in the nucleus. *Nature* **296**, 366-368.

Jacobo-Molina, A., Ding, J., Nanni, R. G., Clark, A. D., Jr., Lu, X., Tantillo, C., Williams, R. L., Kamer, G., Ferris, A. L., Clark, P. & et al. (1993). Crystal structure of human immunodeficiency virus type 1 reverse transcriptase complexed with double-stranded DNA at 3.0 A resolution shows bent DNA. *Proc Natl Acad Sci U S A* **90**, 6320-6324.

Jensen, L. J., Kuhn, M., Stark, M., Chaffron, S., Creevey, C., Muller, J., Doerks, T., Julien, P., Roth, A., Simonovic, M., Bork, P. & von Mering, C. (2009). STRING 8--a global view on proteins and their functional interactions in 630 organisms. *Nucleic Acids Res* **37**, D412-416.

Jo, S., Kawaguchi, A., Takizawa, N., Morikawa, Y., Momose, F. & Nagata, K. (2010). Involvement of vesicular trafficking system in membrane targeting of the progeny influenza virus genome. *Microbes and infection / Institut Pasteur* **12**, 1079-1084.

Jorba, N., Area, E. & Ortin, J. (2008a). Oligomerization of the influenza virus polymerase complex in vivo. *J Gen Virol* **89**, 520-524.

Jorba, N., Coloma, R. & Ortin, J. (2009). Genetic trans-complementation establishes a new model for influenza virus RNA transcription and replication. *PLoS Pathog* **5**, e1000462.

Jorba, N., Juarez, S., Torreira, E., Gastaminza, P., Zamarreno, N., Albar, J. P. & Ortin, J. (2008b). Analysis of the interaction of influenza virus polymerase complex with human cell factors. *Proteomics* **8**, 2077-2088.

Jung, T. E. & Brownlee, G. G. (2006). A new promoter-binding site in the PB1 subunit of the influenza A virus polymerase. *J Gen Virol* **87**, 679-688.

Kajino, T., Ren, H., Iemura, S., Natsume, T., Stefansson, B., Brautigan, D. L., Matsumoto, K. & Ninomiya-Tsuji, J. (2006). Protein phosphatase 6 down-regulates TAK1 kinase activation in the IL-1 signaling pathway. *J Biol Chem* **281**, 39891-39896.

Kamoun, M., Filali, M., Murray, M. V., Awasthi, S. & Wadzinski, B. E. (2013). Protein phosphatase 2A family members (PP2A and PP6) associate with U1 snRNP and the spliceosome during pre-mRNA splicing. *Biochemical and biophysical research communications* **440**, 306-311.

Karlas, A., Machuy, N., Shin, Y., Pleissner, K. P., Artarini, A., Heuer, D., Becker, D., Khalil, H., Ogilvie, L. A., Hess, S., Maurer, A. P., Muller, E., Wolff, T., Rudel, T. & Meyer, T. F. (2010). Genome-wide RNAi screen identifies human host factors crucial for influenza virus replication. *Nature* **463**, 818-822.

Katahira, J. (2012). mRNA export and the TREX complex. *Biochim Biophys Acta* **1819**, 507-513.

Kawaguchi, A. & Nagata, K. (2007). De novo replication of the influenza virus RNA genome is regulated by DNA replicative helicase, MCM. *EMBO J* **26**, 4566-4575.

Kawakami, E., Watanabe, T., Fujii, K., Goto, H., Watanabe, S., Noda, T. & Kawaoka, Y. (2011). Strand-specific real-time RT-PCR for distinguishing influenza vRNA, cRNA, and mRNA. *Journal of virological methods* **173**, 1-6.

Keller, A., Nesvizhskii, A. I., Kolker, E. & Aebersold, R. (2002). Empirical statistical model to estimate the accuracy of peptide identifications made by MS/MS and database search. *Analytical chemistry* **74**, 5383-5392.

Kelly, S. M. & Corbett, A. H. (2009). Messenger RNA export from the nucleus: a series of molecular wardrobe changes. *Traffic* **10**, 1199-1208.

Kerscher, O., Felberbaum, R. & Hochstrasser, M. (2006). Modification of proteins by ubiquitin and ubiquitin-like proteins. *Annual review of cell and developmental biology* **22**, 159-180.

Kim, H. J., Fodor, E., Brownlee, G. G. & Seong, B. L. (1997). Mutational analysis of the RNA-fork model of the influenza A virus vRNA promoter in vivo. *J Gen Virol* **78 (Pt 2)**, 353-357.

Kistner, O., Muller, H., Becht, H. & Scholtissek, C. (1985). Phosphopeptide fingerprints of nucleoproteins of various influenza A virus strains grown in different host cells. *J Gen Virol* **66 (Pt 3)**, 465-472.

Kistner, O., Muller, K. & Scholtissek, C. (1989). Differential phosphorylation of the nucleoprotein of influenza A viruses. *J Gen Virol* **70 (Pt 9)**, 2421-2431.

Kohler, A. & Hurt, E. (2007). Exporting RNA from the nucleus to the cytoplasm. *Nat Rev Mol Cell Biol* **8**, 761-773.

Kohlstaedt, L. A., Wang, J., Friedman, J. M., Rice, P. A. & Steitz, T. A. (1992). Crystal structure at 3.5 A resolution of HIV-1 reverse transcriptase complexed with an inhibitor. *Science* **256**, 1783-1790.

Konig, R., Stertz, S., Zhou, Y., Inoue, A., Hoffmann, H. H., Bhattacharyya, S., Alamares, J. G., Tscherne, D. M., Ortigoza, M. B., Liang, Y., Gao, Q., Andrews, S. E., Bandyopadhyay, S., De Jesus, P., Tu, B. P., Pache, L., Shih, C., Orth, A., Bonamy, G., Miraglia, L., Ideker, T., Garcia-Sastre, A., Young, J. A., Palese, P., Shaw, M. L. & Chanda, S. K. (2010). Human host factors required for influenza virus replication. *Nature* **463**, 813-817.

Krug, R. M. & Fodor, E. (2013). The virus genome and its replication. In *Textbook of Influenza 2nd Edition*, pp. 57-66. Edited by R. G. Webster, A. S. Monto, T. J. Braciale & R. A. Lamb. New York City: John Wiley & Sons, Ltd.

Krug, R. M., Ueda, M. & Palese, P. (1975). Temperature-sensitive mutants of influenza WSN virus defective in virus-specific RNA synthesis. *J Virol* **16**, 790-796.

Kumar, N., Liang, Y. H., Parslow, T. G. & Liang, Y. Y. (2011). Receptor Tyrosine Kinase Inhibitors Block Multiple Steps of Influenza A Virus Replication. *Journal of Virology* **85**, 2818-2827.

Kuo, R. L. & Krug, R. M. (2009). Influenza a virus polymerase is an integral component of the CPSF30-NS1A protein complex in infected cells. *J Virol* **83**, 1611-1616.

Kurokawa, M., Ochiai, H., Nakajima, K. & Niwayama, S. (1990). Inhibitory Effect of Protein-Kinase-C Inhibitor on the Replication of Influenza Type-a Virus. *Journal of General Virology* **71**, 2149-2155.

Lakdawala, S. S., Wu, Y., Wawrzusin, P., Kabat, J., Broadbent, A. J., Lamirande, E. W., Fodor, E., Altan-Bonnet, N., Shroff, H. & Subbarao, K. (2014). Influenza a virus assembly intermediates fuse in the cytoplasm. *PLoS Pathog* **10**, e1003971.

Lamb, R. A. & Choppin, P. W. (1981). Identification of a second protein (M2) encoded by RNA segment 7 of influenza virus. *Virology* **112**, 729-737.

Lamb, R. A., Choppin, P. W., Chanock, R. M. & Lai, C. J. (1980). Mapping of the two overlapping genes for polypeptides NS1 and NS2 on RNA segment 8 of influenza virus genome. *Proc Natl Acad Sci U S A* **77**, 1857-1861.

Lamb, R. A. & Horvath, C. M. (1991). Diversity of coding strategies in influenza viruses. *Trends Genet* **7**, 261-266.

Lamb, R. A. & Lai, C. J. (1980). Sequence of interrupted and uninterrupted mRNAs and cloned DNA coding for the two overlapping nonstructural proteins of influenza virus. *Cell* **21**, 475-485.

Lamb, R. A., Lai, C. J. & Choppin, P. W. (1981). Sequences of mRNAs derived from genome RNA segment 7 of influenza virus: colinear and interrupted mRNAs code for overlapping proteins. *Proc Natl Acad Sci U S A* **78**, 4170-4174.

Leahy, M. B., Dobbyn, H. C. & Brownlee, G. G. (2001a). Hairpin loop structure in the 3' arm of the influenza A virus virion RNA promoter is required for endonuclease activity. *J Virol* **75**, 7042-7049.

Leahy, M. B., Pritlove, D. C., Poon, L. L. & Brownlee, G. G. (2001b). Mutagenic analysis of the 5' arm of the influenza A virus virion RNA promoter defines the sequence requirements for endonuclease activity. *J Virol* **75**, 134-142.

Lee, K. H. & Seong, B. L. (1998). The position 4 nucleotide at the 3' end of the influenza virus neuraminidase vRNA is involved in temporal regulation of transcription and replication of neuraminidase RNAs and affects the repertoire of influenza virus surface antigens. *J Gen Virol* **79 (Pt 8)**, 1923-1934.

Lee, M. K., Bae, S. H., Park, C. J., Cheong, H. K., Cheong, C. & Choi, B. S. (2003). A single-nucleotide natural variation (U4 to C4) in an influenza A virus promoter exhibits a large structural change: implications for differential viral RNA synthesis by RNA-dependent RNA polymerase. *Nucleic Acids Res* **31**, 1216-1223.

Lee, M. T., Bishop, K., Medcalf, L., Elton, D., Digard, P. & Tiley, L. (2002). Definition of the minimal viral components required for the initiation of unprimed RNA synthesis by influenza virus RNA polymerase. *Nucleic Acids Res* **30**, 429-438.

Leser, G. P. & Lamb, R. A. (2005). Influenza virus assembly and budding in raft-derived microdomains: a quantitative analysis of the surface distribution of HA, NA and M2 proteins. *Virology* **342**, 215-227.

Li, G., Zhang, J., Tong, X., Liu, W. & Ye, X. (2011). Heat shock protein 70 inhibits the activity of Influenza A virus ribonucleoprotein and blocks the replication of virus in vitro and in vivo. *PLoS One* **6**, e16546.

Li, M. L., Ramirez, B. C. & Krug, R. M. (1998). RNA-dependent activation of primer RNA production by influenza virus polymerase: different regions of the same protein subunit constitute the two required RNA-binding sites. *EMBO J* **17**, 5844-5852.

Li, M. L., Rao, P. & Krug, R. M. (2001). The active sites of the influenza cap-dependent endonuclease are on different polymerase subunits. *EMBO J* **20**, 2078-2086.

Li, Y., Lu, X., Li, J., Berube, N., Giest, K. L., Liu, Q., Anderson, D. H. & Zhou, Y. (2010). Genetically engineered, biarsenically labeled influenza virus allows visualization of viral NS1 protein in living cells. *J Virol* **84**, 7204-7213.

Liao, T. L., Wu, C. Y., Su, W. C., Jeng, K. S. & Lai, M. M. (2010). Ubiquitination and deubiquitination of NP protein regulates influenza A virus RNA replication. *EMBO J* **29**, 3879-3890.

Lim, F., Downey, T. P. & Peabody, D. S. (2001). Translational repression and specific RNA binding by the coat protein of the Pseudomonas phage PP7. *J Biol Chem* **276**, 22507-22513.

Lim, F. & Peabody, D. S. (2002). RNA recognition site of PP7 coat protein. *Nucleic Acids Res* **30**, 4138-4144.

Lingner, J. & Cech, T. R. (1996). Purification of telomerase from Euplotes aediculatus: requirement of a primer 3' overhang. *Proc Natl Acad Sci U S A* **93**, 10712-10717.

Liu, X., Zhao, Z., Xu, C., Sun, L., Chen, J., Zhang, L. & Liu, W. (2012). Cyclophilin A restricts influenza A virus replication through degradation of the M1 protein. *PLoS One* **7**, e31063.

Lopes, C. T., Franz, M., Kazi, F., Donaldson, S. L., Morris, Q. & Bader, G. D. (2010). Cytoscape Web: an interactive web-based network browser. *Bioinformatics* **26**, 2347-2348.

Luo, G., Chung, J. & Palese, P. (1993). Alterations of the stalk of the influenza virus neuraminidase: deletions and insertions. *Virus Res* **29**, 141-153.

Lyle, J. M., Bullitt, E., Bienz, K. & Kirkegaard, K. (2002). Visualization and functional analysis of RNA-dependent RNA polymerase lattices. *Science* **296**, 2218-2222.

Mahmoudian, S., Auerochs, S., Grone, M. & Marschall, M. (2009). Influenza A virus proteins PB1 and NS1 are subject to functionally important phosphorylation by protein kinase C. *J Gen Virol* **90**, 1392-1397.

Manz, B., Brunotte, L., Reuther, P. & Schwemmle, M. (2012). Adaptive mutations in NEP compensate for defective H5N1 RNA replication in cultured human cells. *Nature communications* **3**, 802.

Manz, B., Schwemmle, M. & Brunotte, L. (2013). Adaptation of avian influenza A virus polymerase in mammals to overcome the host species barrier. *J Virol* **87**, 7200-7209.

Manzoor, R., Kuroda, K., Yoshida, R., Tsuda, Y., Fujikura, D., Miyamoto, H., Kajihara, M., Kida, H. & Takada, A. (2014). Heat shock protein 70 modulates influenza A virus polymerase activity. *J Biol Chem* **289**, 7599-7614.

Marion, R. M., Zurcher, T., de la Luna, S. & Ortin, J. (1997). Influenza virus NS1 protein interacts with viral transcription-replication complexes in vivo. *J Gen Virol* **78 (Pt 10)**, 2447-2451.

Martin-Benito, J., Area, E., Ortega, J., Llorca, O., Valpuesta, J. M., Carrascosa, J. L. & Ortin, J. (2001). Three-dimensional reconstruction of a recombinant influenza virus ribonucleoprotein particle. *EMBO reports* **2**, 313-317.

Martin, K. & Helenius, A. (1991a). Nuclear transport of influenza virus ribonucleoproteins: the viral matrix protein (M1) promotes export and inhibits import. *Cell* **67**, 117-130.

Martin, K. & Helenius, A. (1991b). Transport of Incoming Influenza-Virus Nucleocapsids into the Nucleus. *Journal of Virology* **65**, 232-244.

Matera, A. G. & Wang, Z. (2014). A day in the life of the spliceosome. *Nat Rev Mol Cell Biol* **15**, 108-121.

Matsuoka, Y., Matsumae, H., Katoh, M., Eisfeld, A. J., Neumann, G., Hase, T., Ghosh, S., Shoemaker, J. E., Lopes, T. J., Watanabe, T., Watanabe, S., Fukuyama, S., Kitano, H. & Kawaoka, Y. (2013). A comprehensive map of the influenza A virus replication cycle. *BMC systems biology* **7**, 97.

Mayer, D., Molawi, K., Martinez-Sobrido, L., Ghanem, A., Thomas, S., Baginsky, S., Grossmann, J., Garcia-Sastre, A. & Schwemmle, M. (2007). Identification of cellular interaction partners of the influenza virus ribonucleoprotein complex and polymerase complex using proteomic-based approaches. *J Proteome Res* **6**, 672-682.

McCown, M. F. & Pekosz, A. (2006). Distinct domains of the influenza a virus M2 protein cytoplasmic tail mediate binding to the M1 protein and facilitate infectious virus production. *J Virol* **80**, 8178-8189.

McKeague, M. & Derosa, M. C. (2012). Challenges and opportunities for small molecule aptamer development. *Journal of nucleic acids* **2012**, 748913.

Medcalf, L., Poole, E., Elton, D. & Digard, P. (1999). Temperature-sensitive lesions in two influenza A viruses defective for replicative transcription disrupt RNA binding by the nucleoprotein. *J Virol* **73**, 7349-7356.

Mehle, A. & Doudna, J. A. (2008). An inhibitory activity in human cells restricts the function of an avian-like influenza virus polymerase. *Cell Host Microbe* **4**, 111-122.

Mehle, A. & Doudna, J. A. (2010). A host of factors regulating influenza virus replication. *Viruses* **2**, 566-573.

Mena, I., Jambrina, E., Albo, C., Perales, B., Ortin, J., Arrese, M., Vallejo, D. & Portela, A. (1999). Mutational analysis of influenza A virus nucleoprotein: Identification of mutations that affect RNA replication. *Journal of Virology* **73**, 1186-1194.

Mercer, J., Schelhaas, M. & Helenius, A. (2010). Virus Entry by Endocytosis. *Annual Review of Biochemistry, Vol 79* **79**, 803-833.

Mi, H., Muruganujan, A. & Thomas, P. D. (2013). PANTHER in 2013: modeling the evolution of gene function, and other gene attributes, in the context of phylogenetic trees. *Nucleic Acids Res* **41**, D377-386.

Min, J. Y., Li, S., Sen, G. C. & Krug, R. M. (2007). A site on the influenza A virus NS1 protein mediates both inhibition of PKR activation and temporal regulation of viral RNA synthesis. *Virology* **363**, 236-243.

Mitzner, D., Dudek, S. E., Studtrucker, N., Anhlan, D., Mazur, I., Wissing, J., Jansch, L., Wixler, L., Bruns, K., Sharma, A., Wray, V., Henklein, P., Ludwig, S. & Schubert, U. (2009). Phosphorylation of the influenza A virus

protein PB1-F2 by PKC is crucial for apoptosis promoting functions in monocytes. *Cellular microbiology* **11**, 1502-1516.

Moeller, A., Kirchdoerfer, R. N., Potter, C. S., Carragher, B. & Wilson, I. A. (2012). Organization of the influenza virus replication machinery. *Science* **338**, 1631-1634.

Momose, F., Basler, C. F., O'Neill, R. E., Iwamatsu, A., Palese, P. & Nagata, K. (2001). Cellular splicing factor RAF-2p48/NPI-5/BAT1/UAP56 interacts with the influenza virus nucleoprotein and enhances viral RNA synthesis. *J Virol* **75**, 1899-1908.

Momose, F., Naito, T., Yano, K., Sugimoto, S., Morikawa, Y. & Nagata, K. (2002). Identification of Hsp90 as a stimulatory host factor involved in influenza virus RNA synthesis. *J Biol Chem* **277**, 45306-45314.

Momose, F., Sekimoto, T., Ohkura, T., Jo, S., Kawaguchi, A., Nagata, K. & Morikawa, Y. (2011). Apical transport of influenza A virus ribonucleoprotein requires Rab11-positive recycling endosome. *PLoS One* **6**, e21123.

Moncorge, O., Mura, M. & Barclay, W. S. (2010). Evidence for avian and human host cell factors that affect the activity of influenza virus polymerase. *J Virol* **84**, 9978-9986.

Moore, M. J. & Proudfoot, N. J. (2009). Pre-mRNA processing reaches back to transcription and ahead to translation. *Cell* **136**, 688-700.

Morens, D. M. & Taubenberger, J. K. (2011). Pandemic influenza: certain uncertainties. *Rev Med Virol*.

Morin, B., Kranzusch, P. J., Rahmeh, A. A. & Whelan, S. P. (2013). The polymerase of negative-stranded RNA viruses. *Curr Opin Virol* **3**, 103-110.

Mosley, V. M. & Wyckoff, R. W. (1946). Election micrography of the virus of influenza. *Nature* **157**, 263.

Mukaigawa, J. & Nayak, D. P. (1991). Two signals mediate nuclear localization of influenza virus (A/WSN/33) polymerase basic protein 2. *J Virol* **65**, 245-253.

Muller, K. H., Kakkola, L., Nagaraj, A. S., Cheltsov, A. V., Anastasina, M. & Kainov, D. E. (2012). Emerging cellular targets for influenza antiviral agents. *Trends in pharmacological sciences* **33**, 89-99.

Mullin, A. E., Dalton, R. M., Amorim, M. J., Elton, D. & Digard, P. (2004). Increased amounts of the influenza virus nucleoprotein do not promote higher levels of viral genome replication. *J Gen Virol* **85**, 3689-3698.

Munier, S., Larcher, T., Cormier-Aline, F., Soubieux, D., Su, B., Guigand, L., Labrosse, B., Cherel, Y., Quere, P., Marc, D. & Naffakh, N. (2010). A

genetically engineered waterfowl influenza virus with a deletion in the stalk of the neuraminidase has increased virulence for chickens. *J Virol* **84**, 940-952.

Munier, S., Rolland, T., Diot, C., Jacob, Y. & Naffakh, N. (2013). Exploration of binary virus-host interactions using an infectious protein complementation assay. *Mol Cell Proteomics* **12**, 2845-2855.

Naffakh, N., Tomoiu, A., Rameix-Welti, M. A. & van der Werf, S. (2008). Host restriction of avian influenza viruses at the level of the ribonucleoproteins. *Annual review of microbiology* **62**, 403-424.

Nagata, K., Kawaguchi, A. & Naito, T. (2008). Host factors for replication and transcription of the influenza virus genome. *Rev Med Virol* **18**, 247-260.

Naito, T., Kiyasu, Y., Sugiyama, K., Kimura, A., Nakano, R., Matsukage, A. & Nagata, K. (2007a). An influenza virus replicon system in yeast identified Tat-SF1 as a stimulatory host factor for viral RNA synthesis. *Proc Natl Acad Sci U S A* **104**, 18235-18240.

Naito, T., Momose, F., Kawaguchi, A. & Nagata, K. (2007b). Involvement of Hsp90 in assembly and nuclear import of influenza virus RNA polymerase subunits. *J Virol* **81**, 1339-1349.

Nelson, J., Couceiro, S. S., Paulson, J. C. & Baum, L. G. (1993). Influenza-Virus Strains Selectively Recognize Sialyloligosaccharides on Human Respiratory Epithelium - the Role of the Host-Cell in Selection of Hemagglutinin Receptor Specificity. *Virus Research* **29**, 155-165.

Nesvizhskii, A. I., Keller, A., Kolker, E. & Aebersold, R. (2003). A statistical model for identifying proteins by tandem mass spectrometry. *Analytical chemistry* **75**, 4646-4658.

Neumann, G., Hughes, M. T. & Kawaoka, Y. (2000). Influenza A virus NS2 protein mediates vRNP nuclear export through NES-independent interaction with hCRM1. *EMBO J* **19**, 6751-6758.

Neumann, G., Noda, T. & Kawaoka, Y. (2009). Emergence and pandemic potential of swine-origin H1N1 influenza virus. *Nature* **459**, 931-939.

Neumann, G., Watanabe, T., Ito, H., Watanabe, S., Goto, H., Gao, P., Hughes, M., Perez, D. R., Donis, R., Hoffmann, E., Hobom, G. & Kawaoka, Y. (1999). Generation of influenza A viruses entirely from cloned cDNAs. *Proc Natl Acad Sci U S A* **96**, 9345-9350.

Newcomb, L. L., Kuo, R. L., Ye, Q., Jiang, Y., Tao, Y. J. & Krug, R. M. (2009). Interaction of the influenza a virus nucleocapsid protein with the viral RNA polymerase potentiates unprimed viral RNA replication. *J Virol* **83**, 29-36.

Ng, A. K., Zhang, H., Tan, K., Li, Z., Liu, J. H., Chan, P. K., Li, S. M., Chan, W. Y., Au, S. W., Joachimiak, A., Walz, T., Wang, J. H. & Shaw, P. C. (2008). Structure of the influenza virus A H5N1 nucleoprotein: implications for RNA binding, oligomerization, and vaccine design. *FASEB J* **22**, 3638-3647.

Noda, T., Sagara, H., Yen, A., Takada, A., Kida, H., Cheng, R. H. & Kawaoka, Y. (2006). Architecture of ribonucleoprotein complexes in influenza A virus particles. *Nature* **439**, 490-492.

Noda, T., Sugita, Y., Aoyama, K., Hirase, A., Kawakami, E., Miyazawa, A., Sagara, H. & Kawaoka, Y. (2012). Three-dimensional analysis of ribonucleoprotein complexes in influenza A virus. *Nature communications* **3**, 639.

Noton, S. L., Medcalf, E., Fisher, D., Mullin, A. E., Elton, D. & Digard, P. (2007). Identification of the domains of the influenza A virus M1 matrix protein required for NP binding, oligomerization and incorporation into virions. *J Gen Virol* **88**, 2280-2290.

O'Neill, R. E., Talon, J. & Palese, P. (1998). The influenza virus NEP (NS2 protein) mediates the nuclear export of viral ribonucleoproteins. *EMBO J* **17**, 288-296.

Obayashi, E., Yoshida, H., Kawai, F., Shibayama, N., Kawaguchi, A., Nagata, K., Tame, J. R. & Park, S. Y. (2008). The structural basis for an essential subunit interaction in influenza virus RNA polymerase. *Nature* **454**, 1127-1131.

Oneill, R. E., Jaskunas, R., Blobel, G., Palese, P. & Moroianu, J. (1995). Nuclear Import of Influenza-Virus Rna Can Be Mediated by Viral Nucleoprotein and Transport Factors Required for Protein Import. *Journal of Biological Chemistry* **270**, 22701-22704.

Ortega, J., Martin-Benito, J., Zurcher, T., Valpuesta, J. M., Carrascosa, J. L. & Ortin, J. (2000). Ultrastructural and functional analyses of recombinant influenza virus ribonucleoproteins suggest dimerization of nucleoprotein during virus amplification. *Journal of Virology* **74**, 156-163.

Palese, P. & Shaw, M. L. (2013). *Orthomyxoviridae*. In *Fields Virology*, 6th edn, pp. 1151-1185. Edited by D. M. Knipe & P. M. Howley. Philadelphia: Lippincott Williams and Wilkins.

Paterson, D. & Fodor, E. (2012). Emerging roles for the influenza A virus nuclear export protein (NEP). *PLoS Pathog* **8**, e1003019.

Pavri, R., Zhu, B., Li, G. H., Trojer, P., Mandal, S., Shilatifard, A. & Reinberg, D. (2006). Histone H2B monoubiquitination functions cooperatively with FACT to regulate elongation by RNA polymerase II. *Cell* **125**, 703-717.

Perales, B. & Ortin, J. (1997). The influenza A virus PB2 polymerase subunit is required for the replication of viral RNA. *J Virol* **71**, 1381-1385.

Perales, B., Sanz-Ezquerro, J. J., Gastaminza, P., Ortega, J., Santaren, J. F., Ortin, J. & Nieto, A. (2000). The replication activity of influenza virus polymerase is linked to the capacity of the PA subunit to induce proteolysis. *J Virol* **74**, 1307-1312.

Perez, D. R. & Donis, R. O. (1995). A 48-amino-acid region of influenza A virus PB1 protein is sufficient for complex formation with PA. *J Virol* **69**, 6932-6939.

Perez, D. R. & Donis, R. O. (1998). The matrix 1 protein of influenza A virus inhibits the transcriptase activity of a model influenza reporter genome in vivo. *Virology* **249**, 52-61.

Perez, J. T., Varble, A., Sachidanandam, R., Zlatev, I., Manoharan, M., Garcia-Sastre, A. & tenOever, B. R. (2010). Influenza A virus-generated small RNAs regulate the switch from transcription to replication. *Proc Natl Acad Sci U S A* **107**, 11525-11530.

Perez, J. T., Zlatev, I., Aggarwal, S., Subramanian, S., Sachidanandam, R., Kim, B., Manoharan, M. & tenOever, B. R. (2012). A small-RNA enhancer of viral polymerase activity. *J Virol* **86**, 13475-13485.

Perkins, D. N., Pappin, D. J., Creasy, D. M. & Cottrell, J. S. (1999). Probability-based protein identification by searching sequence databases using mass spectrometry data. *Electrophoresis* **20**, 3551-3567.

Pinto, L. H., Holsinger, L. J. & Lamb, R. A. (1992). Influenza-Virus M2 Protein Has Ion Channel Activity. *Cell* **69**, 517-528.

Pleschka, S., Wolff, T., Ehrhardt, C., Hobom, G., Planz, O., Rapp, U. R. & Ludwig, S. (2001). Influenza virus propagation is impaired by inhibition of the Raf/MEK/ERK signalling cascade. *Nature Cell Biology* **3**, 301-305.

Plotch, S. J., Bouloy, M., Ulmanen, I. & Krug, R. M. (1981). A unique cap(m7GpppXm)-dependent influenza virion endonuclease cleaves capped RNAs to generate the primers that initiate viral RNA transcription. *Cell* **23**, 847-858.

Pons, M. W., Schulze, I. T., Hirst, G. K. & Hauser, R. (1969). Isolation and characterization of the ribonucleoprotein of influenza virus. *Virology* **39**, 250-259.

Poole, E., Elton, D., Medcalf, L. & Digard, P. (2004). Functional domains of the influenza A virus PB2 protein: identification of NP- and PB1-binding sites. *Virology* **321**, 120-133.

Poon, L. L., Fodor, E. & Brownlee, G. G. (2000). Polyuridylated mRNA synthesized by a recombinant influenza virus is defective in nuclear export. *J Virol* **74**, 418-427.

Poon, L. L., Pritlove, D. C., Fodor, E. & Brownlee, G. G. (1999). Direct evidence that the poly(A) tail of influenza A virus mRNA is synthesized by reiterative copying of a U track in the virion RNA template. *J Virol* **73**, 3473-3476.

Potter, C. W. (2001). A history of influenza. *J Appl Microbiol* **91**, 572-579.

Pritlove, D. C., Poon, L. L., Devenish, L. J., Leahy, M. B. & Brownlee, G. G. (1999). A hairpin loop at the 5' end of influenza A virus virion RNA is required for synthesis of poly(A)+ mRNA in vitro. *J Virol* **73**, 2109-2114.

Proudfoot, N. J. (2011). Ending the message: poly(A) signals then and now. *Genes Dev* **25**, 1770-1782.

Proudfoot, N. J. & Brownlee, G. G. (1976). 3' non-coding region sequences in eukaryotic messenger RNA. *Nature* **263**, 211-214.

Qiu, X. B., Shao, Y. M., Miao, S. & Wang, L. (2006). The diversity of the DnaJ/Hsp40 family, the crucial partners for Hsp70 chaperones. *Cellular and molecular life sciences : CMLS* **63**, 2560-2570.

Rameix-Welti, M. A., Tomoiu, A., Dos Santos Afonso, E., van der Werf, S. & Naffakh, N. (2009). Avian Influenza A virus polymerase association with nucleoprotein, but not polymerase assembly, is impaired in human cells during the course of infection. *J Virol* **83**, 1320-1331.

Rao, P., Yuan, W. & Krug, R. M. (2003). Crucial role of CA cleavage sites in the cap-snatching mechanism for initiating viral mRNA synthesis. *EMBO J* **22**, 1188-1198.

Read, E. K. & Digard, P. (2010). Individual influenza A virus mRNAs show differential dependence on cellular NXF1/TAP for their nuclear export. *J Gen Virol* **91**, 1290-1301.

Reed, R. (2003). Coupling transcription, splicing and mRNA export. *Curr Opin Cell Biol* **15**, 326-331.

Resa-Infante, P. & Gabriel, G. (2013). The nuclear import machinery is a determinant of influenza virus host adaptation. *BioEssays : news and reviews in molecular, cellular and developmental biology* **35**, 23-27.

Resa-Infante, P., Jorba, N., Coloma, R. & Ortin, J. (2011). The influenza virus RNA synthesis machine: advances in its structure and function. *RNA Biol* **8**, 207-215.

Resa-Infante, P., Jorba, N., Zamarreno, N., Fernandez, Y., Juarez, S. & Ortin, J. (2008). The host-dependent interaction of alpha-importins with influenza PB2 polymerase subunit is required for virus RNA replication. *PLoS One* **3**, e3904.

Resa-Infante, P., Recuero-Checa, M. A., Zamarreno, N., Llorca, O. & Ortin, J. (2010). Structural and functional characterization of an influenza virus RNA polymerase-genomic RNA complex. *J Virol* **84**, 10477-10487.

Reuther, P., Giese, S., Gotz, V., Kilb, N., Manz, B., Brunotte, L. & Schwemmle, M. (2014a). Adaptive mutations in the nuclear export protein of human-derived H5N1 strains facilitate a polymerase activity-enhancing conformation. *J Virol* **88**, 263-271.

Reuther, P., Giese, S., Gotz, V., Riegger, D. & Schwemmle, M. (2014b). Phosphorylation of highly conserved serine residues in the influenza A virus nuclear export protein NEP plays a minor role in viral growth in human cells and mice. *J Virol*.

Richardson, J. C. & Akkina, R. K. (1991). NS2 protein of influenza virus is found in purified virus and phosphorylated in infected cells. *Archives of virology* **116**, 69-80.

Robb, N. C., Chase, G., Bier, K., Vreede, F. T., Shaw, P. C., Naffakh, N., Schwemmle, M. & Fodor, E. (2011). The influenza A virus NS1 protein interacts with the nucleoprotein of viral ribonucleoprotein complexes. *J Virol* **85**, 5228-5231.

Robb, N. C. & Fodor, E. (2012). The accumulation of influenza A virus segment 7 spliced mRNAs is regulated by the NS1 protein. *J Gen Virol* **93**, 113-118.

Robb, N. C., Jackson, D., Vreede, F. T. & Fodor, E. (2010). Splicing of influenza A virus NS1 mRNA is independent of the viral NS1 protein. *J Gen Virol* **91**, 2331-2340.

Robb, N. C., Smith, M., Vreede, F. T. & Fodor, E. (2009). NS2/NEP protein regulates transcription and replication of the influenza virus RNA genome. *J Gen Virol* **90**, 1398-1407.

Roberts, P. C. & Compans, R. W. (1998). Host cell dependence of viral morphology. *Proc Natl Acad Sci U S A* **95**, 5746-5751.

Roberts, P. C., Lamb, R. A. & Compans, R. W. (1998). The M1 and M2 proteins of influenza A virus are important determinants in filamentous particle formation. *Virology* **240**, 127-137.

Robertson, J. S. (1979). 5' and 3' terminal nucleotide sequences of the RNA genome segments of influenza virus. *Nucleic Acids Res* **6**, 3745-3757.

Robertson, J. S., Schubert, M. & Lazzarini, R. A. (1981). Polyadenylation sites for influenza virus mRNA. *J Virol* **38**, 157-163.

Rodriguez Boulan, E. & Sabatini, D. D. (1978). Asymmetric budding of viruses in epithelial monlayers: a model system for study of epithelial polarity. *Proc Natl Acad Sci U S A* **75**, 5071-5075.

Root, C. N., Wills, E. G., McNair, L. L. & Whittaker, G. R. (2000). Entry of influenza viruses into cells is inhibited by a highly specific protein kinase C inhibitor. *Journal of General Virology* **81**, 2697-2705.

Rossman, J. S., Jing, X., Leser, G. P., Balannik, V., Pinto, L. H. & Lamb, R. A. (2010). Influenza virus m2 ion channel protein is necessary for filamentous virion formation. *J Virol* **84**, 5078-5088.

Rossman, J. S. & Lamb, R. A. (2011). Influenza virus assembly and budding. *Virology* **411**, 229-236.

Ruigrok, R. W. & Baudin, F. (1995). Structure of influenza virus ribonucleoprotein particles. II. Purified RNA-free influenza virus ribonucleoprotein forms structures that are indistinguishable from the intact influenza virus ribonucleoprotein particles. *J Gen Virol* **76 (Pt 4)**, 1009-1014.

Ruigrok, R. W., Crepin, T., Hart, D. J. & Cusack, S. (2010). Towards an atomic resolution understanding of the influenza virus replication machinery. *Curr Opin Struct Biol* **20**, 104-113.

Ruigrok, R. W., Crepin, T. & Kolakofsky, D. (2011). Nucleoproteins and nucleocapsids of negative-strand RNA viruses. *Current opinion in microbiology* **14**, 504-510.

Sanchez, C., Lachaize, C., Janody, F., Bellon, B., Roder, L., Euzenat, J., Rechenmann, F. & Jacq, B. (1999). Grasping at molecular interactions and genetic networks in Drosophila melanogaster using FlyNets, an Internet database. *Nucleic Acids Res* **27**, 89-94.

Sanz-Ezquerro, J. J., Fernandez Santaren, J., Sierra, T., Aragon, T., Ortega, J., Ortin, J., Smith, G. L. & Nieto, A. (1998). The PA influenza virus polymerase subunit is a phosphorylated protein. *J Gen Virol* **79 (Pt 3)**, 471-478.

Satterly, N., Tsai, P. L., van Deursen, J., Nussenzveig, D. R., Wang, Y., Faria, P. A., Levay, A., Levy, D. E. & Fontoura, B. M. (2007). Influenza virus targets the mRNA export machinery and the nuclear pore complex. *Proc Natl Acad Sci U S A* **104**, 1853-1858.

Scheiffele, P., Rietveld, A., Wilk, T. & Simons, K. (1999). Influenza viruses select ordered lipid domains during budding from the plasma membrane. *J Biol Chem* **274**, 2038-2044.

Scheres, S. H. W. (2012). RELION: Implementation of a Bayesian approach to cryo-EM structure determination. *J Struct Biol* **180**, 519-530.

Scheres, S. H. W., Nunez-Ramirez, R., Sorzano, C. O. S., Carazo, J. M. & Marabini, R. (2008). Image processing for electron microscopy single-particle analysis using XMIPP. *Nat Protoc* **3**, 977-990.

Schmidt, T. G. & Skerra, A. (2007). The Strep-tag system for one-step purification and high-affinity detection or capturing of proteins. *Nat Protoc* **2**, 1528-1535.

Selman, M., Dankar, S. K., Forbes, N. E., Jia, J.-J. & Brown, E. G. (2012). Adaptive mutation in influenza A virus non-structural gene is linked to host switching and induces a novel protein by alternative splicing. *Emerg Microbes Infect* **1**, e42.

Seo, S. H., Webby, R. & Webster, R. G. (2004). No apoptotic deaths and different levels of inductions of inflammatory cytokines in alveolar macrophages infected with influenza viruses. *Virology* **329**, 270-279.

Shapira, S. D., Gat-Viks, I., Shum, B. O., Dricot, A., de Grace, M. M., Wu, L., Gupta, P. B., Hao, T., Silver, S. J., Root, D. E., Hill, D. E., Regev, A. & Hacohen, N. (2009). A physical and regulatory map of host-influenza interactions reveals pathways in H1N1 infection. *Cell* **139**, 1255-1267.

Shapiro, G. I., Gurney, T. & Krug, R. M. (1987). Influenza-Virus Gene-Expression - Control Mechanisms at Early and Late Times of Infection and Nuclear-Cytoplasmic Transport of Virus-Specific Rnas. *Journal of Virology* **61**, 764-773.

Shapiro, G. I. & Krug, R. M. (1988). Influenza virus RNA replication in vitro: synthesis of viral template RNAs and virion RNAs in the absence of an added primer. *J Virol* **62**, 2285-2290.

Shaw, M. L. (2011). The host interactome of influenza virus presents new potential targets for antiviral drugs. *Rev Med Virol* **21**, 358-369.

Shaw, M. L., Stone, K. L., Colangelo, C. M., Gulcicek, E. E. & Palese, P. (2008). Cellular proteins in influenza virus particles. *PLoS Pathog* **4**, e1000085.

Shen, Y., Wang, Y., Sheng, K., Fei, X., Guo, Q., Larner, J., Kong, X., Qiu, Y. & Mi, J. (2011). Serine/threonine protein phosphatase 6 modulates the radiation sensitivity of glioblastoma. *Cell death & disease* **2**, e241.

Shi, Y. (2009). Serine/threonine phosphatases: mechanism through structure. *Cell* **139**, 468-484.

Shih, S. R. & Krug, R. M. (1996). Novel exploitation of a nuclear function by influenza virus: the cellular SF2/ASF splicing factor controls the amount of the essential viral M2 ion channel protein in infected cells. *EMBO J* **15**, 5415-5427.

Shih, S. R., Nemeroff, M. E. & Krug, R. M. (1995). The choice of alternative 5' splice sites in influenza virus M1 mRNA is regulated by the viral polymerase complex. *Proc Natl Acad Sci U S A* **92**, 6324-6328.

Shih, S. R., Suen, P. C., Chen, Y. S. & Chang, S. C. (1998). A novel spliced transcript of influenza A/WSN/33 virus. *Virus Genes* **17**, 179-183.

Shimizu, K., Handa, H., Nakada, S. & Nagata, K. (1994). Regulation of influenza virus RNA polymerase activity by cellular and viral factors. *Nucleic Acids Res* **22**, 5047-5053.

Shin, Y. K., Liu, Q., Tikoo, S. K., Babiuk, L. A. & Zhou, Y. (2007). Effect of the phosphatidylinositol 3-kinase/Akt pathway on influenza A virus propagation. *Journal of General Virology* **88**, 942-950.

Shteynberg, D., Deutsch, E. W., Lam, H., Eng, J. K., Sun, Z., Tasman, N., Mendoza, L., Moritz, R. L., Aebersold, R. & Nesvizhskii, A. I. (2011). iProphet: multi-level integrative analysis of shotgun proteomic data improves peptide and protein identification rates and error estimates. *Mol Cell Proteomics* **10**, M111 007690.

Simons, K. & Ikonen, E. (1997). Functional rafts in cell membranes. *Nature* **387**, 569-572.

Skehel, J. J. & Hay, A. J. (1978). Nucleotide sequences at the 5' termini of influenza virus RNAs and their transcripts. *Nucleic Acids Res* **5**, 1207-1219.

Smallwood, S., Cevik, B. & Moyer, S. A. (2002). Intragenic complementation and oligomerization of the L subunit of the sendai virus RNA polymerase. *Virology* **304**, 235-245.

Smed-Sorensen, A., Chalouni, C., Chatterjee, B., Cohn, L., Blattmann, P., Nakamura, N., Delamarre, L. & Mellman, I. (2012). Influenza A virus infection of human primary dendritic cells impairs their ability to cross-present antigen to CD8 T cells. *PLoS Pathog* **8**, e1002572.

Smith, D. B. & Inglis, S. C. (1985). Regulated production of an influenza virus spliced mRNA mediated by virus-specific products. *EMBO J* **4**, 2313-2319.

Smith, G. L. & Hay, A. J. (1982). Replication of the influenza virus genome. *Virology* **118**, 96-108.

Sorrell, E. M., Song, H., Pena, L. & Perez, D. R. (2010). A 27-amino-acid deletion in the neuraminidase stalk supports replication of an avian H2N2 influenza A virus in the respiratory tract of chickens. *J Virol* **84**, 11831-11840.

Srisawat, C. & Engelke, D. R. (2002). RNA affinity tags for purification of RNAs and ribonucleoprotein complexes. *Methods* **26**, 156-161.

Stefansson, B. & Brautigan, D. L. (2007). Protein phosphatase PP6 N terminal domain restricts G1 to S phase progression in human cancer cells. *Cell cycle* **6**, 1386-1392.

Stefansson, B., Ohama, T., Daugherty, A. E. & Brautigan, D. L. (2008). Protein phosphatase 6 regulatory subunits composed of ankyrin repeat domains. *Biochemistry* **47**, 1442-1451.

Stieneke-Grober, A., Vey, M., Angliker, H., Shaw, E., Thomas, G., Roberts, C., Klenk, H. D. & Garten, W. (1992). Influenza virus hemagglutinin with multibasic cleavage site is activated by furin, a subtilisin-like endoprotease. *EMBO J* **11**, 2407-2414.

Stockley, P. G., Stonehouse, N. J., Murray, J. B., Goodman, S. T., Talbot, S. J., Adams, C. J., Liljas, L. & Valegard, K. (1995). Probing sequence-specific RNA recognition by the bacteriophage MS2 coat protein. *Nucleic Acids Res* **23**, 2512-2518.

Su, W. C., Chen, Y. C., Tseng, C. H., Hsu, P. W., Tung, K. F., Jeng, K. S. & Lai, M. M. (2013a). Pooled RNAi screen identifies ubiquitin ligase Itch as crucial for influenza A virus release from the endosome during virus entry. *Proc Natl Acad Sci U S A* **110**, 17516-17521.

Su, Y. T., Gao, C. Z., Liu, Y., Guo, S., Wang, A., Wang, B. L., Erdjument-Bromage, H., Miyagi, M., Tempst, P. & Kao, H. Y. (2013b). Monoubiquitination of Filamin B Regulates Vascular Endothelial Growth Factor-Mediated Trafficking of Histone Deacetylase 7. *Molecular and Cellular Biology* **33**, 1546-1560.

Subbarao, E. K., London, W. & Murphy, B. R. (1993). A single amino acid in the PB2 gene of influenza A virus is a determinant of host range. *J Virol* **67**, 1761-1764.

Sugiyama, K., Obayashi, E., Kawaguchi, A., Suzuki, Y., Tame, J. R., Nagata, K. & Park, S. Y. (2009). Structural insight into the essential PB1-PB2 subunit contact of the influenza virus RNA polymerase. *EMBO J* **28**, 1803-1811.

Sui, B., Bamba, D., Weng, K., Ung, H., Chang, S., Van Dyke, J., Goldblatt, M., Duan, R., Kinch, M. S. & Li, W. B. (2009). The use of Random Homozygous Gene Perturbation to identify novel host-oriented targets for influenza. *Virology* **387**, 473-481.

Tafforeau, L., Chantier, T., Pradezynski, F., Pellet, J., Mangeot, P. E., Vidalain, P. O., Andre, P., Rabourdin-Combe, C. & Lotteau, V. (2011). Generation and comprehensive analysis of an influenza virus polymerase cellular interaction network. *J Virol* **85**, 13010-13018.

Takeda, M., Leser, G. P., Russell, C. J. & Lamb, R. A. (2003). Influenza virus hemagglutinin concentrates in lipid raft microdomains for efficient viral fusion. *Proc Natl Acad Sci U S A* **100**, 14610-14617.

Tarendeau, F., Boudet, J., Guilligay, D., Mas, P. J., Bougault, C. M., Boulo, S., Baudin, F., Ruigrok, R. W., Daigle, N., Ellenberg, J., Cusack, S., Simorre, J. P. & Hart, D. J. (2007). Structure and nuclear import function of the C-terminal domain of influenza virus polymerase PB2 subunit. *Nat Struct Mol Biol* **14**, 229-233.

Tarendeau, F., Crepin, T., Guilligay, D., Ruigrok, R. W., Cusack, S. & Hart, D. J. (2008). Host determinant residue lysine 627 lies on the surface of a discrete, folded domain of influenza virus polymerase PB2 subunit. *PLoS Pathog* **4**, e1000136.

Tarrant, M. K. & Cole, P. A. (2009). The chemical biology of protein phosphorylation. *Annu Rev Biochem* **78**, 797-825.

Taubenberger, J. K. & Morens, D. M. (2006). 1918 Influenza: the mother of all pandemics. *Emerging infectious diseases* **12**, 15-22.

Thierry, F. & Danos, O. (1982). Use of specific single stranded DNA probes cloned in M13 to study the RNA synthesis of four temperature-sensitive mutants of HK/68 influenza virus. *Nucleic Acids Res* **10**, 2925-2938.

Tiley, L. S., Hagen, M., Matthews, J. T. & Krystal, M. (1994). Sequence-specific binding of the influenza virus RNA polymerase to sequences located at the 5' ends of the viral RNAs. *J Virol* **68**, 5108-5116.

Tokunaga, K., Shibuya, T., Ishihama, Y., Tadakuma, H., Ide, M., Yoshida, M., Funatsu, T., Ohshima, Y. & Tani, T. (2006). Nucleocytoplasmic transport of fluorescent mRNA in living mammalian cells: nuclear mRNA export is coupled to ongoing gene transcription. *Genes to cells : devoted to molecular & cellular mechanisms* **11**, 305-317.

Tong, S., Zhu, X., Li, Y., Shi, M., Zhang, J., Bourgeois, M., Yang, H., Chen, X., Recuenco, S., Gomez, J., Chen, L. M., Johnson, A., Tao, Y., Dreyfus, C., Yu, W., McBride, R., Carney, P. J., Gilbert, A. T., Chang, J., Guo, Z., Davis, C. T., Paulson, J. C., Stevens, J., Rupprecht, C. E., Holmes, E. C., Wilson, I. A. & Donis, R. O. (2013). New world bats harbor diverse influenza A viruses. *PLoS Pathog* **9**, e1003657.

Torreira, E., Schoehn, G., Fernandez, Y., Jorba, N., Ruigrok, R. W., Cusack, S., Ortin, J. & Llorca, O. (2007). Three-dimensional model for the isolated recombinant influenza virus polymerase heterotrimer. *Nucleic Acids Res* **35**, 3774-3783.

Toyoda, T., Adyshev, D. M., Kobayashi, M., Iwata, A. & Ishihama, A. (1996). Molecular assembly of the influenza virus RNA polymerase: determination of the subunit-subunit contact sites. *J Gen Virol* **77 (Pt 9)**, 2149-2157.

Trudgian, D. C., Ridlova, G., Fischer, R., Mackeen, M. M., Ternette, N., Acuto, O., Kessler, B. M. & Thomas, B. (2011). Comparative evaluation of label-free SINQ normalized spectral index quantitation in the central proteomics facilities pipeline. *Proteomics* **11**, 2790-2797.

Trudgian, D. C., Thomas, B., McGowan, S. J., Kessler, B. M., Salek, M. & Acuto, O. (2010). CPFP: a central proteomics facilities pipeline. *Bioinformatics* **26**, 1131-1132.

Tsai, P. L., Chiou, N. T., Kuss, S., Garcia-Sastre, A., Lynch, K. W. & Fontoura, B. M. (2013). Cellular RNA binding proteins NS1-BP and hnRNP K regulate influenza A virus RNA splicing. *PLoS Pathog* **9**, e1003460.

Tuerk, C. & Gold, L. (1990). Systematic evolution of ligands by exponential enrichment: RNA ligands to bacteriophage T4 DNA polymerase. *Science* **249**, 505-510.

Turrell, L., Lyall, J. W., Tiley, L. S., Fodor, E. & Vreede, F. T. (2013). The role and assembly mechanism of nucleoprotein in influenza A virus ribonucleoprotein complexes. *Nature communications* **4**, 1591.

Umbach, J. L., Yen, H. L., Poon, L. L. & Cullen, B. R. (2010). Influenza A virus expresses high levels of an unusual class of small viral leader RNAs in infected cells. *mBio* **1**.

Vreede, F. T. & Brownlee, G. G. (2007). Influenza virion-derived viral ribonucleoproteins synthesize both mRNA and cRNA in vitro. *J Virol* **81**, 2196-2204.

Vreede, F. T., Gifford, H. & Brownlee, G. G. (2008). Role of initiating nucleoside triphosphate concentrations in the regulation of influenza virus replication and transcription. *J Virol* **82**, 6902-6910.

Vreede, F. T., Jung, T. E. & Brownlee, G. G. (2004). Model suggesting that replication of influenza virus is regulated by stabilization of replicative intermediates. *J Virol* **78**, 9568-9572.

Wang, Q. M., Hockman, M. A., Staschke, K., Johnson, R. B., Case, K. A., Lu, J., Parsons, S., Zhang, F., Rathnachalam, R., Kirkegaard, K. & Colacino, J.

M. (2002). Oligomerization and cooperative RNA synthesis activity of hepatitis C virus RNA-dependent RNA polymerase. *J Virol* **76**, 3865-3872.

Wang, W., Cui, Z. Q., Han, H., Zhang, Z. P., Wei, H. P., Zhou, Y. F., Chen, Z. & Zhang, X. E. (2008). Imaging and characterizing influenza A virus mRNA transport in living cells. *Nucleic Acids Res* **36**, 4913-4928.

Watanabe, K., Fuse, T., Asano, I., Tsukahara, F., Maru, Y., Nagata, K., Kitazato, K. & Kobayashi, N. (2006). Identification of Hsc70 as an influenza virus matrix protein (M1) binding factor involved in the virus life cycle. *FEBS Lett* **580**, 5785-5790.

Watanabe, K., Handa, H., Mizumoto, K. & Nagata, K. (1996). Mechanism for inhibition of influenza virus RNA polymerase activity by matrix protein. *Journal of Virology* **70**, 241-247.

Watanabe, T., Watanabe, S. & Kawaoka, Y. (2010). Cellular networks involved in the influenza virus life cycle. *Cell Host Microbe* **7**, 427-439.

Whittaker, G., Kemler, I. & Helenius, A. (1995). Hyperphosphorylation of mutant influenza virus matrix protein, M1, causes its retention in the nucleus. *J Virol* **69**, 439-445.

WHOa. Influenza (Seasonal). http://www.who.int/mediacentre/factsheets/fs211/en/ (accessed 2nd June 2014)

WHOb. Cumulative number of confirmed human cases of avian influenza A(H5N1) reported to WHO. http://www.who.int/influenza/human_animal_interface/H5N1_cumulative_table_archives/en/ (accessed 2nd June 2014).

Widjaja, I., de Vries, E., Tscherne, D. M., Garcia-Sastre, A., Rottier, P. J. & de Haan, C. A. (2010). Inhibition of the ubiquitin-proteasome system affects influenza A virus infection at a postfusion step. *J Virol* **84**, 9625-9631.

Winter, G. & Fields, S. (1980). Cloning of influenza cDNA ino M13: the sequence of the RNA segment encoding the A/PR/8/34 matrix protein. *Nucleic Acids Res* **8**, 1965-1974.

Winter, G. & Fields, S. (1981). The structure of the gene encoding the nucleoprotein of human influenza virus A/PR/8/34. *Virology* **114**, 423-428.

Winter, G. & Fields, S. (1982). Nucleotide sequence of human influenza A/PR/8/34 segment 2. *Nucleic Acids Res* **10**, 2135-2143.

Winter, G., Fields, S. & Brownlee, G. G. (1981a). Nucleotide sequence of the haemagglutinin gene of a human influenza virus H1 subtype. *Nature* **292**, 72-75.

Winter, G., Fields, S., Gait, M. J. & Brownlee, G. G. (1981b). The use of synthetic oligodeoxynucleotide primers in cloning and sequencing segment of 8 influenza virus (A/PR/8/34). *Nucleic Acids Res* **9**, 237-245.

Wise, H. M., Hutchinson, E. C., Jagger, B. W., Stuart, A. D., Kang, Z. H., Robb, N., Schwartzman, L. M., Kash, J. C., Fodor, E., Firth, A. E., Gog, J. R., Taubenberger, J. K. & Digard, P. (2012). Identification of a novel splice variant form of the influenza A virus M2 ion channel with an antigenically distinct ectodomain. *PLoS Pathog* **8**, e1002998.

Wisskirchen, C., Ludersdorfer, T. H., Muller, D. A., Moritz, E. & Pavlovic, J. (2011). The cellular RNA helicase UAP56 is required for prevention of double-stranded RNA formation during influenza A virus infection. *J Virol* **85**, 8646-8655.

Wolstenholme, A. J., Barrett, T., Nichol, S. T. & Mahy, B. W. (1980). Influenza virus-specific RNA and protein syntheses in cells infected with temperature-sensitive mutants defective in the genome segment encoding nonstructural proteins. *J Virol* **35**, 1-7.

Wright, P. F., Neumann, G. & Kawaoka, Y. (2013). Orthomyxoviruses. In *Fields Virology*, 6th edn, pp. 1186-1243. Edited by D. M. Knipe & P. M. Howley. Philadelphia: Lippincott Williams and Wilkins.

Xu, Y., Chen, Y., Zhang, P., Jeffrey, P. D. & Shi, Y. (2008). Structure of a protein phosphatase 2A holoenzyme: insights into B55-mediated Tau dephosphorylation. *Mol Cell* **31**, 873-885.

Yamanaka, K., Ishihama, A. & Nagata, K. (1990). Reconstitution of influenza virus RNA-nucleoprotein complexes structurally resembling native viral ribonucleoprotein cores. *J Biol Chem* **265**, 11151-11155.

Yanguez, E. & Nieto, A. (2011). So similar, yet so different: Selective translation of capped and polyadenylated viral mRNAs in the influenza virus infected cell. *Virus Research* **156**, 1-12.

Ye, Q., Krug, R. M. & Tao, Y. J. (2006a). The mechanism by which influenza A virus nucleoprotein forms oligomers and binds RNA. *Nature* **444**, 1078-1082.

Ye, Q. Z., Krug, R. M. & Tao, Y. Z. J. (2006b). The mechanism by which influenza A virus nucleoprotein forms oligomers and binds RNA. *Nature* **444**, 1078-1082.

York, A. & Fodor, E. (2013). Biogenesis, assembly, and export of viral messenger ribonucleoproteins in the influenza A virus infected cell. *RNA Biol* **10**, 1274-1282.

Yuan, P., Bartlam, M., Lou, Z., Chen, S., Zhou, J., He, X., Lv, Z., Ge, R., Li, X., Deng, T., Fodor, E., Rao, Z. & Liu, Y. (2009). Crystal structure of an avian

influenza polymerase PA(N) reveals an endonuclease active site. *Nature* **458**, 909-913.

Zamarin, D., Garcia-Sastre, A., Xiao, X., Wang, R. & Palese, P. (2005). Influenza virus PB1-F2 protein induces cell death through mitochondrial ANT3 and VDAC1. *PLoS Pathog* **1**, e4.

Zamarin, D., Ortigoza, M. B. & Palese, P. (2006). Influenza A virus PB1-F2 protein contributes to viral pathogenesis in mice. *J Virol* **80**, 7976-7983.

Zeng, K., Bastos, R. N., Barr, F. A. & Gruneberg, U. (2010). Protein phosphatase 6 regulates mitotic spindle formation by controlling the T-loop phosphorylation state of Aurora A bound to its activator TPX2. *J Cell Biol* **191**, 1315-1332.

Zhang, J., Leser, G. P., Pekosz, A. & Lamb, R. A. (2000). The cytoplasmic tails of the influenza virus spike glycoproteins are required for normal genome packaging. *Virology* **269**, 325-334.

Zhang, S., Wang, J., Wang, Q. & Toyoda, T. (2010). Internal initiation of influenza virus replication of viral RNA and complementary RNA in vitro. *J Biol Chem* **285**, 41194-41201.

Zhang, Y., Zhang, Q. Y., Kong, H. H., Jiang, Y. P., Gao, Y. W., Deng, G. H., Shi, J. Z., Tian, G. B., Liu, L. L., Liu, J. X., Guan, Y. T., Bu, Z. G. & Chen, H. L. (2013). H5N1 Hybrid Viruses Bearing 2009/H1N1 Virus Genes Transmit in Guinea Pigs by Respiratory Droplet. *Science* **340**, 1459-1463.

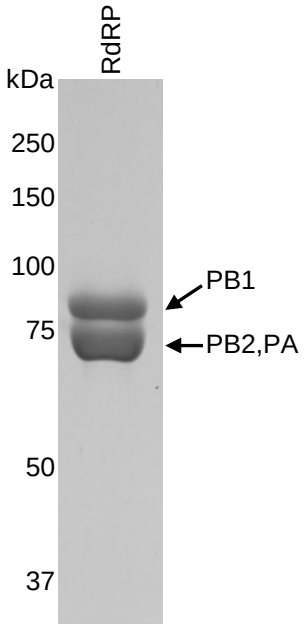
Zhirnov, O. P., Poyarkov, S. V., Vorob'eva, I. V., Safonova, O. A., Malyshev, N. A. & Klenk, H. D. (2007). Segment NS of influenza A virus contains an additional gene NSP in positive-sense orientation. *Doklady Biochemistry and biophysics* **414**, 127-133.

Zhong, J., Liao, J., Liu, X., Wang, P., Liu, J., Hou, W., Zhu, B., Yao, L., Wang, J., Li, J., Stark, J. M., Xie, Y. & Xu, X. (2011). Protein phosphatase PP6 is required for homology-directed repair of DNA double-strand breaks. *Cell cycle* **10**, 1411-1419.

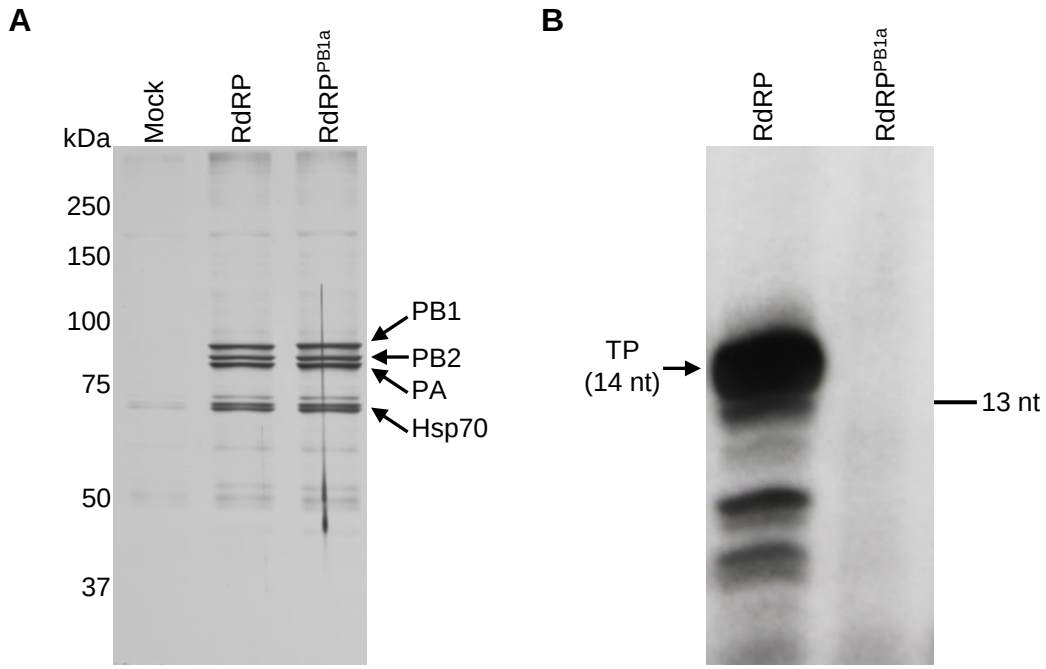
Zhou, H., Yu, Z., Hu, Y., Tu, J., Zou, W., Peng, Y., Zhu, J., Li, Y., Zhang, A., Yu, Z., Ye, Z., Chen, H. & Jin, M. (2009). The special neuraminidase stalk-motif responsible for increased virulence and pathogenesis of H5N1 influenza A virus. *PLoS One* **4**, e6277.

Zhou, Z., Cao, M., Guo, Y., Zhao, L., Wang, J., Jia, X., Li, J., Wang, C., Gabriel, G., Xue, Q., Yi, Y., Cui, S., Jin, Q., Wang, J. & Deng, T. (2014). Fragile X mental retardation protein stimulates ribonucleoprotein assembly of influenza A virus. *Nature communications* **5**, 3259.

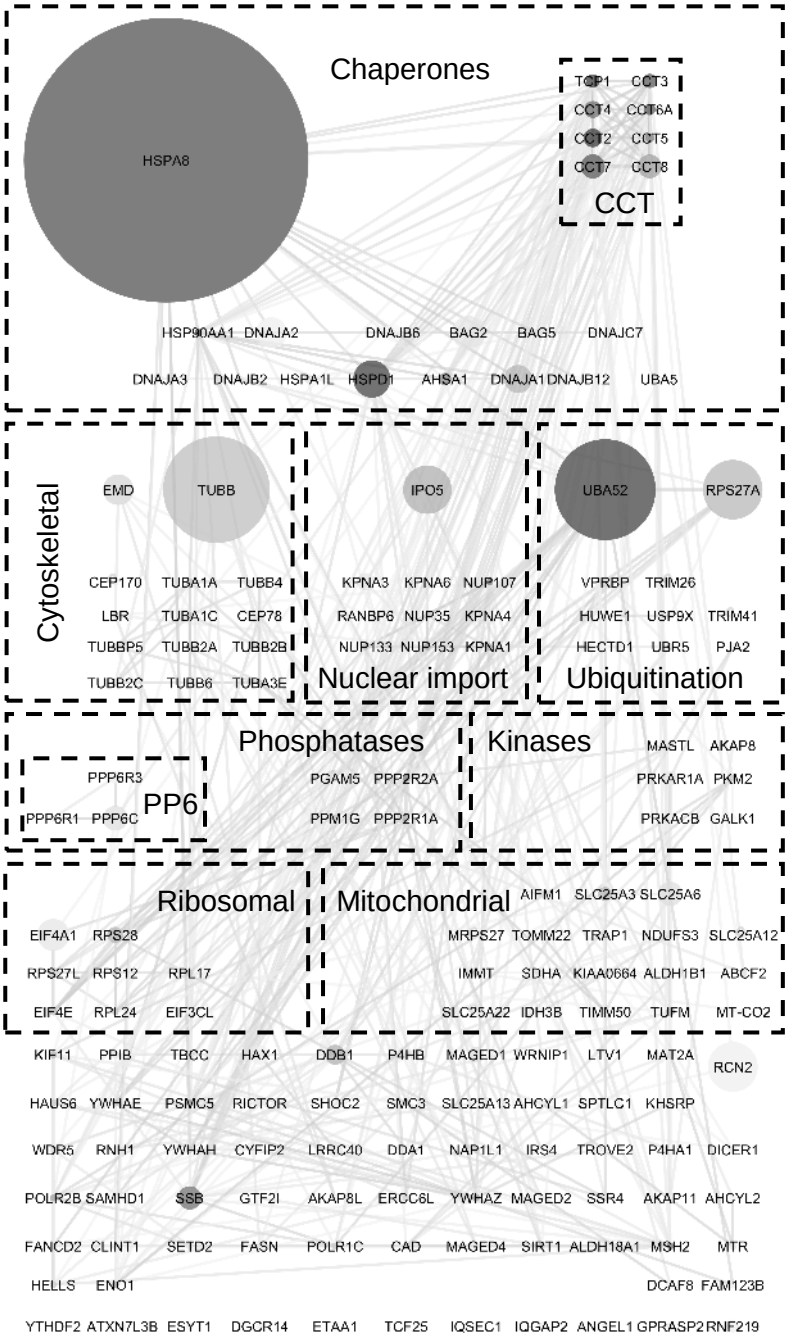
Zurcher, T., de la Luna, S., Sanz-Ezquerro, J. J., Nieto, A. & Ortin, J. (1996). Mutational analysis of the influenza virus A/Victoria/3/75 PA protein: studies of interaction with PB1 protein and identification of a dominant negative mutant. *J Gen Virol* **77 (Pt 8)**, 1745-1749.



Appendix A.1 Recombinant RdRP purified from *Spodoptera frugiperda* (Sf9) cells. Figure and RdRP from Sf9 cells in *in vitro* assays courtesy of Narin Hengrung. Wild-type influenza A/NT/60/68 virus RdRP was purified from recombinant baculovirus-infected Sf9 cells and analysed by SDS-PAGE and staining with Coomassie Brilliant Blue.



Appendix A.2 Recombinant RdRP purified from HEK 293T cells. Wild-type (RdRP) and active site mutant ($RdRP^{PB1a}$) influenza A/WSN/33 virus RdRP were purified from transfected HEK 293T cells. Mock purifications were performed using cells transfected with an empty pcDNA3A vector (Mock). (A) Purified RdRP was analysed by SDS-PAGE and silver staining analysis. (B) Activity of wild-type (RdRP) and active site mutant ($RdRP^{PB1a}$) influenza A virus RdRP, purified from transfected HEK 293T cells, was assayed using an *in vitro* [α-^{32}P]GTP incorporation assay. Transcription products (TP) were analysed by PAGE and bands detected by autoradiography. A 13 nt-long ^{32}P-labelled RNA was used as a size marker.



Appendix B Interaction network of cellular proteins in the viral transcription/replication machinery interactome with node labelling. The interaction network of Figure 5.9, with the short names of proteins shown. See the legend to Figure 5.9 for further details.

Appendix C.1: Mass spectrometry of cRNP complexes – Experiment 1

Mascot score, number of peptide spectrum matches, number of corresponding peptide sequences and % sequence coverage for each identification. Decoy matches and common contaminants have been removed.
aUniProt ID of human protein or viral protein name.
[b] $-10\times\log_{10}(P)$, where P is the absolute probability.

Protein[a]	***Description***	***Mascot Score[b]***	***Peptide Spectrum Matches***	***Peptide Sequences***	***% Sequence Coverage***
NP	NP of influenza A/WSN/33 virus	208	11	9	26.7
P14866	Heterogeneous nuclear ribonucleoprotein L	174	10	9	24.1
PB2	PB2 of influenza A/WSN/33 virus	169	7	6	14.2
P00338	L-lactate dehydrogenase A chain	164	4	4	23.2
Q07065	Cytoskeleton-associated protein 4	156	3	3	11.6
P01876	Ig alpha-1 chain C region	141	5	4	16.1
P07195	L-lactate dehydrogenase B chain	139	4	4	16.2
O43143	Putative pre-mRNA-splicing factor ATP-dependent RNA helicase DHX15	132	8	7	12.2
Q16630	Cleavage and polyadenylation specificity factor subunit 6	128	3	3	10
P01833	Polymeric immunoglobulin receptor	123	2	2	5.4
P01877	Ig alpha-2 chain C region	120	3	2	10.6
P61626	Lysozyme C	100	6	3	27.7
P62701	40S ribosomal protein S4, X isoform	96	3	3	12.5
Q13435	Splicing factor 3B subunit 2	94	3	3	9.2
P08107	Heat shock 70 kDa protein 1A/1B	86	3	3	7.3
Q53H96	Pyrroline-5-carboxylate reductase 3	84	2	1	6.9
Q9H7H0	Methyltransferase-like protein 17, mitochondrial	84	2	1	5.7
P07864	L-lactate dehydrogenase C chain	80	1	1	3.6

Q92499	ATP-dependent RNA helicase DDX1	76	4	4	9.7
Q15427	Splicing factor 3B subunit 4	71	1	1	3.3
Q99700	Ataxin-2	69	1	1	1.3
P0CG05	Ig lambda-2 chain C regions	69	1	1	9.4
Q8IXB1	DnaJ homolog subfamily C member 10	69	4	4	11.2
P01871	Ig mu chain C region	67	1	1	2.7
Q9BU76	Multiple myeloma tumor-associated protein 2	64	1	1	5.3
P04745	Alpha-amylase 1	63	1	1	4.7
PA	PA of influenza A/WSN/33 virus	59	2	2	6.6
Q04726	Transducin-like enhancer protein 3	58	1	1	3.9
P07437	Tubulin beta chain	58	2	1	4.7
Q9GZN8	UPF0687 protein C20orf27	56	1	1	20.7
O75533	Splicing factor 3B subunit 1	56	2	2	3.4
O43488	Aflatoxin B1 aldehyde reductase member 2	55	1	1	7.2
Q86TI2	Dipeptidyl peptidase 9	52	4	3	5.8
Q9H0D6	5~-3~ exoribonuclease 2	50	1	1	2.1
Q02779	Mitogen-activated protein kinase kinase kinase 10	47	2	1	0.6
Q8NDT2	Putative RNA-binding protein 15B	47	1	1	3.5
Q14151	Scaffold attachment factor B2	46	4	4	8
O43809	Cleavage and polyadenylation specificity factor subunit 5	46	2	2	16.3
Q6UN15	Pre-mRNA 3~-end-processing factor FIP1	46	1	1	4.5
Q96GD4	Serine/threonine-protein kinase 12	43	1	1	3.5
Q15428	Splicing factor 3A subunit 2	41	1	1	3
Q15393	Splicing factor 3B subunit 3	41	2	2	2.5
Q8N0Y2	Zinc finger protein 444	41	1	1	4.6
Q8TDL5	Long palate, lung and nasal epithelium carcinoma-associated protein 1	41	2	2	11

Q8TAD8	Smad nuclear-interacting protein 1	40	1	1	8.1
Q15459	Splicing factor 3A subunit 1	40	2	2	12.5
P04083	Annexin A1	39	1	1	7.2
Q5D862	Filaggrin-2	38	1	1	0.5
PB1	PB1 of influenza A/WSN/33 virus	38	2	2	7.3
Q8TD47	40S ribosomal protein S4, Y isoform 2	37	1	1	2.7
Q6UXN9	WD repeat-containing protein 82	37	1	1	6.4
O75152	Zinc finger CCCH domain-containing protein 11A	36	1	1	3.8
Q9BYZ2	L-lactate dehydrogenase A-like 6B	36	1	1	1.6
Q9UKK3	Poly [ADP-ribose] polymerase 4	35	1	1	0.3
P60709	Actin, cytoplasmic 1	35	1	1	5.6
Q96C36	Pyrroline-5-carboxylate reductase 2	35	1	1	2.2
Q4VCS5	Angiomotin	35	1	1	3.9
P12273	Prolactin-inducible protein	34	1	1	11.6
O94763	Unconventional prefoldin RPB5 interactor	33	1	1	2.1
Q4G0X9	Coiled-coil domain-containing protein 40	33	1	1	0.4
Q96K21	Zinc finger FYVE domain-containing protein 19	33	1	1	3
Q7Z4S6	Kinesin-like protein KIF21A	33	1	1	0.4
P16870	Carboxypeptidase E	32	1	1	1.1
P11021	78 kDa glucose-regulated protein	31	1	1	2.8
Q9UDR5	Alpha-aminoadipic semialdehyde synthase, mitochondrial	31	2	2	6.5
P38646	Stress-70 protein, mitochondrial	31	1	1	4.9
Q9NZU0	Leucine-rich repeat transmembrane protein FLRT3	30	1	1	0.9
Q96NJ6	Zinc finger protein 3 homolog	30	2	1	1.4
Q8WWM7	Ataxin-2-like protein	30	1	1	5.4
Q9H857	5~-nucleotidase domain-containing protein 2	30	1	1	2.1

Q69YN4	Protein virilizer homolog	30	1	1	1
Q9BS26	Endoplasmic reticulum resident protein 44	30	1	1	3.2
P06746	DNA polymerase beta	29	1	1	1.8
P36873	Serine/threonine-protein phosphatase PP1-gamma catalytic subunit	29	1	1	3.1
Q9C0J8	WD repeat-containing protein 33	27	1	1	1.7
Q96H79	Zinc finger CCCH-type antiviral protein 1-like	27	1	1	6.3
O15020	Spectrin beta chain, brain 2	26	1	1	0.8
O00410	Importin-5	26	1	1	6.4
Q3MIX3	Uncharacterized aarF domain-containing protein kinase 5	26	1	1	1
Q9HB96	Fanconi anemia group E protein	26	1	1	1.3
Q96DA0	Zymogen granule protein 16 homolog B	26	1	1	18.3
P04279	Semenogelin-1	25	1	1	3.5
Q14152	Eukaryotic translation initiation factor 3 subunit A	24	1	1	0.8
Q8TCC7	Solute carrier family 22 member 8	24	1	1	0.9
P49761	Dual specificity protein kinase CLK3	24	1	1	2
O94779	Contactin-5	21	1	1	1.4
Q96LU7	Uncharacterized protein C12orf28	18	1	1	6.2
Q9P2F8	Signal-induced proliferation-associated 1-like protein 2	17	1	1	0.3
Q14CX7	N-alpha-acetyltransferase 25, NatB auxiliary subunit	16	1	1	1.3

Appendix C.2: Mass spectrometry of cRNP – Experiment 2

Mascot score, number of peptide spectrum matches, number of corresponding peptide sequences and % sequence coverage for each identification.
Decoy matches and common contaminants have been removed.
aUniProt ID of human protein or viral protein name.
[b] $-10\times\log_{10}(P)$, where P is the absolute probability.

Protein[a]	***Description***	***Mascot Score[b]***	***Peptide Spectrum Matches***	***Peptide Sequences***	***% Sequence Coverage***
NP	NP of influenza A/WSN/33 virus	286	15	15	38.6
PB2	PB2 of influenza A/WSN/33 virus	229	18	16	24.5
PA	PA of influenza A/WSN/33 virus	205	11	10	17.2
Q9BQE3	Tubulin alpha-1C chain	87	3	3	15.4
P62829	60S ribosomal protein L23	78	2	2	20
PB1	PB1 of influenza A/WSN/33 virus	74	6	6	9.8
P11387	DNA topoisomerase 1	62	5	5	11.6
Q5D862	Filaggrin-2	52	1	1	0.7
Q7Z417	Nuclear fragile X mental retardation-interacting protein 2	50	3	3	5.5
Q5VTE0	Putative elongation factor 1-alpha-like 3	47	1	1	5
Q3MHD2	Protein LSM12 homolog	46	2	2	17.9
P11142	Heat shock cognate 71 kDa protein	44	2	2	8
P08107	Heat shock 70 kDa protein 1A/1B	43	3	3	8.4
P20930	Filaggrin	40	1	1	0.3
Q86YZ3	Hornerin	37	2	2	0.9
P34931	Heat shock 70 kDa protein 1-like	36	2	2	7.2
P62805	Histone H4	36	2	2	19.4
Q8N684	Cleavage and polyadenylation specificity factor subunit 7	34	1	1	6.4

Q562R1	Beta-actin-like protein 2	33	1	1	4.3
Q08AD1	Calmodulin-regulated spectrin-associated protein 2	32	1	1	1.5
P25490	Transcriptional repressor protein YY1	32	1	1	4.1
P12036	Neurofilament heavy polypeptide	31	1	1	0.8
P17066	Heat shock 70 kDa protein 6	30	2	2	4.4
Q969P6	DNA topoisomerase I, mitochondrial	29	1	1	4
P48736	Phosphatidylinositol-4,5-bisphosphate 3-kinase catalytic subunit gamma isoform	28	1	1	0.5
P0CG38	POTE ankyrin domain family member I	27	1	1	0.9
Q9BWT7	Caspase recruitment domain-containing protein 10	27	2	1	0.6
P15924	Desmoplakin	26	1	1	0.3
P68366	Tubulin alpha-4A chain	25	1	1	5.6
P11021	78 kDa glucose-regulated protein	23	1	1	2.8
P35626	Beta-adrenergic receptor kinase 2	23	3	1	0.9
Q5JV73	FERM and PDZ domain-containing protein 3	22	1	1	0.3
Q8NDA2	Hemicentin-2	21	1	1	0.1
P26196	Probable ATP-dependent RNA helicase DDX6	21	1	1	2.3
P04350	Tubulin beta-4 chain	17	1	1	2
Q99490	Arf-GAP with GTPase, ANK repeat and PH domain-containing protein 2	17	1	1	0.5
Q02880	DNA topoisomerase 2-beta	17	1	1	1.4
Q8TF72	Protein Shroom3	17	1	1	0.5
Q9C0B9	Zinc finger CCHC domain-containing protein 2	16	1	1	0.6
Q9GZN8	UPF0687 protein C20orf27	16	1	1	8
P28288	ATP-binding cassette sub-family D member 3	13	1	1	1.7

Appendix C.3: Mass spectrometry of cRNP – Experiment 3

Mascot score, number of peptide spectrum matches, number of corresponding peptide sequences and % sequence coverage for each identification. Decoy matches and common contaminants have been removed.
aUniProt ID of human protein or viral protein name.
[b] $-10\times\log_{10}(P)$, where P is the absolute probability.

Protein[a]	***Description***	***Mascot Score[b]***	***Peptide Spectrum Matches***	***Peptide Sequences***	***% Sequence Coverage***
NP	NP of influenza A/WSN/33 virus	34	1	1	3.6
PB2	PB2 of influenza A/WSN/33 virus	23	1	1	1.3
Q3MHD2	Protein LSM12 homolog	15	1	1	4.1

Appendix D.1: Mass spectrometry of vRNP – Experiment 1

Mascot score, number of peptide spectrum matches, number of corresponding peptide sequences and % sequence coverage for each identification.
Decoy matches and common contaminants have been removed.
aUniProt ID of human protein or viral protein name.
[b] $-10\times\log_{10}(P)$, where P is the absolute probability.

Protein[a]	***Description***	***Mascot Score[b]***	***Peptide Spectrum Matches***	***Peptide Sequences***	***% Sequence Coverage***
NP	NP of influenza A/WSN/33 virus	669	38	27	62.9
PB2	PB2 of influenza A/WSN/33 virus	147	5	5	10.4
PA	PA of influenza A/WSN/33 virus	86	5	5	14.8
PB1	PB1 of influenza A/WSN/33 virus	102	2	2	9.8
P00338	L-lactate dehydrogenase A chain	89	2	2	14.2
P08107	Heat shock 70 kDa protein 1A/1B	88	2	2	14.4
P17066	Heat shock 70 kDa protein 6	72	1	1	7.3
P62701	40S ribosomal protein S4, X isoform	50	1	1	10.6
Q53H96	Pyrroline-5-carboxylate reductase 3	48	1	1	4
Q08188	Protein-glutamine gamma-glutamyltransferase E	44	1	1	1.3
Q9UDR5	Alpha-aminoadipic semialdehyde synthase, mitochondrial	44	2	1	2.7
O43143	Putative pre-mRNA-splicing factor ATP-dependent RNA helicase DHX15	42	2	2	3.8
P34931	Heat shock 70 kDa protein 1-like	39	1	1	9.2
P12036	Neurofilament heavy polypeptide	35	1	1	3
Q8IYT1	Protein FAM71A	35	2	1	1
P60709	Actin, cytoplasmic 1	35	1	1	6.7
Q4G0X9	Coiled-coil domain-containing protein 40	33	1	1	0.4
Q9NUL7	Probable ATP-dependent RNA helicase DDX28	32	1	1	2.6

P54652	Heat shock-related 70 kDa protein 2	31	1	1	6.9
Q14119	Vascular endothelial zinc finger 1	31	1	1	3.6
P05141	ADP/ATP translocase 2	31	1	1	2.3
O75152	Zinc finger CCCH domain-containing protein 11A	29	1	1	1.5
P08670	Vimentin	28	1	1	3.4
O15020	Spectrin beta chain, brain 2	28	1	1	0.5
Q9NQX0	Putative histone-lysine N-methyltransferase PRDM6	26	1	1	0.8
P55196	Afadin	24	1	1	0.3
Q07283	Trichohyalin	24	2	2	0.8
Q9HCE3	Zinc finger protein 532	24	1	1	1.1
Q92949	Forkhead box protein J1	24	1	1	17.1
O43809	Cleavage and polyadenylation specificity factor subunit 5	22	1	1	6.6
B1AK53	Espin	21	1	1	0.6
Q8NDZ9	Putative uncharacterized protein LOC439951	15	1	1	3.3
Q8WVV9	Heterogeneous nuclear ribonucleoprotein L-like	0	1	1	1.3

Appendix D.2: Mass spectrometry of vRNP – Experiment 2

Mascot score, number of peptide spectrum matches, number of corresponding peptide sequences and % sequence coverage for each identification. Decoy matches and common contaminants have been removed.
aUniProt ID of human protein or viral protein name.
[b] $-10\times\log_{10}(P)$, where P is the absolute probability.

Protein[a]	***Description***	***Mascot Score[b]***	***Peptide Spectrum Matches***	***Peptide Sequences***	***% Sequence Coverage***
NP	NP of influenza A/WSN/33 virus	362	20	15	46.4
PB2	PB2 of influenza A/WSN/33 virus	131	7	7	12.4
P07195	L-lactate dehydrogenase B chain	64	3	3	9.3
PA	PA of influenza A/WSN/33 virus	61	3	3	5.2
Q8N684	Cleavage and polyadenylation specificity factor subunit 7	49	1	1	5.7
P11142	Heat shock cognate 71 kDa protein	44	2	2	7.7
Q02413	Desmoglein-1	40	1	1	0.7
PB1	PB1 of influenza A/WSN/33 virus	36	3	3	6.5
Q12882	Dihydropyrimidine dehydrogenase [NADP+]	31	1	1	0.7
P15924	Desmoplakin	28	1	1	0.4
P11387	DNA topoisomerase 1	28	4	4	6
Q9BX26	Synaptonemal complex protein 2	26	1	1	0.4
Q6UXN9	WD repeat-containing protein 82	25	1	1	1.9
P06746	DNA polymerase beta	25	1	1	1.8
Q969P6	DNA topoisomerase I, mitochondrial	24	1	1	2.3
O00410	Importin-5	22	1	1	0.5
P22626	Heterogeneous nuclear ribonucleoproteins A2/B1	20	1	1	5.1
Q7Z417	Nuclear fragile X mental retardation-interacting protein 2	18	1	1	1.9

Q6EMK4	Vasorin	18	1	1	1
Q6PEY2	Tubulin alpha-3E chain	17	1	1	6.2
P62269	40S ribosomal protein S18	16	1	1	7.2
P02768	Serum albumin	15	1	1	2.8
Q9H0G5	Coiled-coil domain-containing protein 55	15	1	1	2.2
P12036	Neurofilament heavy polypeptide	13	1	1	0.8
Q9H7H0	Methyltransferase-like protein 17, mitochondrial	13	1	1	3.1

Appendix D.3: Mass spectrometry of vRNP – Experiment 3

Mascot score, number of peptide spectrum matches, number of corresponding peptide sequences and % sequence coverage for each identification. Decoy matches and common contaminants have been removed.
aUniProt ID of human protein or viral protein name.
[b] $-10\times\log_{10}(P)$, where P is the absolute probability.

Protein[a]	***Description***	***Mascot Score[b]***	***Peptide Spectrum Matches***	***Peptide Sequences***	***% Sequence Coverage***
NP	NP of influenza A/WSN/33 virus	489	40	24	48.4
PB2	PB2 of influenza A/WSN/33 virus	456	22	21	34.7
PA	PA of influenza A/WSN/33 virus	206	14	13	28.4
P68871	Haemoglobin subunit beta	112	4	4	29.9
Q71U36	Tubulin alpha-1A chain	94	2	2	10
P04792	Heat shock protein beta-1	79	2	2	16.6
Q08188	Protein-glutamine gamma-glutamyltransferase E	72	2	2	6.8
PB1	PB1 of influenza A/WSN/33 virus	69	6	6	13.9
P05089	Arginase-1	67	3	2	8.4
Q13748	Tubulin alpha-3C/D chain	64	1	1	8
P60709	Actin, cytoplasmic 1	58	3	2	9.9
P69905	Haemoglobin subunit alpha	54	7	5	28.2
P14923	Junction plakoglobin	52	1	1	5
Q02413	Desmoglein-1	51	1	1	2.9
Q8WWM7	Ataxin-2-like protein	51	2	2	3.4
P02042	Haemoglobin subunit delta	50	2	2	15
A5A3E0	POTE ankyrin domain family member F	49	1	1	2.5
P05109	Protein S100-A8	49	2	2	24.7

Q8WXF1	Paraspeckle component 1	46	1	1	4.6
Q13835	Plakophilin-1	45	1	1	2
P04406	Glyceraldehyde-3-phosphate dehydrogenase	43	4	3	12.2
P08107	Heat shock 70 kDa protein 1A/1B	42	3	3	8.1
P34931	Heat shock 70 kDa protein 1-like	41	1	1	6.4
P11142	Heat shock cognate 71 kDa protein	40	2	2	7
P12273	Prolactin-inducible protein	40	1	1	8.2
P06702	Protein S100-A9	38	3	3	35.1
P61626	Lysozyme C	37	2	2	23.6
P68366	Tubulin alpha-4A chain	36	1	1	6.5
Q86VP1	Tax1-binding protein 1	35	1	1	1.3
P20930	Filaggrin	35	1	1	0.5
Q06830	Peroxiredoxin-1	31	1	1	5.5
Q8TF72	Protein Shroom3	30	1	1	1.4
P07195	L-lactate dehydrogenase B chain	28	3	3	12.9
Q8TE73	Dynein heavy chain 5, axonemal	28	1	1	0.1
Q8IYT1	Protein FAM71A	27	1	1	1
Q5QNW6	Histone H2B type 2-F	25	1	1	56.3
Q9H5Q4	Dimethyladenosine transferase 2, mitochondrial	25	1	1	1.5
Q15828	Cystatin-M	24	1	1	7.4
O94763	Unconventional prefoldin RPB5 interactor	22	1	1	1.1
O00410	Importin-5	22	1	1	0.5
Q3MHD2	Protein LSM12 homolog	22	1	1	6.7
Q8NDA2	Hemicentin-2	21	1	1	0.1
P68371	Tubulin beta-2C chain	21	1	1	9.7
P04083	Annexin A1	21	1	1	2.3

Q8TAL5	Uncharacterized protein C9orf43	21	1	1	1.5
Q4G0N8	Sodium/hydrogen exchanger 10	20	1	1	0.7
P31944	Caspase-14	20	1	1	5
Q96P63	Serpin B12	20	1	1	6.2
P00338	L-lactate dehydrogenase A chain	18	1	1	9.6
P17612	cAMP-dependent protein kinase catalytic subunit alpha	17	1	1	2.6
P62805	Histone H4	17	1	1	17.5
Q8IXN7	N-acetylaspartyl-glutamate synthetase A	17	1	1	1.5
Q9Y3B4	Pre-mRNA branch site protein p14	15	1	1	6.4
P17066	Heat shock 70 kDa protein 6	14	1	1	5.1
O00423	Echinoderm microtubule-associated protein-like 1	14	1	1	1.5
Q9NPH0	Lysophosphatidic acid phosphatase type 6	14	1	1	4.2
Q8N998	Coiled-coil domain-containing protein 89	14	1	1	4.3
Q9UK08	Guanine nucleotide-binding protein G(I)/G(S)/G(O) subunit gamma-8	13	1	1	10

Appendix E: Raw SINQ scores for identified proteins

SINQ scores of identified proteins in PB2-Strep and WT (negative control) samples. Raw data from three experiments are shown. Decoy matches and common contaminants have been removed.
[a]UniProt ID of human protein or viral protein name.

		Experiment 1		Experiment 2		Experiment 3	
Protein[a]	***Description***	***PB2-Strep***	***WT***	***PB2-Strep***	***WT***	***PB2-Strep***	***WT***
HA	HA of influenza A/WSN/33	8.928E-07	6.33E-07	2.87E-06	4.59E-06	1.71E-06	2.97E-06
M1	M1 of influenza A/WSN/33	1.229E-06	1.1E-05	5.1E-06	1.88E-05	1.08E-06	4.55E-05
NA	NA of influenza A/WSN/33	1.626E-07	4.95E-08	3.24E-07	1.15E-07	5.16E-07	
NP	NP of influenza A/WSN/33	0.0009755	7.56E-05	0.001128	4.57E-05	0.001287	4.65E-05
NS1	NS1 of influenza A/WSN/33	3.973E-06	5.45E-05	2.92E-05	0.000182	1.08E-05	0.000103
PA	PA of influenza A/WSN/33	0.0001127	8.57E-07	7.93E-05	2.91E-06	6.67E-05	5.68E-07
PB1	PB1 of influenza A/WSN/33	0.00012	1.16E-06	0.000115	1.9E-06	0.000101	1.08E-06
PB2-Strep	PB2-Strep of influenza A/WSN/33	0.0001574	3.86E-06	0.000149	5.17E-06	0.000123	1.47E-06
O00267	Transcription elongation factor SPT5	1.927E-07		8.67E-08	1.12E-07	1.25E-07	3.85E-07
O00410	Importin-5	2.349E-06		2.31E-06		1.99E-06	
O00505	Importin subunit alpha-4	8.294E-07		9.23E-07	1.5E-07	6.94E-07	
O00571	ATP-dependent RNA helicase DDX3X	3.957E-07	1.16E-06	4.69E-07	5.79E-06	1.17E-07	1.07E-05
O00629	Importin subunit alpha-3	6.319E-07		6.18E-07	7.28E-08	5.1E-07	
O00743	Serine/threonine-protein phosphatase 6 catalytic subunit	0.0000017		7.44E-07		9.83E-07	
O00763	Acetyl-CoA carboxylase 2	3.268E-07	6.09E-07	2.34E-08	4.4E-07		
O14654	Insulin receptor substrate 4	1.959E-07		2.84E-07	3.87E-08	3.53E-07	
O14979	Heterogeneous nuclear ribonucleoprotein D-like		1.03E-06	3.18E-08	6.36E-07	4.17E-09	1.07E-06
O43164	E3 ubiquitin-protein ligase Praja-2	1.766E-07		4.66E-07		3.73E-07	
O43390	Heterogeneous nuclear ribonucleoprotein R	7.728E-08	8.62E-07	6.16E-08	1.14E-06	1.2E-08	3.11E-06
O43865	Putative adenosylhomocysteinase 2	1.655E-08		8.83E-08		1.1E-07	
O60506	Heterogeneous nuclear ribonucleoprotein Q	1.158E-08	3.44E-07	5.56E-07	5.87E-06	2.77E-08	1.39E-05
O60518	Ran-binding protein 6	2.086E-08					
O60684	Importin subunit alpha-7	2.27E-08		5.22E-07	4.5E-08	4.09E-07	6.58E-08

O60814	Histone H2B type 1-K	2.081E-07	4.35E-05	4.8E-07	4.4E-06	1.72E-07	5.54E-06
O60884	DnaJ homolog subfamily A member 2	1.257E-07		2.48E-06	4.18E-08	1.48E-06	
O75153	Clustered mitochondria protein homolog	5.577E-08		4.91E-08		5.78E-08	
O75190	DnaJ homolog subfamily B member 6	1.871E-07		6.01E-07		1.41E-06	
O75367	Core histone macro-H2A.1		3.23E-07				
O75531	Barrier-to-autointegration factor		8.54E-08	7.24E-07	1.03E-05	1.3E-07	3.2E-06
O95831	Apoptosis-inducing factor 1, mitochondrial	1.311E-07		4.48E-07	1.81E-07	3.62E-07	
P00915	Carbonic anhydrase 1	7.766E-08	9.99E-08				
P00918	Carbonic anhydrase 2	4.444E-08	5.68E-08				
P02545	Prelamin-A/C		1.89E-08	1.08E-06	1.14E-05	9.63E-08	8.37E-06
P04406	Glyceraldehyde-3-phosphate dehydrogenase		1.2E-06	5.75E-07	3.82E-06	6.63E-07	1.75E-06
P05141	ADP/ATP translocase 2	2.443E-06	1.63E-06	8.52E-07	1.96E-06	6.11E-07	8.36E-07
P05165	Propionyl-CoA carboxylase alpha chain, mitochondrial	1.311E-05	3.42E-05	8.56E-06	5.87E-05	6.25E-06	4.35E-05
P05166	Propionyl-CoA carboxylase beta chain, mitochondrial	1.762E-05	3.77E-05	6.5E-06	5.08E-05	8.08E-06	5.08E-05
P06748	Nucleophosmin	9.709E-08	7.96E-06	4.52E-06	8.15E-05	9.96E-07	3.23E-05
P07437	Tubulin beta chain	5.747E-07	5.33E-08	9.56E-06	3.7E-06	4.27E-06	1.73E-06
P08107	Heat shock 70 kDa protein 1A/1B	8.283E-06	2.7E-06	1.49E-05	1.61E-05	1.22E-05	1.27E-05
P08670	Vimentin		1.88E-06				
P09651	Heterogeneous nuclear ribonucleoprotein A1	3.048E-06	1.07E-05	1.1E-05	6.32E-05	4.88E-06	9.33E-05
P09874	Poly [ADP-ribose] polymerase 1	2.577E-06	8.27E-06	8.78E-07	5.88E-06	7.44E-08	1.25E-05
P0C0S5	Histone H2A.Z		3.05E-06	1.64E-07	9.27E-07		
P10155	60 kDa SS-A/Ro ribonucleoprotein	2.067E-07		8.08E-08		3.63E-07	
P10809	60 kDa heat shock protein, mitochondrial	9.024E-09		2.73E-06	9.1E-07	2.15E-06	3.62E-08
P11021	78 kDa glucose-regulated protein		5.99E-07	6.47E-07	2.31E-06	5.38E-07	1.24E-06
P11142	Heat shock cognate 71 kDa protein	1.383E-05	3.56E-06	1.42E-05	8.44E-06	1.11E-05	6.07E-06
P11182	Branched-chain alpha-keto acid dehydrogenase complex component E2	1.906E-06	1.27E-05	4.23E-06	2E-05	2.62E-06	2.21E-05
P11387	DNA topoisomerase 1		1.75E-07	9.89E-08	3.46E-06		2.33E-06
P11388	DNA topoisomerase 2-alpha	3.12E-07	5.76E-06	1.78E-06	1.6E-05	6.11E-07	1.29E-05
P11498	Pyruvate carboxylase, mitochondrial	8.731E-06	2.88E-05	1.71E-06	1.36E-05	1.4E-06	1.05E-05
P12236	ADP/ATP translocase 3	3.426E-06	3.69E-08	1.98E-07	1.64E-07	4.37E-08	7.17E-07

P12956	X-ray repair cross-complementing protein 6	1.163E-07	1.45E-06	3.68E-07	5.24E-06	4.33E-08	8.73E-06
P13010	X-ray repair cross-complementing protein 5	3.164E-07	2.59E-06	2.75E-07	3.83E-06	7.19E-08	6.12E-06
P14678	Small nuclear ribonucleoprotein-associated proteins B and B'		5.18E-07	1.81E-07	1.4E-06	2.2E-08	4.92E-07
P14866	Heterogeneous nuclear ribonucleoprotein L	6.51E-07	7.59E-06	2.8E-06	3.14E-05	6.77E-07	2.83E-05
P15880	40S ribosomal protein S2	1.077E-06	2.46E-06	1.97E-06	2.09E-06	1.75E-06	1.98E-06
P16104	Histone H2AX	2.981E-06	2.87E-05		3.11E-08		
P16403	Histone H1.2	8.479E-07	5.66E-06	2.61E-07	1.75E-06	2.98E-07	1.03E-06
P17612	cAMP-dependent protein kinase catalytic subunit alpha	1.862E-07	1.14E-07	1.44E-07		1.31E-08	
P17844	Probable ATP-dependent RNA helicase DDX5	4.979E-09	5.62E-07	3.23E-07	3.66E-06	1.77E-07	5.99E-06
P17987	T-complex protein 1 subunit alpha	5.027E-07		5.64E-07		7.29E-07	
P19338	Nucleolin	1.163E-08	2.12E-06	4.92E-07	3.02E-06	2.86E-07	3.18E-06
P20700	Lamin-B1	2.816E-07	1.64E-06	2.58E-06	2.35E-05	2.34E-07	2.6E-05
P22061	Protein-L-isoaspartate(D-aspartate) O-methyltransferase		1.59E-06	6.5E-07	1.01E-05	2.84E-07	2.41E-06
P22087	rRNA 2'-O-methyltransferase fibrillarin		1.74E-07	1.11E-07	2.46E-06	2.99E-08	2.35E-06
P22626	Heterogeneous nuclear ribonucleoproteins A2/B1	5.596E-06	7.16E-05	8.33E-06	0.000223	7.06E-06	0.000135
P22694	cAMP-dependent protein kinase catalytic subunit beta	8.702E-09		7.96E-09		2.74E-07	
P23246	Splicing factor, proline- and glutamine-rich		1.66E-07	3.65E-07	2.19E-06	3.07E-08	4.83E-06
P23396	40S ribosomal protein S3	5.056E-06	8.44E-06	3.58E-06	1.12E-05	4.16E-06	5.8E-06
P26196	Probable ATP-dependent RNA helicase DDX6	1.27E-07	9.2E-07	1.74E-07	5.14E-06	2.37E-07	6.33E-06
P26368	Splicing factor U2AF 65 kDa subunit		2.27E-07	2.07E-07	2.4E-06		5.11E-06
P26599	Polypyrimidine tract-binding protein 1	9.447E-08	6.96E-06	9.84E-07	1.54E-05	1.77E-07	1.75E-05
P26641	Elongation factor 1-gamma	7.107E-08		1.51E-07	1.07E-06	1.15E-07	
P27708	CAD protein	6.754E-08		8.07E-08	2.03E-08	9.33E-08	
P30050	60S ribosomal protein L12	3.98E-07	1.8E-06	4.74E-06	4.12E-05	6.57E-07	4.22E-05
P31689	DnaJ homolog subfamily A member 1	5.794E-07		2.04E-06	1.5E-07	1.17E-06	3.11E-07
P31942	Heterogeneous nuclear ribonucleoprotein H3	1.987E-08	1.23E-06	6.57E-07	7.11E-06	1.56E-07	2.17E-06
P31943	Heterogeneous nuclear ribonucleoprotein H	5.95E-08	1.29E-06	5.77E-07	2.22E-06	7.66E-07	7.85E-06
P32969	60S ribosomal protein L9	9.301E-08	1.71E-07	2.15E-07	0.000012	1.34E-07	1.76E-05
P34931	Heat shock 70 kDa protein 1-like	5.774E-08					
P35268	60S ribosomal protein L22		4.39E-06	2.24E-06	1.64E-05	4.36E-07	1.05E-05
P38159	RNA-binding motif protein, X chromosome	8.015E-08	5.88E-06	3.22E-07	4.5E-06	2.65E-07	2.46E-06

P38646	Stress-70 protein, mitochondrial	1.923E-07	6.01E-06	3.8E-06	1.01E-05	2.3E-06	7.09E-06
P38919	Eukaryotic initiation factor 4A-III		5.79E-07	2.05E-09	8.54E-07		1.19E-06
P40227	T-complex protein 1 subunit zeta	2.467E-07		8.07E-07		4.8E-07	
P40939	Trifunctional enzyme subunit alpha, mitochondrial	1.912E-06	3.03E-07	1.32E-06	3.25E-06	9.64E-07	1.83E-06
P41159	Leptin	1.053E-07	3.09E-07				
P42166	Lamina-associated polypeptide 2, isoform alpha		3.76E-07				
P42677	40S ribosomal protein S27	3.002E-06	4.01E-06	9.92E-06	9.03E-06	1.2E-05	2.7E-06
P43243	Matrin-3	1.004E-08	1.53E-06	3.95E-07	3.63E-06	2.06E-07	2.7E-06
P45880	Voltage-dependent anion-selective channel protein 2		1.28E-06	6.26E-07	3.66E-06	5.22E-07	2.33E-06
P46013	Antigen KI-67		1.13E-07	3.59E-09	4.66E-08		
P46781	40S ribosomal protein S9	5.184E-07	6.93E-07	8.9E-07	3.71E-06	5.07E-07	2.27E-06
P48643	T-complex protein 1 subunit epsilon	1.627E-07		5.6E-07		5E-07	
P49368	T-complex protein 1 subunit gamma	2.634E-07		1.08E-06		5.87E-07	
P49411	Elongation factor Tu, mitochondrial	9.824E-07	1.57E-08	8.1E-08		2.05E-07	
P49916	DNA ligase 3		2.86E-07	1.36E-08	2.41E-07		1.99E-07
P50402	Emerin	1.79E-07		2.17E-06	6.31E-07	1.69E-06	
P50991	T-complex protein 1 subunit delta	1.074E-07		1.16E-06		9.79E-07	4.3E-08
P51571	Translocon-associated protein subunit delta	3.794E-07		2.15E-07		3.31E-07	
P51991	Heterogeneous nuclear ribonucleoprotein A3	1.052E-08	3.03E-06	8.33E-07	1.06E-05	1.75E-07	1.69E-05
P52272	Heterogeneous nuclear ribonucleoprotein M	1.743E-07	3.23E-06	1.91E-07	1.38E-06	2.68E-08	2.1E-06
P52292	Importin subunit alpha-1		1.64E-06	2.74E-07	4.33E-06	1.14E-07	3.04E-06
P52294	Importin subunit alpha-5	2.269E-07		1.88E-07		8.17E-08	
P52597	Heterogeneous nuclear ribonucleoprotein F		2.28E-08	5.63E-07	1.08E-06	5.41E-07	4.79E-07
P55084	Trifunctional enzyme subunit beta, mitochondrial	1.839E-06	2.72E-08	1.58E-06	3.45E-06	8.03E-07	2.54E-06
P55884	Eukaryotic translation initiation factor 3 subunit B		2.91E-08			5.99E-09	
P61247	40S ribosomal protein S3a	1.265E-07	2.03E-06	8.21E-07	1.72E-06	7.97E-07	3.53E-07
Q5T6W5	Heterogeneous nuclear ribonucleoprotein K	6.531E-08	3.07E-06	4.36E-08	2.35E-07		5.81E-07
P62081	40S ribosomal protein S7	1.679E-07	9.66E-08	1.16E-06	2.17E-05	2.23E-07	3.34E-05
P62140	Serine/threonine-protein phosphatase PP1-beta catalytic subunit	1.701E-08	7.49E-07	2.23E-08	2.05E-07		3.79E-07
P62241	40S ribosomal protein S8	7.112E-07	2.54E-06	3.8E-07	2.08E-06	5.72E-07	1.04E-06

P62244	40S ribosomal protein S15a	7.33E-07	7.32E-06	1.46E-06	1.03E-05	8.15E-07	1.04E-05
P62249	40S ribosomal protein S16	1.264E-06	2.51E-06	1.61E-06	7.5E-06	2.57E-06	3.98E-06
P62263	40S ribosomal protein S14	1.152E-07	2.07E-06	3E-06	1.28E-05	4.34E-06	8.24E-06
P62266	40S ribosomal protein S23		1.12E-07			1.21E-07	
P62277	40S ribosomal protein S13		1.09E-07	5.23E-07	1.36E-06	3.84E-07	4.39E-07
P62280	40S ribosomal protein S11	3.438E-06	3.01E-06	9.38E-07	1.34E-06	9.94E-07	9.35E-07
P62314	Small nuclear ribonucleoprotein Sm D1	1.349E-06	2.39E-07	5.29E-08	3.83E-06		2.13E-05
P62701	40S ribosomal protein S4, X isoform	8.853E-07	1.37E-05	2.58E-06	1.31E-05	2.01E-06	1.81E-05
P62753	40S ribosomal protein S6	1.858E-07	4.57E-07	3.18E-07	5.66E-07	4.69E-07	5.08E-07
P62805	Histone H4	5.7E-07	9.37E-05	4.06E-07	1.3E-05	1.94E-07	1.4E-05
P62829	60S ribosomal protein L23	4.833E-06	6.65E-06	5.78E-06	1.77E-05	4.8E-06	7.69E-06
P62899	60S ribosomal protein L31	1.632E-07		9.38E-07	1.53E-06	7.35E-08	1.99E-06
P62913	60S ribosomal protein L11	4.667E-07	1.68E-06	1.87E-07	4.19E-06	3.21E-07	3.38E-06
P62987	Ubiquitin-60S ribosomal protein L40	5.933E-06	2.69E-06	4.02E-06	2.97E-06		
P62995	Transformer-2 protein homolog beta	8.357E-08	4.49E-07	7.68E-09	1.01E-06		1.39E-06
P63173	60S ribosomal protein L38	3.985E-07	2.1E-06	3.1E-06	2.3E-06	9.6E-07	1.55E-05
P63261	Actin, cytoplasmic 2	3.057E-07	1.01E-05				
P67809	Nuclease-sensitive element-binding protein 1	5.384E-08	7.16E-08	5.04E-07	9.16E-07	3.36E-07	6.83E-08
P68104	Elongation factor 1-alpha 1	4.513E-06	6.89E-06	2.4E-06	1.99E-05	1.84E-06	1.1E-05
P68363	Tubulin alpha-1B chain	1.016E-07	1.22E-08	4E-08	3.42E-07	2.6E-07	6.02E-07
P68371	Tubulin beta-4B chain	1.102E-06	5.81E-07	2.5E-06	9.21E-07	8.25E-07	6.97E-08
P68431	Histone H3.1		2.28E-06				
P78527	DNA-dependent protein kinase catalytic subunit	3.258E-09		3.63E-08	9.08E-08	2.96E-08	4.17E-08
P81605	Dermcidin	1.737E-06	2.91E-07	4.01E-07	2.35E-06	7.03E-06	1.31E-05
P84098	60S ribosomal protein L19	5.472E-08	9.14E-08	7.79E-07	1.37E-06	7.2E-07	1.13E-07
P84103	Serine/arginine-rich splicing factor 3	9.121E-08	2.27E-06	1.22E-06	1.53E-05		7.45E-06
P84243	Histone H3.3		7.59E-07				
Q00325	Phosphate carrier protein, mitochondrial	1.225E-06		1.88E-07	2.67E-07		
Q00610	Clathrin heavy chain 1	3.122E-09	2.23E-08	3.75E-08	6.35E-07	3.38E-08	1.79E-07
Q00839	Heterogeneous nuclear ribonucleoprotein U	1.546E-07	2.9E-06	5.86E-07	6.31E-06	1.94E-07	7.3E-06
Q02878	60S ribosomal protein L6	1.435E-08	5.36E-08				

Q02880	DNA topoisomerase 2-beta	6.495E-07	5.43E-06	9.57E-07	1.13E-05	4.15E-07	1.17E-05
Q02978	Mitochondrial 2-oxoglutarate/malate carrier protein	1.07E-07	8.63E-08				
Q03252	Lamin-B2		5.19E-08	1.68E-06	1.82E-05	1.3E-07	1.27E-05
Q07666	KH domain-containing, RNA-binding, signal transduction-associated protein 1		2.45E-08	8.61E-07	1.1E-05	8.62E-07	3.7E-06
Q07955	Serine/arginine-rich splicing factor 1		2.85E-06	2.05E-06	1.35E-05	1.29E-06	6.3E-06
Q08211	ATP-dependent RNA helicase A	8.054E-08	7.05E-07	4.78E-07	3.61E-06	2.06E-07	5.99E-06
Q08945	FACT complex subunit SSRP1	8.103E-07	3.27E-06	1.64E-06	1.05E-05	1.85E-07	2.08E-05
Q12899	Tripartite motif-containing protein 26	2.441E-07					
Q12905	Interleukin enhancer-binding factor 2	9.402E-08	3.44E-06	8.61E-07	6.12E-06	5.55E-08	9.84E-06
Q12906	Interleukin enhancer-binding factor 3	1.712E-08	1.34E-06	4.73E-07	7.33E-06	7.11E-08	5.72E-06
Q13085	Acetyl-CoA carboxylase 1	1.167E-05	4.17E-05	1.02E-06	1.08E-05	1.01E-06	1.58E-05
Q13151	Heterogeneous nuclear ribonucleoprotein A0	5.213E-08	1.14E-06	2.57E-07	5.23E-06		4.88E-06
Q13509	Tubulin beta-3 chain	4.148E-08		1.17E-07	3.07E-08	6.54E-08	
Q14103	Heterogeneous nuclear ribonucleoprotein D0		3.41E-06	9.3E-07	1.02E-05	8.84E-08	6.3E-06
Q14257	Reticulocalbin-2	7.331E-08		3.31E-06		3.11E-06	
Q14676	Mediator of DNA damage checkpoint protein 1	3.684E-08	1.8E-06	5.16E-07	3.68E-06	1.65E-08	5.35E-06
Q14974	Importin subunit beta-1	3.398E-08	1.84E-08	4.56E-07	1.1E-06	1.62E-07	1.69E-06
S4R341	Nucleolar and coiled-body phosphoprotein 1		4.29E-08		9.48E-08		
Q14980	Nuclear mitotic apparatus protein 1		1.73E-08				
Q15233	Non-POU domain-containing octamer-binding protein	3.248E-08	4.58E-07	3.09E-07	4.09E-06	8E-08	7.11E-06
Q15287	RNA-binding protein with serine-rich domain 1		7.1E-09				
Q15366	Poly(rC)-binding protein 2		1.25E-06	3.23E-07	3.93E-06	6.29E-08	2.85E-06
Q15393	Splicing factor 3B subunit 3		1.48E-07	1.57E-08	6.06E-08	2.8E-08	
Q15424	Scaffold attachment factor B1	6.289E-08	8.9E-07	4.3E-07	4.7E-06	1.48E-07	5.15E-06
Q15717	ELAV-like protein 1		8.71E-06	7.48E-07	9.92E-06	3.6E-07	1.02E-05
Q16531	DNA damage-binding protein 1	1.107E-06	3.98E-07	9.74E-07	8.85E-07	6.92E-07	2.43E-07
Q16629	Serine/arginine-rich splicing factor 7	3.093E-08	7.72E-08	5.87E-08	1.63E-06	6.77E-08	1.98E-06
Q16777	Histone H2A type 2-C	2.248E-06	4.45E-05				
Q1KMD3	Heterogeneous nuclear ribonucleoprotein U-like protein 2		1.21E-07				
Q3MHD2	Protein LSM12 homolog	1.032E-06	5.13E-06	4.38E-07	9.96E-06	1.7E-06	5.14E-06

Q5H9R7	Serine/threonine-protein phosphatase 6 regulatory subunit 3	9.773E-07		3.97E-07		3.99E-07	
Q5JTC6	APC membrane recruitment protein 1	1.103E-07		3.75E-08			
Q5TAQ9	DDB1- and CUL4-associated factor 8	8.057E-08		5.47E-07	8.43E-08	4.55E-07	
Q71DI3	Histone H3.2		7.79E-06				
Q71U36	Tubulin alpha-1A chain	1.301E-07	3.12E-09	3.53E-08	5.44E-08		
Q7L576	Cytoplasmic FMR1-interacting protein 1	1.446E-07	9.49E-07	1.27E-07	1.44E-06	2.84E-08	2.78E-07
Q7Z417	Nuclear fragile X mental retardation-interacting protein 2		2.19E-07	3.9E-07	2.43E-06	2.05E-07	4.44E-07
Q7Z6Z7	E3 ubiquitin-protein ligase HUWE1	6.549E-08		1.38E-07	1.3E-08	6.12E-08	
Q7Z7K6	Centromere protein V		6.89E-08				
Q8IZP0	Abl interactor 1		1.06E-06	1.49E-07	1.27E-06	7.58E-08	9.14E-07
Q8WWM7	Ataxin-2-like protein	3.104E-07	5.35E-06	6.04E-07	3.7E-06	1.27E-06	4.18E-06
Q92499	ATP-dependent RNA helicase DDX1		4.75E-07	1.58E-08	7.94E-07		6.98E-07
Q92841	Probable ATP-dependent RNA helicase DDX17		4.28E-07	3.64E-07	1.37E-06	1.47E-07	2.01E-06
Q96D09	G-protein coupled receptor-associated sorting protein 2	4.305E-08		5.52E-07		4.18E-07	
Q96EY1	DnaJ homolog subfamily A member 3, mitochondrial	7.543E-08		3.38E-07	1.31E-07	1.98E-07	
Q96HN2	Putative adenosylhomocysteinase 3	4.207E-07		9.01E-08		1.78E-07	
Q96PK6	RNA-binding protein 14		7.27E-07		9.45E-07	9.46E-09	3.97E-07
Q96RQ3	Methylcrotonoyl-CoA carboxylase subunit alpha, mitochondrial	1.628E-06	7.89E-06	4.86E-07	4.01E-06	3.97E-07	4.34E-06
Q99623	Prohibitin-2	2.172E-08	7.06E-08	9.47E-07	4.12E-06	5.86E-07	1.99E-06
Q99832	T-complex protein 1 subunit eta	1.115E-06		1.13E-06		1.05E-06	
Q9BQ70	Transcription factor 25	1.839E-08		4.24E-07		7.57E-08	
Q9BQE3	Tubulin alpha-1C chain	3.596E-07	1.45E-07	2.26E-07	2.11E-08	2.13E-07	
Q9BVA1	Tubulin beta-2B chain	3.498E-08		3.42E-07	4.8E-08	7.39E-07	
Q9BY77	Polymerase delta-interacting protein 3		1.06E-06	2.17E-07	2.32E-06	1.89E-07	1.12E-06
Q9H0S4	Probable ATP-dependent RNA helicase DDX47		2.91E-08	3.58E-07	2.86E-06		3.28E-06
Q9HAV7	GrpE protein homolog 1, mitochondrial		5.63E-06	1.35E-06	1.42E-05	9.46E-07	7.06E-06
Q9HCC0	Methylcrotonoyl-CoA carboxylase beta chain, mitochondrial	5.077E-06	1.25E-05	2.21E-06	1.57E-05	1.19E-06	1.78E-05
Q9HCD5	Nuclear receptor coactivator 5	1.177E-07	1.17E-06	6.66E-07	5.53E-06	4.8E-07	7.83E-06
Q9NW64	Pre-mRNA-splicing factor RBM22		2.18E-08				
Q9NZI8	Insulin-like growth factor 2 mRNA-binding protein 1	4.228E-08	1.05E-06	3.39E-07	2.35E-06	2.1E-07	9.54E-07
Q9UJS0	Calcium-binding mitochondrial carrier protein Aralar2	3.475E-08		2.28E-07		2.77E-07	

Q9UKD2	mRNA turnover protein 4 homolog		1.84E-06	1.34E-06	1.1E-05		1.88E-05
S4R3H4	Apoptotic chromatin condensation inducer in the nucleus	2.892E-08	9.73E-08	2.6E-07	1.56E-06	2.09E-08	1.95E-06
Q9UNK9	Protein angel homolog 1	6.009E-08		2.98E-07		1.95E-07	
Q9Y2A7	Nck-associated protein 1	1.403E-07	6.24E-07	2.38E-07	1.65E-06	1.83E-07	7.03E-07
Q9Y4B6	Protein VPRBP	7.165E-07		3.88E-07		2.13E-07	
Q9Y5A9	YTH domain family protein 2	2.057E-08		3.13E-07		4.16E-07	
Q9Y5B9	FACT complex subunit SPT16	3.639E-07	8.17E-06	1.44E-06	1.07E-05	1.25E-07	1.26E-05
Q9Y5V3	Melanoma-associated antigen D1	1.039E-06		6.92E-07	4.87E-09	5.2E-07	
D6R9P3	Heterogeneous nuclear ribonucleoprotein A/B		5.57E-07	6.49E-07	5.75E-06	4.07E-07	2.48E-06
K7EII5	Acetyl-CoA carboxylase 1 (Fragment)		3.46E-06				
M2	Influenza A/WSN/33 M2			3.83E-07	3.07E-06	9.25E-07	
A6NKZ8	Putative tubulin beta chain-like protein ENSP00000290377			2.79E-07		2.25E-07	
B5ME19	Eukaryotic translation initiation factor 3 subunit C-like protein			6.18E-09			
O00148	ATP-dependent RNA helicase DDX39A				5.51E-07		
O00165	HCLS1-associated protein X-1			1.71E-06	4.66E-08	1.19E-07	
O00255	Menin			4.13E-08	9.9E-08		
O00422	Histone deacetylase complex subunit SAP18			8.71E-07	9.39E-06		6.92E-07
O00425	Insulin-like growth factor 2 mRNA-binding protein 3			3.14E-09	1.67E-07	3.56E-09	2.85E-07
O00483	NADH dehydrogenase [ubiquinone] 1 alpha subcomplex subunit 4			2.88E-07	2.02E-07		
O00541	Pescadillo homolog			2.39E-08	1.34E-07		2.42E-07
O15027	Protein transport protein Sec16A			2.06E-08		7.75E-09	
O15160	DNA-directed RNA polymerases I and III subunit RPAC1			1.92E-08			
O15269	Serine palmitoyltransferase 1			4.25E-08			
O15355	Protein phosphatase 1G			2.64E-07		3.1E-07	
O15498	Synaptobrevin homolog YKT6			1.08E-08	2.35E-07		
O43143	Putative pre-mRNA-splicing factor ATP-dependent RNA helicase DHX15			1.82E-09	1.64E-07	1.1E-08	4.19E-07
O43172	U4/U6 small nuclear ribonucleoprotein Prp4				5.77E-07		5.84E-07
O43175	D-3-phosphoglycerate dehydrogenase			3.92E-07	4.05E-07	1.84E-07	9.78E-08
O43290	U4/U6.U5 tri-snRNP-associated protein 1			3.04E-08	1.93E-07		

O43347	RNA-binding protein Musashi homolog 1		8.32E-08		
O43395	U4/U6 small nuclear ribonucleoprotein Prp3		4.22E-07		
O43423	Acidic leucine-rich nuclear phosphoprotein 32 family member C	4.5E-08			
O43719	HIV Tat-specific factor 1	3.18E-08	5.48E-08	9.45E-08	
O43823	A-kinase anchor protein 8	5.95E-08		5.82E-08	
O43837	Isocitrate dehydrogenase [NAD] subunit beta, mitochondrial	1.11E-08			
O43913	Origin recognition complex subunit 5	4.1E-08	1.16E-06		2.51E-06
O43929	Origin recognition complex subunit 4	5.62E-08	1.59E-06		8.73E-07
O60264	Sucrose nonfermenting protein 2 homolog		8.77E-08		
O60832	H/ACA ribonucleoprotein complex subunit 4	2.98E-08	4.84E-07		7.52E-07
O75152	Zinc finger CCCH domain-containing protein 11A	8.93E-09	5.99E-07		
O75400	Pre-mRNA-processing factor 40 homolog A		3.7E-07	4.75E-08	3.66E-08
O75475	PC4 and SFRS1-interacting protein	8.03E-07	6.46E-06		7.49E-06
O75489	NADH dehydrogenase iron-sulfur protein 3, mitochondrial	2E-08			
O75494	Serine/arginine-rich splicing factor 10	3.3E-09	5.29E-07		
O75533	Splicing factor 3B subunit 1	2.45E-08	1.11E-07	4.88E-08	2.77E-08
O75746	Calcium-binding mitochondrial carrier protein Aralar1	2.73E-09		2.2E-08	
O75964	ATP synthase subunit g, mitochondrial	3.95E-07	4.02E-07		
O94776	Metastasis-associated protein MTA2	3.17E-08			
O94906	Pre-mRNA-processing factor 6	2.33E-08	3.55E-07	3.32E-09	7.75E-08
O95071	E3 ubiquitin-protein ligase UBR5	4.85E-08		3.49E-08	
O95218	Zinc finger Ran-binding domain-containing protein 2	6E-08	2.32E-07		
O95232	Luc7-like protein 3	5E-08	3.59E-07		2.17E-07
O95251	Histone acetyltransferase KAT7	1.55E-08	1.13E-07		
O95758	Polypyrimidine tract-binding protein 3		6.31E-09		
O95816	BAG family molecular chaperone regulator 2	2.13E-06		8.65E-07	
O96019	Actin-like protein 6A	4.08E-08	6.53E-07		
O96028	Histone-lysine N-methyltransferase NSD2		6.06E-08		
P00403	Cytochrome c oxidase subunit 2	1.17E-07			
P02788	Lactotransferrin		1.59E-08		
P04279	Semenogelin-1		6.79E-07		

P04350	Tubulin beta-4A chain	2.01E-07	9.93E-09	1.46E-07	
P04637	Cellular tumor antigen p53	9.29E-08	6.29E-08	5.19E-08	3.86E-07
P04843	Ribophorin-1	2.73E-07	2.16E-06	3.56E-07	1.03E-06
P04844	Ribophorin-2		6.58E-08		
P05023	Sodium/potassium-transporting ATPase subunit alpha-1	1.06E-07	9.12E-08	7.52E-08	
P05114	Non-histone chromosomal protein HMG-14	6E-08	8.68E-07		
P05204	Non-histone chromosomal protein HMG-17	2.38E-07	7.09E-07		
P05388	60S acidic ribosomal protein P0	8.49E-07	5.28E-06	2.29E-07	2.14E-06
P05455	Lupus La protein	1.26E-06	5.74E-07	8.02E-07	
P06576	ATP synthase subunit beta, mitochondrial	6.86E-07	3.32E-06	4.08E-07	4.56E-06
P06730	Eukaryotic translation initiation factor 4E	2.73E-07		3.59E-07	
P07237	Protein disulfide-isomerase	4.04E-08		2.66E-08	
P07814	Bifunctional glutamate/proline--tRNA ligase	1.48E-08	1E-07	1.78E-08	
P07900	Heat shock protein HSP 90-alpha	1.18E-07	4.9E-08	2.17E-07	
P07910	Heterogeneous nuclear ribonucleoproteins C1/C2	1.51E-07	1.47E-06	1.07E-07	4.39E-06
P08238	Heat shock protein HSP 90-beta	1.57E-07	1.27E-07	3.54E-08	1.95E-07
P08579	U2 small nuclear ribonucleoprotein B''	1.16E-07	1.78E-07		
P08621	U1 small nuclear ribonucleoprotein 70 kDa	1.26E-07	1.51E-06	1.18E-08	2.96E-06
P08708	40S ribosomal protein S17	3.5E-07	1.93E-06		
P08865	40S ribosomal protein SA	1.07E-06	2.2E-06	7.76E-07	7.57E-07
P09012	U1 small nuclear ribonucleoprotein A	9.43E-08	9.86E-07		1.19E-06
P09622	Dihydrolipoyl dehydrogenase, mitochondrial	1.77E-09	7.97E-07		
P09661	U2 small nuclear ribonucleoprotein A'	1.24E-07	6.54E-07		
P10644	cAMP-dependent protein kinase type I-alpha regulatory subunit	6.78E-07		6E-07	
P11908	Ribose-phosphate pyrophosphokinase 2		9.87E-08		
P11940	Polyadenylate-binding protein 1	1.51E-07	1.01E-06	1.22E-07	3.96E-07
P12268	Inosine-5'-monophosphate dehydrogenase 2	1.04E-07	3.76E-07		
P12273	Prolactin-inducible protein	2.14E-08	1.97E-06	3.37E-08	1.45E-06
P13489	Ribonuclease inhibitor	4.45E-08			
P13639	Elongation factor 2	3.56E-09	4.6E-08	3.29E-09	
P13674	Prolyl 4-hydroxylase subunit alpha-1	3.42E-07		2.42E-07	

P14868	Aspartate--tRNA ligase, cytoplasmic	4.08E-08	1.51E-07		
P14923	Junction plakoglobin	1.82E-08	6.76E-08	7.54E-08	8.97E-07
P15924	Desmoplakin	5.17E-09	2.44E-08	6.8E-08	5.79E-07
P15927	Replication protein A 32 kDa subunit	2.13E-08	7.41E-07		3.81E-07
P16615	Sarcoplasmic/endoplasmic reticulum calcium ATPase 2	4.76E-08	1.54E-07	2.14E-08	
P16989	Y-box-binding protein 3	9.62E-08	1.61E-07	5.32E-08	
P17096	High mobility group protein HMG-I/HMG-Y	2.64E-07	1.03E-06		
P18085	ADP-ribosylation factor 4	1.14E-07	4.51E-07		
P18754	Regulator of chromosome condensation	6.99E-07	6.08E-06		6.5E-06
P21796	Voltage-dependent anion-selective channel protein 1	6.26E-07	3.76E-06	4.95E-07	2.65E-06
P22695	Cytochrome b-c1 complex subunit 2, mitochondrial	2.36E-08	6.59E-08		
P23284	Peptidyl-prolyl cis-trans isomerase B	3.65E-07			
P24539	ATP synthase F(0) complex subunit B1, mitochondrial	4.32E-08	7.92E-07	1.48E-07	
P25398	40S ribosomal protein S12	5.74E-08			
P25686	DnaJ homolog subfamily B member 2	2.41E-08			
P25705	ATP synthase subunit alpha, mitochondrial	1.08E-06	6.71E-06	1.46E-06	6.3E-06
P27348	14-3-3 protein theta		1.02E-07		
P27635	60S ribosomal protein L10	5.1E-07	4.01E-07	2.43E-07	
P27694	Replication protein A 70 kDa DNA-binding subunit	2.18E-07	2.26E-06	2.8E-08	2.93E-06
P27816	Microtubule-associated protein 4	6.03E-09	2.52E-08		
P27824	Calnexin	5.21E-08	1.27E-07		
P28288	ATP-binding cassette sub-family D member 3		4.64E-07		
P30153	Serine/threonine-protein phosphatase 2A 65 kDa regulatory subunit A alpha isoform	5.7E-08			
P30876	DNA-directed RNA polymerase II subunit RPB2	4.85E-08		2.32E-08	
P31040	Succinate dehydrogenase flavoprotein subunit, mitochondrial	9.39E-08		1.29E-07	
P31350	Ribonucleoside-diphosphate reductase subunit M2	9.67E-08	1.37E-06		
P31483	Nucleolysin TIA-1 isoform p40		6.55E-07		
P35232	Prohibitin	6.22E-07	2.74E-06	4.12E-07	
P35637	RNA-binding protein FUS	2.43E-07	1.54E-06		1.45E-06
P36507	Dual specificity mitogen-activated protein kinase kinase 2	1.17E-07	2.64E-07	4.31E-08	

P36542	ATP synthase subunit gamma, mitochondrial	4.82E-07	2.39E-07	2.33E-07	1.34E-06
P36873	Serine/threonine-protein phosphatase PP1-gamma catalytic subunit	2.05E-07	1.71E-06	7.23E-08	1.58E-06
P36957	2-oxoglutarate dehydrogenase complex component E2	1.09E-07	1.65E-06	1.6E-07	1.24E-07
P37108	Signal recognition particle 14 kDa protein	2.01E-07	5.42E-06		2.93E-06
P39019	40S ribosomal protein S19	4.01E-06	6.96E-06	1.26E-06	3.55E-06
P41252	Isoleucine--tRNA ligase, cytoplasmic		6.93E-09		
P42167	Lamina-associated polypeptide 2, isoforms beta/gamma	1.41E-06	1.12E-05	6.07E-08	7.23E-06
P43694	Transcription factor GATA-4	1.33E-08	1.06E-07		
P45973	Chromobox protein homolog 5		2.91E-07		
P46060	Ran GTPase-activating protein 1		1.08E-07		
P46776	60S ribosomal protein L27a	2.76E-07	2.96E-07	1.85E-07	9.2E-07
P46777	60S ribosomal protein L5	1.33E-07	7.04E-06	3.55E-09	6.22E-06
P46782	40S ribosomal protein S5	2.04E-06	6.64E-06	3.54E-07	9.86E-07
P46783	40S ribosomal protein S10	1.7E-06	4.81E-06	4.2E-06	4.67E-06
P48047	ATP synthase subunit O, mitochondrial	4.03E-07	2.66E-06	1.84E-07	6.96E-07
P49327	Fatty acid synthase	3.93E-09			
P49756	RNA-binding protein 25	2.11E-08	8.84E-07	6.3E-08	2.65E-07
P49790	Nuclear pore complex protein Nup153	1.15E-08			
P50990	T-complex protein 1 subunit theta	9.29E-07	3.48E-08	1.1E-06	
P51532	Transcription activator BRG1	2.04E-08	9.36E-08		1.85E-07
P51659	Peroxisomal multifunctional enzyme type 2	4.1E-08	2.87E-07		
P52701	DNA mismatch repair protein Msh6	5.67E-08	1.33E-07	5.84E-08	
P52907	F-actin-capping protein subunit alpha-1	1.07E-07	8.98E-08	4.63E-08	
P52926	High mobility group protein HMGI-C	1.65E-08	1.57E-07		
P54886	Delta-1-pyrroline-5-carboxylate synthase	4.39E-07	1.08E-07	3.33E-07	
P55209	Nucleosome assembly protein 1-like 1	1.83E-07	2.19E-08		
P55265	Double-stranded RNA-specific adenosine deaminase	1.32E-08	1.18E-07		1.73E-07
P55316	Forkhead box protein G1		6.95E-08		
P55795	Heterogeneous nuclear ribonucleoprotein H2	7.36E-09	2.86E-07		
P56270	Myc-associated zinc finger protein		1.4E-07		

P57740	Nuclear pore complex protein Nup107	2.52E-08		4.2E-08	
P60866	40S ribosomal protein S20	2.14E-06	5.19E-06	5.68E-07	4.55E-06
P60891	Ribose-phosphate pyrophosphokinase 1	4.75E-08	1.52E-07	9.09E-08	
P61081	NEDD8-conjugating enzyme Ubc12	3.34E-08	9.18E-07		
P61254	60S ribosomal protein L26	1.07E-07	1.5E-06	3.5E-07	2.81E-06
P61964	WD repeat-containing protein 5	2.08E-08			
P61978	Heterogeneous nuclear ribonucleoprotein K	1.73E-06	2.49E-06	4.04E-07	3.5E-06
P62136	Serine/threonine-protein phosphatase PP1-alpha catalytic subunit	6.68E-08	2.67E-06	1.38E-09	4.17E-07
P62195	26S protease regulatory subunit 8	1.12E-07	2.07E-08		
P62258	14-3-3 protein epsilon	2.86E-07	6.63E-08		
P62269	40S ribosomal protein S18	2.66E-06	8.36E-06	1.59E-06	8.11E-07
P62304	Small nuclear ribonucleoprotein E	1.57E-07	3.01E-07	2.17E-07	2.26E-06
P62306	Small nuclear ribonucleoprotein F	3.29E-07	2.51E-07		
P62316	Small nuclear ribonucleoprotein Sm D2	1.74E-06	1.46E-05	3.66E-07	7.15E-06
P62318	Small nuclear ribonucleoprotein Sm D3	2E-07		1.86E-07	3.98E-06
P62424	60S ribosomal protein L7a		2.88E-07		
P62750	60S ribosomal protein L23a	4.5E-07	3.19E-06	3.36E-07	3.7E-06
P62826	GTP-binding nuclear protein Ran	8.72E-07	5.7E-06	5.85E-08	7.1E-06
P62851	40S ribosomal protein S25	1.44E-06	2.98E-06	1.27E-06	2.19E-06
P62857	40S ribosomal protein S28	4.04E-07		9.34E-07	
P62888	60S ribosomal protein L30	6.12E-08	4.7E-06	1.53E-08	1.18E-06
P62979	Ubiquitin-40S ribosomal protein S27a	1.13E-07	3.09E-07	4.59E-06	1.24E-06
P63104	14-3-3 protein zeta/delta	1.58E-08		8.15E-08	
P78371	T-complex protein 1 subunit beta	8.53E-07	7.57E-07	7.68E-07	1.29E-07
P78549	Endonuclease III-like protein 1		2.71E-07		
Q00059	Transcription factor A, mitochondrial	2.36E-07	1.34E-06		8.62E-07
Q00587	Cdc42 effector protein 1	1.55E-07		7.52E-08	
Q01081	Splicing factor U2AF 35 kDa subunit	2.69E-07	3.16E-06		2.12E-06
Q01105	Protein SET	3.48E-07	2.52E-06	3.53E-07	1.38E-06
Q01130	Serine/arginine-rich splicing factor 2	2.27E-08	1.47E-06		

Q02218	2-oxoglutarate dehydrogenase, mitochondrial	2.41E-08	2.2E-08		
Q02447	Transcription factor Sp3		1.09E-07		
Q04837	Single-stranded DNA-binding protein, mitochondrial	5.55E-07	1.2E-06		
Q04917	14-3-3 protein eta	1.6E-07			
Q05D32	CTD small phosphatase-like protein 2		1.36E-07		
Q07021	Complement component 1 Q subcomponent-binding protein, mitochondrial	1.15E-06	2.33E-06	3.88E-07	1.46E-06
Q07065	Cytoskeleton-associated protein 4	8.93E-08	6.7E-08		
Q08170	Serine/arginine-rich splicing factor 4	3.69E-08	5.63E-07		2.14E-07
Q09028	Histone-binding protein RBBP4	2.11E-08	3.19E-07		5.31E-07
Q12788	Transducin beta-like protein 3		6.98E-08		
Q12874	Splicing factor 3A subunit 3	5.79E-08	2.83E-07		
Q13011	Delta(3,5)-Delta(2,4)-dienoyl-CoA isomerase, mitochondrial	1.78E-08	8.84E-07		
Q13112	Chromatin assembly factor 1 subunit B	2.5E-08	1.09E-07		5.89E-07
Q13148	TAR DNA-binding protein 43	5.25E-07	4.4E-06	8.17E-08	3.52E-06
Q13185	Chromobox protein homolog 3	1.69E-08	2.56E-07		
Q13242	Serine/arginine-rich splicing factor 9	3.53E-07	2.59E-06		4.87E-07
Q13243	Serine/arginine-rich splicing factor 5	3.13E-08	1.84E-07		
Q13247	Serine/arginine-rich splicing factor 6	1.63E-07	3.41E-06		2.08E-06
Q13257	Mitotic spindle assembly checkpoint protein MAD2A	3.46E-07	4.13E-07	4.16E-07	
Q13330	Metastasis-associated protein MTA1	2.3E-08	1.28E-07		
Q13415	Origin recognition complex subunit 1	2.41E-08	3.29E-07		2.67E-07
Q13416	Origin recognition complex subunit 2	5.18E-08	1.19E-06		1.23E-06
Q13435	Splicing factor 3B subunit 2	1.36E-08	5.61E-08		
Q13595	Transformer-2 protein homolog alpha	9.44E-09	5.84E-07		6.72E-07
Q13617	Cullin-2	2.21E-08	1.3E-07		
Q13620	Cullin-4B	7.14E-08	1.67E-07		
Q13885	Tubulin beta-2A chain	2.9E-07		6.4E-08	
Q14011	Cold-inducible RNA-binding protein	1.8E-07	7.73E-07		7.71E-07
Q14151	Scaffold attachment factor B2	2.31E-08	5.09E-07	2.17E-08	3.6E-07
Q14157	Ubiquitin-associated protein 2-like	9.74E-08	5.31E-08	6.71E-09	

Q14204	Cytoplasmic dynein 1 heavy chain 1	8.65E-09	5.19E-08		
Q14444	Caprin-1		1.65E-07		
Q14498	RNA-binding protein 39	1.59E-07	5.58E-07	1.04E-07	4.36E-07
Q14669	E3 ubiquitin-protein ligase TRIP12		2.24E-08		
Q14677	Clathrin interactor 1	4.11E-08		4.85E-08	
Q14739	Lamin-B receptor	1.49E-08			
Q14807	Kinesin-like protein KIF22		2.93E-07		
Q14839	Chromodomain-helicase-DNA-binding protein 4		3.58E-08		
Q14978	Nucleolar and coiled-body phosphoprotein 1	5.27E-07	6E-06	1.31E-07	3.34E-06
Q15007	Pre-mRNA-splicing regulator WTAP	2.63E-08	1.28E-07		
Q15029	116 kDa U5 small nuclear ribonucleoprotein component	1.92E-08	2.56E-07	2.29E-08	1.15E-08
Q15365	Poly(rC)-binding protein 1	2.38E-07	1E-06	1.77E-07	8E-07
Q15459	Splicing factor 3A subunit 1	2.26E-08	1.59E-07	2.58E-08	
Q16630	Cleavage and polyadenylation specificity factor subunit 6		1.05E-07		
Q16775	Hydroxyacylglutathione hydrolase, mitochondrial	1.75E-07	3.14E-06	1.27E-07	4.69E-07
Q27J81	Inverted formin-2	1.83E-08	7.85E-08		
Q2NKX8	DNA excision repair protein ERCC-6-like	2.18E-08			
Q2TAY7	WD40 repeat-containing protein SMU1		1.14E-07		4.65E-07
Q3ZCQ8	Mitochondrial import inner membrane translocase subunit TIM50	2.98E-07	1.97E-08	1.5E-07	
Q53GQ0	Estradiol 17-beta-dehydrogenase 12	1.05E-08	2.4E-07		
Q53GS9	U4/U6.U5 tri-snRNP-associated protein 2	9.86E-09	5.57E-07		5.36E-07
Q562R1	Beta-actin-like protein 2		3.39E-07		
Q5JTV8	Torsin-1A-interacting protein 1	7.07E-09	1.71E-08		
Q5SW79	Centrosomal protein of 170 kDa	1.82E-08		1.68E-08	
Q5T4S7	E3 ubiquitin-protein ligase UBR4	7.53E-09	1.81E-08		
Q5T8P6	RNA-binding protein 26		5.62E-08		
Q5UIP0	Telomere-associated protein RIF1	7.99E-08	6.73E-07		7.5E-07
Q5W0B1	RING finger protein 219	5.89E-07		4.76E-07	
Q6P1J9	Parafibromin	2.08E-08	3.69E-08		
Q6P2Q9	Pre-mRNA-processing-splicing factor 8	7.76E-10	9.63E-08		

Q6PJT7	Zinc finger CCCH domain-containing protein 14	1.12E-07	6.98E-07		
Q6R327	Rapamycin-insensitive companion of mTOR	3.57E-08		1.17E-08	
Q6YN16	Hydroxysteroid dehydrogenase-like protein 2	5.01E-08	1.55E-07	1.09E-07	
Q7Z4H7	HAUS augmin-like complex subunit 6	9.07E-08		1.67E-07	
Q7Z739	YTH domain family protein 3		4.82E-08	3.37E-08	
Q86U42	Polyadenylate-binding protein 2	8.07E-07	1.2E-05	1.27E-06	1.87E-05
Q86UA1	Pre-mRNA-processing factor 39	1.93E-08	6.75E-08		
Q86UY6	N-alpha-acetyltransferase 40		4.84E-07		
Q86V15	Zinc finger protein castor homolog 1	1.66E-09	2.93E-08		
Q86YP4	Transcriptional repressor p66-alpha		1.22E-07		
Q8IWS0	PHD finger protein 6	1.03E-08	6.01E-08		
Q8N1F7	Nuclear pore complex protein Nup93	7.09E-08	5.78E-07	7.66E-08	1.96E-07
Q8N5D0	WD and tetratricopeptide repeats protein 1	2.86E-08	3.59E-08	3.46E-08	
Q8NC51	Plasminogen activator inhibitor 1 RNA-binding protein	5.26E-08	7.96E-08	5.39E-08	2.94E-07
Q8NCA5	Protein FAM98A		3.67E-07		1.05E-06
Q8NDX6	Zinc finger protein 740		9.61E-07		
Q8NF91	Nesprin-1		5.41E-09		
Q8NFH5	Nucleoporin NUP53	7.17E-08	4.11E-08		
Q8WV44	E3 ubiquitin-protein ligase TRIM41	4.76E-08		3.97E-08	
Q8WWY3	U4/U6 small nuclear ribonucleoprotein Prp31		7.31E-08		
Q8WXF1	Paraspeckle component 1		5.07E-08		
Q8WXI9	Transcriptional repressor p66-beta		1.87E-07		
Q92552	28S ribosomal protein S27, mitochondrial	2.37E-08			
Q92598	Heat shock protein 105 kDa	2.81E-08	2.35E-08		
Q92621	Nuclear pore complex protein Nup205		1.5E-08		
Q92769	Histone deacetylase 2		3.86E-07		
Q92785	Zinc finger protein ubi-d4		3.22E-07		
Q92879	CUGBP Elav-like family member 1	3.68E-08	1.93E-07		1.06E-06
Q92922	SWI/SNF complex subunit SMARCC1		1.27E-07		1.04E-07
Q92945	Far upstream element-binding protein 2	5.47E-08			
Q92979	Ribosomal RNA small subunit methyltransferase NEP1	2.96E-07	6.96E-06		9.44E-06

Q93008	Probable ubiquitin carboxyl-terminal hydrolase FAF-X	5.86E-08		3.95E-08	
Q93034	Cullin-5	1.35E-07	1.48E-06	2.37E-07	6.62E-07
Q96AG4	Leucine-rich repeat-containing protein 59	6.21E-08	4.16E-08		
Q96C36	Pyrroline-5-carboxylate reductase 2	2.31E-08	2.03E-07		
Q96DF8	Protein DGCR14	7.72E-08			
Q96EB6	NAD-dependent protein deacetylase sirtuin-1	1.34E-08			
Q96GA3	Protein LTV1 homolog	5.26E-09			
Q96GX5	Serine/threonine-protein kinase greatwall	1.13E-08			
Q96P16	Regulation of nuclear pre-mRNA domain-containing protein 1A	1.71E-08	1.5E-07		
Q96S55	ATPase WRNIP1	2.09E-08		3.27E-08	
Q96ST2	Protein IWS1 homolog	6.34E-08	4.07E-07		9.32E-07
Q96T37	Putative RNA-binding protein 15	1.29E-08	1.82E-07		1.35E-07
Q96T58	Msx2-interacting protein		1.88E-08		
Q96T88	E3 ubiquitin-protein ligase UHRF1	2.05E-08	7.67E-07		3.02E-07
Q99459	Cell division cycle 5-like protein	1.8E-09	2.63E-07		
Q99615	DnaJ homolog subfamily C member 7	1.53E-07		5.88E-08	
Q99986	Serine/threonine-protein kinase VRK1		5.03E-07		9.98E-07
Q9BQ67	Glutamate-rich WD repeat-containing protein 1	1.06E-08	3.19E-07		
Q9BQG0	Myb-binding protein 1A	2.85E-09	1.75E-08		1.87E-07
Q9BSJ8	Extended synaptotagmin-1	3.6E-09			
Q9BUF5	Tubulin beta-6 chain	6.63E-07	9.41E-08	4.98E-07	
Q9BUJ2	Heterogeneous nuclear ribonucleoprotein U-like protein 1	5.35E-08	8.99E-08	1.34E-08	
Q9BUQ8	Probable ATP-dependent RNA helicase DDX23	3.51E-08	9.54E-09		2.35E-07
Q9BW61	DET1- and DDB1-associated protein 1	2.91E-07			
Q9BWF3	RNA-binding protein 4	1.87E-08	8.55E-07		1.5E-07
Q9BXP5	Serrate RNA effector molecule homolog	9.25E-08	1.32E-07		
Q9BXW9	Fanconi anemia group D2 protein	6.64E-09			
Q9BZC1	CUGBP Elav-like family member 4		4.33E-07		
Q9BZE1	39S ribosomal protein L37, mitochondrial	4.25E-08	8.13E-08		
Q9GZZ9	Ubiquitin-like modifier-activating enzyme 5	1.06E-07		3.49E-08	
Q9H078	Caseinolytic peptidase B protein homolog	3.81E-07	2.7E-07	2.95E-07	

Q9H0A0	N-acetyltransferase 10	3.58E-09	1.49E-08		
Q9H307	Pinin	3.33E-08	4.03E-07		
Q9H3P2	Negative elongation factor A		9.33E-08		
Q9H9A6	Leucine-rich repeat-containing protein 40	4.97E-07		7.5E-07	
Q9HCN4	GPN-loop GTPase 1	1.42E-07	9.58E-08		
Q9NQ29	Putative RNA-binding protein Luc7-like 1	5.04E-08	9.05E-08		
Q9NRG9	Aladin		1.36E-07		
Q9NRZ9	Lymphoid-specific helicase	6.87E-08			
Q9NS69	Mitochondrial import receptor subunit TOM22 homolog	2.75E-07			
Q9NSI2	Protein FAM207A	3.74E-08	9.24E-07		
Q9NTI5	Sister chromatid cohesion protein PDS5 homolog B	8.85E-09	2.49E-08		
Q9NUU7	ATP-dependent RNA helicase DDX19A	5.55E-08	1.68E-07		
Q9NVH2	Integrator complex subunit 7		2.69E-08		
Q9NVI7	ATPase family AAA domain-containing protein 3A	1.37E-07	3.03E-07	1.01E-07	
Q9NXW2	DnaJ homolog subfamily B member 12	8.88E-08			
Q9NYF8	Bcl-2-associated transcription factor 1	1.88E-08	2E-07		
Q9NZB2	Constitutive coactivator of PPAR-gamma-like protein 1	6.74E-09	6.69E-08		
Q9P035	Very-long-chain (3R)-3-hydroxyacyl-[acyl-carrier protein] dehydratase 3	8.52E-09	2.89E-07		
Q9P2D1	Chromodomain-helicase-DNA-binding protein 7	1.3E-09	4.68E-08		
Q9UBD5	Origin recognition complex subunit 3	1.47E-08	9.18E-07		1.01E-06
Q9UBU9	Nuclear RNA export factor 1	3.79E-08	2.26E-07		
Q9UFC0	Leucine-rich repeat and WD repeat-containing protein 1	1.92E-08	1.12E-06		4.62E-07
Q9UG63	ATP-binding cassette sub-family F member 2	3.51E-08			
Q9UHX1	Poly(U)-binding-splicing factor PUF60	5.42E-08	8.64E-07	1.77E-08	3.43E-07
Q9UJV9	Probable ATP-dependent RNA helicase DDX41	1.42E-08	6.6E-08		
Q9UJZ1	Stomatin-like protein 2, mitochondrial	9.13E-08	1.27E-07		
Q9UKA9	Polypyrimidine tract-binding protein 2	2.07E-08	3.81E-08		
Q9UL15	BAG family molecular chaperone regulator 5	3.02E-08			
Q9ULT8	E3 ubiquitin-protein ligase HECTD1	6.44E-09			
Q9ULX6	A-kinase anchor protein 8-like	3.78E-07		2.87E-07	

Q9UMS4	Pre-mRNA-processing factor 19	1.21E-07	2.58E-06	8.51E-08	2.66E-06
Q9UNF1	Melanoma-associated antigen D2	2.83E-08			
Q9UPN7	Serine/threonine-protein phosphatase 6 regulatory subunit 1	1.21E-07		5.19E-08	
Q9UPY3	Endoribonuclease Dicer	1.08E-08			
Q9UQ13	Leucine-rich repeat protein SHOC-2	4.03E-08			
Q9UQ35	Serine/arginine repetitive matrix protein 2		3.95E-08		
Q9UQR1	Zinc finger protein 148		1.17E-07		
Q9Y230	RuvB-like 2	5.38E-07	6.79E-07	3.43E-07	7.37E-07
Q9Y265	RuvB-like 1	6.88E-07	1.46E-06	4.84E-07	1.27E-06
Q9Y277	Voltage-dependent anion-selective channel protein 3	3.27E-08	5E-07		
Q9Y2K7	Lysine-specific demethylase 2A		1.04E-07		1.52E-07
Q9Y2W1	Thyroid hormone receptor-associated protein 3	2.68E-08	1.83E-07		
Q9Y333	U6 snRNA-associated Sm-like protein LSm2	3.23E-07	2.91E-06		
Q9Y383	Putative RNA-binding protein Luc7-like 2	3.05E-08	1.44E-07		4.97E-07
Q9Y3F4	Serine-threonine kinase receptor-associated protein	1.91E-08	3.83E-07	6.75E-08	
Q9Y3I0	tRNA-splicing ligase RtcB homolog	2.47E-08	8.48E-08		
Q9Y3Z3	Deoxynucleoside triphosphate triphosphohydrolase SAMHD1	6.79E-08			
Q9Y5M8	Signal recognition particle receptor subunit beta	8.6E-08	1.7E-07		
Q9Y6G9	Cytoplasmic dynein 1 light intermediate chain 1	1.42E-08	1.15E-07		
Q9Y6K1	DNA (cytosine-5)-methyltransferase 3A		6.2E-08		
Q9Y6V7	Probable ATP-dependent RNA helicase DDX49		6.27E-08		
Q9Y6W5	Wiskott-Aldrich syndrome protein family member 2		2.18E-07		
A8MQB8	Fragile X mental retardation protein 1		8.23E-08		
E9PAU2	Ribonucleoprotein PTB-binding 1	3.24E-08	1.08E-07		
E9PCY5	DNA topoisomerase 2 (Fragment)	1.11E-06	0.000013	4.87E-07	1.2E-05
H3BUF6	Ataxin-2-like protein	1.86E-08	9.03E-08		
M0QZM1	Heterogeneous nuclear ribonucleoprotein M (Fragment)		6.33E-08		
Q59FY4	Acetyl-CoA carboxylase 1 (Fragment)		2.65E-08		
Q5T6W1	Heterogeneous nuclear ribonucleoprotein K		8.04E-08		1.49E-07
S4R3J4	Heterogeneous nuclear ribonucleoprotein R		1.71E-08		
O75694	Nuclear pore complex protein Nup155			4.11E-09	5.23E-08

O95433	Activator of 90 kDa heat shock protein ATPase homolog 1	4.93E-07	
P04908	Histone H2A type 1-B/E		1.8E-06
P05089	Arginase-1	3.83E-08	3.08E-07
P05109	Protein S100-A8	8E-08	8.55E-06
P06702	Protein S100-A9		7.4E-06
P06733	Alpha-enolase	4.45E-08	
P0CG38	POTE ankyrin domain family member I	4.78E-08	2.56E-07
P14618	Pyruvate kinase PKM	1.97E-08	
P18621	60S ribosomal protein L17	2.61E-07	
P30837	Aldehyde dehydrogenase X, mitochondrial	5.5E-08	
P31153	S-adenosylmethionine synthase isoform type-2	5.2E-09	
P31944	Caspase-14		5.74E-07
P42766	60S ribosomal protein L35	2.87E-07	9.44E-07
P43246	DNA mismatch repair protein Msh2	1.15E-08	
P51570	Galactokinase	4.29E-08	
P52732	Kinesin-like protein KIF11	1.35E-08	
P60842	Eukaryotic initiation factor 4A-I	1.26E-06	1.45E-07
P63151	Serine/threonine-protein phosphatase 2A 55 kDa regulatory subunit B alpha isoform	4.48E-09	
P78347	General transcription factor II-I	2.81E-08	
P83731	60S ribosomal protein L24	1.32E-07	
Q01469	Fatty acid-binding protein, epidermal		6.07E-07
Q02413	Desmoglein-1	2.02E-08	4.43E-07
Q06830	Peroxiredoxin-1	5.37E-08	3.13E-07
Q12931	Heat shock protein 75 kDa, mitochondrial	8.54E-09	
Q13576	Ras GTPase-activating-like protein IQGAP2	5.19E-09	
Q15517	Corneodesmosin	5.76E-08	1.95E-07
Q15814	Tubulin-specific chaperone C	3.81E-08	
Q16891	Mitochondrial inner membrane protein	2.29E-08	
Q5JTW2	Centrosomal protein of 78 kDa	9.07E-09	
Q6DN90	IQ motif and SEC7 domain-containing protein 1	2.8E-08	

Q6PEY2	Tubulin alpha-3E chain	5.64E-08	
Q6UWP8	Suprabasin	6.11E-09	2.22E-07
Q71UM5	40S ribosomal protein S27-like	4.19E-07	
Q86V81	THO complex subunit 4		7.19E-07
Q8N680	Zinc finger and BTB domain-containing protein 2		3.98E-07
Q8WUM0	Nuclear pore complex protein Nup133	2.79E-08	
Q96EP5	DAZ-associated protein 1		8.34E-07
Q96F07	Cytoplasmic FMR1-interacting protein 2	4.11E-08	
Q96GX2	Putative ataxin-7-like protein 3B	2.3E-07	
Q96HS1	Serine/threonine-protein phosphatase PGAM5, mitochondrial	9.37E-08	
Q96JG8	Melanoma-associated antigen D4	8.79E-08	
Q96P63	Serpin B12	5.15E-09	2.87E-07
Q99707	Methionine synthase	6.51E-09	
Q9BYW2	Histone-lysine N-methyltransferase SETD2	4.89E-09	
Q9H936	Mitochondrial glutamate carrier 1	9.31E-08	
Q9NY74	Ewing's tumor-associated antigen 1	9.5E-09	
Q9UKA4	A-kinase anchor protein 11	7.25E-09	
Q9UQE7	Structural maintenance of chromosomes protein 3	1.55E-09	
Q9Y2X9	Zinc finger protein 281	3.91E-08	

Appendix F: Identity and relative SINQ scores of proteins that co-purified with PB2-Strep

Protein SINQ scores were normalised and non-specific binding proteins were removed (see Materials and Methods for details).
Identified protein SINQ scores were normalised to PB2-Strep SINQ score.
[a]UniProt ID of human protein or viral protein name.
[b]Short gene name for each identified protein.
[c]Mean SINQ score of each protein (missing data did not contribute to the mean).
[d]SD ($N > 2$) or half-range ($N=2$).
[e]Number of experiments in which the protein was identified.

Protein[a]	***Short Name[b]***	***Description***	***Mean SINQ Score[c]***	***(+/–)[d]***	***N[e]***
NP	NP	Influenza A/WSN/33 NP	8.076611961	2.183442	3
PB2-Strep	PB2-Strep	Influenza A/WSN/33 PB2-Strep	1		3
PB1	PB1	Influenza A/WSN/33 PB1	0.786299188	0.033873	3
PA	PA	Influenza A/WSN/33 PA	0.596522858	0.103631	3
P11142	HSPA8	Heat shock cognate 71 kDa protein	0.091249799	0.003725	3
P07437	TUBB	Tubulin beta chain	0.034142773	0.0302	3
P62987	UBA52	Ubiquitin-60S ribosomal protein L40	0.032312034	0.005382	2
P62979	RPS27A	Ubiquitin-40S ribosomal protein S27a	0.019067003	0.018313	2
Q14257	RCN2	Reticulocalbin-2	0.015968216	0.013516	3
O00410	IPO5	Importin-5	0.015526085	0.000637	3
P10809	HSPD1	60 kDa heat shock protein, mitochondrial	0.011939713	0.010298	3
O95816	BAG2	BAG family molecular chaperone regulator 2	0.010648861	0.003614	2
P60842	EIF4A1	Eukaryotic initiation factor 4A	0.010235964		1
P68371	TUBB4B	Tubulin beta-4B chain	0.010159805	0.005726	3
O60884	DNAJA2	DnaJ homolog subfamily A member 2	0.009808361	0.008133	3
P50402	EMD	Emerin	0.009800935	0.007514	3
P31689	DNAJA1	DnaJ homolog subfamily A member 1	0.008964199	0.005032	3
O00743	PPP6C	Serine/threonine-protein phosphatase 6 catalytic subunit	0.007929034	0.002908	3
P12236	SLC25A6	ADP/ATP translocase 3	0.007816372	0.012091	3

Q99832	CCT7	T-complex protein 1 subunit eta	0.007711209	0.000724	3
P50990	CCT8	T-complex protein 1 subunit theta	0.007604392	0.001379	2
P05455	SSB	Lupus La protein	0.007476909	0.000948	2
Q16531	DDB1	DNA damage-binding protein 1	0.006396893	0.000712	3
O00165	HAX1	HCLS1-associated protein X-1	0.006218454	0.005249	2
P78371	CCT2	T-complex protein 1 subunit beta	0.005982113	0.000264	2
O00505	KPNA3	Importin subunit alpha-4	0.00569974	0.000459	3
O75190	DNAJB6	DnaJ homolog subfamily B member 6	0.005574937	0.005329	3
P50991	CCT4	T-complex protein 1 subunit delta	0.005464235	0.004143	3
Q9Y5V3	MAGED1	Melanoma-associated antigen D1	0.005157536	0.001266	3
P62857	RPS28	40S ribosomal protein S28	0.005152026	0.002444	2
Q9H9A6	LRRC40	Leucine-rich repeat-containing protein 40	0.004716811	0.001386	2
P10644	PRKAR1A	cAMP-dependent protein kinase type I-alpha regulatory subunit	0.004710566	0.000169	2
P49368	CCT3	T-complex protein 1 subunit gamma	0.004568045	0.002795	3
Q00325	SLC25A3	Phosphate carrier protein, mitochondrial	0.004522392	0.00326	2
P17987	CCT1	T-complex protein 1 subunit alpha	0.004301543	0.001441	3
Q9BUF5	TUBB6	Tubulin beta-6 chain	0.004248102	0.000194	2
O00629	KPNA4	Importin subunit alpha-3	0.004101055	7.49E-05	3
Q5H9R7	PPP6R3	Serine/threonine-protein phosphatase 6 regulatory subunit 3	0.004039222	0.001902	3
O95433	AHSA1	Activator of 90 kDa heat shock protein ATPase homolog 1	0.004014646		1
Q5W0B1	RNF219	RING finger protein 219	0.003909317	3.71E-05	2
P40227	CCT6A	T-complex protein 1 subunit zeta	0.003627412	0.001935	3
Q71UM5	RPS27L	40S ribosomal protein S27-like	0.003410903		1
Q9Y4B6	VPRBP	Protein VPRBP	0.00296147	0.001444	3
P48643	CCT5	T-complex protein 1 subunit epsilon	0.002952142	0.001669	3
Q9BVA1	TUBB2B	Tubulin beta-2B chain	0.002841552	0.002934	3
P54886	ALDH18A1	Delta-1-pyrroline-5-carboxylate synthase	0.00282716	0.000115	2
P49411	TUFM	Elongation factor Tu, mitochondrial	0.002818283	0.003018	3
Q5TAQ9	DCAF8	DDB1- and CUL4-associated factor 8	0.002624835	0.00183	3
NA	NA	Influenza A/WSN/33 NA	0.002469202	0.001605	3
Q96D09	GPRASP2	G-protein coupled receptor-associated sorting protein 2	0.002457759	0.001898	3

P23284	PPIB	Peptidyl-prolyl cis-trans isomerase B	0.002449062		1
Q9ULX6	AKAP8L	A-kinase anchor protein 8-like	0.002435664	9.72E-05	2
O43164	PJA2	E3 ubiquitin-protein ligase Praja-2	0.002427387	0.001131	3
P06730	EIF4E	Eukaryotic translation initiation factor 4E	0.002376757	0.000544	2
O60684	KPNA6	Importin subunit alpha-7	0.002322559	0.001888	3
O95831	AIFM1	Apoptosis-inducing factor 1, mitochondrial	0.00226055	0.001237	3
P51571	SSR4	Translocon-associated protein subunit delta	0.002180429	0.000655	3
O15355	PPM1G	Protein phosphatase 1G	0.00214739	0.000377	2
P13674	P4HA1	Prolyl 4-hydroxylase subunit alpha-1	0.002131323	0.000162	2
P18621	RPL17	60S ribosomal protein L17	0.002123678		1
O14654	IRS4	Insulin receptor substrate 4	0.002007418	0.000821	3
Q9BW61	DDA1	DET1- and DDB1-associated protein 1	0.001947721		1
P62258	YWHAE	14-3-3 protein epsilon	0.00191622		1
Q9Y5A9	YTHDF2	YTH domain family protein 2	0.001873114	0.001641	3
Q96GX2	ATXN7L3B	Putative ataxin-7-like protein 3B	0.001867372		1
A6NKZ8	TBB	Putative tubulin beta chain-like protein ENSP00000290377	0.001852663	1.87E-05	2
Q9NS69	TOMM22	Mitochondrial import receptor subunit TOM22 homolog	0.001845174		1
Q9BQE3	TUBA1C	Tubulin alpha-1C chain	0.00184362	0.000397	3
Q3ZCQ8	TIMM50	Mitochondrial import inner membrane translocase subunit TIM50	0.001610467	0.000388	2
P10155	TROVE2	60 kDa SS-A/Ro ribonucleoprotein	0.001602436	0.001232	3
Q96HN2	AHCYL2	Putative adenosylhomocysteinase 3	0.001575258	0.00104	3
Q12899	TRIM26	Tripartite motif-containing protein 26	0.001550826		1
Q96EY1	DNAJA3	DnaJ homolog subfamily A member 3, mitochondrial	0.001451599	0.000902	3
Q9UJS0	SLC25A13	Calcium-binding mitochondrial carrier protein Aralar2	0.001335348	0.001032	3
Q9UNK9	ANGEL1	Protein angel homolog 1	0.001322951	0.00084	3
P07900	HSP90AA1	Heat shock protein HSP 90-alpha	0.001276455	0.000488	2
P04350	TUBB4A	Tubulin beta-4A chain	0.001266686	8.12E-05	2
Q13885	TUBB2A	Tubulin beta-2A chain	0.001232641	0.000712	2
P55209	NAP1L1	Nucleosome assembly protein 1-like 1	0.001223861		1
Q9BQ70	TCF25	Transcription factor 25	0.001191177	0.001451	3
P52294	KPNA1	Importin subunit alpha-5	0.001121115	0.000406	3

P83731	RPL24	60S ribosomal protein L24	0.001076485		1
Q04917	YWHAH	14-3-3 protein eta	0.001073056		1
Q7Z4H7	HAUS6	HAUS augmin-like complex subunit 6	0.000982249	0.000374	2
P31040	SDHA	Succinate dehydrogenase flavoprotein subunit, mitochondrial	0.000838648	0.000209	2
Q00587	CDC42EP1	Cdc42 effector protein 1	0.000824493	0.000212	2
P00403	MT-CO2	Cytochrome c oxidase subunit 2	0.000781501		1
P22694	PRKACB	cAMP-dependent protein kinase catalytic subunit beta	0.00077855	0.001254	3
Q96HS1	PGAM5	Serine/threonine-protein phosphatase PGAM5, mitochondrial	0.000762164		1
Q9H936	SLC25A22	Mitochondrial glutamate carrier 1	0.000757608		1
Q99615	DNAJC7	DnaJ homolog subfamily C member 7	0.00075237	0.000274	2
P62195	PSMC5	26S protease regulatory subunit 8	0.00075134		1
Q96JG8	MAGED4	Melanoma-associated antigen D4	0.000714809		1
Q9UPN7	PPP6R1	Serine/threonine-protein phosphatase 6 regulatory subunit 1	0.000617811	0.000195	2
Q7Z6Z7	HUWE1	E3 ubiquitin-protein ligase HUWE1	0.00061249	0.000273	3
Q9NXW2	DNAJB12	DnaJ homolog subfamily B member 12	0.000595241		1
P27708	CAD	CAD protein	0.000576443	0.000168	3
Q71U36	TUBA1A	Tubulin alpha-1A chain	0.000531576	0.000295	2
O43865	AHCYL1	Putative adenosylhomocysteinase 2	0.00053033	0.000398	3
Q13509	TUBB3	Tubulin beta-3 chain	0.000526449	0.00026	3
Q96DF8	DGCR14	Protein DGCR14	0.00051756		1
Q9GZZ9	UBA5	Ubiquitin-like modifier-activating enzyme 5	0.000498137	0.000214	2
Q8NFH5	NUP35	Nucleoporin NUP53	0.000480697		1
Q5JTC6	AMER1	APC membrane recruitment protein 1	0.000475951	0.000225	2
Q9NRZ9	HELLS	Lymphoid-specific helicase	0.000460389		1
Q6PEY2	TUBA3E	Tubulin alpha-3E chain	0.000458828		1
Q9Y3Z3	SAMHD1	Deoxynucleoside triphosphate triphosphohydrolase SAMHD1	0.000455027		1
P30837	ALDH1B1	Aldehyde dehydrogenase X, mitochondrial OS=Homo sapiens	0.000447356		1
O43823	AKAP8	A-kinase anchor protein 8	0.000436187	3.71E-05	2
P63104	YWHAZ	14-3-3 protein zeta/delta	0.000384816	0.000279	2
O75153	CLUH	Clustered mitochondria protein homolog	0.000384686	7.53E-05	3
P25398	RPS12	40S ribosomal protein S12	0.000384517		1

P30153	PPP2R1A	Serine/threonine-protein phosphatase 2A 65 kDa regulatory subunit A alpha isoform	0.000381702		1
P34931	HSPA1L	Heat shock 70 kDa protein 1-like	0.000366836		1
Q92945	KHSRP	Far upstream element-binding protein 2	0.000366756		1
P06733	ENO1	Alpha-enolase OS=Homo sapiens	0.000362246		1
Q93008	USP9X	Probable ubiquitin carboxyl-terminal hydrolase FAF-X	0.000357006	3.57E-05	2
P51570	GALK1	Galactokinase	0.000348902		1
Q14677	CLINT1	Clathrin interactor 1	0.000334935	5.95E-05	2
Q96F07	CYFIP2	Cytoplasmic FMR1-interacting protein 2	0.000334011		1
Q8WV44	TRIM41	E3 ubiquitin-protein ligase TRIM41	0.000320945	2.24E-06	2
Q9Y2X9	ZNF281	Zinc finger protein 281	0.000317738		1
Q15814	TBCC	Tubulin-specific chaperone C	0.000310334		1
O95071	UBR5	E3 ubiquitin-protein ligase UBR5	0.000304627	2.06E-05	2
O43423	ANP32C	Acidic leucine-rich nuclear phosphoprotein 32 family member C	0.000301542		1
P13489	RNH1	Ribonuclease inhibitor	0.000297922		1
O15269	SPTLC1	Serine palmitoyltransferase 1	0.000284517		1
Q9UQ13	SHOC2	Leucine-rich repeat protein SHOC-2	0.000270107		1
P30876	POLR2B	DNA-directed RNA polymerase II subunit RPB2	0.000256711	6.8E-05	2
P57740	NUP107	Nuclear pore complex protein Nup107	0.000255113	8.65E-05	2
P07237	P4HB	Protein disulfide-isomerase	0.000243399	2.7E-05	2
Q9UG63	ABCF2	ATP-binding cassette sub-family F member 2	0.000235255		1
P78347	GTF2I	General transcription factor II-I	0.000228723		1
Q6DN90	IQSEC1	IQ motif and SEC7 domain-containing protein 1	0.000227583		1
Q8WUM0	NUP133	Nuclear pore complex protein Nup133	0.000227177		1
O94776	MTA2	Metastasis-associated protein MTA2	0.000212131		1
Q96S55	WRNIP1	ATPase WRNIP1 OS=Homo sapiens	0.000202972	6.27E-05	2
Q9UL15	BAG5	BAG family molecular chaperone regulator 5	0.000202413		1
Q9UNF1	MAGED2	Melanoma-associated antigen D2	0.000189611		1
Q16891	IMMT	Mitochondrial inner membrane protein	0.000185924		1
Q6R327	RICTOR	Rapamycin-insensitive companion of mTOR	0.000167164	7.2E-05	2
P25686	DNAJB2	DnaJ homolog subfamily B member 2	0.000161394		1

P14618	PKM	Pyruvate kinase PKM	0.00016013		1
Q92552	MRPS27	28S ribosomal protein S27, mitochondrial	0.000159115		1
Q2NKX8	ERCC6L	DNA excision repair protein ERCC-6-like	0.000145845		1
P61964	WDR5	WD repeat-containing protein 5	0.000139276		1
O75489	NDUFS3	NADH dehydrogenase [ubiquinone] iron-sulfur protein 3, mitochondrial	0.000134182		1
O60518	RANBP6	Ran-binding protein 6	0.000132529		1
Q5SW79	CEP170	Centrosomal protein of 170 kDa	0.000129118	7.33E-06	2
O15160	POLR1C	DNA-directed RNA polymerases I and III subunit RPAC1	0.000128954		1
P52732	KIF11	Kinesin-like protein KIF11	0.00010952		1
O15027	SEC16A	Protein transport protein Sec16A	0.000100418	3.74E-05	2
Q14739	LBR	Lamin-B receptor	0.000100134		1
O75746	SLC25A12	Calcium-binding mitochondrial carrier protein Aralar1	9.84624E-05	8.01E-05	2
P43246	MSH2	DNA mismatch repair protein Msh2	9.38975E-05		1
Q96EB6	SIRT1	NAD-dependent protein deacetylase sirtuin-1	8.98794E-05		1
P49790	NUP153	Nuclear pore complex protein Nup153	7.73458E-05		1
Q9NY74	ETAA1	Ewing's tumor-associated antigen 1	7.73149E-05		1
Q96GX5	MASTL	Serine/threonine-protein kinase greatwall	7.55362E-05		1
O43837	IDH3B	Isocitrate dehydrogenase [NAD] subunit beta, mitochondrial	7.45979E-05		1
Q5JTW2	CEP78	Centrosomal protein of 78 kDa	7.37673E-05		1
Q9UPY3	DICER1	Endoribonuclease Dicer	7.25201E-05		1
Q12931	TRAP1	Heat shock protein 75 kDa, mitochondrial	6.95037E-05		1
Q9UKA4	AKAP11	A-kinase anchor protein 11	5.8991E-05		1
Q99707	MTR	Methionine synthase	5.29618E-05		1
Q9BXW9	FANCD2	Fanconi anemia group D2 protein	4.45308E-05		1
Q9ULT8	HECTD1	E3 ubiquitin-protein ligase HECTD1	4.31568E-05		1
P31153	MAT2A	S-adenosylmethionine synthase isoform type-2	4.22864E-05		1
Q13576	IQGAP2	Ras GTPase-activating-like protein IQGAP2	4.21888E-05		1
B5ME19	EIF3CL	Eukaryotic translation initiation factor 3 subunit C-like protein	4.14343E-05		1
Q9BYW2	SETD2	Histone-lysine N-methyltransferase SETD2	3.9764E-05		1
P63151	PPP2R2A	Serine/threonine-protein phosphatase 2A 55 kDa regulatory subunit B alpha isoform	3.64849E-05		1

Q96GA3	LTV1	Protein LTV1 homolog	3.52212E-05	1
P49327	FASN	Fatty acid synthase	2.63271E-05	1
Q9BSJ8	ESYT1	Extended synaptotagmin-1	2.41354E-05	1
Q9UQE7	SMC3	Structural maintenance of chromosomes protein 3	1.25712E-05	1

Isolation and characterization of the positive-sense replicative intermediate of a negative-strand RNA virus

Ashley York[a], Narin Hengrung[a,b], Frank T. Vreede[a], Juha T. Huiskonen[b,1], and Ervin Fodor[a,1]

[a]Sir William Dunn School of Pathology, University of Oxford, Oxford OX1 3RE, United Kingdom; and [b]Division of Structural Biology, Wellcome Trust Centre for Human Genetics, University of Oxford, Oxford OX3 7BN, United Kingdom

Edited by Robert A. Lamb, Northwestern University, Evanston, IL, and approved September 25, 2013 (received for review August 8, 2013)

Negative-strand RNA viruses represent a significant class of important pathogens that cause substantial morbidity and mortality in human and animal hosts worldwide. A defining feature of these viruses is that their single-stranded RNA genomes are of opposite polarity to messenger RNA and are replicated through a positive-sense intermediate. The replicative intermediate is thought to exist as a complementary ribonucleoprotein (cRNP) complex. However, isolation of such complexes from infected cells has never been accomplished. Here we report the development of an RNA-based affinity-purification strategy for the isolation of cRNPs of influenza A virus from infected cells. This technological advance enabled the structural and functional characterization of this elusive but essential component of the viral RNA replication machine. The cRNP exhibits a filamentous double-helical organization with defined termini, containing the viral RNA-dependent RNA polymerase (RdRp) at one end and a loop structure at the other end. In vitro characterization of cRNP activity yielded mechanistic insights into the workings of this RNA synthesis machine. In particular, we found that cRNPs show activity in vitro only in the presence of added RdRp. Intriguingly, a replication-inactive RdRp mutant was also able to activate cRNP-templated viral RNA synthesis. We propose a model of influenza virus genome replication that relies on the *trans*-activation of the cRNP-associated RdRp. The described purification strategy should be applicable to other negative-strand RNA viruses and will promote studies into their replication mechanisms.

Negative-strand RNA viruses include several major human and animal pathogens that cause substantial morbidity and deaths worldwide, as well as several important plant pathogens that are responsible for plant diseases with considerable economic impact. Notable examples of human pathogens are influenza, rabies, mumps, measles, and respiratory syncytial virus, as well as zoonotic, hemorrhagic fever-causing Ebola and Lassa viruses. A defining feature of these viruses is that their single-stranded RNA genomes are of opposite polarity to messenger RNA and are replicated through a cRNA intermediate (1). The genomic viral RNA (vRNA) molecules of negative-strand RNA viruses are assembled into viral ribonucleoprotein particles (vRNPs) containing an oligomer of nucleoprotein (NP) and the RNA-dependent RNA polymerase (RdRp), which is responsible for transcription and replication of the viral genome. High-resolution structures of the genomic ribonucleoproteins of negative-strand RNA viruses have been determined by means of EM, the best-studied example of which is the vRNP of influenza A virus (2, 3).

The genome of influenza A virus is segmented into eight individual vRNP complexes that display a double-helical arrangement resembling a large loop twisted into a helical filament. One copy of the 250-kDa heterotrimeric RdRp, containing the polymerase basic 1 (PB1), polymerase basic 2 (PB2), and polymerase acidic (PA) subunits, binds at one end of the filament interacting with both the 5′ and the 3′ ends of the vRNA (2, 3). Influenza viruses initiate infection by delivering these highly specialized RNA synthesis machines into the nucleus of a host cell for the expression of viral genes. Upon entry into the nucleus, the vRNP-associated RdRp is responsible for transcription of the parental vRNAs into capped and polyadenylated mRNAs using 5′-capped RNA primers snatched from host pre-mRNAs (4, 5). The capped RNA primers are generated by the viral RdRp. Specifically, the PB2 subunit of the RdRp binds to the cap structure of host pre-mRNAs by sandwiching the 7-methyl guanine between two aromatic amino acid residues, whereas the PA subunit endonucleolytically cleaves the capped RNA 9–15 nt downstream of the cap. Subsequently, these primers are extended by condensation of nucleoside triphosphates by the RdRp catalytic domain within the PB1 subunit. Polyadenylation occurs by stuttering of the RdRp on a stretch of uridine residues ∼16 nt from the 5′ end of the vRNA template. Replication of the viral genome is also catalyzed by the viral RdRp, first by synthesizing full-length positive polarity cRNA de novo, which is believed to assemble with NP and the RdRp into a complementary ribonucleoprotein (cRNP). This cRNP then serves as a replication intermediate for the synthesis of multiple copies of progeny vRNPs, which subsequently serve for secondary rounds of transcription, genome amplification, or are exported from the nucleus for packaging into progeny virions (6). Although a cRNP complex has long been assumed to serve as a replicative intermediate for all negative-strand RNA viruses, such complexes have never been isolated. This shortcoming can be attributed to the technical difficulties of separating cRNPs from vRNPs during purification from infected cells and the low ratio of cRNPs to vRNPs in infected cells (7, 8). Consequently, cRNP complexes remain uncharacterized both structurally and functionally, greatly hampering our understanding of an essential aspect in the replication process of negative-strand RNA virus genomes.

Significance

The negative-strand RNA viruses comprise several significant human, animal, and plant pathogens that have considerable health and economic impact globally. During infection, replication of the single-stranded negative-sense RNA genome occurs through a complementary RNA intermediate, which is believed to complex with viral proteins to form a complementary ribonucleoprotein (cRNP). The isolation of these complexes from infected cells has never been accomplished, greatly hampering our understanding of genome replication. We report a technological advance for the isolation of this elusive but essential component of the influenza A virus replication machine. Structural and functional characterization of the influenza A virus cRNP has led to the proposal of a model of genome replication that relies on a *trans*-activating viral RNA-dependent RNA polymerase.

Author contributions: A.Y., N.H., F.T.V., J.T.H., and E.F. designed research; A.Y., N.H., and J.T.H. performed research; A.Y., N.H., F.T.V., J.T.H., and E.F. analyzed data; and A.Y., J.T.H., and E.F. wrote the paper.

The authors declare no conflict of interest.

This article is a PNAS Direct Submission.

[1]To whom correspondence may be addressed. E-mail: juha@strubi.ox.ac.uk or ervin.fodor@path.ox.ac.uk.

This article contains supporting information online at www.pnas.org/lookup/suppl/doi:10.1073/pnas.1315068110/-/DCSupplemental.

To understand the overall molecular architecture of the influenza virus ribonucleoprotein complexes and the basic molecular requirements of influenza virus genome replication, we set out to isolate the replicative cRNP intermediate from infected cells using an RNA tag and affinity purification. Electron microscopy and single particle analysis revealed that the cRNPs isolated from infected cells exist as individual particles that exhibit a double-helical arrangement consisting of cRNA, NP, and the RdRp. Unexpectedly, it was shown in vRNA synthesis assays that cRNP activity requires a *trans*-activating RdRp for initiation and processivity by the resident RdRp. By using a replication-inactive mutant of the RdRp, we show that the role of this *trans*-activating RdRp is not enzymatic. These findings allow us to propose a model for genomic vRNA synthesis by the influenza virus replicative intermediate cRNP.

Results

RNA-Affinity Tag-Based Strategy for cRNP and vRNP Purification. To isolate influenza virus cRNPs and vRNPs separately from infected cells we sought to use an affinity purification of RNPs based on an RNA tag. We took advantage of the translational operator RNA hairpin from the *Pseudomonas aeruginosa* bacteriophage PP7 (PP7) that binds with high affinity (K_d = ~1 nM) to the coat protein of PP7 (PP7CP) (9, 10). We generated recombinant influenza A/WSN/33 viruses by reverse genetics (11) that encode the PP7 RNA tag in the neuraminidase (NA) gene allowing the isolation of either cRNA or vRNA, depending on the orientation of the tag (Fig. 1*A*). The RNA-tag was inserted into the region of the NA gene that encodes the NA stalk (12). Analysis of wild-type and recombinant viruses revealed that virus growth was unaffected by the presence of the RNA tag (Fig. 1 *B* and *C*), demonstrating that heterologous RNA secondary structures can be introduced into the influenza virus genome without impairing genome encapsidation. Furthermore, the corresponding insertion in the NA protein did not hamper virus release from the host cells in cell culture conditions, consistent with previous reports showing that insertions and deletions in the NA stalk can be tolerated by the virus (13–16).

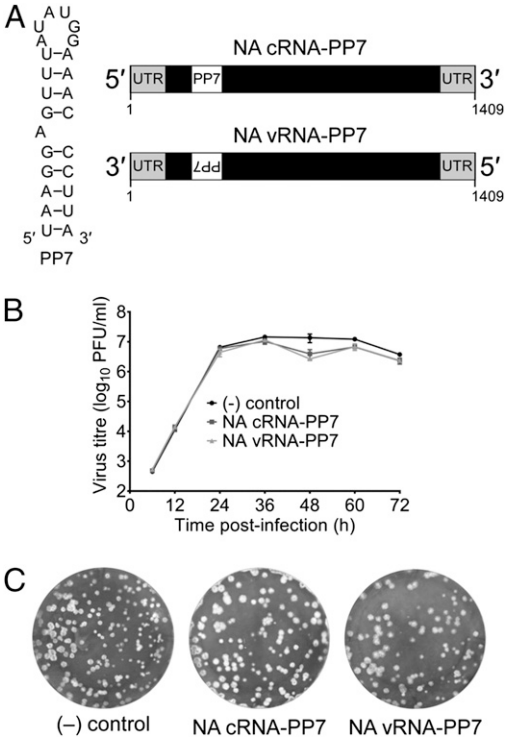


Fig. 1. Generation of recombinant influenza A viruses containing PP7 RNA tag in the NA. (*A*) PP7 RNA was inserted into the NA gene of influenza A/WSN/33 virus to allow RNA-affinity purification of cRNA or vRNA. (*Left*) Sequence of the PP7 RNA tag. (*Right*) Position of the PP7 RNA tag in the NA cRNA and vRNA. Untranslated terminal sequences (UTR), the NA ORF (black box), and the PP7 RNA tag are shown. (*B*) Growth curves of wild-type [(–) control] and tagged cRNA-PP7 and vRNA-PP7 viruses in MDBK cells. (*C*) Plaque phenotype of wild-type [(–) control] and tagged cRNA-PP7 and vRNA-PP7 viruses on MDBK cells infected for 72 h before staining with Coomassie Brilliant Blue.

Purification of Influenza A Virus cRNP and vRNP Separately from Infected Cells. To purify PP7-tagged RNA, we established a stable HEK 293T cell line that expresses PP7CP. Alternatively, expression was achieved transiently by transfection. Infection of cells expressing PP7CP resulted in endogenous assembly of viral RNP complexes containing PP7CP for affinity purification. Target viral NA cRNPs and vRNPs were separated with high specificity using RNA-based affinity chromatography and density gradient centrifugation (Fig. 2 and Figs. S1 and S2). Analysis of RNA and protein revealed that the cRNP and vRNP contained RdRp, NP, and cRNA or vRNA, respectively (Fig. 2). On average, 20.0% of the total cRNA and 11.8% of the total vRNA from cell lysates could be purified. However, only 3.2% of total mRNA could be recovered in the purification process (Fig. 2*B*). These data demonstrate that an RNA tag-based affinity purification allows the separate isolation of influenza virus cRNPs and vRNPs and that sufficient flexibility exists within the cRNPs and vRNPs for secondary RNA structures to form that are not eliminated as a result of encapsidation by oligomeric NP.

Influenza Virus cRNP Exhibits a Double-Helical Arrangement Consisting of cRNA, NP, and the RdRp. Negative-stain EM of NA cRNPs revealed filamentous particles (Fig. 3*A*) with a median length of 72 nm (n = 231), in agreement with the length of influenza virus vRNP segments of intermediate length in nucleotides (17). A dataset of 2,456 cRNP images was obtained, revealing that the filaments were often highly flexible (Fig. S3). This flexibility resulted in disorder in the 2D class averages of the particles, especially at the termini (Fig. 3*B*). To gain insight into the molecular architecture of the central filament and the termini, the corresponding subimages were classified independently. The central filament class averages revealed repeating triangular structural motifs, consistent with a double-helical arrangement of NP (Fig. 3*C*). We classified the termini and then split them into two groups, comprising either arrowhead-shaped (Fig. 3*D*) or looped structures (Fig. 3*E*), and these were interpreted to correspond to side views of the RdRp and NP-RNA loops, respectively. The RdRp structure exhibited a large and a small polymerase domain and adopted different angles relative to the central filament (Fig. 3*D*). The NP-RNA loops displayed varying diameters (~14–23 nm) corresponding to approximately three to seven NP molecules, suggesting a degree of flexibility of the loop structure.

Purified vRNPs but Not cRNPs Are Active in Vitro. The separation of cRNP and vRNP from infected cells enabled us to determine and compare the basic molecular requirements for viral RNA synthesis between these viral RNP complexes in in vitro activity assays. Viral RNAs were detected by performing a primer extension assay by using two radiolabeled primers that analyze the 5′ end of the template and product, one specific for NA mRNA and cRNA and the other specific for vRNA (7, 18). As demonstrated by the synthesis of de novo initiated cRNA, vRNPs were able to replicate (Fig. 4*A*). Replication activity was greatly enhanced in the presence of an ApG dinucleotide primer that is complementary to the 3′ end of the vRNA template (Fig. 4*A*). vRNPs were also able to synthesize 5′ capped mRNA when β-globin mRNA was provided as a cap donor. In the presence of the cap donor, vRNPs also synthesized de novo initiated cRNA, as reported previously (19), although we cannot exclude entirely

MICROBIOLOGY

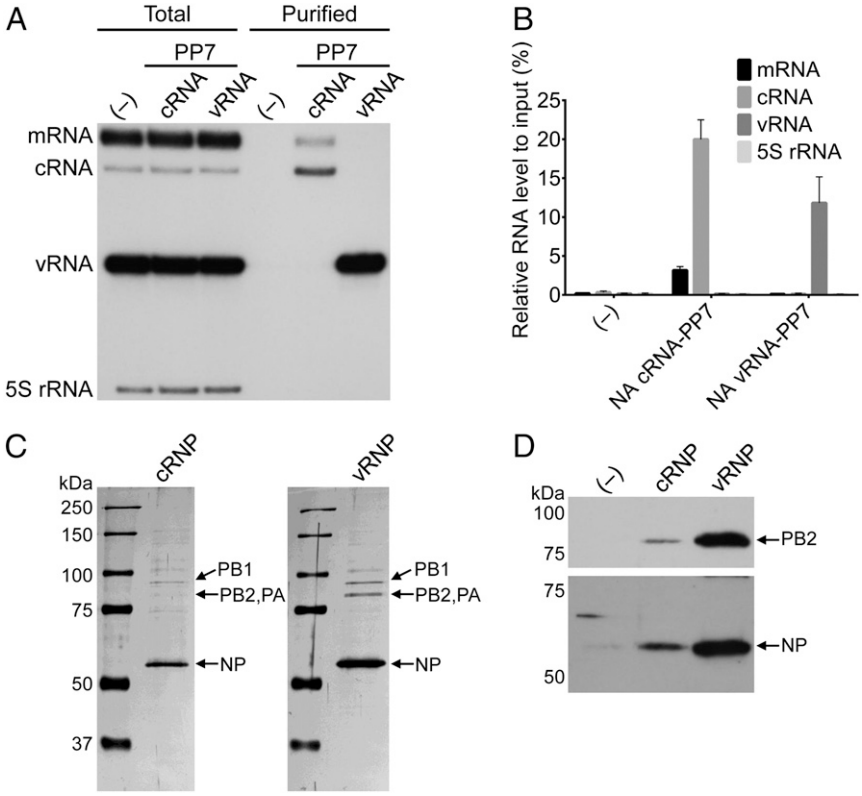


Fig. 2. Isolation of a cRNP replicative intermediate and vRNP from influenza virus-infected cells. (*A*) Primer extension analysis of total and purified NA-specific RNA from HEK 293T-PP7CP cells infected with wild-type (–), cRNA-PP7, or vRNA-PP7 viruses. Viral RNAs were analyzed by primer extension using primers specific for positive sense (mRNA and cRNA) and negative sense (vRNA) NA-specific viral RNAs that generate cDNAs with an expected size of 169–177 nt from mRNA (dependent on the length of the capped mRNA primer), 160 nt from cRNA, and 129 nt from vRNA. Primer extension analysis of 5S rRNA was used as a control producing a cDNA product of 100 nt. Ten times more sample of purified RNA was analyzed relative to total RNA. (*B*) Quantitation of primer extension analysis of purified RNA. RNA levels represent the mean, and the error bars represent SDs from three biological repeats. (*C*) Analysis of purified cRNP and vRNP fractions from RNA-affinity purifications and density glycerol gradients by SDS/PAGE and staining with silver. Note that lower amounts of cRNPs were purified compared with vRNPs owing to a lower accumulation of cRNA in infected cells (7, 8). In the cRNP lane the intensity of the PB1 band appears stronger than that of the PB2/PA bands owing to the presence of a contaminating cellular protein that migrates at the same position (Fig. S2). (*D*) Analysis of PB2 and NP in purified RNPs by Western blot.

that some of these products represent de-capped viral mRNAs. In contrast, cRNPs were unable to synthesize detectable amounts of vRNA de novo or in the presence of an ApG dinucleotide that is complementary to the 3′ end of the cRNA template (Fig. 4*A*).

A *Trans*-Activating RdRp Is Required for cRNP Activity. Earlier work has proposed a model whereby vRNA synthesis relies on a *trans*-acting RdRp for replication (20). We therefore hypothesized that the inability of the cRNP to synthesize vRNA is due to the absence of an RdRp acting in *trans*. To test this hypothesis, we included recombinant RdRp purified from *Spodoptera frugiperda* cells (Fig. S4*A*) in the cRNP activity assays. Only in the presence of additional RdRp did we observe the synthesis of vRNA from the cRNA template. Two primer extension products with slightly different sizes were observed (Fig. 4*B*), the shorter product likely representing vRNA initiated internally at position 4 on the cRNA promoter, consistent with the previously proposed internal initiation model for the cRNA promoter (21). In the absence of a vRNA-specific radiolabeled primer the products of cRNP activity were not detected (Fig. 4*B*). A 4.1-fold increase in vRNA signal was observed in the presence of added recombinant RdRp, compared with no recombinant RdRp being present.

The *Trans*-Activating RdRp Acts Cooperatively with the Resident RdRp, Which Carries Out the vRNA Synthesis. Does the recombinant RdRp act in *trans* in agreement with previously proposed models (3, 20), or does it instead have an uncharacterized function for supporting the cRNP-associated RdRp to act in *cis*? To address this question, recombinant wild-type RdRp or PB1 active-site mutant (PB1a) RdRp was purified from mammalian cells (Fig. S4 *B* and *C*) and included in the in vitro assays. Unexpectedly, both wild-type and active-site mutant RdRp were able to promote cRNP activity, resulting in the synthesis of vRNA 3.1-fold and 2.8-fold over background for the wild-type and the active-site mutant RdRp, respectively (Fig. 5*A*). These results suggest that the recombinant RdRp does not act as a replicase in *trans*, but instead, it acts cooperatively with the resident RdRp, which acts as a replicase in *cis*.

To investigate this further, we used an alternative in vitro transcription assay that involves the incorporation of radiolabeled nucleoside triphosphates. To analyze vRNP activity we set up a reaction leaving out UTP, expecting a 14-nt-long transcription product as the first ATP occurs at position 15 in the vRNA template. Analogously, to analyze cRNP activity we left out CTP, expecting an 8-nt-long transcription product. Consistent with previous results (Fig. 5*A*), cRNPs showed activity in presence of wild-type RdRp as well as in the presence of the PB1a active-site mutant RdRp (Fig. 5*B*). Taken together, these data show that the cRNP-associated RdRp requires a *trans*-activating RdRp with a nonenzymatic role.

Discussion

The principal advancement of this study is the isolation of a replicative intermediate of a negative-strand virus, permitting

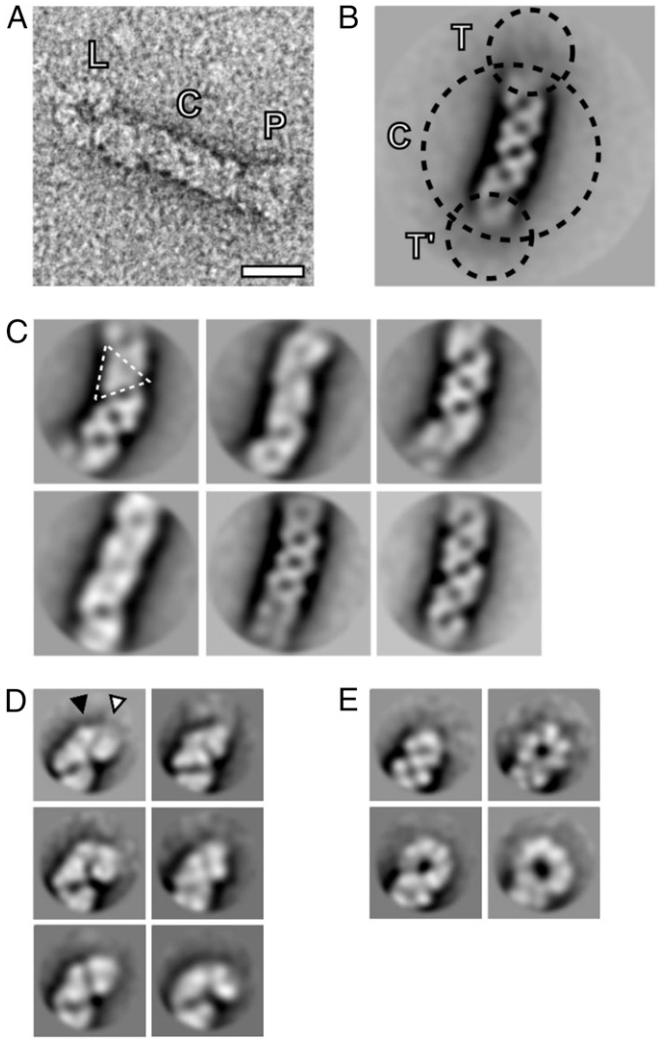


Fig. 3. Structural organization of the influenza virus cRNP replicative intermediate. (*A*) One cRNP particle, extracted from an electron micrograph, is shown. NP-RNA loop end (L), central helical filament (C), and RdRp end (P) are labeled. (Scale bar, 20 nm.) (*B*) Class averages of cRNP particles. The two termini (T and T′) were not resolved in initial class averages. Further classification concentrated on subimages of the termini and the central filament (C). (*C*) Class averages of the central filament reveal variation due to variable curvature of the filament and different orientations around the filament long axis. Depending on the orientation, repeating triangular structural motifs were visible (triangle). (*D*) Class averages of the termini representing RdRp side views. Two globular densities, putatively corresponding to a large (white triangle) and small (black triangle) structural feature of RdRp are indicated. (*E*) Class averages of the NP-RNA loop side views reveal variation in loop diameter. The scale of *B*–*E* is the same as in *A*.

visualization and functional characterization of such complexes. Our data revealed that the replicative intermediate of influenza virus exists as an individual structured particle that comprises cRNA, NP, and RdRp. We observed that the cRNP particle contains three major domains, the central filament and two distinct termini, one terminus harboring a loop and the other a structure that we interpret as the RdRp, on the basis of analogy to previously published structures of vRNPs (2, 3). The central filament exhibited a helical arrangement, similar to the reported vRNP filament structure (2, 3) in which the helical arrangement of the filament is facilitated by NP–NP interactions. We observed a varying diameter of the loop at the terminus of the cRNP, with three to seven NP molecules being present within the loop. This observation is consistent with previous reports that the loop end of the vRNP comprises five to eight NP molecules in one study (3) and three NP molecules in another study (2). In contrast to previous studies, which analyzed a mixture of vRNPs corresponding to RNA segments of various lengths, here we analyze one particular cRNP with an RNA segment of a defined length. The fact that these cRNPs exhibit loops with varying numbers of NP molecules implies either slightly different degrees of helical winding in the central filament or, perhaps more likely, different degrees of unwinding at the loop-end of the filament. The opposite terminus contained the RdRp exhibiting a small and a large structural feature. Previous EM studies of vRNP-associated RdRp also found that the RdRp shows two structural features, the larger feature possibly corresponding to PB1, PB2, and the N terminus of PA, whereas the smaller feature corresponds to the C-terminal domain of PA (3). Further studies using higher-resolution approaches (e.g. cryo-EM) are required to answer whether a similar or different arrangement of subunits exists within the cRNP-associated RdRp.

The specific purification of PP7 RNA-tagged RNPs relies on the accessibility of a surface exposed RNA tag that is not bound by NP. It remains unclear whether the formation of the PP7 RNA secondary structure is sufficient to prevent encapsidation by NP or the binding of PP7CP is required to stabilize the RNA structure and prevent the melting by NP. The presence of an RNA tag that is accessible within the vRNP and cRNP structures

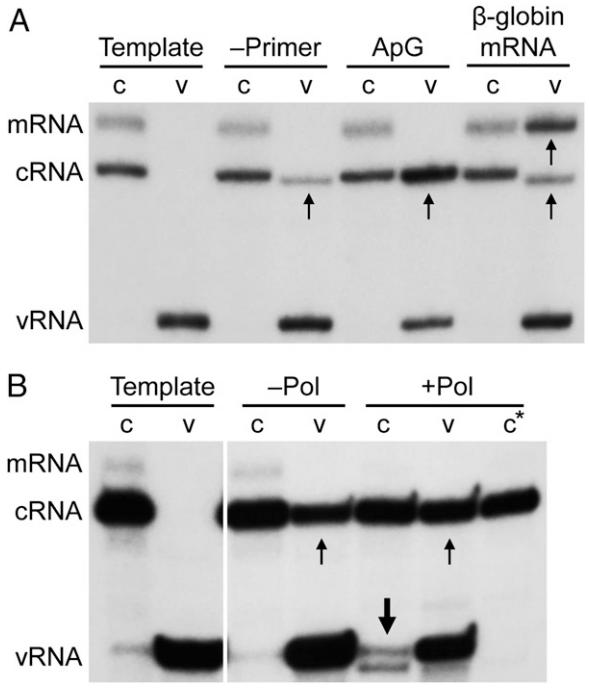


Fig. 4. A *trans*-activating RdRp is required for cRNP activity. In vitro activity assays of purified NA cRNPs (c) and vRNPs (v) in the absence of rNTPs as a negative control to indicate template RNA (Template) or (*A*) in the presence of rNTPs but absence of primer (–Primer), presence of ApG dinucleotide primer (ApG), or capped RNA (β-globin mRNA), (*B*) in the presence of rNTPs and ApG dinucleotide primer without (–Pol) or with (+Pol) added recombinant influenza virus RdRp purified from insect cells. Templates and transcription products were analyzed by primer extension using primers specific for positive sense (mRNA and cRNA) or negative sense (vRNA) NA-specific viral RNAs as described for Fig 2*A*. c* denotes primer extension analysis in the absence of vRNA-specific primer. Small arrows indicate products of vRNP activity, and large arrows indicate products of cRNP activity that form a doublet. Note that the weak vRNA-specific signals observed in the Template and –Pol cRNP lanes represent small amounts of vRNA that copurify with cRNPs.

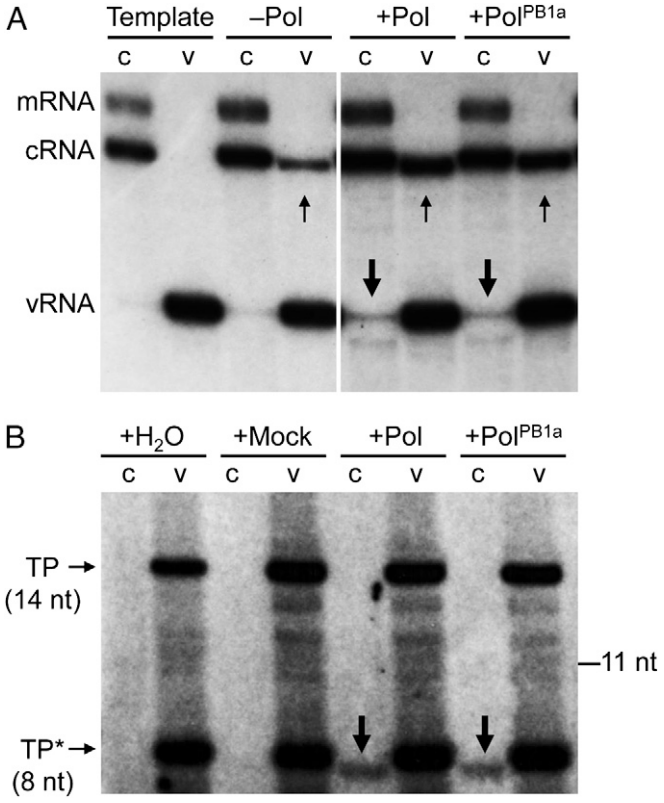


Fig. 5. *Trans*-activating RdRp acts cooperatively with the resident RdRp, which carries out vRNA synthesis. (*A*) In vitro activity assays of purified NA cRNPs (c) and vRNPs (v) in the absence of rNTPs as a negative control to indicate template RNA (Template) or in the presence of rNTPs without (–Pol) or with added recombinant wild-type (+Pol) or active-site mutant (+Pol^{PB1a}) influenza virus RdRp purified from transfected HEK 293T cells. Templates and transcription products were analyzed by primer extension using primers specific for positive sense (mRNA and cRNA) or negative sense (vRNA) NA-specific viral RNAs. Small arrows indicate products of vRNP activity, and large arrows indicate products of cRNP activity that form a doublet. Note that small amounts of vRNA copurifying with cRNP were detected in the Template and –Pol cRNP lanes. (*B*) In vitro activity assays of purified NA cRNPs (c) and vRNPs (v) using [α-^{32}P]NTP incorporation in the presence of ApG primer and water (+H_2O), mock polymerase (+Mock), wild-type (+Pol), or active-site mutant (+Pol^{PB1a}) RdRp purified from transfected HEK 293T cells. TP (14 nt) denotes the transcription product derived from the vRNA template, and TP* (8 nt) denotes a premature termination product due to limiting CTP concentrations. The 8-nt-long transcription product derived from the cRNA template is denoted by large arrows.

of influenza virus for the binding of PP7CP provides experimental evidence that sufficient flexibility exists within viral ribonucleoproteins for secondary RNA structures to form and that such structures do not prevent read-through by the RdRp. Local secondary RNA structures are also believed to play a role in the packaging process of the eight vRNP complexes into progeny virions. Interactions between such RNA secondary structures may mediate the interaction between the eight vRNPs, leading to the observed 7+1 arrangement of vRNPs within budding virions as visualized by EM (22–25).

Interestingly, viral mRNA was purified with a significantly lower efficiency than cRNA or vRNA (Fig. 2*B*). This finding suggests that the PP7 RNA tag is less accessible for PP7CP binding in the NA mRNPs, possibly reflecting the association of viral mRNAs with numerous cellular factors involved in their processing, nuclear export, and translation (26). The potential for secondary RNA structures to form in the ribonucleoproteins of other negative-strand RNA viruses is not known. In contrast to influenza virus RNPs, the RNA associated with the majority of negative-strand RNA virus RNPs is more resistant to nuclease digestion, suggesting a tighter packaging of RNA within the RNP structure (27). The described method using an RNA tag might help to address the question of whether RNA secondary structures can form within these RNPs.

The isolation of cRNPs presented in this study allowed us to advance the model of genome replication for influenza viruses by performing in vitro functional assays. Previously proposed models of influenza virus RNP function suggest that replication is performed by a *trans*-acting RdRp (3, 20). It has been observed, by using a genetic *trans*-complementation approach, that the replication activity of a replication-defective RNP could be rescued in the presence of a replication-competent *trans*-acting RdRp (20). Consistent with this observation, EM studies of RNPs purified from transfected cells revealed short RNPs branching from longer RNPs with an RdRp being present at both the branch point and termini (3).

In contrast to this model, our model on cRNP function suggests that replication (cRNA→vRNA) is performed by the RdRp that is resident in the cRNP complex and that a *trans*-activating polymerase is required for activation of vRNA synthesis. This model is supported by two findings from our in vitro experiments. First, cRNP showed no detectable activity in vRNA synthesis assays, but activity could be gained by the addition of purified RdRp in *trans*. Second, the result that the addition of an RNA synthesis inactive mutant of the RdRp had the same effect as the wild-type RdRp demonstrates that replication is performed by the resident RdRp in *cis*. The *trans*-activating RdRp, however, is required for activation of the resident RdRp. It could be argued that there is an exchange at the cRNA promoter between the active and inactive RdRps such that the active RdRp could then act in *trans* on the template. Although this possibility cannot be excluded, previous data showed that binding of RdRp to the 5′ end of the promoter cannot be outcompeted by a pre-expressed RdRp (19, 20), suggesting that an exchange is unlikely. We speculate that the *trans*-activating RdRp either provides structural support or induces a conformational change of the resident RdRp. This may occur through the formation of a quaternary structure by an interaction between the two RdRps. Indeed, it has been proposed that the influenza virus RdRp can form oligomers, possibly through interactions between PB1 and/or PB2 subunits (28, 29).

The cooperation and oligomerization between RdRps has been reported to be necessary for viral RNA synthesis in several RNA viruses, including poliovirus (30), hepatitis C virus (31), and Sendai virus (32). Additionally, the HIV-1 reverse transcriptase functions as a dimeric complex of the p66 subunit and a processed product p51 (33). Together with our study, these findings suggest that multimerization-driven stimulation of RNA polymerase activity is a common theme in RNA viruses. Whether the arrangement of RdRps plays an architectural role, required for the reorganization of RNA structural motifs or the rearrangement of the active site of the cRNP-associated replicating RdRp, remains unknown.

To conclude, the presented approach for isolating the replicative intermediates of negative-strand RNA viruses represents a powerful method for understanding how vRNA replication works in influenza virus infection. The approach should be applicable to the study of any other negative-strand RNA virus. This will undoubtedly yield new mechanistic insights into the workings of the RNA synthesis machines shared by a broad group of important human, animal, and plant pathogens.

Materials and Methods

Cells. Human embryonic kidney 293T (HEK 293T) cells and Madin-Darby bovine kidney epithelial (MDBK) cells were maintained in DMEM (PAA) or modified Eagle medium with Earle's salts (MEM; PAA), respectively, sup-

plemented with 2 mM L-glutamine (PAA) and 10% FCS (PAA). An HEK 293T-PP7CP stable cell line was produced under the selection of hygromycin-B (Roche). For this purpose, 30 μg of pcDNA-PP7CP-His was transfected using Lipofectamine 2000 (Invitrogen) according to the manufacturer's instructions into ~4 × 10^6 HEK 293T cells in 10-cm dishes. After 48 h, the cells were replated into 15-cm dishes containing DMEM supplemented with 10% FCS and hygromycin-B (500 μg/mL). Stable clone selection occurred in the presence of hygromycin-B (500 μg/mL) for ~30 d. Stable colonies resistant to hygromycin-B were picked and recultured, and protein expression was confirmed by Western blotting.

Viruses. Influenza A/WSN/33 virus (WSN) was cultured on MDBK cells in MEM supplemented with 2 mM L-glutamine and 0.5% FCS. Influenza A/WSN/33 NA cRNA-PP7 and vRNA-PP7 influenza viruses were generated using the 12 plasmid-based reverse genetics rescue system (11). An XbaI site was introduced into the pPOLI-NA-RT plasmid by site-directed mutagenesis [(5′-GGCAGCATTACCTCTAGAGTTGTTGC-3′) and (5′-GCAACAACTCTAGAGGTAATGCTGCC-3′)]. The PP7 RNA tag was inserted by annealing two complementary oligonucleotides with XbaI restriction sites at the 5′ and 3′ ends [(5′-CTAGTAAGGAGTTTATATGGAAACCCTTAT-3′) and (5′-CTAGATAAGGGTTTCCATATAAACTCCTTA-3′)] for NA cRNA-PP7 and [(5′-CTAGTAAGGGTTTCCATATAAACTCCTTAT-3′) and (5′-CTAGATAAGGAGTTTATATGGAAACCCTTA-3′)] for NA vRNA-PP7 and ligating into the XbaI-digested pPOLI-NA-XbaI plasmid. Underlined nucleotides correspond to the PP7 RNA tag recognized by PP7CP. Insertion of the PP7 RNA tag resulted in the replacement of amino acids Y56 and K57 in the NA stalk with SSKEFIWKPLSR in NA cRNA-PP7 and SSKGFHINSLSR in NA vRNA-PP7.

Plasmids. The pcDNA-PP7CP-His and pcDNA-PP7CP-Strep expression plasmids were constructed by PCR amplifying the PP7 gene from pETZZ-tev-PP7CP (kind gift from J. Robert Hogg, National Heart, Lung, and Blood Institute, National Institutes of Health, Bethesda) (10) with NotI or KpnI at the 5′ end and a 6-His tag or One-Strep and a XbaI or NotI restriction site at the 3′ end, respectively. The PCR product and pcDNA3A (34) were double-digested with the relevant restriction endonucleases, and the PCR amplified gene was ligated into pcDNA3A.

Growth Curve Analysis. Growth curve analysis was performed by infecting 80% confluent MDBK cells in 3.5-cm dishes at a multiplicity of infection (MOI) of 0.001 with wild-type or PP7-tagged influenza/A/WSN/33 viruses and harvesting the supernatant every 12 h after infection for 72 h. Viral titers were determined by plaque assay.

Isolation of RNPs by RNA-Based Affinity Purification. Approximately 3 × 10^7 HEK 293T-PP7CP-His cells were seeded into 15-cm dishes and cultured for 48 h in DMEM supplemented with 10% FCS and hygromycin-B (500 μg/mL) at 37 °C, 5% CO_2. Alternatively, ~3 × 10^7 HEK 293T cells were transfected with pcDNA-PP7CP-Strep using Lipofectamine 2000 according to the manufacturer's instructions and incubated for 48 h in DMEM supplemented with 10% FCS at 37 °C, 5% CO_2. Cells were rinsed with PBS and infected at an MOI of 5 for 1 h at room temperature with wild-type or PP7-tagged influenza A/WSN/33 viruses and incubated for a further 6–9 h in DMEM (0.5% FCS) at 37 °C, 5% CO_2. Six to nine hours after infection, cells were collected by centrifugation at 200 × *g* for 5 min at 4 °C and washed with ice-cold PBS. Cells were collected by centrifugation at 200 × *g* for 5 min at 4 °C, flash-frozen, and stored at −80 °C.

vRNPs were purified either by Ni-NTA or Strep-tag affinity purification. For Ni-NTA affinity purification of RNPs, cells were thawed on ice and lysed in 4 mL of Tris lysis buffer [50 mM Tris·HCl (pH 8.0), 200 mM NaCl, 33% (vol/vol) glycerol, 20 mM imidazole, 0.5% (vol/vol) Igepal CA-630 (Sigma), 1 mM DTT, and 1× complete EDTA-free protease inhibitor mixture (Roche)] by rotation for 1 h at 4 °C, and then the soluble and insoluble fractions were separated by centrifugation at 17,000 × *g* for 5 min at 4 °C. The soluble fraction was diluted 1:5 with Ni-NTA binding buffer [20 mM Tris·HCl (pH 8.0), 200 mM NaCl, 20 mM imidazole, 1 mM $MgCl_2$, and 1× complete EDTA-free protease inhibitor mixture] and incubated with 4 mL Ni-NTA agarose (Qiagen) for 2 h by rotation at 4 °C. Ni-NTA agarose was washed extensively with Ni-NTA wash buffer [20 mM Tris·HCl (pH 8.0), 200 mM NaCl, 40 mM imidazole, 1 mM $MgCl_2$, 0.1% (vol/vol) Igepal CA-630, 10% (vol/vol) glycerol, and 1× phenylmethanesulfonylfluoride], and PP7CP-bound RNPs were eluted in 5 mL of Ni-NTA elution buffer [20 mM Tris·HCl (pH 8.0), 200 mM NaCl, 250 mM imidazole, 1 mM $MgCl_2$, 0.1% (vol/vol) Igepal CA-630, 10% (vol/vol) glycerol, and 1× complete EDTA-free protease inhibitor mixture] for 2 h at 4 °C by rotation. Eluates were subsequently analyzed for proteins by SDS/PAGE and silver staining, and RNA was extracted and analyzed for by primer extension using NA-specific primers as previously described (18). Quantitation of primer extension products was performed by phosphorimage analysis using Aida software (Raytest). Eluates were concentrated to 1 mL using Amicon Ultra-4 (100K MWCO) centrifugation devices (Millipore) before density gradient centrifugation.

For Strep-tag affinity-purification of RNPs, cells were thawed on ice and lysed in 4 mL of Tris lysis buffer [50 mM Tris·HCl (pH 8.0), 200 mM NaCl, 33% (vol/vol) glycerol, 0.5% (vol/vol) Igepal CA-630, 1 mM DTT, and 1× complete EDTA-free protease inhibitor mixture] by rotation for 1 h at 4 °C, and then the soluble and insoluble fractions were separated by centrifugation at 17,000 × *g* for 5 min at 4 °C. The soluble fraction was diluted 1:5 with Strep-Tactin binding buffer [20 mM Tris·HCl (pH 8.0), 200 mM NaCl, 1 mM $MgCl_2$, and 1× complete EDTA-free protease inhibitor mixture] and incubated overnight at 4 °C with 0.5 mL of 50% suspension Strep-Tactin Superflow high-capacity resin (IBA GmbH). Strep-Tactin resin was washed extensively with Strep-Tactin wash buffer [20 mM Tris·HCl (pH 8.0), 200 mM NaCl, 1 mM $MgCl_2$, 0.1% (vol/vol) Igepal CA-630, 10% (vol/vol) glycerol, and 1× phenylmethanesulfonylfluoride], and PP7CP-bound RNPs were eluted in 5 mL of Strep-Tactin elution buffer [20 mM Tris·HCl (pH 8.0), 200 mM NaCl, 1 mM $MgCl_2$, 0.1% (vol/vol) Igepal CA-630, 10% (vol/vol) glycerol, 2 mM *d*-Desthiobiotin (IBA GmbH), and 1× complete EDTA-free protease inhibitor mixture] for 2 h at 4 °C by rotation. Eluates were subsequently analyzed for proteins by SDS/PAGE and silver staining, and RNA was extracted and analyzed for by primer extension using NA-specific primers. Eluates were concentrated to 1 mL using Amicon Ultra-4 (100K MWCO) centrifugation devices (Millipore) before density gradient centrifugation.

RNPs were isolated by ultracentrifugation on a discontinuous glycerol gradient [1 mL each of 70%, 50%, 40%, and 33% (vol/vol)] in 50 mM Tris·HCl (pH 8.0), 200 mM NaCl, and 1 mM $MgCl_2$. The gradients were centrifuged at 192,000 × *g* in a Beckman SW55Ti rotor for 4 h at 4 °C. Fractions of ~300 μL were collected dropwise from the bottom of the tube. Fractions were analyzed for RNA by primer extension using NA-specific primers. Proteins were analyzed by SDS/PAGE and silver staining and Western blotting using polyclonal antibodies directed against PB2 and NP. Fractions enriched with RNPs were pooled and used for EM and in vitro activity assays.

EM and Image Processing. A 5-μL aliquot of purified cRNP was applied to a glow-discharged 200 mesh carbon-formvar copper grid, and grids were stained with 2% uranyl acetate. Images were taken on CCD (UltraScan 4000SP; Gatan) with a transmission electron microscope (Tecnai F30; FEI) operated at 200 kV and at 39,000× nominal magnification. Contrast transfer function estimation and phase flipping was carried out using XMIPP (http://xmipp.cnb.csic.es/) (35). Images were down-sampled by a factor of two, resulting in a pixel size of 6.08 Å/pixels. In total, 529 images were taken, resulting in a dataset of 2,456 cRNP particles. Extracted particles (150 × 150 pixels) were subjected to simultaneous alignment and classification in Relion (http://www2.mrc-lmb.cam.ac.uk/relion/) (36). The approximate coordinates of the termini were defined in the selected class averages, and 2,456 corresponding subimages (80 × 80 pixels) were extracted from the original micrographs. Subimages were aligned and classified using the in-plane rotation angle of the central filament (psi) as prior information. To derive final class-average images of the RdRp and NP-RNA loop ends, particles assigned to either group were subjected to further 2D classification.

Recombinant Influenza Virus RdRp Purification. Recombinant influenza A/NT/60/68 virus RdRp with a protein-A tag on the PB2 subunit was expressed using the Multibac system in Sf9 insect cells (37, 38). Sf9 cell suspension cultures at 2.0 ×10^6 cells/mL were infected with recombinant baculovirus at an MOI of 0.5–1.0 and incubated for 72 h at 27 °C. Cells were harvested by centrifugation and lysed by sonication in lysis buffer [50 mM Hepes·NaOH (pH 7.5), 500 mM NaCl, 10% (vol/vol) glycerol, 0.05% (wt/vol) octylthioglucoside, 1× complete EDTA-free protease inhibitor mixture, and 100 μg/mL RNase A]. The lysate was clarified by centrifugation, and the supernatant was incubated with washed IgG Sepharose (GE Healthcare; ~2 mL bead slurry per liter of original culture) for 3–4 h at 4 °C. After binding, the beads were washed with 50 mM Hepes·NaOH (pH 7.5), 500 mM NaCl, 10% (vol/vol) glycerol, and 0.05% (wt/vol) octylthioglucoside. The polymerase was released using AcTEV protease (150 U per mL of IgG Sepharose) at 4 °C overnight in the above wash buffer supplemented with 2.5 mM reduced glutathione. The final purification step was size exclusion chromatography through a HiLoadTM 16/60 Superdex S200 column (GE Healthcare) at 4 °C, using 500 mM NaCl, 50 mM Hepes·NaOH (pH 7.5), 10% (vol/vol) glycerol, 1 mM $MgCl_2$, and 0.1 mM $MnCl_2$.

Recombinant influenza A/WSN/33 virus RdRp expressed in mammalian cells was prepared by tandem affinity purification (37) by transiently

transfecting ~2×10^7 HEK 293T cells with 60 μg of each of the RdRp expression plasmids (pcDNA-PA, pcDNA-PB2-TAP, and pcDNA-PB1 for wild-type RdRp or pcDNA-PB1a for active-site mutant RdRp) (7, 34, 39) using Lipofectamine 2000 according to the manufacturer's instructions. Cells were incubated for 48 h in DMEM supplemented with 10% FCS at 37 °C, 5% CO_2 before collection by centrifugation at 200 × *g* for 5 min at 4 °C. Cells were then washed with ice-cold PBS and pelleted by centrifugation at 200 × *g* for 5 min at 4 °C and then lysed in 2 mL of Tris lysis buffer [50 mM Tris·HCl (pH 8.0), 200 mM NaCl, 33% (vol/vol) glycerol, 0.5% (vol/vol) Igepal CA-630, 1 mM DTT, and 1× complete EDTA-free protease inhibitor mixture] by rotation for 1 h at 4 °C. The soluble and insoluble fractions were separated by centrifugation at 17,000 × *g* for 5 min at 4 °C, and the soluble fraction was diluted 1:5 with binding buffer [20 mM Tris·HCl (pH 8.0), 150 mM NaCl, and 1× complete EDTA-free protease inhibitor mixture] and incubated with 400 μL of IgG Sepharose (GE Healthcare) for 2 h by rotation at 4 °C. IgG Sepharose was washed extensively with wash buffer [20 mM Tris·HCl (pH 8.0), 150 mM NaCl, 0.1% (vol/vol) Igepal CA-630, 10% (vol/vol) glycerol, and 1× phenylmethanesulfonylfluoride], and the RdRp was released by cleavage overnight at 4 °C with 20 U of AcTEV (Invitrogen) in 500 μL of cleavage buffer [10 mM Tris·HCl (pH 8.0), 150 mM NaCl, 0.1% (vol/vol) Igepal CA-630, 10% (vol/vol) glycerol, 1 mM DTT, and 1× complete EDTA-free protease inhibitor mixture]. AcTEV was removed by binding the eluate to 100 μL Ni-NTA agarose for 30 min at 4 °C by rotation and centrifuging at 17,000 × *g* for 5 min at 4 °C. The supernatant was concentrated to 50 μL using Amicon Ultra-4 (100K MWCO) centrifugation devices (Millipore) and stored at 4 °C. Mock samples as negative controls were prepared by processing HEK 293T cells transfected with empty vector (pcDNA3A) as described above.

In Vitro Activity Assays of RNPs. RNP activity was assessed in a 20-μl reaction mixture containing 10 μL of purified RNPs, incubated for 16 h at 30 °C with 1 mM ATP, 0.5 mM of each CTP, GTP, and UTP (Amersham), 5 mM $MgCl_2$, 2 mM DTT, and 5 U RNasin (Promega), with 360 ng β-globin mRNA (Sigma) or 0.5 mM ApG (Sigma) as indicated. Where indicated, 500 ng of purified recombinant influenza virus RdRp expressed in Sf9 cells or 40 ng of wild-type or PB1a mutant RdRp expressed in mammalian HEK 293T cells was included. Transcription products were extracted using TRIzol reagent (Invitrogen) according to the manufacturer's instructions and precipitated with isopropanol in the presence of 10 μg of tRNA from *Escherichia coli* MRE 600 (Roche) before analysis by NA gene-specific primer extension and 6% PAGE in 7 M urea as described previously (7). Quantitation of primer extension products was performed by phosphorimage analysis using Aida software (Raytest).

Alternatively, RNP activity was assessed in a 10-μL reaction mixture containing 5 μl of purified RNPs incubated for 2 h at 30 °C with 1 mM ATP, 0.5 mM GTP, and 0.16 μM of [α-^{32}P]UTP (3,000 Ci/mmole; Perkin-Elmer) for cRNPs or 0.16 μM of [α-^{32}P]CTP (3,000 Ci/mmole; Perkin-Elmer) for vRNPs, 0.5 mM ApG, 5 mM $MgCl_2$, 2 mM DTT, and 5 U RNasin, with 10 ng of wild-type RdRp, PB1a active-site mutant RdRp, or mock sample. RNA was extracted by adding an equal volume of phenol/chloroform 1:1 (vol/vol) (pH 4.3) and vortexing for 5 min at room temperature before centrifuging at 17,000 × *g* for 20 min at 4 °C. RNA was precipitated from the aqueous fraction by adding 5 volumes of acetone/ethanol 3:1 (vol/vol) in the presence of 10 μg of tRNA from *E. coli* MRE 600 and incubating for 30 min at −20 °C before centrifuging at 17,000 × *g* for 20 min at 4 °C. The RNA pellet was washed in ice-cold 70% ethanol before dissolving in 10 μL formamide [90% (vol/vol) formamide (Sigma), 10 mM EDTA, 0.001% (wt/vol) bromophenol blue, and 0.001% (wt/vol) xylene cyanol] and heating to 95 °C for 3 min and cooling directly on ice before being analyzed by 20% PAGE containing 7 M urea.

In Vitro Activity Assay of Recombinant RdRp. Activity of purified recombinant RdRp polymerase was assessed using an [α-^{32}P]GTP incorporation assay as previously described (40). Briefly, 1.5 μL of purified polymerase and 15 pmol of each of 5′ end [15 nt (5′-AGUAGAAACAAGGCC-3′)] and 3′ end [14 nt (5′- GGCCUGCUUUUGCU-3′)] promoter templates were incubated in a 3-μL reaction mixture for 2 h at 30 °C with 1 mM ATP, 0.5 mM CTP, 0.5 mM UTP, 0.1 μM [α-^{32}P]GTP (3,000 Ci/mmole; Perkin-Elmer), 0.5 mM ApG, 5 mM $MgCl_2$, 2 mM DTT, and 5 U RNasin. After 2 h, 10 μL formamide was added [90% (vol/vol) formamide (Sigma), 10 mM EDTA, 0.001% (wt/vol) bromophenol blue, and 0.001% (wt/vol) xylene cyanol] and heated to 95 °C for 3 min and cooling directly on ice before being analyzed by 20% PAGE containing 7 M urea.

ACKNOWLEDGMENTS. We thank J. Robert Hogg for the pET-ZZ-tev-PP7CP plasmid, Otto Haller for the NP antibody, Imre Berger for providing the baculovirus technology, Zoe Gage for assistance with protein expression optimization, and Errin Johnson and Alistair Siebert for assistance with EM. This work was supported by Medical Research Council (MRC) Grants G0700848 and MR/K000241/1 (to E.F.) and G1100138 (to F.T.V.), an MRC studentship (to A.Y.), by Wellcome Trust Studentship 092931/Z/10/Z (to N.H.), and by Academy of Finland Grants 130750 and 218080 (to J.T.H.). The Wellcome Trust Centre for Human Genetics is supported by Wellcome Trust Core Award 090532/Z/09/Z. The Oxford Particle Imaging Centre EM facility was founded by Wellcome Trust Joint Infrastructure Fund Award 060208/Z/00/Z and is supported by Wellcome Trust Equipment Grant 093305/Z/10/Z.

1. Morin B, Kranzusch PJ, Rahmeh AA, Whelan SP (2013) The polymerase of negative-stranded RNA viruses. *Curr Opin Virol* 3(2):103–110.
2. Arranz R, et al. (2012) The structure of native influenza virion ribonucleoproteins. *Science* 338(6114):1634–1637.
3. Moeller A, Kirchdoerfer RN, Potter CS, Carragher B, Wilson IA (2012) Organization of the influenza virus replication machinery. *Science* 338(6114):1631–1634.
4. Fodor E (2013) The RNA polymerase of influenza a virus: Mechanisms of viral transcription and replication. *Acta Virol* 57(2):113–122.
5. Krug RM, Fodor E (2013) The virus genome and its replication. *Textbook of Influenza*, eds Webster RG, Monto AS, Braciale TJ, Lamb RA (John Wiley & Sons, New York), 2nd Ed, pp 57–66.
6. Palese P, Shaw ML (2013) *Orthomyxoviridae*. *Fields Virology*, eds Knipe DM, Howley PM (Lippincott Williams and Wilkins, Philadelphia), 6th Ed, pp 1151–1185.
7. Vreede FT, Jung TE, Brownlee GG (2004) Model suggesting that replication of influenza virus is regulated by stabilization of replicative intermediates. *J Virol* 78(17): 9568–9572.
8. Hatada E, Hasegawa M, Mukaigawa J, Shimizu K, Fukuda R (1989) Control of influenza virus gene expression: Quantitative analysis of each viral RNA species in infected cells. *J Biochem* 105(4):537–546.
9. Lim F, Peabody DS (2002) RNA recognition site of PP7 coat protein. *Nucleic Acids Res* 30(19):4138–4144.
10. Hogg JR, Collins K (2007) RNA-based affinity purification reveals 7SK RNPs with distinct composition and regulation. *RNA* 13(6):868–880.
11. Fodor E, et al. (1999) Rescue of influenza A virus from recombinant DNA. *J Virol* 73 (11):9679–9682.
12. Air GM (2012) Influenza neuraminidase. *Influenza Other Respi Viruses* 6(4):245–256.
13. Luo G, Chung J, Palese P (1993) Alterations of the stalk of the influenza virus neuraminidase: Deletions and insertions. *Virus Res* 29(2):141–153.
14. Castrucci MR, Kawaoka Y (1993) Biologic importance of neuraminidase stalk length in influenza A virus. *J Virol* 67(2):759–764.
15. Sorrell EM, Song H, Pena L, Perez DR (2010) A 27-amino-acid deletion in the neuraminidase stalk supports replication of an avian H2N2 influenza A virus in the respiratory tract of chickens. *J Virol* 84(22):11831–11840.
16. Munier S, et al. (2010) A genetically engineered waterfowl influenza virus with a deletion in the stalk of the neuraminidase has increased virulence for chickens. *J Virol* 84(2):940–952.
17. Compans RW, Content J, Duesberg PH (1972) Structure of the ribonucleoprotein of influenza virus. *J Virol* 10(4):795–800.
18. Robb NC, Smith M, Vreede FT, Fodor E (2009) NS2/NEP protein regulates transcription and replication of the influenza virus RNA genome. *J Gen Virol* 90(Pt 6):1398–1407.
19. Vreede FT, Brownlee GG (2007) Influenza virion-derived viral ribonucleoproteins synthesize both mRNA and cRNA in vitro. *J Virol* 81(5):2196–2204.
20. Jorba N, Coloma R, Ortín J (2009) Genetic trans-complementation establishes a new model for influenza virus RNA transcription and replication. *PLoS Pathog* 5(5):e1000462.
21. Deng T, Vreede FT, Brownlee GG (2006) Different de novo initiation strategies are used by influenza virus RNA polymerase on its cRNA and viral RNA promoters during viral RNA replication. *J Virol* 80(5):2337–2348.
22. Noda T, et al. (2006) Architecture of ribonucleoprotein complexes in influenza A virus particles. *Nature* 439(7075):490–492.
23. Hutchinson EC, von Kirchbach JC, Gog JR, Digard P (2010) Genome packaging in influenza A virus. *J Gen Virol* 91(Pt 2):313–328.
24. Fournier E, et al. (2012) A supramolecular assembly formed by influenza A virus genomic RNA segments. *Nucleic Acids Res* 40(5):2197–2209.
25. Noda T, et al. (2012) Three-dimensional analysis of ribonucleoprotein complexes in influenza A virus. *Nat Commun* 3:639.
26. York A, Fodor E (2013) Biogenesis, assembly and export of viral messenger ribonucleoproteins in the influenza A virus infected cell. *RNA Biol* 10(8):1274–1282.
27. Ruigrok RW, Crépin T, Kolakofsky D (2011) Nucleoproteins and nucleocapsids of negative-strand RNA viruses. *Curr Opin Microbiol* 14(4):504–510.
28. Jorba N, Area E, Ortín J (2008) Oligomerization of the influenza virus polymerase complex in vivo. *J Gen Virol* 89(Pt 2):520–524.
29. Digard P, Blok VC, Inglis SC (1989) Complex formation between influenza virus polymerase proteins expressed in *Xenopus oocytes*. *Virology* 171(1):162–169.
30. Lyle JM, Bullitt E, Bienz K, Kirkegaard K (2002) Visualization and functional analysis of RNA-dependent RNA polymerase lattices. *Science* 296(5576):2218–2222.
31. Wang QM, et al. (2002) Oligomerization and cooperative RNA synthesis activity of hepatitis C virus RNA-dependent RNA polymerase. *J Virol* 76(8):3865–3872.

32. Smallwood S, Cevik B, Moyer SA (2002) Intragenic complementation and oligomerization of the L subunit of the sendai virus RNA polymerase. *Virology* 304(2):235–245.
33. Kohlstaedt LA, Wang J, Friedman JM, Rice PA, Steitz TA (1992) Crystal structure at 3.5 A resolution of HIV-1 reverse transcriptase complexed with an inhibitor. *Science* 256 (5065):1783–1790.
34. Fodor E, et al. (2002) A single amino acid mutation in the PA subunit of the influenza virus RNA polymerase inhibits endonucleolytic cleavage of capped RNAs. *J Virol* 76 (18):8989–9001.
35. Scheres SHW, Núñez-Ramírez R, Sorzano COS, Carazo JM, Marabini R (2008) Image processing for electron microscopy single-particle analysis using XMIPP. *Nat Protoc* 3(6):977–990.
36. Scheres SHW (2012) RELION: Implementation of a Bayesian approach to cryo-EM structure determination. *J Struct Biol* 180(3):519–530.
37. Puig O, et al. (2001) The tandem affinity purification (TAP) method: A general procedure of protein complex purification. *Methods* 24(3):218–229.
38. Bieniossek C, Richmond TJ, Berger I (2008) MultiBac: Multigene baculovirus-based eukaryotic protein complex production. *Curr Protoc Protein Sci* Chapter 5:Unit 5.20.
39. Engelhardt OG, Smith M, Fodor E (2005) Association of the influenza A virus RNA-dependent RNA polymerase with cellular RNA polymerase II. *J Virol* 79(9):5812–5818.
40. Brownlee GG, Sharps JL (2002) The RNA polymerase of influenza A virus is stabilized by interaction with its viral RNA promoter. *J Virol* 76(14):7103–7113.

Supporting Information

York et al. 10.1073/pnas.1315068110

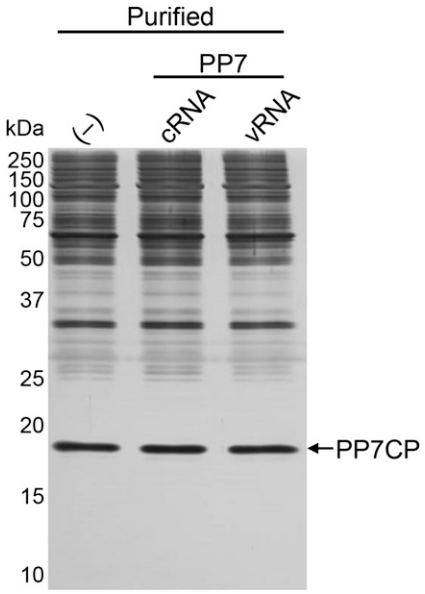


Fig. S1. RNA-based affinity purification of influenza virus ribonucleoprotein (RNP) complexes from infected HEK 293T-PP7CP-His cells. SDS/PAGE and silver stain analysis of PP7CP purified by Ni-NTA chromatography from HEK 293T-PP7CP-His cells infected with wild-type (–), neuraminidase (NA) cRNA-PP7, or NA vRNA-PP7 influenza/A/WSN/33 viruses. PP7, *Pseudomonas aeruginosa* bacteriophage PP7; PP7CP, coat protein of PP7.

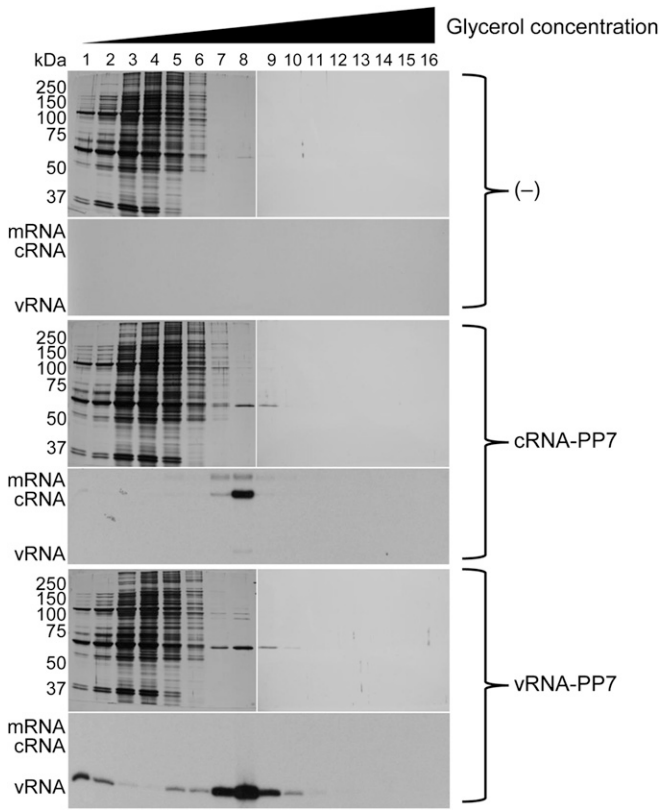


Fig. S2. Purification of NA complementary ribonucleoprotein (cRNP) and viral ribonucleoprotein (vRNP) complexes by density gradient ultracentrifugation. RNA-affinity purified material obtained from cells infected with wild-type (–), NA cRNA-PP7, or NA vRNA-PP7 influenza/A/WSN/33 viruses was fractionated on glycerol gradients, and fractions were analyzed by SDS/PAGE and staining with silver (*Upper*). RNA isolated from the fractions was analyzed by NA-specific primer extension (*Lower*) to detect NA mRNA, cRNA, and vRNA.

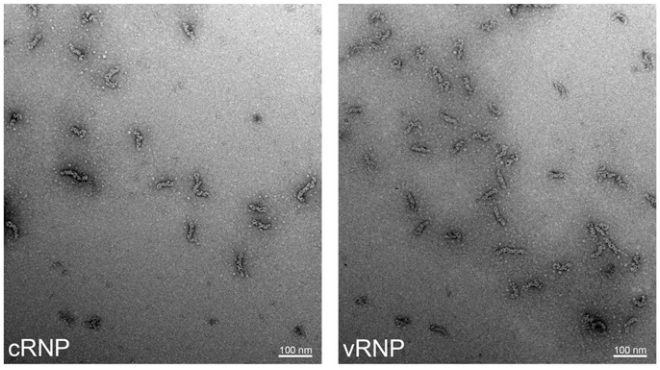


Fig. S3. Negative stain EM of purified influenza A/WSN/33 virus RNPs. Examples of images obtained from negative-stained samples used in 2D single particle analysis of cRNPs and vRNPs isolated by RNA-based affinity purification and density gradient centrifugation.

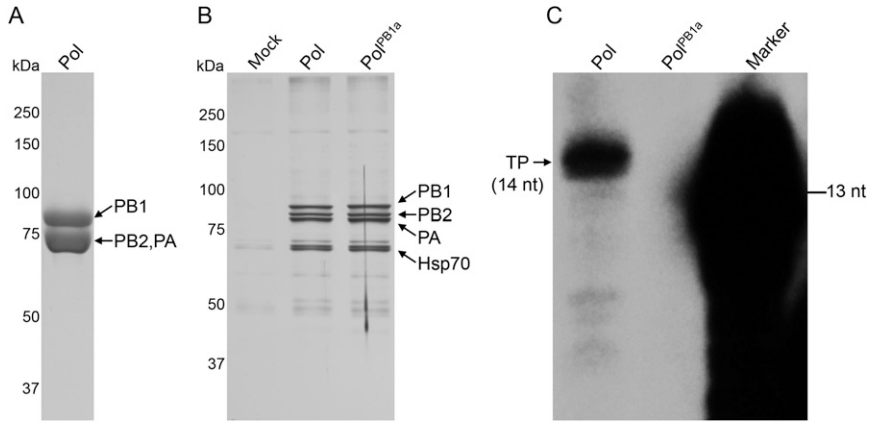


Fig. S4. Purification and activity of recombinant influenza A virus RdRp from Sf9 and HEK 293T cells. (*A*) Wild-type influenza virus RdRp (Pol) was purified from recombinant baculovirus-infected Sf9 cells and analyzed by SDS/PAGE and staining with Coomassie Brilliant Blue. (*B*) Wild-type (Pol) and active-site mutant (Pol^{PB1a}) influenza virus RdRp were purified from transfected HEK 293T cells, and mock purifications were performed using cells transfected with empty pcDNA3A vector (Mock). Purified material was analyzed by SDS/PAGE followed by staining with silver. (*C*) Activity of wild-type (Pol) and active-site mutant (Pol^{PB1a}) influenza virus RdRp, purified from transfected HEK 293T cells, was assayed using an in vitro [α-^{32}P]GTP incorporation activity assay. Transcription products (TP) were analyzed by 20% PAGE and detected by autoradiography. A 13-nt-long ^{32}P-labeled RNA was used as a size marker.

JVI Journals.ASM.org

Interactome Analysis of the Influenza A Virus Transcription/Replication Machinery Identifies Protein Phosphatase 6 as a Cellular Factor Required for Efficient Virus Replication

Ashley York, Edward C. Hutchinson, Ervin Fodor

Sir William Dunn School of Pathology, University of Oxford, Oxford, United Kingdom

ABSTRACT

The negative-sense RNA genome of influenza A virus is transcribed and replicated by the viral RNA-dependent RNA polymerase (RdRP). The viral RdRP is an important host range determinant, indicating that its function is affected by interactions with cellular factors. However, the identities and the roles of most of these factors remain unknown. Here, we employed affinity purification followed by mass spectrometry to identify cellular proteins that interact with the influenza A virus RdRP in infected human cells. We purified RdRPs using a recombinant influenza virus in which the PB2 subunit of the RdRP is fused to a Strep-tag. When this tagged subunit was purified from infected cells, copurifying proteins included the other RdRP subunits (PB1 and PA) and the viral nucleoprotein and neuraminidase, as well as 171 cellular proteins. Label-free quantitative mass spectrometry revealed that the most abundant of these host proteins were chaperones, cytoskeletal proteins, importins, proteins involved in ubiquitination, kinases and phosphatases, and mitochondrial and ribosomal proteins. Among the phosphatases, we identified three subunits of the cellular serine/threonine protein phosphatase 6 (PP6), including the catalytic subunit PPP6C and regulatory subunits PPP6R1 and PPP6R3. PP6 was found to interact directly with the PB1 and PB2 subunits of the viral RdRP, and small interfering RNA (siRNA)-mediated knockdown of the catalytic subunit of PP6 in infected cells resulted in the reduction of viral RNA accumulation and the attenuation of virus growth. These results suggest that PP6 interacts with and positively regulates the activity of the influenza virus RdRP.

IMPORTANCE

Influenza A viruses are serious clinical and veterinary pathogens, causing substantial health and economic impacts. In addition to annual seasonal epidemics, occasional global pandemics occur when viral strains adapt to humans from other species. To replicate efficiently and cause disease, influenza viruses must interact with a large number of host factors. The reliance of the viral RNA-dependent RNA polymerase (RdRP) on host factors makes it a major host range determinant. This study describes and quantifies host proteins that interact, directly or indirectly, with a subunit of the RdRP. It increases our understanding of the role of host proteins in viral replication and identifies a large number of potential barriers to pandemic emergence. Identifying host factors allows their importance for viral replication to be tested. Here, we demonstrate a role for the cellular phosphatase PP6 in promoting viral replication, contributing to our emerging knowledge of regulatory phosphorylation in influenza virus biology.

Viruses are obligate intracellular parasites that have been compelled by evolutionary processes to encode a minimal number of proteins for the completion of an infectious life cycle, in order to infect naive hosts and to persist in nature. This is exemplified by RNA viruses, the genomes of which are generally smaller than the genomes of DNA viruses, and therefore they greatly rely on the exploitation and subversion of host cellular proteins, structures, and pathways to facilitate virus replication (1). Transcription and replication of the influenza A virus genome are performed by the virally encoded RNA-dependent RNA polymerase (RdRP), a major determinant of species tropism and pathogenicity and a key player in the adaptation of avian influenza A viruses to mammalian hosts. These characteristics of the viral RdRP are thought to be governed by numerous interactions with cellular factors (reviewed in references 2 and 3). It is therefore of great importance to understand the relationship between the viral transcription/replication machinery and host cellular factors in order to understand how the host cell can influence the function of the viral transcription/replication machinery and vice versa. Insight into the molecular biology of these relationships could lead to novel antiviral strategies and has the potential to identify host-specific interactions that would act as a barrier to pandemic emergence.

The genome of influenza A virus, like that of other members of the *Orthomyxoviridae*, is segmented and consists of eight individual viral ribonucleoprotein (vRNP) complexes. Each vRNP contains single-stranded viral RNA (vRNA) that is encapsidated by viral nucleoprotein (NP) and bound at the 5′ and 3′ ends by the viral RdRP, a 250-kDa heterotrimer containing polymerase acidic (PA), polymerase basic 1 (PB1), and polymerase basic 2 (PB2)

Received 22 June 2014 **Accepted** 25 August 2014

Published ahead of print 3 September 2014

Editor: A. García-Sastre

Address correspondence to Ervin Fodor, ervin.fodor@path.ox.ac.uk.

Supplemental material for this article may be found at http://dx.doi.org/10.1128/JVI.01813-14.

Copyright © 2014, American Society for Microbiology. All Rights Reserved.

doi:10.1128/JVI.01813-14

subunits. The PB1 subunit contains the polymerase active site, while PB2 and PA are responsible for cap snatching (4–7). The viral RdRP transcribes and replicates the vRNA genome in the host cell nucleus, where it can be found within RNP complexes and in a free form (reviewed in references 8 and 9). Numerous cellular factors have been identified as interaction partners of components of vRNP complexes, and some of these have been shown to play a role in transcription and replication of the viral genome (reviewed in reference 10).

We set out to identify the interactome of the influenza A virus transcription/replication machinery in the context of an infected cell with the aim of discovering cellular proteins that are involved in the influenza A virus life cycle. We employed an affinity purification mass spectrometry (AP-MS) strategy in which the viral RdRP is isolated from infected cells and then copurifying host factors are identified by liquid chromatography/tandem mass spectrometry (LC/MS-MS), exploiting recent advances in mass spectrometer instrument sensitivity and label-free quantitation. Using this approach, we identified 171 cellular interactors of the viral transcription/replication machinery. This method complements previous studies that have aimed to identify critical cellular factors that are involved in the virus life cycle, including a number of genome-wide screens (11–15). Although informative, these genome-wide screens have failed to identify the specific stages of the virus life cycle at which particular cellular factors are critical. Furthermore, these methods do not distinguish between those factors that are required for virus replication due to direct interaction with a viral component and those factors that can contribute to virus replication indirectly. Additional techniques have been employed with the aim of identifying host factors that interact with the viral transcription/replication machinery, including yeast two-hybrid screens (15, 16), complementation assays (17), and AP-MS (18–21). However, these studies have been limited either by the number of cellular factors that can be cloned and screened or because the identifications were not carried out in the context of the infected cell.

In our interactome study, we identified three individual subunits of cellular serine/threonine protein phosphatase 6 (PP6). PP6 is a member of the PP2A subfamily of protein phosphatases, cellular enzymes that catalyze the liberation of inorganic phosphate from proteins and peptides at serine or threonine residues (22). PP6 is a significant regulator of a number of cellular processes, including chromosome stability and the DNA damage response (23–27), mitosis and the regulation of cell cycle progression (22, 28–31), signaling (32, 33), pre-mRNA splicing (34), and vesicular trafficking (35). The catalytic subunit PPP6C and the regulatory subunits PPP6R1 and PPP6R3 were found to copurify with the viral RdRP. Knockdown experiments in human cells revealed that physiological levels of PPP6C are required for efficient virus growth and for transcription and replication of the viral genome, suggesting an important role for PP6 and for the regulation of phosphorylation in the influenza A virus life cycle. Indeed, previous studies have identified numerous sites of phosphorylation in the proteomes of influenza A and B viruses, with roles for phosphorylation being implicated in virus entry and exit, nuclear localization, and protein oligomerization (36–49).

The data presented in this study contribute to the understanding of the role of cellular proteins in influenza virus replication and underpin further studies into the molecular mechanisms that govern transcription and replication of the influenza A virus RNA genome. In addition, the study also contributes to the emerging evidence for an important regulatory role for the phosphorylation of viral proteins in influenza virus biology.

MATERIALS AND METHODS

Cells and viruses. Human embryonic kidney 293T (HEK 293T) cells were maintained in Dulbecco's modified Eagle medium (DMEM; Sigma) supplemented with 10% fetal calf serum (FCS; Sigma). Human adenocarcinoma alveolar basal epithelial (A549) cells and Madin-Darby bovine kidney epithelial (MDBK) cells were maintained in modified Eagle medium with Earle's salts (MEM; Sigma) supplemented with 2 mM L-glutamine (Invitrogen) and 10% FCS. Mammalian cells were maintained in humidified incubators at 37°C, 5% CO_2. *Spodoptera frugiperda* (Sf9) cells were propagated at 28°C in Insect-XPRESS medium (Lonza) supplemented with 1% penicillin-streptomycin. Influenza A viruses were cultured in MDBK cells in MEM supplemented with 2 mM L-glutamine and 0.5% FCS. The influenza A/WSN/33 PB2-Strep virus was generated by reverse genetics (50) using the pHW2000-PB2-Strep construct (51).

Plasmids and antibodies. The plasmids for use in reverse genetics have been described previously (50–52). The pcDNA-PB1-Strep and pcDNA-PA-Strep mammalian expression plasmids were constructed by digesting pcDNA-PB1-TAP and pcDNA-PA-TAP plasmids (53) with NotI and XbaI restriction endonucleases and ligating into the digested plasmids two preannealed complementary oligonucleotides with NotI and XbaI overhangs at the 5′ and 3′ ends [(5′-GGCCGCAAGCGCTTGGAGCCACCCGCAGTTCGAGAAAGGTGGAGGTTCCGGAGGTGGATCGGGAGGTGGATCGTGGAGCCACCCGCAGTTCGAAAAATAGT-3′) and (5′-CTAGACTATTTTTCGAACTGCGGGTGGCTCCACGATCCACCTCCCGATCCACCTCCGGAACCTCCACCTTTCTCGAACTGCGGGTGGCTCCAAGCGCTTGC-3′)]. The pcDNA-PB2-Strep plasmid was constructed by PCR amplifying the PB2-Strep gene from pHW2000-PB2-Strep with KpnI and NotI restriction sites at the 5′ and 3′ ends, respectively. The PCR product and pcDNA3A (52, 54) were digested with KpnI and NotI restriction endonucleases, and the PCR-amplified gene was ligated into pcDNA3A. The pcDNA-PP7CP-Strep mammalian expression plasmid has been described previously (55). The pGEX-6P1-GST, pGEX-6P1-GST-PPP6C, pGEX-4T1-GST-PPP6R1, pGEX-4T1-GST-PPP6R2, and pGEX-4T1-GST-PPP6R3 *Escherichia coli* expression plasmids have been described previously (23). Antibodies to PPP6C (A300-844A) and PPP6R3 (A300-972A) were purchased from Bethyl Laboratories. Antibodies to actin (A2066) and influenza A virus NP (Ab128193) were purchased from Sigma and Abcam, respectively. A custom polyclonal antibody for the influenza A virus RdRP was produced by Eurogentec. Briefly, recombinant RdRP to be used as an antigen was expressed using the MultiBac insect cell expression system (56) and purified as described previously (55). Two rabbits were immunized with 140 μg of antigen, followed by three further boosts of 140 μg of antigen each over a period of 3 months.

Strep-tag affinity-purifications. To purify PB2-Strep complexes by Strep-tag affinity chromatography (57), infections were carried out with PB2-Strep or wild-type (WT) virus at a multiplicity of infection (MOI) of 5 using approximately 4×10^7 HEK 293T cells in two 15-cm dishes. Alternatively, transfections were carried out using Lipofectamine 2000 (Invitrogen) with 60 μg of each of the indicated pcDNA plasmids (total, 180 μg) using approximately 2×10^7 HEK 293T cells in two 15-cm dishes. At 7 h postinfection (p.i.) or 48 h posttransfection, cells were harvested, washed in ice-cold phosphate-buffered saline (PBS), and pelleted at 450 × *g* for 5 min at 4°C. Lysates were prepared by incubating cells on a rotating wheel for 1 h at 4°C in lysis buffer (50 mM Tris-HCl [pH 8.0], 200 mM NaCl, 33% glycerol [vol/vol], 0.5% Igepal CA-630 [vol/vol], and 1 mM dithiothreitol [DTT] with 1× complete EDTA-free protease inhibitor cocktail [Roche]). The soluble fraction was separated by centrifugation at 17,000 × *g* for 5 min at 4°C, diluted 1:5 with binding buffer (20 mM Tris-HCl [pH 8.0], 200 mM NaCl, and 1× complete EDTA-free protease inhibitor cocktail), and incubated overnight at 4°C with 200 μl of washed

50% suspension Strep-Tactin Superflow high-capacity resin (IBA GmbH). The resin was washed extensively with wash buffer (20 mM Tris-HCl [pH 8.0], 150 mM NaCl, 1 mM EDTA, 0.1% Igepal CA-630 [vol/vol], 10% glycerol [vol/vol], and 1 mM phenylmethylsulfonyl fluoride [PMSF]), and proteins were eluted in 2 ml of elution buffer (20 mM Tris-HCl [pH 8.0], 150 mM NaCl, 1 mM EDTA, 0.1% Igepal CA-630 [vol/vol], 10% glycerol [vol/vol], 1× complete EDTA-free protease inhibitor cocktail, and 2 mM *d*-desthiobiotin) for 2 h on a rotating wheel at 4°C. Eluates were concentrated using Amicon Ultra-4 (3-kDa-molecular-mass cutoff) centrifugation devices prior to analyzing by SDS-PAGE and silver staining or primer extension analysis using NA-specific primers as previously described (58) or mass spectrometry.

Mass spectrometry. Affinity-purified samples from infected cells were prepared for mass spectrometry by boiling in Laemmli buffer and running a short distance into a polyacrylamide gel (Thermo Scientific) to remove detergent and salts. The entire sample was then excised from the gel with a clean scalpel. Samples were then washed with 50 mM ammonium bicarbonate in 50% (vol/vol) acetonitrile, reduced with 10 mM DTT and 55 mM chloroacetamide, and then digested with 0.5 μg trypsin (Promega) at 37°C for 16 h. Peptides were extracted with 0.1% (vol/vol) formic acid in 50% (vol/vol) acetonitrile, lyophilized in a SpeedVac (Thermo Savant), and then desalted using an in-house manufactured C_{18} purification tip. Samples were lyophilized and stored at −20°C and then dissolved in 0.1% (vol/vol) formic acid prior to mass spectrometry analysis. Three experiments were performed, and for each experiment two samples were analyzed, one purified from cells infected with a WT virus and the other purified from cells infected with the PB2-Strep virus. The WT sample was always analyzed first. Samples from each experiment were analyzed on two separate occasions. Samples were analyzed on an Ultimate 3000 RSLCnano HPLC (Dionex, Camberley, United Kingdom) system run in direct injection mode coupled to a Q Exactive Orbitrap mass spectrometer (Thermo Electron, Hemel Hempstead, United Kingdom). Samples were resolved on a 25-cm by 75-μm inner-diameter picotip analytical column (New Objective, Woburn, MA, USA), which was packed in-house with ProntoSIL 120-3 C_{18} Ace-EPS phase, 3-μm beads (Bischoff Chromatography, Germany). The system was operated at a flow rate of 300 nl min^{-1}. A 120-min gradient was used to separate the peptides. The mass spectrometer was operated in a "Top 10" data-dependent acquisition mode. Precursor scans were performed in the Orbitrap at a resolving power of 70,000, from which the 10 most intense precursor ions were selected by the quadrupole and fragmented by high cell density (HCD) at a normalized collision energy of 28%. The quadrupole isolation window was set at 3 *m/z*. Charge state +1 ions and undetermined charge state ions were rejected from selection for fragmentation. Dynamic exclusion was enabled for 40 s. Data files were converted from .RAW to .MGF using ProteoWizard (59).

Analysis of mass spectrometry. Mass spectra were analyzed using the Central Proteomics Facilities Pipeline (CPFP) (60). Data from experimental replicates were merged. Peptide spectral matches were made to custom databases that concatenated the sequence of the tagged PB2-Strep protein with the proteomes of *Homo sapiens* and of the influenza A/WSN/33 virus, as well as common contaminants and decoy sequences. The viral proteome in the database was expanded to include hypothetical as well as experimentally confirmed proteins, as previously described (36). For the identification of peptides, CPFP uses iProphet (61) to combine searches made with Mascot (Matrix Science, London, United Kingdom), OMSSA (62), and X!TANDEM (63), with peptide identifications validated using PeptideProphet (64). Combined protein identifications were assigned using ProteinProphet (65) with a 1% false-discovery rate (FDR). Searches were made for peptides with up to two missed cleavages, with carbamidomethylation of cysteine as a fixed modification and oxidation of methionine and deamidation of glutamine and asparagine as variable modifications. A minimum of 2 peptides were required to make positive protein identifications. Label-free protein quantitation was performed using spectral index normalized quantitation (SINQ) in CPFP (66). The nature of ubiquitination means that in most cases it was not clear which proteins ubiquitin was conjugated to. Tryptic peptides of ubiquitin were assigned to the limited number of ubiquitin conjugates currently annotated in the human proteome. Common contaminants, keratins, serum albumin, and decoy sequences were manually removed from the data before further processing. To control for nonspecific binding, proteins that were present in all three experiments in both the PB2-Strep and the WT samples were identified (93 proteins from the 619 identified). The median intensity of this set of proteins was used to normalize protein abundance, and the mean abundance of each protein in the PB2-Strep and WT samples was then calculated (missing data did not contribute to the means). The majority of the proteins consistently found in both the WT and the PB2-Strep samples had an abundance in the PB2-Strep sample that was within a 10-fold difference of their abundance in the WT sample after normalization. Proteins that did not increase at least 10-fold in abundance in the PB2-Strep sample compared to WT were therefore excluded from further analysis. Finally, for each PB2-Strep sample, protein abundance was normalized by the amount of PB2-Strep present.

Raw files for all mass spectra used in the analysis have been deposited at the Mass spectrometry Interactive Virtual Environment (MassIVE; Center for Computational Mass Spectrometry at the University of California, San Diego) and can be accessed at http://massive.ucsd.edu/ProteoSAFe/datasets.jsp using the MassIVE ID MSV000078741.

To construct an interaction network, protein-protein interactions were taken from STRING (Search Tool for the Retrieval of Interacting Genes/Proteins) version 9.1 (http://string-db.org) on 10 June 2014 (67) and illustrated using Cytoscape version 3.1.0 (68). Gene Ontology (GO) mapping to high-level GO parent (GO Slim) terms was performed by the Generic Gene Ontology Term Mapper (http://go.princeton.edu/cgi-bin/GOTermMapper) (69, 70) using a GO slim list published by the European Bioinformatics Institute (EBI) (goa_human generic, downloaded on 7 March 2014). The statistical significance of GO term enrichment was calculated using a hypergeometric test, with the background distribution of terms in the human genome taken from the GO slim list.

Recombinant influenza A virus RdRP purification. Recombinant influenza A/NT/60/68 virus RdRP with a protein A tag on the PB2 subunit was expressed using the MultiBac system in Sf9 insect cells (56) as previously described (55). Sf9 cell suspension cultures (1 liter) at 1.2 × 10^6 cells/ml were infected with recombinant baculovirus at an MOI of 1 and incubated for 72 h at 27°C. Infected Sf9 cells were harvested by centrifugation at 800 × *g* for 15 min at 4°C and lysed by continuous sonication for 90 s with a Soniprep 150 (MSE) at 10-μm amplitude in lysis buffer (50 mM Tris-HCl [pH 8.0], 500 mM NaCl, 10% [vol/vol] glycerol, 0.05% [wt/vol] octylthioglucoside, 1× complete EDTA-free protease inhibitor cocktail [Roche], and 100 μg/ml RNase A). The lysate was clarified by centrifugation at 35,000 × *g* for 45 min at 4°C, and the supernatant was incubated with washed IgG Sepharose (approximately 2 ml bead slurry per liter of original culture; GE Healthcare) for 3 h at 4°C. After binding, the beads were washed extensively with 50 mM Tris-HCl (pH 8.0), 500 mM NaCl, 10% (vol/vol) glycerol, and 0.05% (wt/vol) octylthioglucoside. The recombinant RdRP was released using AcTEV protease (150 U/ml of IgG Sepharose) at 4°C overnight in 50 mM Tris-HCl (pH 8.0), 500 mM NaCl, 10% (vol/vol) glycerol, 0.05% (wt/vol) octylthioglucoside, and 2.5 mM reduced glutathione. Released recombinant protein was subsequently analyzed by SDS-PAGE and Coomassie brilliant blue staining (Invitrogen).

GST pulldown assay. Glutathione S-transferase (GST), GST-PPP6C, GST-PPP6R1, GST-PPP6R2, and GST-PPP6R3 were expressed in *E. coli* BL21(DE3) by isopropyl β-D-1-thiogalactopyranoside (IPTG) induction at a concentration of 0.1 mM overnight at 21°C. Cells were harvested by centrifugation at 5,000 × *g* for 20 min at 4°C. Cell pellets were resuspended in lysis buffer (20 mM Tris-HCl [pH 8.0], 150 mM NaCl, 1 mM $MgCl_2$, 10% glycerol [vol/vol], 1× complete EDTA-free protease inhibitor cocktail, and 0.25 mg/ml lysozyme) and sonicated for 5 min (30 s on/off) with a Soniprep 150 (MSE) at 10-μm amplitude. The lysate was

clarified by centrifugation at 35,000 × *g* for 30 min at 4°C, and the supernatant was incubated with 100 μl of washed glutathione Sepharose (GE Healthcare) for 3 h at 4°C. After binding, the beads were washed extensively with 20 mM Tris-HCl (pH 8.0), 200 mM NaCl, 1 mM $MgCl_2$, 10% glycerol (vol/vol), 0.1% Igepal CA-630 (vol/vol), and 1 mM phenylmethylsulfonyl fluoride (PMSF). Beads were then incubated for 2 h at 4°C with 40 μg of recombinant RdRP in a total volume of 1 ml in 20 mM Tris-HCl (pH 8.0), 200 mM NaCl, 1 mM $MgCl_2$, 10% glycerol (vol/vol), 0.1% Igepal CA-630 (vol/vol), and 1× complete EDTA-free protease inhibitor cocktail. After binding, the beads were washed extensively with 20 mM Tris-HCl (pH 8.0), 200 mM NaCl, 1 mM $MgCl_2$, 10% glycerol (vol/vol), 0.1% Igepal CA-630 (vol/vol), and 1 mM PMSF. Recombinant proteins were eluted at room temperature for 15 min in 250 μl of 50 mM Tris-HCl (pH 8.0), 200 mM NaCl, 10 mM reduced glutathione, 1 mM $MgCl_2$, 10% glycerol (vol/vol), and 1× complete EDTA-free protease inhibitor cocktail. Eluates were analyzed by SDS-PAGE, Coomassie brilliant blue staining, and Western blotting with an anti-RdRP antibody.

Design of siRNAs and knockdown of PPP6C. Small interfering RNAs (siRNAs; Sigma) were designed using the Dharmacon siDESIGN center. Three independent siRNA duplexes with 3′ dTT overhangs were designed against the PPP6C gene (GenBank accession number, NM_001123369) with different starting positions 239 (siPPP6C1 [GGACAAGTATGTGG AAATA]), 494 (siPPP6C2 [TCATGAGAGTAGACAGATA]), and 875 (siPPP6C3 [GCACGAAGGCTATAAATTT]). To knock down PPP6C, HEK 293T cells or A549 cells were transfected in suspension or as a monolayer, respectively, with 0.18 nmol/ml of siRNA using Lipofectamine 2000 (Invitrogen) according to the manufacturer's instructions. The AllStars negative-control siRNA (Qiagen) was used as a negative control. The transfection was repeated 24 h later on the cell monolayers, and the cells were incubated for a further 24 h prior to infection. After two consecutive transfections with siRNAs, HEK 293T and A549 cells in 24-well dishes were resuspended in PBS, and the cell viability was determined using a CellTiter-Glo luminescent assay (Promega) according to the manufacturer's instructions. PPP6C protein levels were determined by densitometry of Western blots with a PPP6C polyclonal antibody.

Growth curve analysis. To assess virus growth in cells treated with siRNA against PPP6C or with negative-control siRNA, HEK 293T cells in 6-well plates were infected with WT virus at an MOI of 0.001, supernatants were harvested at 12, 24, 36, 48, 60, and 72 h p.i., and the virus titer was determined by plaque assay on MDBK cells. To compare the growths of WT and PB2-Strep viruses, MDBK cells in 6-well plates were infected at an MOI of 0.001, supernatants were harvested 12, 24, 36, 48, 60, and 72 h p.i., and the virus titer was determined by plaque assay on MDBK cells.

RNA analysis. To compare viral RNA synthesis in infected cells, HEK 293T cells were treated with siRNA against PPP6C or with negative-control siRNA in 24-well plates and were infected at an MOI of 1. RNA was extracted at 0, 6, and 8 h p.i. using TRIzol (Invitrogen) according to the manufacturer's instructions. To compare primary transcription in infected cells, HEK 293T cells in 24-well plates were treated with siRNA against PPP6C or with negative-control siRNA and were infected at an MOI of 10 or mock infected in the presence of cycloheximide (CHX; 100 μg/ml). RNA was extracted at 6 h p.i. using TRIzol. RNA pellets were dissolved in 10 μl of RNase-free water, and RNA was analyzed in a primer extension assay using NA segment-specific primers as previously described (58). Signals were detected by autoradiography, and images were quantitated using phosphorimage analysis in Aida.

Indirect immunofluorescence and confocal microscopy analysis. To analyze the cellular localization of viral NP in infected cells that were knocked down for PPP6C or negative-control cells, A549 cells on 13-mm cover glasses in 24-well plates were infected with WT virus at an MOI of 1. At 0, 4, 6, and 8 h p.i., cells were washed with PBS and fixed with 4% paraformaldehyde in 250 mM HEPES (pH 7.5) for 15 min at room temperature. Cells were permeabilized with 0.5% Triton X-100 (vol/vol) in PBS for 15 min at room temperature, washed with PBS, and subsequently blocked in blocking PBS containing 1% bovine serum albumin (wt/vol), 0.2% porcine gelatin (wt/vol), and 0.1% Tween 20 (vol/vol) overnight at 4°C. Indirect immunofluorescence was performed using a mouse monoclonal NP antibody at a 1:500 dilution in blocking PBS for 1 h at room temperature. Coverslips were washed extensively with PBS before labeling with a Cy3-conjugated anti-mouse secondary antibody (Jackson ImmunoResearch Laboratories) at a 1:500 dilution in blocking PBS for 1 h at room temperature. Coverslips were washed extensively with PBS prior to mounting in Mowiol (Calbiochem) containing 1 μg/ml 4′,6′-diamidino-2-phenylindole (DAPI; Sigma). Cells were imaged on an Olympus Flouview FV1000 confocal laser scanning microscope, using a 60×/1.35 Oil UPlanSApo objective for detailed imaging and a 40×/1.30 Oil UPlan FLN objective to capture four images in a random field of view from each sample for scoring. Images were processed using ImageJ and scored using the Cell Counter plugin.

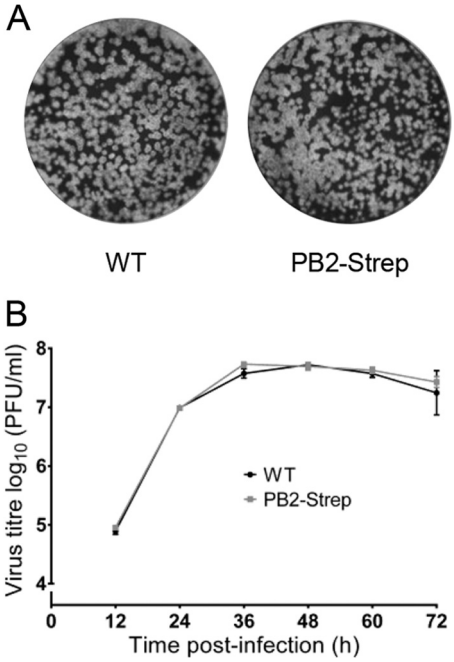


FIG 1 Characterization of a recombinant influenza A virus encoding a PB2-Strep protein. (A) Plaques of WT and PB2-Strep viruses on MDBK cells at 72 h p.i. stained with Coomassie brilliant blue. (B) Growth kinetics of WT virus and PB2-Strep virus in MDBK cells infected at an MOI of 0.001. At the indicated time points, cell supernatants were collected and virus titers were determined by plaque assay on MDBK cells. The means and standard deviations (SD) of three experiments are shown.

RESULTS

Isolation of influenza A virus RdRP complexes and the associated interactome from infected HEK 293T cells. For the isolation of the influenza A virus RdRP from infected HEK 293T cells, we used a recombinant influenza A/WSN/33 virus that expresses the PB2 subunit of the RdRP with a Strep-tag at the C terminus (PB2-Strep virus) (51). The Strep-tag is a small polypeptide tag that exhibits intrinsic reversible affinity for Strep-Tactin, an engineered streptavidin that allows highly selective single-step purification of Strep-tag fusion proteins under physiological conditions (57). The PB2-Strep virus exhibited a plaque phenotype and growth kinetics indistinguishable from that of wild-type virus (Fig. 1). This showed that the presence of the Strep-tag on the C terminus of PB2 does not affect the efficiency of viral replication and therefore indicated that it does not affect the function of PB2.

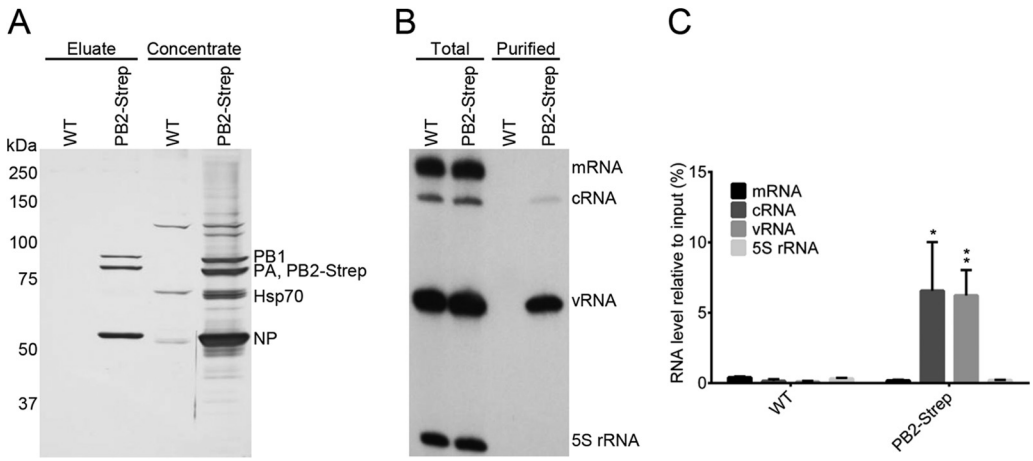


FIG 2 Isolation of influenza A virus RdRP and the associated interactome from infected HEK 293T cells. HEK 293T cells were infected with WT virus (negative control) or PB2-Strep virus at an MOI of 5 for 7 h. PB2-Strep complexes were purified by Strep-tag affinity-purification from cell lysates. (A) Purified proteins were analyzed by SDS-PAGE and silver staining. (B) Viral RNAs isolated from total cell lysates or purified material were analyzed by primer extension using radiolabeled primers for positive-sense (mRNA and cRNA) and negative-sense (vRNA) NA-specific viral RNAs. Primer extension analysis of 5S rRNA was used as a control. Ten times more sample of copurified RNA than of total RNA was analyzed. (C) Quantitation of primer extension analyses of copurified RNA, showing the means and SD of three biological repeats. Asterisks indicate a significant difference from WT (*, $P < 0.05$; **, $P < 0.01$, based on a two-sample Student's *t* test).

HEK 293T cells were infected with the PB2-Strep virus or WT virus (negative control) at a multiplicity of infection (MOI) of 5. Whole-cell lysates were prepared 7 h p.i., and PB2-Strep complexes were affinity purified with Strep-Tactin resin using a batch method. PB2-Strep complexes were eluted, concentrated, and analyzed by SDS-PAGE and silver staining, and RNA was analyzed by primer extension analysis using neuraminidase (NA) segment-specific primers. Viral RdRP-containing complexes were isolated from cells infected with the PB2-Strep virus but not from the cells infected with WT virus (Fig. 2A). Concentration of the eluates revealed a number of cellular proteins copurifying with PB2-Strep that were absent in the WT negative control (Fig. 2A). Analyses of the viral RNAs showed that viral cRNA and vRNA, but not viral mRNA or the highly abundant 5S rRNA, were isolated using PB2-Strep affinity purification (Fig. 2B). Approximately 6% of total cRNA and vRNA was isolated from infected cells using PB2-Strep affinity purification (Fig. 2C). This showed that the viral RdRP and ribonucleoprotein complexes in association with cellular factors had been specifically isolated from infected cells.

Identification of the interactome of the influenza A virus replication machinery by mass spectrometry. Mass spectrometry analysis was used to identify proteins that form complexes with PB2-Strep in infected cells. HEK 293T cells were infected with the PB2-Strep virus or with WT virus, and affinity purifications were carried out using Strep-Tactin. Proteins copurifying with PB2-Strep were identified by mass spectrometry and quantified using spectral index normalized quantitation (SINQ), a label-free method that uses the intensities of the peptide fragment ions to measure protein abundance (see Table S1 in the supplemental material) (66). Background binding was determined by identifying proteins purified from cells infected with WT virus, which lacks a Strep-tag (see Materials and Methods for details). As expected, the viral RdRP subunits and NP were the most abundant proteins in three separate experiments (see Table S2 in the supplemental material). All three RdRP subunits were detected, consistent with the purification of RdRP trimers. However, there was an excess of approximately one-third of PB2-Strep, indicating that not all of the PB2-Strep purified was incorporated into trimeric RdRPs. NP was also purified, confirming that a number of the RdRPs had been incorporated into RNPs. This is also consistent with the identification of vRNA and cRNA in the purified samples (Fig. 2B and C). The ratio of NP to PB2-Strep was 8. Each NP is thought to bind approximately 24 nucleotides (nt) of RNA (71, 72), so even for the shortest segment of the viral genome (890 nt), this would not be sufficient for all of the purified RdRPs to be incorporated into RNPs. Assuming equimolar binding of all eight genome segments (with an average length of 1,700 nt per vRNP and hence an average binding capacity of 71 copies of NP), approximately 1 in 9 of the PB2-Strep proteins analyzed could be part of an RNP. We therefore conclude that our sample contained a mixture of RNPs, free trimeric RdRPs, and free PB2 polymerase subunits. Intriguingly, we also found small amounts of the viral neuraminidase copurifying with PB2-Strep.

In addition to these viral proteins, 171 cellular proteins were specifically purified. The abundance of these proteins, which corresponds to their relative likelihood of being bound directly or indirectly to PB2-Strep, varied over approximately 4 orders of magnitude. The majority of these proteins could be identified reproducibly (Fig. 3A), with reproducible observations more likely for the more abundant proteins (see Table S2 in the supplemental material). The most abundant of the interacting host proteins was the Hsp70 molecular chaperone, which is clearly visible by PAGE and silver staining (Fig. 2A and 3B; see also Fig. S1 in the supplemental material). Other categories of particularly abundant protein are shown in Fig. 3B. These include the chaperonin-containing TCP1 complex (CCT), nuclear import factors such as RanBP5 and importin α3, α4, α5, and α7, ubiquitin and ubiquitin ligases, cytoskeletal proteins (in particular tubulin), ribosomal proteins, mitochondrial proteins, phosphatases, and kinases. Most of the bound proteins could interact with at least one of the other bound proteins, suggesting that complexes of interacting proteins may have been purified (Fig. 3B; see also Fig. S1 in the supplemental

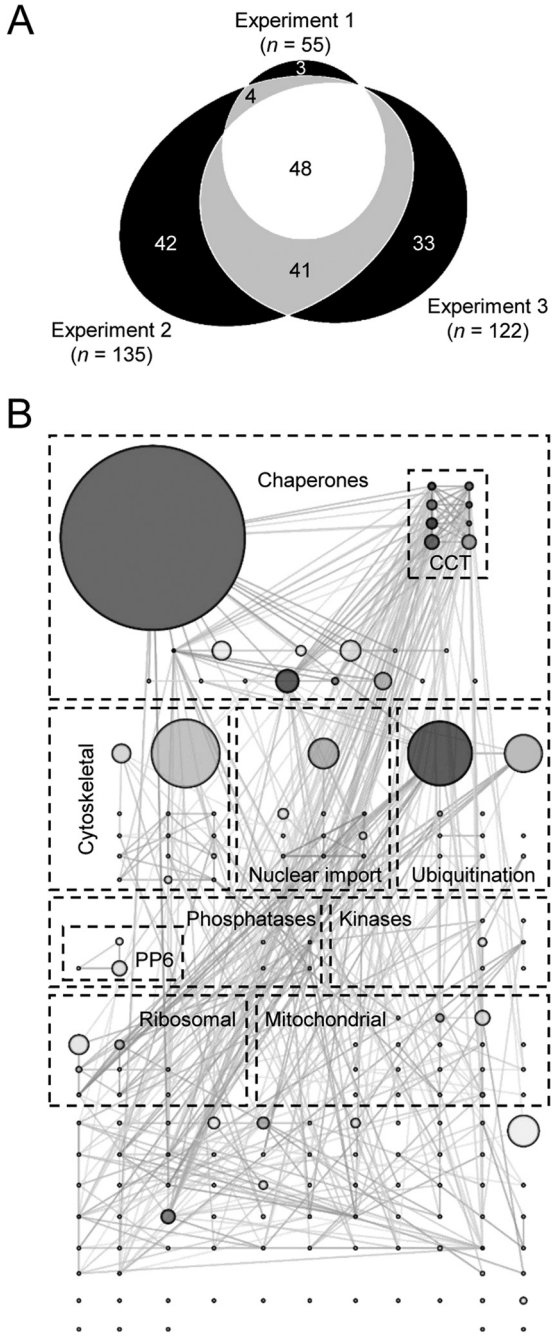


FIG 3 Identification of the interactome of the influenza A virus transcription/replication machinery by mass spectrometry. (A) Venn diagram representing 171 cellular proteins identified by affinity purification mass spectrometry of PB2-Strep complexes from infected HEK 293T cells, highlighting the number of identifications that overlap between three independent biological repeats. (B) Interaction network of host proteins in the viral transcription/replication machinery interactome. Abundant proteins have been manually sorted into the indicated categories. The shading of nodes indicates their connectivity in the network, with darker shading for highly connected nodes. The size of nodes is proportional to protein abundance in the sample, an indication of each protein's likelihood of being bound to PB2-Strep. For reasons of clarity, no node has an area less than 1/40 of the largest node.

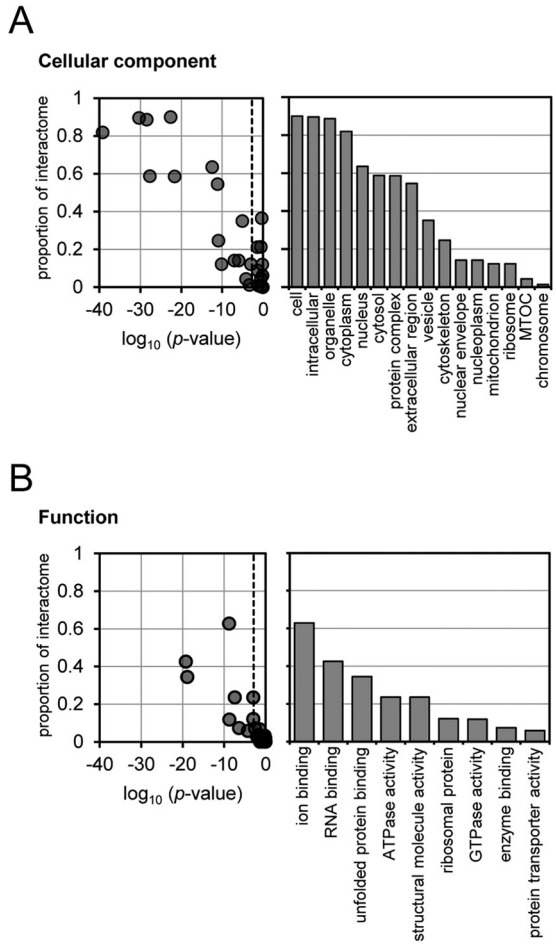


FIG 4 Gene Ontology (GO) cellular component terms (A) and functional terms (B) enriched in the interactome of the viral transcription/replication machinery and the proportion of the interactome assigned to those terms. The probability that terms were enriched in the interactome was calculated by comparing it to the annotation of the total human proteome, and the proportion of interactome proteins with particular terms was calculated by label-free quantitation of mass spectra.

material). Consistent with this, the eight subunits of the chaperonin CCT were purified in approximately equal quantities (Fig. 3B). Gene Ontology mapping showed that the interactome of the viral replication machinery was highly enriched for proteins from numerous cellular components with varied molecular functions, reflecting the isolation of PB2 at different stages of the virus life cycle (Fig. 4).

Among the interactome, we were particularly interested by the subunits of the cellular serine/threonine protein phosphatase PP6 due to the relatively high abundance of these proteins in the interactome and to the importance of phosphorylation in regulating influenza virus replication (36). By molar abundance, PPP6C, the catalytic subunit of the PP6 complex, comprised approximately 1.5% of the viral replication machinery's interactome, with two alternative regulatory subunits, PPP6R3 and PPP6R1, comprising around 0.8% and 0.1%, respectively (see Table S2 in the supplemental material). Western blotting confirmed that PPP6C and PPP6R3 copurified with the viral RdRP from HEK 293T cells infected with PB2-Strep virus but were absent in the negative control (Fig. 5A).

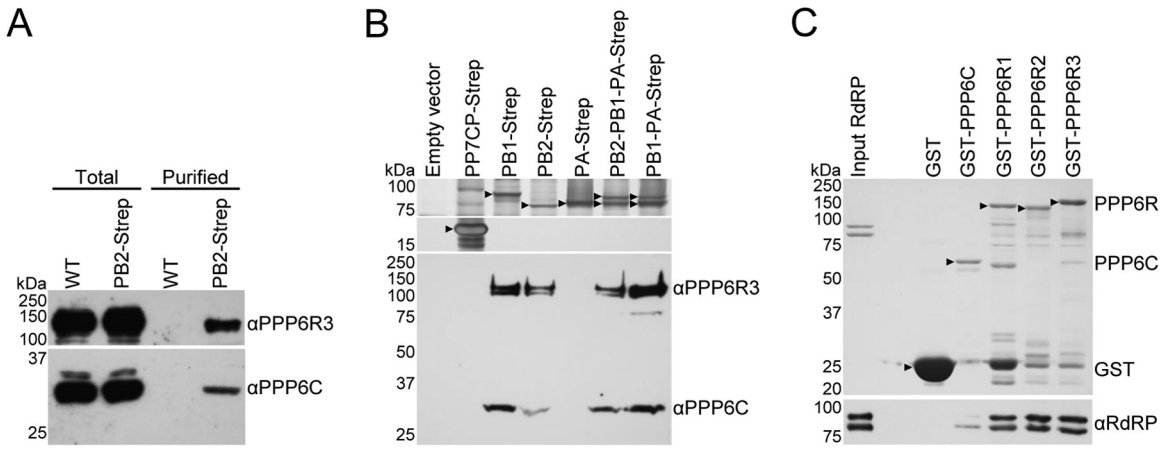


FIG 5 Analyses of the interaction between PP6 and the influenza A virus RdRP. (A) Western blot analyses of total cell lysate and Strep-tag affinity purified material from HEK 293T cells infected with WT or PB2-Strep virus, using antibodies specific to PPP6R3 (upper panel) and PPP6C (lower panel). (B) SDS-PAGE and silver staining analysis (upper panels) and Western blot analysis (lower panel) using PPP6R3 and PPP6C antibodies of purified Strep-tagged viral RdRP subunits or negative-control samples from HEK 293T cells transfected with the indicated plasmids. Black arrowheads indicate Strep-purified proteins. (C) GST pulldown assay whereby GST, GST-PPP6C, GST-PPP6R1, GST-PPP6R2, and GST-PPP6R3 were expressed separately in *E. coli* and immobilized on glutathione Sepharose beads. Recombinant influenza A virus RdRP purified from *Spodoptera frugiperda* (Sf9) cells was incubated with immobilized GST-tagged proteins. Bound material was analyzed by SDS-PAGE and staining with Coomassie brilliant blue (upper panel) and Western blotting with an RdRP antibody (lower panel). Black arrowheads indicate the positions of full-length GST-tagged proteins.

We hypothesized that the interaction between the RdRP and PP6 had evolved because PP6 played a role in regulating influenza virus replication, and we decided to investigate this interaction further.

The PB1 and PB2 subunits of the viral RdRP interact directly with PP6. In order to address the specificity of the interaction of PP6 with the viral RdRP, individual polymerase subunits, trimeric RdRP, or PB1-PA dimer were purified from HEK 293T cells transfected with mammalian expression plasmids encoding a Strep-tagged polymerase subunit. Cells were transfected with an empty expression vector or a mammalian expression vector encoding the coat protein of the *Pseudomonas aeruginosa* bacteriophage PP7 (PP7CP) fused to a Strep-tag (PP7CP-Strep) to control for background binding of PP6 to Strep-Tactin beads or the Strep-tag, respectively. To analyze copurification of PP6, Western blotting was performed using antibodies specific to PPP6C and PPP6R3. PP6 did not copurify from the negative-control cells transfected with an empty vector or the PP7CP-Strep expression vector or with PA-Strep in the absence of other RdRP subunits. However, PP6 copurified with PB1-Strep, PB2-Strep, trimeric PB2-PB1-PA-Strep, and a PB1-PA-Strep dimer, indicating that PP6 could interact with PB1 and PB2, both individually and as part of the RdRP complex (Fig. 5B).

To determine whether the interaction between the viral RdRP and PP6 was direct, an *in vitro* GST pulldown assay was performed. N-terminally GST-tagged PPP6C, PPP6R1, PPP6R2, and PPP6R3 subunits of PP6 or GST alone (negative control) was individually expressed in *E. coli*. After cell lysis, the lysate was incubated with glutathione Sepharose beads, and after washing, the beads were incubated with recombinant influenza A virus RdRP purified from *Spodoptera frugiperda* (Sf9) cells. After a further washing step, the GST fusion proteins were eluted and Western blotting was performed using an antibody specific to the viral RdRP. Viral RdRP was not detected when GST was expressed alone, but GST-tagged PP6 subunits could pull down RdRP *in vitro*, indicating that their interaction was direct. GST-tagged PP6C could pull down only a small quantity of RdRP, but relatively large amounts of RdRP were pulled down by each of the three GST-tagged PP6 regulatory subunits (Fig. 5C). Thus, the catalytic and regulatory subunits of PP6 interact directly with the viral RdRP. This mode of interaction is typical of phosphatases, as the catalytic subunit must interact with the target protein for activity while the specificity of the interaction is primarily determined by the regulatory subunit. Although we found that each of the three PP6 regulatory subunits could pull down the viral polymerase complex, it remains to be determined whether either of the regulatory subunits facilitates the interaction of PPP6C with either PB1 or PB2. Nevertheless, the results shown in Fig. 5B clearly demonstrate that PP6 can interact with both PB1 and PB2 independently of each other.

Knockdown of PPP6C reduces influenza A virus replication. To assess the biological significance of PP6 in the influenza A virus life cycle, siRNA-mediated knockdown of the PP6 catalytic subunit was performed and growth of influenza A virus was assessed. We opted to knock down the catalytic subunit because the catalytic activity of the phosphatase resides in PPP6C and knocking down a single regulatory subunit might not be appropriate to assess the function of PP6 in the viral life cycle, considering that all three regulatory subunits, which might have redundant functions, were found to interact with the viral RNA polymerase. Three independent siRNAs specific for the PPP6C subunit, targeting the mRNA transcript at different positions, were transfected independently into HEK 293T cells (siPPP6C1, siPPP6C2, and siPPP6C3), alongside AllStars negative-control siRNA (siNegative). Cell lysates were analyzed for the levels of PPP6C by Western blotting. siRNA treatment resulted in a reduction of PPP6C protein levels to 5 to 20% of the untreated level (Fig. 6A). To ensure that the same number of viable cells were infected for each treatment, HEK 293T cells were transfected with siPPP6C1, siPPP6C2, siPPP6C3, or the negative-control siRNA and levels of ATP were measured to assess their metabolic activity. The numbers of viable cells were comparable (Fig. 6B). To investigate the effect of PPP6C knock-

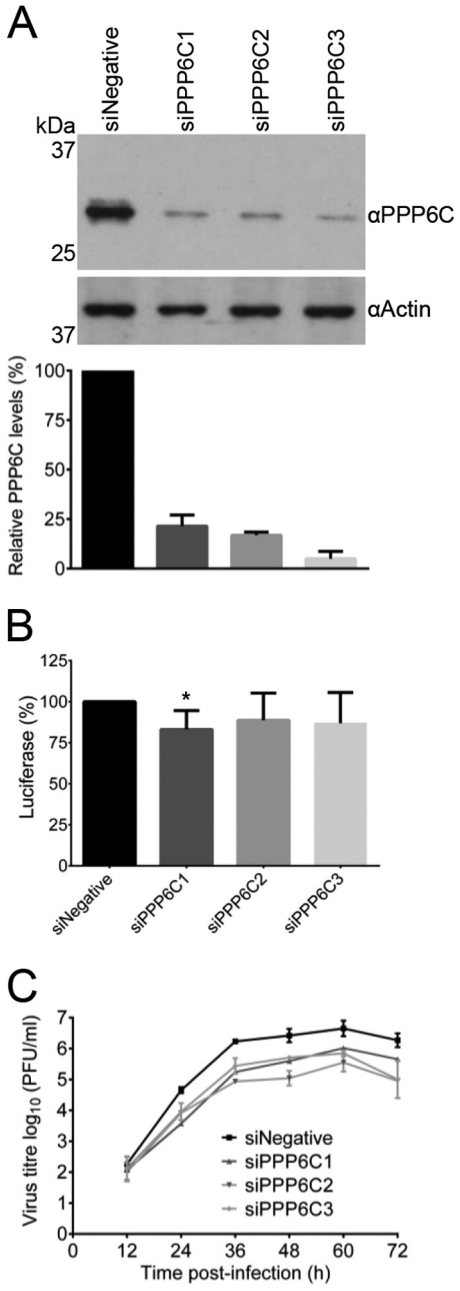


FIG 6 Effect of PPP6C knockdown in HEK 293T cells on influenza A virus growth. (A) Western blot analysis of PPP6C in HEK 293T cells treated with PPP6C-targeting siRNAs (siPPP6C1, siPPP6C2, and siPPP6C3) or a negative-control siRNA (siNegative). PPP6C (upper panel) was detected with a PPP6C-specific antibody. Actin (lower panel) was used as a loading control. PPP6C levels were normalized to the levels of actin and expressed as a percentage of PPP6C levels in cells treated with siNegative. The means and SD of three experiments are shown. (B) Viability assay of HEK 293T cells treated with PPP6C siRNAs or a negative-control siRNA as described above. The levels of ATP were determined by a CellTiter-Glo luminescent assay. The means and SD of three experiments are shown. The asterisk indicates a significant difference from 100% (*, $P < 0.05$, based on a one-sample Student's t test). (C) Growth curves of WT virus in PPP6C knockdown or control cells. Cells were treated with the indicated siRNAs and infected at an MOI of 0.001. At the indicated time points postinfection, cell supernatants were collected and virus titers were determined by plaque assay on MDBK cells. The means and SD of three experiments are shown. Knockdown of PPP6C significantly reduced replication compared to a negative-control siRNA for all time points from 24 h onwards (Student's two-tail t test, $P < 0.05$).

down on the virus life cycle, cells that were knocked down for PPP6C and control cells were infected with WT virus at an MOI of 0.001 and viral growth kinetics were measured (Fig. 6C). At 12 h p.i., there was no statistically significant difference between control and knockdown cells, but at all subsequent time points there was approximately a 10-fold, statistically significant reduction in virus accumulation in PPP6C knockdown cells, indicating an important role for PP6 in the influenza A virus life cycle.

Knockdown of PPP6C reduces viral RNA accumulation in influenza A virus-infected cells. In order to investigate the mechanisms that resulted in approximately 10-fold reduction of virus growth in PPP6C knockdown cells, viral RNA accumulation was assessed in PPP6C knockdown cells at 0, 6, and 8 h p.i. HEK 293T cells were transfected with three independent siRNAs that target PPP6C or a control siRNA. Levels of PPP6C protein in cell lysates were assessed by Western blotting. siRNA treatment resulted in reduction of PPP6C protein levels to 9 to 17% of the untreated level (Fig. 7A). Cells were infected at an MOI of 1, and RNA was isolated from infected cells at 0, 6, and 8 h p.i. Primer extension analyses using NA segment-specific primers showed that there was a significant reduction in mRNA, cRNA, and vRNA accumulation compared to what was seen in control cells at 6 h p.i. (Fig. 7B). However, at 8 h p.i. a significant reduction in cRNA and vRNA accumulation was observed only with the PPP6C-targeting siRNA that gave the greatest reduction in PPP6C levels (siPPP6C3), and no significant reduction was observed for viral mRNA accumulation (Fig. 7C). These data suggest that RNA accumulation is delayed in PPP6C knockdown cells. In order to assess whether the requirement of PP6 for efficient viral RNA synthesis takes place at a stage of the influenza A virus life cycle that precedes primary transcription, PPP6C knockdown or negative-control cells were infected or mock infected at an MOI of 10 in the presence of cycloheximide (CHX), an inhibitor of protein synthesis in eukaryotic cells, and the levels of viral mRNA were analyzed. Knockdown of PPP6C was confirmed by Western blotting, and quantitation showed that siRNA treatment resulted in reduction of PPP6C protein levels to 4 to 19% of control levels (Fig. 8A). At 6 h p.i., RNA was extracted from the infected cells, and primer extension analyses using NA segment-specific primers showed that levels of primary transcription in knockdown cells were not significantly different from those of negative-control cells (Fig. 8B and C). This result indicates that the requirement of PP6 for efficient viral RNA accumulation occurs at a stage of the viral life cycle after nuclear import of genomic vRNPs and primary transcription. Taken together, these data strongly suggest that the phosphatase activity of PP6 is required for efficient viral RNA accumulation after primary transcription and, consequently, virus growth in infected cells. However, it remains unclear whether the requirement for PP6 for early viral RNA accumulation is solely responsible for the reduction observed in viral growth or if PP6 might play additional roles in the viral replication cycle.

Reduced nuclear export of vRNPs is observed in PPP6C knockdown cells infected with influenza A virus. To further understand the mechanisms behind the reduction of influenza A virus growth in PPP6C knockdown cells, the nuclear export of vRNPs was compared in human alveolar basal epithelial (A549) cells with and without PPP6C knockdown. Levels of PPP6C protein in knockdown cells were reduced to 5 to 11% of those of negative-control cells (Fig. 9A). To assess the viability of A549 cells treated with PPP6C-targeting siRNAs, ATP levels were measured;

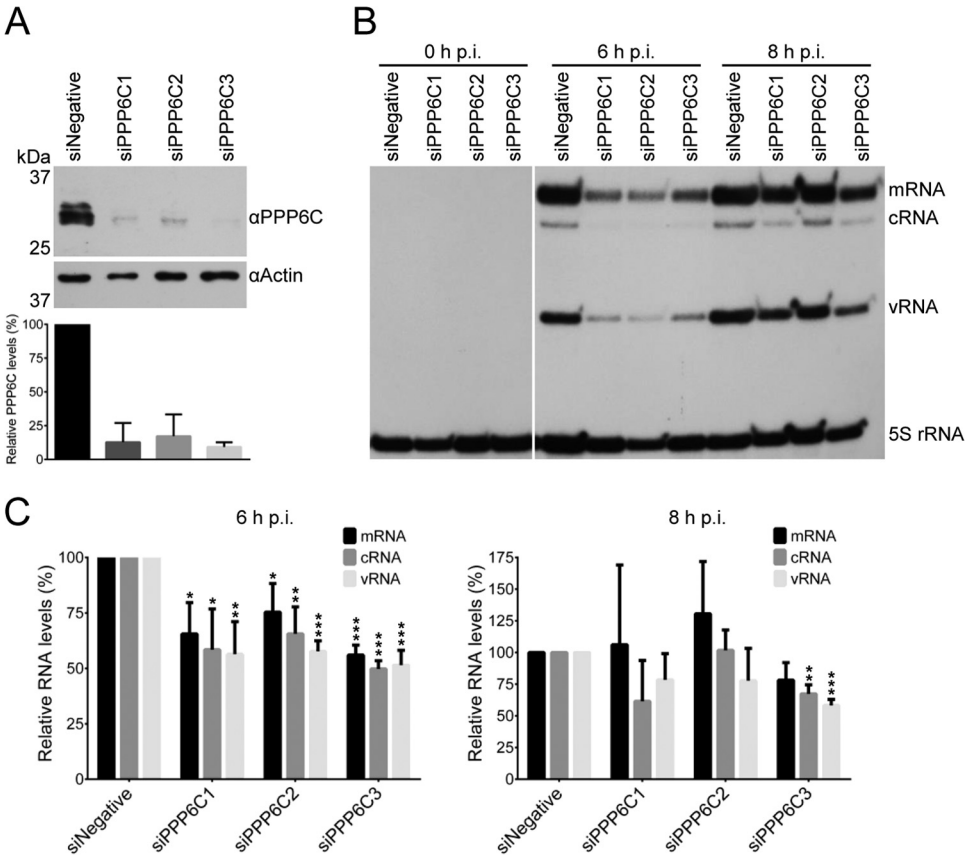


FIG 7 Effect of PPP6C knockdown in HEK 293T cells on the accumulation of viral RNAs. (A) Western blot analysis of PPP6C in HEK 293T cells treated with PPP6C-targeting siRNAs (siPPP6C1, siPPP6C2, and siPPP6C3) or a negative-control siRNA (siNegative). PPP6C (upper panel) was detected with a PPP6C-specific antibody. Actin (lower panel) was used as a loading control. PPP6C levels were normalized to the levels of actin and expressed as a percentage of PPP6C levels in cells treated with siNegative. The means and SD of three experiments are shown. (B) Primer extension analysis of viral NA segment-specific mRNA, cRNA, and vRNA in PPP6C knockdown or control cells. Cells were treated with the indicated siRNAs and infected at an MOI of 1. At the indicated time points postinfection, RNA was extracted from infected cells and viral RNAs were analyzed by primer extension using radiolabeled primers for positive-sense (mRNA and cRNA) and negative-sense (vRNA) NA-specific viral RNAs. 5S rRNA was used as a loading control. (C) Quantitation of primer extension analysis. The means and SD of three experiments are shown. Asterisks indicate a significant difference from 100% (*, $P < 0.05$; **, $P < 0.01$; ***, $P < 0.001$, based on a one-sample Student's *t* test).

these did not vary significantly between PPP6C knockdown cells and negative-control cells (Fig. 9B). The cellular localization of viral NP was determined in PPP6C knockdown or negative-control cells infected at an MOI of 1 with WT virus at 0, 4, 6, and 8 h p.i. The cellular localization of NP was scored in random fields of view in three biological replicates. NP signal was absent at 0 h p.i., as expected (Fig. 9C and D). At 4 h p.i., 100% of both the knockdown and the negative-control infected cells showed nuclear NP staining, indicating that significant vRNP export is not undertaken at this time point (Fig. 9C and D). At 6 h p.i., an average of 30% of negative-control cells showed a nucleocytoplasmic NP localization, representing the nuclear export of vRNPs that had occurred in these infected cells. However, on average, only 6%, 7%, and 11% of the PPP6C knockdown cells treated with the three different siRNAs showed nucleocytoplasmic NP localization (Fig. 9C and D). At 8 h p.i., the average proportion of infected negative-control cells that had a nucleocytoplasmic NP localization increased to 71%. However, the average proportions of infected knockdown cells with a nucleocytoplasmic NP localization reached only 44%, 49%, and 45% for each PPP6C siRNA, respectively (Fig. 9C and D). These results demonstrate that when the levels of the catalytic subunit of PP6 are reduced in infected cells, there is a marked delay in the nuclear export of vRNPs.

DISCUSSION

An in-depth understanding of the physical interactions that occur between viral proteins and cellular proteins within an infected cell is necessary for elucidating the molecular mechanisms that underlie virus replication. During infection, the influenza virus transcription/replication machinery makes numerous interactions with the host cell (reviewed in references 10, 73, and 74). Following infection, vRNPs from virions enter the host cell nucleus and recruit host factors to enable them to transcribe and replicate vRNA. Subsequently, new viral RdRP subunits are translated in the cytoplasm and must be imported into the nucleus for trimer assembly and incorporation into RNPs. This requires the viral RdRP to interface with molecular chaperones and the host nuclear import machinery (reviewed in references 75, 76, and 77). While many interactions between the viral RdRP and the host cell have been reported and some of the molecular biology of these interactions has been elucidated, a full description of the cellular proteins interacting with the viral RdRP in an infected host is lacking.

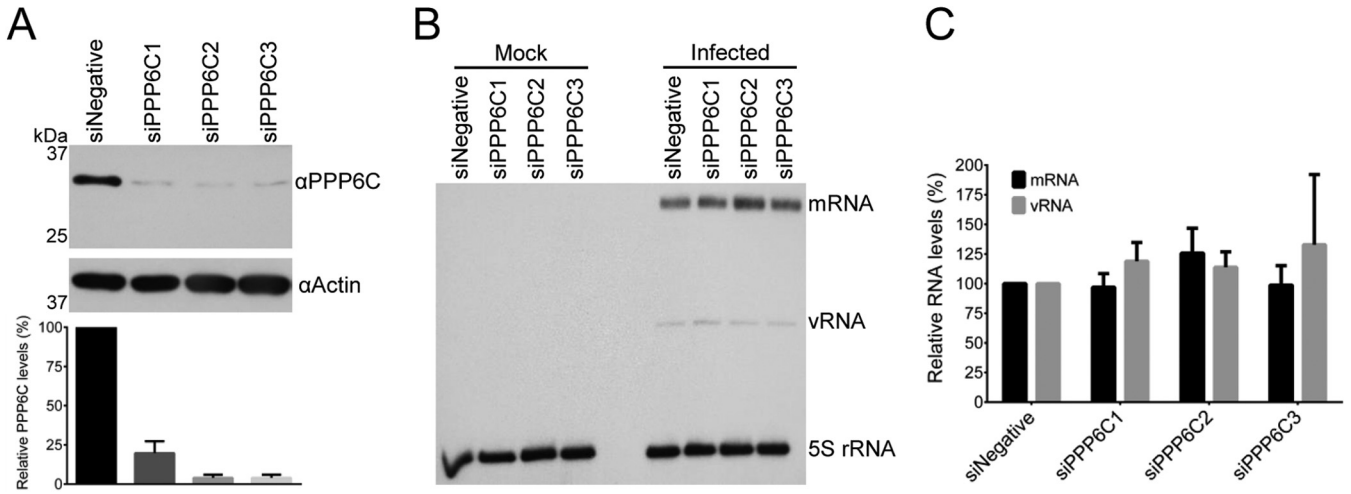


FIG 8 Effects of PPP6C knockdown in HEK 293T cells on primary transcription by parental vRNPs. (A) Western blot analysis of PPP6C in HEK 293T cells treated with PPP6C-targeting siRNAs (siPPP6C1, siPPP6C2, and siPPP6C3) or a negative-control siRNA (siNegative). PPP6C (upper panel) was detected with a PPP6C-specific antibody. Actin (lower panel) was used as a loading control. PPP6C levels were normalized to the levels of actin and expressed as a percentage of PPP6C levels in cells treated with siNegative. The means and SD of three experiments are shown. (B) Primer extension analysis of viral NA segment-specific mRNA, cRNA, and vRNA in PPP6C knockdown or control cells. Cells were treated with the indicated siRNAs and mock infected or infected at an MOI of 10 in the presence of cycloheximide (100 μg/ml). At 6 h p.i., RNA was extracted from infected cells and viral RNAs were analyzed by primer extension using radiolabeled primers for positive-sense (mRNA and cRNA) and negative-sense (vRNA) NA-specific viral RNAs. 5S rRNA was used as a loading control. (C) Quantitation of primer extension analysis. The means and SD of three experiments are shown.

Furthermore, much of the mechanistic details and roles of previously identified host-pathogen interactions is not understood.

In this study, an affinity purification mass spectrometry proteomic approach was employed with the aim of identifying the cellular interactome of the viral transcription/replication machinery. We sought to identify interactions occurring during infection by purifying the RdRP subunit PB2. Unlike what was done in previous studies, in which the viral RdRP was expressed by transient transfection (18–21), we were able to purify material from infected human cells. To do this, we took advantage of a recombinant influenza A virus encoding a Strep-tag at the C terminus of the PB2 subunit of the viral RdRP to isolate protein complexes containing PB2 (51). These complexes included vRNPs and cRNPs as demonstrated by the presence of NP, vRNA, and cRNA in the isolated complexes. In contrast, viral mRNA did not copurify at detectable levels with PB2-Strep, confirming that the viral RdRP does not stably associate with viral mRNA and the viral RdRP is unlikely to form a stable component of viral mRNPs (78, 79). In addition to PB2 being present in vRNPs and cRNPs, PB2 was present as a monomer and as part of RdRP that had not been incorporated into RNPs. We identified 171 cellular factors that copurified with PB2 from infected cells. This interactome was subjected to GO term analysis, revealing that interaction partners of the viral RdRP have a range of molecular functions. For example, a significant number of identified proteins are RNA-binding proteins. Considering the RNA-binding functions of the viral RdRP in transcription and replication of the viral genome (reviewed in references 8 and 80) and the reported association of the viral RdRP with cellular DNA-dependent RNA polymerase II and chromatin (81, 82), it is plausible that many of these factors are involved in viral RNA synthesis.

To our knowledge, our study is the first to use the relative abundance of copurifying cellular proteins to assess the likelihood that they are bound to the influenza virus RdRP in infected cells. We were able to place the most abundant host proteins in 8 major categories: chaperones, cytoskeletal proteins, importins, proteins involved in ubiquitination, kinases and phosphatases, mitochondrial proteins, and ribosomal proteins. The category of host proteins most likely to copurify with PB2-Strep was that of molecular chaperones, including Hsp70. Hsp70 family members have been reported to interact with the PB1 and PB2 subunits of the viral RdRP, with roles for Hsp70 being described in the nuclear export of vRNP complexes (83, 84) and in regulating RNA synthesis (85, 86). A number of additional molecular chaperones were present in the interactome, including Hsp90 and members of the CCT complex. Hsp90 has been shown to interact with PB1 and PB2 to stimulate viral RNA synthesis *in vitro* (87) and to facilitate nuclear import (88). Members of the CCT chaperonin have been proposed to aid in the folding of PB2 for its incorporation into a trimeric RdRP (20). The high abundance of molecular chaperones in the interactome reflects the importance of protein folding, proteome integrity, and proteostasis for the biological function of viral proteins.

Nuclear transport proteins were also enriched in the interactome. The most abundant of these proteins was importin-5 (RanBP5), a member of the importin-β family. Importin-5 is known to play a role in the nuclear import of the PB1-PA dimer by interacting with PB1 (89, 90). However, the nuclear import of PB2 is believed to occur independently of importin-5 and to be facilitated instead by the classical α/β-importin pathway (91–93). The identification of importin-5 as an abundant interactor of PB2, possibly as part of an RNP complex, suggests a role for importin-5 beyond its role in the nuclear import of the PB1-PA dimer. In addition to importin-5, members of the importin-α family of proteins, including importin-α3, -α4, -α5, and -α7, were also present, most likely due to the use of the α/β-importin pathway for nuclear import of PB2, NP, and vRNP complexes (reviewed in reference

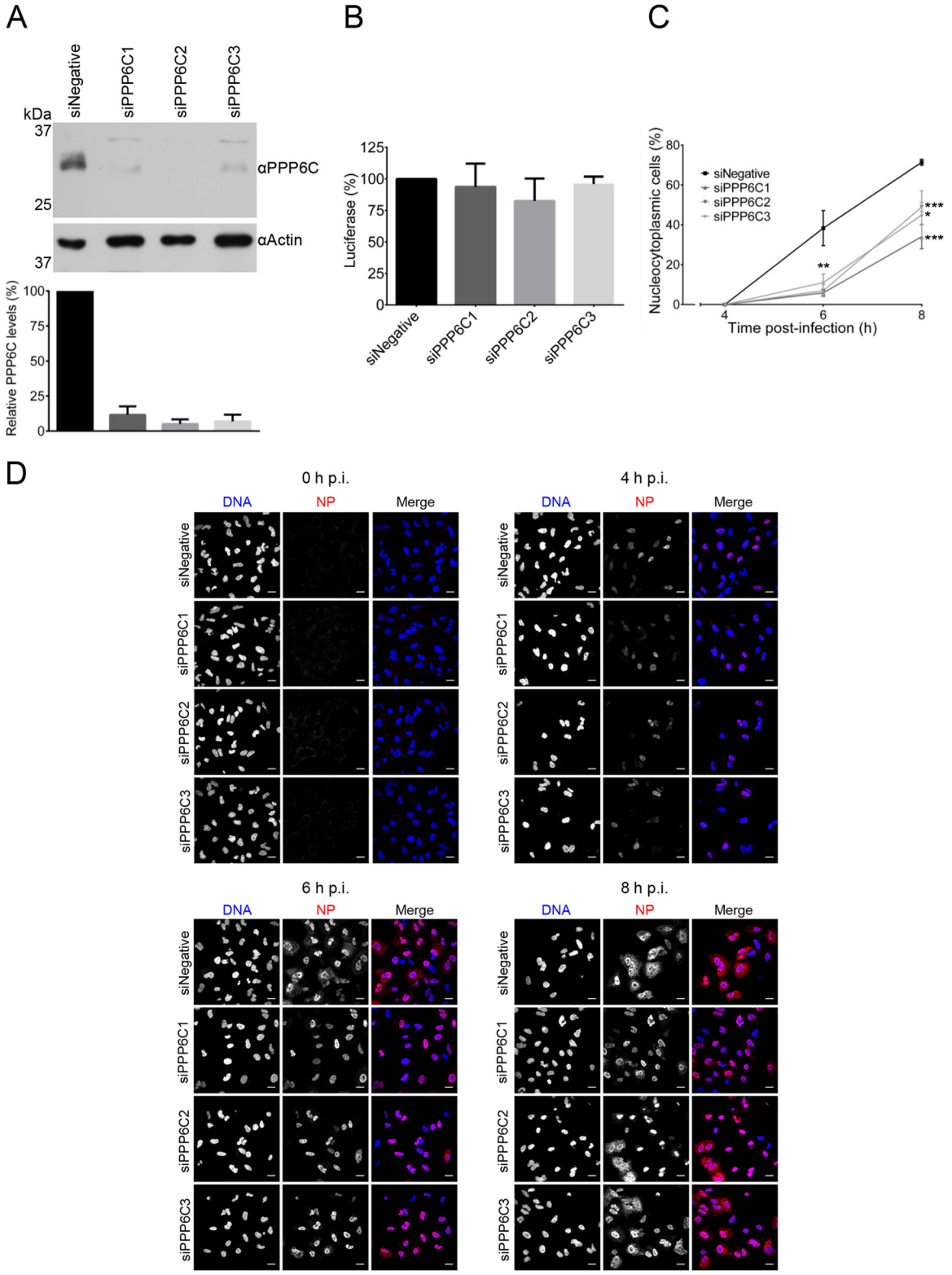


FIG 9 Effects of PPP6C knockdown on NP nucleocytoplasmic distribution in influenza A virus-infected A549 cells. (A) Western blot analysis of PPP6C in HEK 293T cells treated with PPP6C-targeting siRNAs (siPPP6C1, siPPP6C2, and siPPP6C3) or a negative-control siRNA (siNegative). PPP6C (upper panel) was detected with a PPP6C-specific antibody. Actin (lower panel) was used as a loading control. PPP6C levels were normalized to the levels of actin and expressed as a percentage of PPP6C levels in cells treated with siNegative. The means and SD of three experiments are shown. (B) Viability assay of A549 cells treated with PPP6C siRNAs or a negative-control siRNA as described above. The levels of ATP were determined by a CellTiter-Glo luminescent assay. The means and SD of three experiments are shown. (C) Confocal microscopy analysis of the nucleocytoplasmic distribution of NP in infected PPP6C knockdown cells. A549 cells treated with the indicated siRNAs were infected at an MOI of 1. NP was detected by indirect immunofluorescence using a monoclonal NP antibody and confocal

75); however, a noncanonical function for importin-α proteins in viral transcription/replication has also been proposed (91, 94).

Among the cytoskeletal proteins identified, tubulins, the major constituents of microtubules, were found to be the most abundant. This is likely to be related to the microtubule-dependent transport of vRNPs across the cytoplasm prior to virion assembly at the plasma membrane (95–98). A number of mitochondrial proteins were also present in the interactome. In previous studies, PB2 of human-adapted influenza viruses has been shown to accumulate in the mitochondria of infected cells and suppress beta interferon (IFN-β) production by associating with the mitochondrial antiviral signaling protein (MAVS) (99–101). Although MAVS has not been identified in this study, we found a range of mitochondrial proteins copurifying with PB2, including the apoptosis-inducing factor AIFM1. A previous study has shown that this protein, along with over 30 other mitochondrial proteins, associates with the PA subunit of the RdRP (21). The presence of a number of mitochondrial proteins in the interactome implies that uncharacterized associations exist between mitochondria and the viral transcription/replication machinery for the control of innate immune responses and apoptosis.

Posttranslational modifications are known to play an important role in influenza virus biology, and we identified factors involved in ubiquitination as interactors of the viral RdRP. Influenza virus proteins have been shown to be polyubiquitinated, leading to their degradation by the 26S proteasome (102–105). For example, the IFN-inducible antiviral protein TRIM22 has been shown to target NP for degradation in order to curtail virus replication (103). However, nondegradative roles of ubiquitination in influenza virus replication have also been proposed. Viral NP is reversibly monoubiquitinated, which has been proposed to regulate its RNA-binding activity (106). The identification of specific ubiquitin ligases in the RdRP interactome could help to elucidate the molecular mechanisms of a targeted response by the innate immune system to downregulate virus replication and could facilitate the understanding of the role of reversible monoubiquitination in the regulation of the viral transcription/replication machinery.

The influenza virus RdRP and NP are known to be phosphorylated in infected cells (36–38, 43, 46, 107, 108), and kinase activity has been shown to be essential for influenza virus replication. The treatment of cells with protein kinase inhibitors has been shown to interfere with different stages in the virus life cycle, including nuclear import, transcription, translation, nuclear export, and viral egress (109–113). Consistent with this, we found that a number of kinases and phosphatases were present in the interactome. We decided to investigate one of these interactions further, focusing on the cellular phosphatase PP6, as it was present at a relatively high abundance in the interactome. The PP6 heterotrimeric holoenzyme has been proposed to be composed of the catalytic subunit PPP6C, an ankyrin repeat domain 28 protein (Ankrd28), and one of the regulatory subunits PPP6R1, PPP6R2, and PPP6R3 (29). PPP6C, PPP6R1, and PPP6R3 were identified by mass spectrometry as interactors of the viral RdRP. However, Ankrd28 was not detected in the mass spectrometry. This absence could be explained by a proposed model of PP6 holoenzyme assembly in which Ankrd28 is not required for the interaction between the catalytic and regulatory subunits of PP6 (29).

The biological significance of PP6 in the influenza A virus life cycle was assessed by functional experiments in which the catalytic subunit of PP6 was knocked down in infected cells. Knockdown of PP6 resulted in a 10-fold reduction in viral growth, most likely caused by a delay in viral RNA accumulation. We found a significant reduction in viral RNA accumulation early in infection, although primary transcription was not affected. This suggests that PP6 function is required for viral RNA replication and, consequently, secondary transcription. These processes are known to depend on newly synthesized RdRP and NP, and therefore it is plausible that PP6 is required for the nuclear import and assembly of fully functional RdRP and/or viral RNPs. It is also possible that PP6 acts directly on the viral RdRP to positively regulate its replicative activity.

We found that PP6 interacted with monomeric PB1 and PB2, dimeric PB1-PA, and the trimeric RdRP in mammalian cells. This is consistent with a previous report that PPP6C interacts with a PB1-PA dimer in transiently transfected cells (21). We determined that the interaction between PP6 and the viral RdRP is direct, with both the catalytic and regulatory subunits being able to bind to the RdRP independently. However, more RdRP was found to interact with the regulatory subunits, in agreement with the substrate specificity of PP2A phosphatases being defined by their regulatory subunits (31, 114). Although there is no high-resolution structural information available for the PP6 holoenzyme, the crystal structure of the PP2A holoenzyme shows that a substrate-binding groove within the regulatory subunit is located in close proximity to the active site of the catalytic subunit, supporting the view that the regulatory subunits are responsible for target specificity and the positioning of the phosphorylated substrate close to the catalytic center for dephosphorylation (115). We found that PP6 binds directly to the PB1 and PB2 subunits of the viral RdRP, suggesting that it could dephosphorylate PB1 or PB2.

All three subunits of the viral RdRP as well as NP are phosphorylated (36–38, 43, 46, 107, 108, 116), and PP6 could be involved in the regulation of their phosphorylation. For example, phosphorylation of PB1 and PB2 could regulate their interactions with importins. The structure of the C terminus of PB2 in complex with importin-α5 reveals that S742, a residue that can be phosphorylated (36), is positioned close to two basic residues on the surface of importin-α5 (92). Phosphorylation of S742 could therefore regulate PB2 binding to importins. The PB1 subunit of the viral RdRP can be phosphorylated at position T223. This is close to a nuclear localization signal (NLS) and a region that is believed to be involved in promoter binding, indicating a potential role in regulating the cellular localization or RNA binding of PB1 (36, 90, 117–120).

As PP6 interacts directly with PB1 and PB2, they represent the most obvious substrates. However, it is possible that PP6 could dephosphorylate another viral or host protein in close proximity to PB1 or PB2. The viral RdRP forms a compact structure, and

microscopy at the indicated time points p.i. The percentage of infected cells with a nucleocytoplasmic NP localization at each time point is shown. The means and SD of three experiments are shown. Asterisks indicate a significant difference from siNegative (*, $P < 0.05$; **, $P < 0.01$; ***, $P < 0.001$, based on a two-sample Student's *t* test). (D) Representative images of NP localization. Scale bars, 20 μm.

therefore it is conceivable that PP6 could dephosphorylate PA (121–124), which can be phosphorylated at positions S224/S225, in an unstructured region linking the PA endonuclease and C-terminal domains (6, 7, 36, 125, 126). The viral NP can be phosphorylated at multiple sites (36–38, 42, 116), and therefore it is also possible that PP6 could bind to the viral RdRP and dephosphorylate a proximal NP molecule within a viral RNP complex, perhaps serving to regulate the oligomerization of NP as has been previously proposed (36, 116). Nuclear export protein (NEP), a viral factor for the nuclear export of genomic vRNPs and a regulator of viral RNA synthesis, has been found to be phosphorylated at a position between S23 and S25 (36, 127). NEP is known to interact with and modulate the activity of the viral RdRP (58, 127–129), and therefore it could be subject to PP6-mediated regulatory phosphorylation. In support of this hypothesis, a recent study described a minor role for phosphorylation of NEP in controlling vRNP export and the polymerase cofactor activity in regulating RNA synthesis (130).

We cannot exclude the possibility that PP6 also plays an additional role in the virus life cycle, independent of binding to the viral RdRP. PP6 regulates the activities of many host proteins (22–35), and it is therefore possible that PP6 silencing perturbs the virus life cycle by affecting other cellular processes. However, the fact that PP6 interacts directly with the viral RdRP suggests that it plays a direct role in the viral life cycle by regulating the posttranslational modifications of viral proteins. Further studies will be required to identify the precise substrate and residues targeted by PP6 and to determine the molecular function that dephosphorylation by PP6 plays in the influenza virus life cycle.

In summary, 171 components of the interactome of the influenza A virus transcription/replication machinery were identified by highly sensitive LC/MS-MS and label-free quantitative analysis of affinity-purified PB2 complexes from virus-infected human cells. One of the identified proteins, the cellular phosphatase PP6, was shown to be important for the influenza A virus life cycle, as siRNA-mediated knockdown resulted in the downregulation of viral RNA synthesis and, consequently, vRNP export and virus growth. This study identifies cellular factors that interact with the viral transcription/replication machinery during influenza A virus infection and highlights the significance of regulatory phosphorylation in influenza virus biology.

ACKNOWLEDGMENTS

We thank Martin Schwemmle, Nadia Naffakh, Susan P. Lees-Miller, and J. Robert Hogg for providing plasmids. We thank Benjamin Thomas and Svenja Hester (Central Proteomics Facility, Sir William Dunn School of Pathology, University of Oxford) for mass spectrometry analysis.

This work was supported by Medical Research Council (MRC) grants G0700848 and MR/K000241/1 (to E.F.) and an MRC studentship (to A.Y.).

REFERENCES

1. **Holmes EC.** 2013. Virus evolution, p 286–313. *In* Knipe DM, Howley PM (ed), Fields virology, 6th ed. Lippincott Williams and Wilkins, Philadelphia, PA.
2. **Cauldwell AV, Long JS, Moncorge O, Barclay WS.** 2014. Viral determinants of influenza A virus host range. J. Gen. Virol. **95:**1193–1210. http://dx.doi.org/10.1099/vir.0.062836-0.
3. **Manz B, Schwemmle M, Brunotte L.** 2013. Adaptation of avian influenza A virus polymerase in mammals to overcome the host species barrier. J. Virol. **87:**7200–7209. http://dx.doi.org/10.1128/JVI.00980-13.
4. **Biswas SK, Nayak DP.** 1994. Mutational analysis of the conserved motifs of influenza A virus polymerase basic protein 1. J. Virol. **68:**1819–1826.
5. **Guilligay D, Tarendeau F, Resa-Infante P, Coloma R, Crepin T, Sehr P, Lewis J, Ruigrok RW, Ortin J, Hart DJ, Cusack S.** 2008. The structural basis for cap binding by influenza virus polymerase subunit PB2. Nat. Struct. Mol. Biol. **15:**500–506. http://dx.doi.org/10.1038/nsmb.1421.
6. **Yuan P, Bartlam M, Lou Z, Chen S, Zhou J, He X, Lv Z, Ge R, Li X, Deng T, Fodor E, Rao Z, Liu Y.** 2009. Crystal structure of an avian influenza polymerase PA(N) reveals an endonuclease active site. Nature **458:**909–913. http://dx.doi.org/10.1038/nature07720.
7. **Dias A, Bouvier D, Crepin T, McCarthy AA, Hart DJ, Baudin F, Cusack S, Ruigrok RW.** 2009. The cap-snatching endonuclease of influenza virus polymerase resides in the PA subunit. Nature **458:**914–918. http://dx.doi.org/10.1038/nature07745.
8. **Resa-Infante P, Jorba N, Coloma R, Ortin J.** 2011. The influenza virus RNA synthesis machine: advances in its structure and function. RNA Biol. **8:**207–215. http://dx.doi.org/10.4161/rna.8.2.14513.
9. **Fodor E.** 2013. The RNA polymerase of influenza a virus: mechanisms of viral transcription and replication. Acta Virol. **57:**113–122. http://dx.doi.org/10.4149/av_2013_02_113.
10. **Matsuoka Y, Matsumae H, Katoh M, Eisfeld AJ, Neumann G, Hase T, Ghosh S, Shoemaker JE, Lopes TJ, Watanabe T, Watanabe S, Fukuyama S, Kitano H, Kawaoka Y.** 2013. A comprehensive map of the influenza A virus replication cycle. BMC Syst. Biol. **7:**97. http://dx.doi.org/10.1186/1752-0509-7-97.
11. **Karlas A, Machuy N, Shin Y, Pleissner KP, Artarini A, Heuer D, Becker D, Khalil H, Ogilvie LA, Hess S, Maurer AP, Muller E, Wolff T, Rudel T, Meyer TF.** 2010. Genome-wide RNAi screen identifies human host factors crucial for influenza virus replication. Nature **463:**818–822. http://dx.doi.org/10.1038/nature08760.
12. **Konig R, Stertz S, Zhou Y, Inoue A, Hoffmann HH, Bhattacharyya S, Alamares JG, Tscherne DM, Ortigoza MB, Liang Y, Gao Q, Andrews SE, Bandyopadhyay S, De Jesus P, Tu BP, Pache L, Shih C, Orth A, Bonamy G, Miraglia L, Ideker T, Garcia-Sastre A, Young JA, Palese P, Shaw ML, Chanda SK.** 2010. Human host factors required for influenza virus replication. Nature **463:**813–817. http://dx.doi.org/10.1038/nature08699.
13. **Hao L, Sakurai A, Watanabe T, Sorensen E, Nidom CA, Newton MA, Ahlquist P, Kawaoka Y.** 2008. Drosophila RNAi screen identifies host genes important for influenza virus replication. Nature **454:**890–893. http://dx.doi.org/10.1038/nature07151.
14. **Sui B, Bamba D, Weng K, Ung H, Chang S, Van Dyke J, Goldblatt M, Duan R, Kinch MS, Li WB.** 2009. The use of random homozygous gene perturbation to identify novel host-oriented targets for influenza. Virology **387:**473–481. http://dx.doi.org/10.1016/j.virol.2009.02.046.
15. **Shapira SD, Gat-Viks I, Shum BO, Dricot A, de Grace MM, Wu L, Gupta PB, Hao T, Silver SJ, Root DE, Hill DE, Regev A, Hacohen N.** 2009. A physical and regulatory map of host-influenza interactions reveals pathways in H1N1 infection. Cell **139:**1255–1267. http://dx.doi.org/10.1016/j.cell.2009.12.018.
16. **Tafforeau L, Chantier T, Pradezynski F, Pellet J, Mangeot PE, Vidalain PO, Andre P, Rabourdin-Combe C, Lotteau V.** 2011. Generation and comprehensive analysis of an influenza virus polymerase cellular interaction network. J. Virol. **85:**13010–13018. http://dx.doi.org/10.1128/JVI.02651-10.
17. **Munier S, Rolland T, Diot C, Jacob Y, Naffakh N.** 2013. Exploration of binary virus-host interactions using an infectious protein complementation assay. Mol. Cell. Proteomics **12:**2845–2855. http://dx.doi.org/10.1074/mcp.M113.028688.
18. **Jorba N, Juarez S, Torreira E, Gastaminza P, Zamarreno N, Albar JP, Ortin J.** 2008. Analysis of the interaction of influenza virus polymerase complex with human cell factors. Proteomics **8:**2077–2088. http://dx.doi.org/10.1002/pmic.200700508.
19. **Mayer D, Molawi K, Martinez-Sobrido L, Ghanem A, Thomas S, Baginsky S, Grossmann J, Garcia-Sastre A, Schwemmle M.** 2007. Identification of cellular interaction partners of the influenza virus ribonucleoprotein complex and polymerase complex using proteomic-based approaches. J. Proteome Res. **6:**672–682. http://dx.doi.org/10.1021/pr060432u.
20. **Fislova T, Thomas B, Graef KM, Fodor E.** 2010. Association of the influenza virus RNA polymerase subunit PB2 with the host chaperonin CCT. J. Virol. **84:**8691–8699. http://dx.doi.org/10.1128/JVI.00813-10.
21. **Bradel-Tretheway BG, Mattiacio JL, Krasnoselsky A, Stevenson C, Purdy D, Dewhurst S, Katze MG.** 2011. Comprehensive proteomic

analysis of influenza virus polymerase complex reveals a novel association with mitochondrial proteins and RNA polymerase accessory factors. J. Virol. **85:**8569–8581. http://dx.doi.org/10.1128/JVI.00496-11.
22. **Bastians H, Ponstingl H.** 1996. The novel human protein serine/threonine phosphatase 6 is a functional homologue of budding yeast Sit4p and fission yeast ppe1, which are involved in cell cycle regulation. J. Cell Sci. **109**(Part 12):2865–2874.
23. **Douglas P, Zhong J, Ye R, Moorhead GB, Xu X, Lees-Miller SP.** 2010. Protein phosphatase 6 interacts with the DNA-dependent protein kinase catalytic subunit and dephosphorylates gamma-H2AX. Mol. Cell. Biol. **30:**1368–1381. http://dx.doi.org/10.1128/MCB.00741-09.
24. **Zhong J, Liao J, Liu X, Wang P, Liu J, Hou W, Zhu B, Yao L, Wang J, Li J, Stark JM, Xie Y, Xu X.** 2011. Protein phosphatase PP6 is required for homology-directed repair of DNA double-strand breaks. Cell Cycle **10:**1411–1419. http://dx.doi.org/10.4161/cc.10.9.15479.
25. **Hosing AS, Valerie NC, Dziegielewski J, Brautigan DL, Larner JM.** 2012. PP6 regulatory subunit R1 is bidentate anchor for targeting protein phosphatase-6 to DNA-dependent protein kinase. J. Biol. Chem. **287:**9230–9239. http://dx.doi.org/10.1074/jbc.M111.333708.
26. **Hammond D, Zeng K, Espert A, Bastos RN, Baron RD, Gruneberg U, Barr FA.** 2013. Melanoma-associated mutations in protein phosphatase 6 cause chromosome instability and DNA damage owing to dysregulated Aurora-A. J. Cell Sci. **126:**3429–3440. http://dx.doi.org/10.1242/jcs.128397.
27. **Shen Y, Wang Y, Sheng K, Fei X, Guo Q, Larner J, Kong X, Qiu Y, Mi J.** 2011. Serine/threonine protein phosphatase 6 modulates the radiation sensitivity of glioblastoma. Cell Death Dis. **2:**e241. http://dx.doi.org/10.1038/cddis.2011.126.
28. **Stefansson B, Brautigan DL.** 2007. Protein phosphatase PP6 N terminal domain restricts G1 to S phase progression in human cancer cells. Cell Cycle **6:**1386–1392. http://dx.doi.org/10.4161/cc.6.11.4276.
29. **Stefansson B, Ohama T, Daugherty AE, Brautigan DL.** 2008. Protein phosphatase 6 regulatory subunits composed of ankyrin repeat domains. Biochemistry **47:**1442–1451. http://dx.doi.org/10.1021/bi7022877.
30. **Zeng K, Bastos RN, Barr FA, Gruneberg U.** 2010. Protein phosphatase 6 regulates mitotic spindle formation by controlling the T-loop phosphorylation state of Aurora A bound to its activator TPX2. J. Cell Biol. **191:**1315–1332. http://dx.doi.org/10.1083/jcb.201008106.
31. **Barr FA, Elliott PR, Gruneberg U.** 2011. Protein phosphatases and the regulation of mitosis. J. Cell Sci. **124:**2323–2334. http://dx.doi.org/10.1242/jcs.087106.
32. **Kajino T, Ren H, Iemura S, Natsume T, Stefansson B, Brautigan DL, Matsumoto K, Ninomiya-Tsuji J.** 2006. Protein phosphatase 6 down-regulates TAK1 kinase activation in the IL-1 signaling pathway. J. Biol. Chem. **281:**39891–39896. http://dx.doi.org/10.1074/jbc.M608155200.
33. **Dai M, Terzaghi W, Wang H.** 2013. Multifaceted roles of Arabidopsis PP6 phosphatase in regulating cellular signaling and plant development. Plant Signal. Behav. **8**(1):e22508. http://dx.doi.org/10.4161/psb.22508.
34. **Kamoun M, Filali M, Murray MV, Awasthi S, Wadzinski BE.** 2013. Protein phosphatase 2A family members (PP2A and PP6) associate with U1 snRNP and the spliceosome during pre-mRNA splicing. Biochem. Biophys. Res. Commun. **440:**306–311. http://dx.doi.org/10.1016/j.bbrc.2013.09.068.
35. **Bhandari D, Zhang J, Menon S, Lord C, Chen S, Helm JR, Thorsen K, Corbett KD, Hay JC, Ferro-Novick S.** 2013. Sit4p/PP6 regulates ER-to-Golgi traffic by controlling the dephosphorylation of COPII coat subunits. Mol. Biol. Cell **24:**2727–2738. http://dx.doi.org/10.1091/mbc.E13-02-0114.
36. **Hutchinson EC, Denham EM, Thomas B, Trudgian DC, Hester SS, Ridlova G, York A, Turrell L, Fodor E.** 2012. Mapping the phosphoproteome of influenza A and B viruses by mass spectrometry. PLoS Pathog. **8:**e1002993. http://dx.doi.org/10.1371/journal.ppat.1002993.
37. **Almond JW, Felsenreich V.** 1982. Phosphorylation of the nucleoprotein of an avian influenza virus. J. Gen. Virol. **60:**295–305. http://dx.doi.org/10.1099/0022-1317-60-2-295.
38. **Arrese M, Portela A.** 1996. Serine 3 is critical for phosphorylation at the N-terminal end of the nucleoprotein of influenza virus A/Victoria/3/75. J. Virol. **70:**3385–3391.
39. **Gregoriades A, Christie T, Markarian K.** 1984. The membrane (M1) protein of influenza virus occurs in two forms and is a phosphoprotein. J. Virol. **49:**229–235.
40. **Gregoriades A, Guzman GG, Paoletti E.** 1990. The phosphorylation of the integral membrane (M1) protein of influenza virus. Virus Res. **16:**27–41. http://dx.doi.org/10.1016/0168-1702(90)90041-9.
41. **Holsinger LJ, Shaughnessy MA, Micko A, Pinto LH, Lamb RA.** 1995. Analysis of the posttranslational modifications of the influenza virus M2 protein. J. Virol. **69:**1219–1225.
42. **Kistner O, Muller K, Scholtissek C.** 1989. Differential phosphorylation of the nucleoprotein of influenza A viruses. J. Gen. Virol. **70**(Part 9):2421–2431.
43. **Mahmoudian S, Auerochs S, Grone M, Marschall M.** 2009. Influenza A virus proteins PB1 and NS1 are subject to functionally important phosphorylation by protein kinase C. J. Gen. Virol. **90:**1392–1397. http://dx.doi.org/10.1099/vir.0.009050-0.
44. **Mitzner D, Dudek SE, Studtrucker N, Anhlan D, Mazur I, Wissing J, Jansch L, Wixler L, Bruns K, Sharma A, Wray V, Henklein P, Ludwig S, Schubert U.** 2009. Phosphorylation of the influenza A virus protein PB1-F2 by PKC is crucial for apoptosis promoting functions in monocytes. Cell. Microbiol. **11:**1502–1516. http://dx.doi.org/10.1111/j.1462-5822.2009.01343.x.
45. **Richardson JC, Akkina RK.** 1991. NS2 protein of influenza virus is found in purified virus and phosphorylated in infected cells. Arch. Virol. **116:**69–80. http://dx.doi.org/10.1007/BF01319232.
46. **Sanz-Ezquerro JJ, Fernandez Santaren J, Sierra T, Aragon T, Ortega J, Ortin J, Smith GL, Nieto A.** 1998. The PA influenza virus polymerase subunit is a phosphorylated protein. J. Gen. Virol. **79**(Part 3):471–478.
47. **Whittaker G, Kemler I, Helenius A.** 1995. Hyperphosphorylation of mutant influenza virus matrix protein, M1, causes its retention in the nucleus. J. Virol. **69:**439–445.
48. **Hale BG, Knebel A, Botting CH, Galloway CS, Precious BL, Jackson D, Elliott RM, Randall RE.** 2009. CDK/ERK-mediated phosphorylation of the human influenza A virus NS1 protein at threonine-215. Virology **383:**6–11. http://dx.doi.org/10.1016/j.virol.2008.10.002.
49. **Hsiang TY, Zhou L, Krug RM.** 2012. Roles of the phosphorylation of specific serines and threonines in the NS1 protein of human influenza A viruses. J. Virol. **86:**10370–10376. http://dx.doi.org/10.1128/JVI.00732-12.
50. **Fodor E, Devenish L, Engelhardt OG, Palese P, Brownlee GG, Garcia-Sastre A.** 1999. Rescue of influenza A virus from recombinant DNA. J. Virol. **73:**9679–9682.
51. **Rameix-Welti MA, Tomoiu A, Dos Santos Afonso E, van der Werf S, Naffakh N.** 2009. Avian influenza A virus polymerase association with nucleoprotein, but not polymerase assembly, is impaired in human cells during the course of infection. J. Virol. **83:**1320–1331. http://dx.doi.org/10.1128/JVI.00977-08.
52. **Fodor E, Crow M, Mingay LJ, Deng T, Sharps J, Fechter P, Brownlee GG.** 2002. A single amino acid mutation in the PA subunit of the influenza virus RNA polymerase inhibits endonucleolytic cleavage of capped RNAs. J. Virol. **76:**8989–9001. http://dx.doi.org/10.1128/JVI.76.18.8989-9001.2002.
53. **Deng T, Sharps J, Fodor E, Brownlee GG.** 2005. In vitro assembly of PB2 with a PB1-PA dimer supports a new model of assembly of influenza A virus polymerase subunits into a functional trimeric complex. J. Virol. **79:**8669–8674. http://dx.doi.org/10.1128/JVI.79.13.8669-8674.2005.
54. **Brownlee GG, Sharps JL.** 2002. The RNA polymerase of influenza a virus is stabilized by interaction with its viral RNA promoter. J. Virol. **76:**7103–7113. http://dx.doi.org/10.1128/JVI.76.14.7103-7113.2002.
55. **York A, Hengrung N, Vreede FT, Huiskonen JT, Fodor E.** 2013. Isolation and characterization of the positive-sense replicative intermediate of a negative-strand RNA virus. Proc. Natl. Acad. Sci. U. S. A. **110:**E4238–E4245. http://dx.doi.org/10.1073/pnas.1315068110.
56. **Bieniossek C, Richmond TJ, Berger I.** 2008. MultiBac: multigene baculovirus-based eukaryotic protein complex production. Curr. Protoc. Protein Sci. **Chapter 5:**Unit 5.20. http://dx.doi.org/10.1002/0471140864.ps0520s51.
57. **Schmidt TG, Skerra A.** 2007. The Strep-tag system for one-step purification and high-affinity detection or capturing of proteins. Nat. Protoc. **2:**1528–1535. http://dx.doi.org/10.1038/nprot.2007.209.
58. **Robb NC, Smith M, Vreede FT, Fodor E.** 2009. NS2/NEP protein regulates transcription and replication of the influenza virus RNA genome. J. Gen. Virol. **90:**1398–1407. http://dx.doi.org/10.1099/vir.0.009639-0.
59. **Chambers MC, Maclean B, Burke R, Amodei D, Ruderman DL, Neumann S, Gatto L, Fischer B, Pratt B, Egertson J, Hoff K, Kessner D, Tasman N, Shulman N, Frewen B, Baker TA, Brusniak MY, Paulse**

C, Creasy D, Flashner L, Kani K, Moulding C, Seymour SL, Nuwaysir LM, Lefebvre B, Kuhlmann F, Roark J, Rainer P, Detlev S, Hemenway T, Huhmer A, Langridge J, Connolly B, Chadick T, Holly K, Eckels J, Deutsch EW, Moritz RL, Katz JE, Agus DB, MacCoss M, Tabb DL, Mallick P. 2012. A cross-platform toolkit for mass spectrometry and proteomics. Nat. Biotechnol. **30:**918–920. http://dx.doi.org/10.1038/nbt.2377.

60. **Trudgian DC, Thomas B, McGowan SJ, Kessler BM, Salek M, Acuto O.** 2010. CPFP: a central proteomics facilities pipeline. Bioinformatics **26:**1131–1132. http://dx.doi.org/10.1093/bioinformatics/btq081.
61. **Shteynberg D, Deutsch EW, Lam H, Eng Sun JKZ, Tasman N, Mendoza L, Moritz RL, Aebersold R, Nesvizhskii AI.** 2011. iProphet: multi-level integrative analysis of shotgun proteomic data improves peptide and protein identification rates and error estimates. Mol. Cell. Proteomics **10:**M111.007690. http://dx.doi.org/10.1074/mcp.M111.007690.
62. **Geer LY, Markey SP, Kowalak JA, Wagner L, Xu M, Maynard DM, Yang X, Shi W, Bryant SH.** 2004. Open mass spectrometry search algorithm. J. Proteome Res. **3:**958–964. http://dx.doi.org/10.1021/pr0499491.
63. **Craig R, Beavis RC.** 2004. TANDEM: matching proteins with tandem mass spectra. Bioinformatics **20:**1466–1467. http://dx.doi.org/10.1093/bioinformatics/bth092.
64. **Keller A, Nesvizhskii AI, Kolker E, Aebersold R.** 2002. Empirical statistical model to estimate the accuracy of peptide identifications made by MS/MS and database search. Anal. Chem. **74:**5383–5392. http://dx.doi.org/10.1021/ac025747h.
65. **Nesvizhskii AI, Keller A, Kolker E, Aebersold R.** 2003. A statistical model for identifying proteins by tandem mass spectrometry. Anal. Chem. **75:**4646–4658. http://dx.doi.org/10.1021/ac0341261.
66. **Trudgian DC, Ridlova G, Fischer R, Mackeen MM, Ternette N, Acuto O, Kessler BM, Thomas B.** 2011. Comparative evaluation of label-free SINQ normalized spectral index quantitation in the central proteomics facilities pipeline. Proteomics **11:**2790–2797. http://dx.doi.org/10.1002/pmic.201000800.
67. **Jensen LJ, Kuhn M, Stark M, Chaffron S, Creevey C, Muller J, Doerks T, Julien P, Roth A, Simonovic M, Bork P, von Mering C.** 2009. STRING 8–a global view on proteins and their functional interactions in 630 organisms. Nucleic Acids Res. **37:**D412–D416. http://dx.doi.org/10.1093/nar/gkn760.
68. **Lopes CT, Franz M, Kazi F, Donaldson SL, Morris Q, Bader GD.** 2010. Cytoscape Web: an interactive web-based network browser. Bioinformatics **26:**2347–2348. http://dx.doi.org/10.1093/bioinformatics/btq430.
69. **Boyle EI, Weng S, Gollub J, Jin H, Botstein D, Cherry JM, Sherlock G.** 2004. GO::TermFinder–open source software for accessing Gene Ontology information and finding significantly enriched Gene Ontology terms associated with a list of genes. Bioinformatics **20:**3710–3715. http://dx.doi.org/10.1093/bioinformatics/bth456.
70. **Harris MA, Clark J, Ireland A, Lomax J, Ashburner M, Foulger R, Eilbeck K, Lewis S, Marshall B, Mungall C, Richter J, Rubin GM, Blake JA, Bult C, Dolan M, Drabkin H, Eppig JT, Hill DP, Ni L, Ringwald M, Balakrishnan R, Cherry JM, Christie KR, Costanzo MC, Dwight SS, Engel S, Fisk DG, Hirschman JE, Hong EL, Nash RS, Sethuraman A, Theesfeld CL, Botstein D, Dolinski K, Feierbach B, Berardini T, Mundodi S, Rhee SY, Apweiler R, Barrell D, Camon E, Dimmer E, Lee V, Chisholm R, Gaudet P, Kibbe W, Kishore R, Schwarz EM, Sternberg P, Gwinn M, Hannick L, Wortman J, Berriman M, Wood V, de la Cruz N, Tonellato P, Jaiswal P, Seigfried T, White R, Gene Ontology Consortium.** 2004. The Gene Ontology (GO) database and informatics resource. Nucleic Acids Res. **32:**D258–D261. http://dx.doi.org/10.1093/nar/gkh036.
71. **Ye QZ, Krug RM, Tao YZJ.** 2006. The mechanism by which influenza A virus nucleoprotein forms oligomers and binds RNA. Nature **444:**1078–1082. http://dx.doi.org/10.1038/nature05379.
72. **Ortega J, Martin-Benito J, Zurcher T, Valpuesta JM, Carrascosa JL, Ortin J.** 2000. Ultrastructural and functional analyses of recombinant influenza virus ribonucleoproteins suggest dimerization of nucleoprotein during virus amplification. J. Virol. **74:**156–163. http://dx.doi.org/10.1128/JVI.74.1.156-163.2000.
73. **Watanabe T, Watanabe S, Kawaoka Y.** 2010. Cellular networks involved in the influenza virus life cycle. Cell Host Microbe **7:**427–439. http://dx.doi.org/10.1016/j.chom.2010.05.008.
74. **Shaw ML.** 2011. The host interactome of influenza virus presents new potential targets for antiviral drugs. Rev. Med. Virol. **21:**358–369. http://dx.doi.org/10.1002/rmv.703.
75. **Hutchinson EC, Fodor E.** 2012. Nuclear import of the influenza A virus transcriptional machinery. Vaccine **30:**7353–7358. http://dx.doi.org/10.1016/j.vaccine.2012.04.085.
76. **Resa-Infante P, Gabriel G.** 2013. The nuclear import machinery is a determinant of influenza virus host adaptation. Bioessays **35:**23–27. http://dx.doi.org/10.1002/bies.201200138.
77. **Geller R, Taguwa S, Frydman J.** 2012. Broad action of Hsp90 as a host chaperone required for viral replication. Biochim. Biophys. Acta **1823:**698–706. http://dx.doi.org/10.1016/j.bbamcr.2011.11.007.
78. **Bier K, York A, Fodor E.** 2011. Cellular cap-binding proteins associate with influenza virus mRNAs. J. Gen. Virol. **92:**1627–1634. http://dx.doi.org/10.1099/vir.0.029231-0.
79. **York A, Fodor E.** 2013. Biogenesis, assembly, and export of viral messenger ribonucleoproteins in the influenza A virus infected cell. RNA Biol. **10:**1274–1282. http://dx.doi.org/10.4161/rna.25356.
80. **Krug RM, Fodor E.** 2013. The virus genome and its replication, p 57–66. *In* Webster RG, Monto AS, Braciale TJ, Lamb RA (ed), Textbook of influenza, 2nd ed. John Wiley & Sons, Ltd., New York, NY.
81. **Engelhardt OG, Smith M, Fodor E.** 2005. Association of the influenza A virus RNA-dependent RNA polymerase with cellular RNA polymerase II. J. Virol. **79:**5812–5818. http://dx.doi.org/10.1128/JVI.79.9.5812-5818.2005.
82. **Chase GP, Rameix-Welti MA, Zvirbliene A, Zvirblis G, Gotz V, Wolff T, Naffakh N, Schwemmle M.** 2011. Influenza virus ribonucleoprotein complexes gain preferential access to cellular export machinery through chromatin targeting. PLoS Pathog. **7:**e1002187. http://dx.doi.org/10.1371/journal.ppat.1002187.
83. **Hirayama E, Atagi H, Hiraki A, Kim J.** 2004. Heat shock protein 70 is related to thermal inhibition of nuclear export of the influenza virus ribonucleoprotein complex. J. Virol. **78:**1263–1270. http://dx.doi.org/10.1128/JVI.78.3.1263-1270.2004.
84. **Watanabe K, Fuse T, Asano I, Tsukahara F, Maru Y, Nagata K, Kitazato K, Kobayashi N.** 2006. Identification of Hsc70 as an influenza virus matrix protein (M1) binding factor involved in the virus life cycle. FEBS Lett. **580:**5785–5790. http://dx.doi.org/10.1016/j.febslet.2006.09.040.
85. **Li G, Zhang J, Tong X, Liu W, Ye X.** 2011. Heat shock protein 70 inhibits the activity of influenza A virus ribonucleoprotein and blocks the replication of virus in vitro and in vivo. PLoS One **6:**e16546. http://dx.doi.org/10.1371/journal.pone.0016546.
86. **Manzoor R, Kuroda K, Yoshida R, Tsuda Y, Fujikura D, Miyamoto H, Kajihara M, Kida H, Takada A.** 2014. Heat shock protein 70 modulates influenza A virus polymerase activity. J. Biol. Chem. **289:**7599–7614. http://dx.doi.org/10.1074/jbc.M113.507798.
87. **Momose F, Naito T, Yano K, Sugimoto S, Morikawa Y, Nagata K.** 2002. Identification of Hsp90 as a stimulatory host factor involved in influenza virus RNA synthesis. J. Biol. Chem. **277:**45306–45314. http://dx.doi.org/10.1074/jbc.M206822200.
88. **Naito T, Momose F, Kawaguchi A, Nagata K.** 2007. Involvement of Hsp90 in assembly and nuclear import of influenza virus RNA polymerase subunits. J. Virol. **81:**1339–1349. http://dx.doi.org/10.1128/JVI.01917-06.
89. **Deng T, Engelhardt OG, Thomas B, Akoulitchev AV, Brownlee GG, Fodor E.** 2006. Role of ran binding protein 5 in nuclear import and assembly of the influenza virus RNA polymerase complex. J. Virol. **80:**11911–11919. http://dx.doi.org/10.1128/JVI.01565-06.
90. **Hutchinson EC, Orr OE, Man Liu S, Engelhardt OG, Fodor E.** 2011. Characterization of the interaction between the influenza A virus polymerase subunit PB1 and the host nuclear import factor Ran-binding protein 5. J. Gen. Virol. **92:**1859–1869. http://dx.doi.org/10.1099/vir.0.032813-0.
91. **Resa-Infante P, Jorba N, Zamarreno N, Fernandez Y, Juarez S, Ortin J.** 2008. The host-dependent interaction of alpha-importins with influenza PB2 polymerase subunit is required for virus RNA replication. PLoS One **3:**e3904. http://dx.doi.org/10.1371/journal.pone.0003904.
92. **Tarendeau F, Boudet J, Guilligay D, Mas PJ, Bougault CM, Boulo S, Baudin F, Ruigrok RW, Daigle N, Ellenberg J, Cusack S, Simorre JP, Hart DJ.** 2007. Structure and nuclear import function of the C-terminal domain of influenza virus polymerase PB2 subunit. Nat. Struct. Mol. Biol. **14:**229–233. http://dx.doi.org/10.1038/nsmb1212.
93. **Gabriel G, Klingel K, Otte A, Thiele S, Hudjetz B, Arman-Kalcek G, Sauter M, Shmidt T, Rother F, Baumgarte S, Keiner B, Hartmann E, Bader M, Brownlee GG, Fodor E, Klenk HD.** 2011. Differential

use of importin-alpha isoforms governs cell tropism and host adaptation of influenza virus. Nat. Commun. **2:**156. http://dx.doi.org/10.1038/ncomms1158.
94. **Hudjetz B, Gabriel G.** 2012. Human-like PB2 627K influenza virus polymerase activity is regulated by importin-alpha1 and -alpha7. PLoS Pathog. **8:**e1002488. http://dx.doi.org/10.1371/journal.ppat.1002488.
95. **Momose F, Kikuchi Y, Komase K, Morikawa Y.** 2007. Visualization of microtubule-mediated transport of influenza viral progeny ribonucleoprotein. Microbes Infect. **9:**1422–1433. http://dx.doi.org/10.1016/j.micinf.2007.07.007.
96. **Liu SL, Zhang LJ, Wang ZG, Zhang ZL, Wu QM, Sun EZ, Shi YB, Pang DW.** 2014. Globally visualizing the microtubule-dependent transport behaviors of influenza virus in live cells. Anal. Chem. **86:**3902–3908. http://dx.doi.org/10.1021/ac500640u.
97. **Amorim MJ, Bruce EA, Read EK, Foeglein A, Mahen R, Stuart AD, Digard P.** 2011. A Rab11- and microtubule-dependent mechanism for cytoplasmic transport of influenza A virus viral RNA. J. Virol. **85:**4143–4156. http://dx.doi.org/10.1128/JVI.02606-10.
98. **Bruce EA, Digard P, Stuart AD.** 2010. The Rab11 pathway is required for influenza A virus budding and filament formation. J. Virol. **84:**5848–5859. http://dx.doi.org/10.1128/JVI.00307-10.
99. **Graef KM, Vreede FT, Lau YF, McCall AW, Carr SM, Subbarao K, Fodor E.** 2010. The PB2 subunit of the influenza virus RNA polymerase affects virulence by interacting with the mitochondrial antiviral signaling protein and inhibiting expression of beta interferon. J. Virol. **84:**8433–8445. http://dx.doi.org/10.1128/JVI.00879-10.
100. **Carr SM, Carnero E, Garcia-Sastre A, Brownlee GG, Fodor E.** 2006. Characterization of a mitochondrial-targeting signal in the PB2 protein of influenza viruses. Virology **344:**492–508. http://dx.doi.org/10.1016/j.virol.2005.08.041.
101. **Iwai A, Shiozaki T, Kawai T, Akira S, Kawaoka Y, Takada A, Kida H, Miyazaki T.** 2010. Influenza A virus polymerase inhibits type I interferon induction by binding to interferon beta promoter stimulator 1. J. Biol. Chem. **285:**32064–32074. http://dx.doi.org/10.1074/jbc.M110.112458.
102. **Finley D.** 2009. Recognition and processing of ubiquitin-protein conjugates by the proteasome. Annu. Rev. Biochem. **78:**477–513. http://dx.doi.org/10.1146/annurev.biochem.78.081507.101607.
103. **Di Pietro A, Kajaste-Rudnitski A, Oteiza A, Nicora L, Towers GJ, Mechti N, Vicenzi E.** 2013. TRIM22 inhibits influenza A virus infection by targeting the viral nucleoprotein for degradation. J. Virol. **87:**4523–4533. http://dx.doi.org/10.1128/JVI.02548-12.
104. **Liu X, Zhao Z, Xu C, Sun L, Chen J, Zhang L, Liu W.** 2012. Cyclophilin A restricts influenza A virus replication through degradation of the M1 protein. PLoS One **7:**e31063. http://dx.doi.org/10.1371/journal.pone.0031063.
105. **Su WC, Chen YC, Tseng CH, Hsu PW, Tung KF, Jeng KS, Lai MM.** 2013. Pooled RNAi screen identifies ubiquitin ligase Itch as crucial for influenza A virus release from the endosome during virus entry. Proc. Natl. Acad. Sci. U. S. A. **110:**17516–17521. http://dx.doi.org/10.1073/pnas.1312374110.
106. **Liao TL, Wu CY, Su WC, Jeng KS, Lai MM.** 2010. Ubiquitination and deubiquitination of NP protein regulates influenza A virus RNA replication. EMBO J. **29:**3879–3890. http://dx.doi.org/10.1038/emboj.2010.250.
107. **Kistner O, Muller H, Becht H, Scholtissek C.** 1985. Phosphopeptide fingerprints of nucleoproteins of various influenza A virus strains grown in different host cells. J. Gen. Virol. **66**(Part 3)**:**465–472.
108. **Perales B, Sanz-Ezquerro JJ, Gastaminza P, Ortega J, Santaren JF, Ortin J, Nieto A.** 2000. The replication activity of influenza virus polymerase is linked to the capacity of the PA subunit to induce proteolysis. J. Virol. **74:**1307–1312. http://dx.doi.org/10.1128/JVI.74.3.1307-1312.2000.
109. **Pleschka S, Wolff T, Ehrhardt C, Hobom G, Planz O, Rapp UR, Ludwig S.** 2001. Influenza virus propagation is impaired by inhibition of the Raf/MEK/ERK signalling cascade. Nat. Cell Biol. **3:**301–305. http://dx.doi.org/10.1038/35060098.
110. **Root CN, Wills EG, McNair LL, Whittaker GR.** 2000. Entry of influenza viruses into cells is inhibited by a highly specific protein kinase C inhibitor. J. Gen. Virol. **81:**2697–2705.
111. **Kurokawa M, Ochiai H, Nakajima K, Niwayama S.** 1990. Inhibitory effect of protein-kinase-C inhibitor on the replication of influenza type-A virus. J. Gen. Virol. **71:**2149–2155. http://dx.doi.org/10.1099/0022-1317-71-9-2149.
112. **Kumar N, Liang YH, Parslow TG, Liang YY.** 2011. Receptor tyrosine kinase inhibitors block multiple steps of influenza A virus replication. J. Virol. **85:**2818–2827. http://dx.doi.org/10.1128/JVI.01969-10.
113. **Hui EKW, Nayak DP.** 2002. Role of G protein and protein kinase signalling in influenza virus budding in MDCK cells. J. Gen. Virol. **83:**3055–3066.
114. **Shi Y.** 2009. Serine/threonine phosphatases: mechanism through structure. Cell **139:**468–484. http://dx.doi.org/10.1016/j.cell.2009.10.006.
115. **Xu Y, Chen Y, Zhang P, Jeffrey PD, Shi Y.** 2008. Structure of a protein phosphatase 2A holoenzyme: insights into B55-mediated Tau dephosphorylation. Mol. Cell **31:**873–885. http://dx.doi.org/10.1016/j.molcel.2008.08.006.
116. **Chenavas S, Estrozi LF, Slama-Schwok A, Delmas B, Di Primo C, Baudin F, Li X, Crepin T, Ruigrok RW.** 2013. Monomeric nucleoprotein of influenza A virus. PLoS Pathog. **9:**e1003275. http://dx.doi.org/10.1371/journal.ppat.1003275.
117. **Mukaigawa J, Nayak DP.** 1991. Two signals mediate nuclear localization of influenza virus (A/WSN/33) polymerase basic protein 2. J. Virol. **65:**245–253.
118. **Gonzalez S, Ortin J.** 1999. Characterization of influenza virus PB1 protein binding to viral RNA: two separate regions of the protein contribute to the interaction domain. J. Virol. **73:**631–637.
119. **Gonzalez S, Ortin J.** 1999. Distinct regions of influenza virus PB1 polymerase subunit recognize vRNA and cRNA templates. EMBO J. **18:**3767–3775. http://dx.doi.org/10.1093/emboj/18.13.3767.
120. **Jung TE, Brownlee GG.** 2006. A new promoter-binding site in the PB1 subunit of the influenza A virus polymerase. J. Gen. Virol. **87:**679–688. http://dx.doi.org/10.1099/vir.0.81453-0.
121. **Coloma R, Valpuesta JM, Arranz R, Carrascosa JL, Ortin J, Martin-Benito J.** 2009. The structure of a biologically active influenza virus ribonucleoprotein complex. PLoS Pathog. **5:**e1000491. http://dx.doi.org/10.1371/journal.ppat.1000491.
122. **Area E, Martin-Benito J, Gastaminza P, Torreira E, Valpuesta JM, Carrascosa JL, Ortin J.** 2004. 3D structure of the influenza virus polymerase complex: localization of subunit domains. Proc. Natl. Acad. Sci. U. S. A. **101:**308–313. http://dx.doi.org/10.1073/pnas.0307127101.
123. **Torreira E, Schoehn G, Fernandez Y, Jorba N, Ruigrok RW, Cusack S, Ortin J, Llorca O.** 2007. Three-dimensional model for the isolated recombinant influenza virus polymerase heterotrimer. Nucleic Acids Res. **35:**3774–3783. http://dx.doi.org/10.1093/nar/gkm336.
124. **Resa-Infante P, Recuero-Checa MA, Zamarreno N, Llorca O, Ortin J.** 2010. Structural and functional characterization of an influenza virus RNA polymerase-genomic RNA complex. J. Virol. **84:**10477–10487. http://dx.doi.org/10.1128/JVI.01115-10.
125. **He X, Zhou J, Bartlam M, Zhang R, Ma J, Lou Z, Li X, Li J, Joachimiak A, Zeng Z, Ge R, Rao Z, Liu Y.** 2008. Crystal structure of the polymerase PA(C)-PB1(N) complex from an avian influenza H5N1 virus. Nature **454:**1123–1126. http://dx.doi.org/10.1038/nature07120.
126. **Obayashi E, Yoshida H, Kawai F, Shibayama N, Kawaguchi A, Nagata K, Tame JR, Park SY.** 2008. The structural basis for an essential subunit interaction in influenza virus RNA polymerase. Nature **454:**1127–1131. http://dx.doi.org/10.1038/nature07225.
127. **Paterson D, Fodor E.** 2012. Emerging roles for the influenza A virus nuclear export protein (NEP). PLoS Pathog. **8:**e1003019. http://dx.doi.org/10.1371/journal.ppat.1003019.
128. **Manz B, Brunotte L, Reuther P, Schwemmle M.** 2012. Adaptive mutations in NEP compensate for defective H5N1 RNA replication in cultured human cells. Nat. Commun. **3:**802. http://dx.doi.org/10.1038/ncomms1804.
129. **Reuther P, Giese S, Gotz V, Kilb N, Manz B, Brunotte L, Schwemmle M.** 2014. Adaptive mutations in the nuclear export protein of human-derived H5N1 strains facilitate a polymerase activity-enhancing conformation. J. Virol. **88:**263–271. http://dx.doi.org/10.1128/JVI.01495-13.
130. **Reuther P, Giese S, Gotz V, Riegger D, Schwemmle M.** 2014. Phosphorylation of highly conserved serine residues in the influenza A virus nuclear export protein NEP plays a minor role in viral growth in human cells and mice. J. Virol. **88:**7668–7673. http://dx.doi.org/10.1128/JVI.00854-14.